Faculty of Biomedical and Life Sciences

INVESTIGATING MOLECULAR MECHANISMS OF NEURONAL REGENERATION: A MICROARRAY APPROACH

Alison Margaret Blain

Thesis submitted for the degree of Doctor of Philosophy

September 2008

Abstract

Injury to the peripheral nervous system (PNS) stimulates a finely regulated regenerative response that generally leads to some recovery of function. In contrast, the response to injury in the adult mammalian central nervous system (CNS) is abortive and adult CNS neurons do not normally regenerate. We used a microarray approach to identify putative regeneration-associated changes in gene expression in the L4 dorsal root ganglion (DRG) in rat models of PNS and CNS injury.

Our models included crush injury to both branches of the bifurcating axon of sensory neurons with cell bodies in the DRG (DRGNs). Injury to the peripheral branch at the level of the spinal nerve (SN) results in axonal regeneration and reinnervation. Crush injury of the central branch in the dorsal root (DR) results in active regeneration up to the point of CNS entry at the DR entry zone (DREZ) and subsequent arrest of further growth, while transection injury within the CNS at the level of the dorsal columns (DC) results in abortive and unsuccessful regeneration attempts. These DRGN injury models therefore allowed us to compare the gene expression programmes elicited during active, arrested and abortive regeneration.

Following a pilot microarray experiment to optimize experimental parameters and tract tracing and electrophysiological experiments to confirm time points for harvest of DRGs after DR and SN injury, respectively, male Sprague-Dawley rats underwent an L4 SN crush, an L4 DR crush or a bilateral DC transection at the L3/L4 spinal segment boundary. L4 DRGs were collected at 2 weeks (active regeneration) and 6 weeks (arrested regeneration) after DR crush. DRGs were harvested at 6 weeks after SN crush and 2 weeks after DC transection. DRGs harvested from naïve rats served as a control group.

Microarray analysis (Affymetrix Rat genome 230 2.0 array) identified genes showing differential expression (5% FDR) in regenerating and non-regenerating conditions. Selected genes chosen for validation by qRT-PCR included WISP2 and TFPI2- genes that were regulated specifically in the regenerating conditions. These genes could represent putative regeneration-associated genes and may suggest novel therapeutic interventions to encourage regeneration of the spinal cord following injury. Additionally, we have identified genes upregulated in the DR active regeneration state relative to DR arrested state, which have relevance to root avulsion injury and may provide insight into the mechanisms that prevent regeneration of DR axons through the DREZ to re-enter the spinal cord. We also present evidence that a transcriptional programme consistent with regeneration is mounted within the DRG following DC transection. This lends support to the idea that CNS neurons have intrinsic regenerative capability and that manipulations of the CNS environment may be sufficient to permit regeneration of CNS axons.

Acknowledgements

First of all I would like to say a massive thank you to my supervisors, Mark and John for their support and guidance throughout the project. Thank you Mark for all your encouragement, especially during the write up and a special thank you to John for performing the very technical surgical procedures that were required for this project.

There have been a number of other people who have helped in this project; thank you to the staff of the Sir Henry Wellcome Functional Genomics unit- thank you to Jing Wang who performed the chip hybridisations and to Pawel Herzyk for guidance on the data analysis aspects of the project. Thank you also to Dugald Scott for help in performing the electrophysiology experiments, and to Andrew Toft for helping me with dissection and immunohistochemistry. Thank you to Timothy Hems for providing us with our human samples. Thank you also to my assessors, Julian and Brian.

To all my fellow tea Jennys (and coffee addicts) on Level 5- thank you so much for being such fantastic friends as well as great people to work with.

Mum and dad, thank you so much for supporting me all these years. I promise I will now make the trip North more often. Finally, thank you to Tom for helping me to look on the bright side.

Table of contents

List of tables

List of figures

Author's Declaration

I certify that this thesis does not contain material previously published or written by any other person. The research reported in this thesis is my own original work, except where otherwise stated, and has not been submitted for any other degree.

Alison Blain.

September 2008

Definitions

ºC	Degrees Celsius
µ	Micro (10^{6})
ANOVA	Analysis of variance
b	Base
bp	Base pair
cDNA	Complementary deoxyribonucleic acid
CAP	Compound action potential
CDP	Cord dorsum potential
CNS	Central nervous system
dATP	2'-Deoxyadenosine-5'-triphosphate
dCTP	2'-Deoxycytidine-5'-triphosphate
dGTP	2'-Deoxyguanine-5'-triphosphate
dTTP	2'-Deoxythymidine-5'-triphosphate
DEPC	Diethylpyrocarbonate
DNA	Deoxyribonucleic acid
dNTP	Deoxyribonucleotidetriphosphate
DREZ	Dorsal root entry zone
DRG	Dorsal root ganglion
DTT	Dithiotheitol
EDTA	Ethylenediaminetetracetic acid
EtBr	Ethidium bromide
g	Gram
K	Kilo (10^{3})
l	Litre
L4	Lumbar 4
L5	Lumbar 5
m	Milli (10^{-3})
M	Molar
mRNA	Messenger ribonucleic acid
MW	Molecular weight
N	Nano (10^{-9})
P	Pico (10^{-12})
PBS	Phosphate buffered saline
PCR	Polymerase chain reaction
PFA	Paraformaldehyde
PNS	Peripheral nervous system
RNA	Ribonucleic acid
RT	Reverse transcriptase
TBS	Tris-buffered saline
Tm	Melting temperature
Tris	Tris(hydroxymethyl)amino methane
U	Unit
UV	Ultraviolet
v	Volume
V	Volt
w	Weight
W	Watt

In adult centres the nerve paths are something fixed, ended, immutable. Everything may die, nothing may be regenerated. It is for the science of the future to change if possible, this harsh decree.

Santiago Ramon y Cajal, 1911.

1 Introduction

1.1 Regeneration in the central and peripheral nervous systems

Injury to the peripheral nervous system (PNS) stimulates a complex and finely regulated regenerative response that generally leads to some recovery of function. In contrast, in the adult mammalian central nervous system (CNS), the response to injury is abortive and in normal circumstances, adult CNS neurons do not regenerate. Thus damage to the CNS has permanent and debilitating consequences such as paralysis (in the case of spinal cord injury (SCI)). It is therefore of significant clinical importance to elucidate the molecular mechanisms underlying the failure of CNS regeneration, and to explore ways in which they can be manipulated to stimulate regeneration. This project aims to compare and contrast the transcriptional response of dorsal root ganglion (DRG) neurons to injuries to their central or peripheral branch and to gain insight into the molecular mechanisms that dictate their respective injury response programmes.

1.2 Injury to the PNS

1.2.1 Aetiology

Aetiologically, a number of factors including malignancy, toxins, connective tissue diseases (e.g. Systemic Erythematosus Lupus), metabolic factors (e.g. as in diabetes mellitus) and thermal and mechanical disruption can cause injury to peripheral nerves. Of most relevance to this project and of wider clinical significance is mechanical injury, which can result from a number of primary injuries, including laceration, fracture, surgery and gunshot wounds.

The clinical prognosis following any peripheral nerve injury will depend on the nature of the primary injury. For example, the probability of functional recovery following a crush lesion is much greater than following a transection lesion as in nerve crush the preserved basal lamina (a layer of extracellular matrix on which epithelia sits) provides guidance for regenerating axons from the proximal nerve stump to their targets. In contrast, the proximal and distal stumps are completely separated in transection injuries and thus reinnervation of targets is impeded and a swelling of the nerve, called a neuroma, may form. Despite these differences in clinical outcome, the initial regenerative response elicited by peripheral nerve crush and peripheral nerve transection follows the same characteristic pattern.

1.2.2 Wallerian Degeneration and regeneration

In the PNS, the response to injury comprises a degenerative and subsequent regenerative phase that has been described in detail in a number of reviews (Stoll and Muller 1999; Stoll *et al.* 2002; Burnett and Zager 2004; Rodiguez *et al*. 2004). The degenerative phase was first described by Augustus Waller, who in the transected hypoglossal and glossopharyngeal nerves of frogs, observed histological alterations in the 'medulla' of the nerve and in the nerve-tubes of the papillae (Waller 1850). It is now recognised that these early observations describe a process that applies to all peripheral and central nerve lesions and is widely known as 'Wallerian Degeneration' (WD).

WD (Figure 1-1) serves to create a microenvironment favouring axonal regeneration. It begins within hours of injury with fragmentation of microtubules and degradation of the axoplasm and axolemma in the distal nerve segment. This is mediated by increased calcium influx (George *et al.* 1995) and the subsequent activation of ubiquitin-regulatory enzymes and axonal proteases such as calpain (Glass *et al*. 2002; Zhai *et al.* 2003; Ehlers 2004). Zhai *et al.* (2003) demonstrated, using pharmacological methods, a critical role for the Ubiquitin-Proteasome System (UPS) in the early stages of WD. UPS inhibitors retarded the development of the early signs of WD and more specifically, microtubule fragmentation. Modification of proteins by addition of ubiquitin can target them for destruction by the proteosome and thus ubiquitinisation may be a suitable candidate mechanism for the destruction of cellular structures as seen in WD.

Schwann cells (the myelin producing cells of the PNS) play a pivotal role in WD and subsequent axonal elongation. In response to axonal loss, Schwann cells proliferate in the distal section of the injured nerve to form daughter cells that upregulate genes involved in the degenerative and regenerative processes, and down-regulate steady-state mRNA levels for the myelin components (LeBlanc and Poduslo 1990). As will be discussed later, the downregulation of myelin-associated components in the PNS may contribute to the creation of an environment permissive to neural regeneration, as such molecules are known to be growth inhibitory. Schwann cells fragment their own myelin sheaths and have a role in the removal of the debris of WD by sequestration of small coils of myelin debris for phagocytosis. Phagocytosis of the myelin debris is achieved partly through the action of the Schwann cells themselves but also through haematogenous macrophages that infiltrate the injured area. Following phagocytosis of their myelin and axonal components, the basal lamina of Schwann cells (the endoneurial tubes) collapse and form stacked processes called bands of Büngner. The bands of Büngner later serve as guidance tubes for the regenerating nerve fibres.

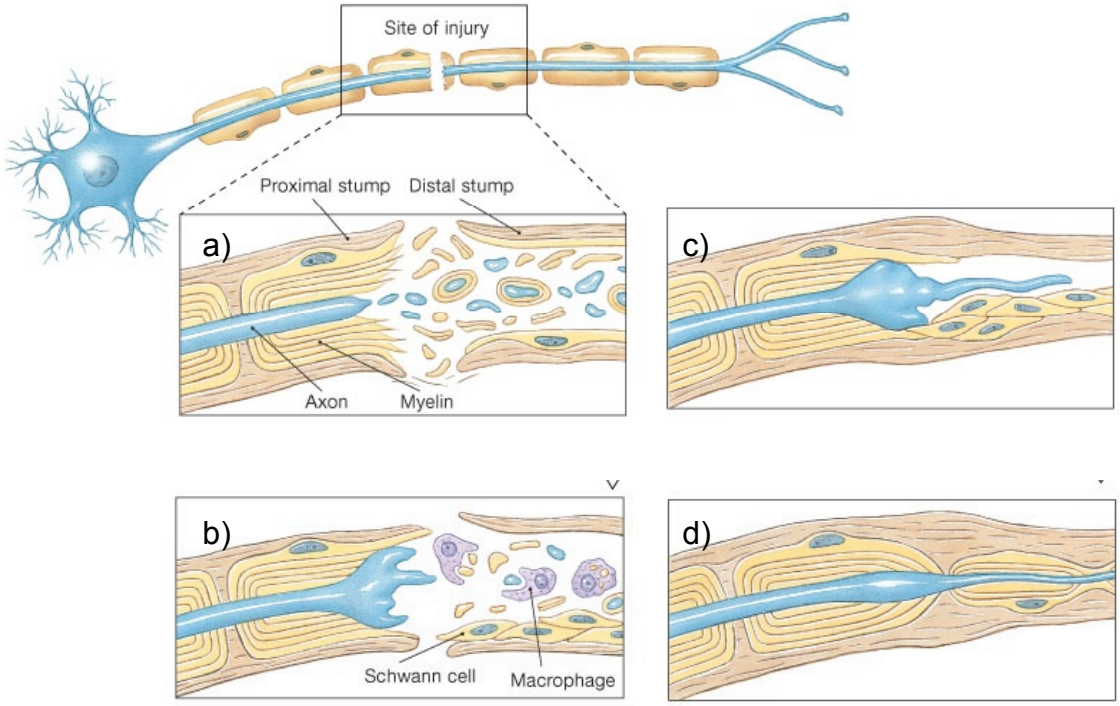

Figure 1-1: Wallerian degeneration. a) Fragmentation of myelin occurs in the distal stump. b) Schwann cells proliferate in the distal stump and macrophages engulf debris. c) Axons bud and grow along schwann cells d) Schwann cells collapse to form bands of Bü**n**gner which guide regenerating nerve fibres. Adapted from www.iupucanatomy.com.

The regenerative phase of the peripheral response to injury may begin after completion of WD (in the case of severe nerve injuries), or almost immediately after injury (following milder injuries), and can continue for a number of months. The first signs of regeneration are seen in the neuronal cell body where there are visible changes marking the reversal of chromatolysis (the dissolution and breaking up of chromatin). Chromatolysis is a hallmark feature of the PNS response to injury, occurring immediately following injury and marking a shift from synaptic transmission to cellular repair. With initiation of regeneration, the cell nucleus returns to the cell centre, nucleoproteins reorganise into compact Nissl granules and subcellular metabolic functions that were altered during chromatolysis revert to their original states.

Regeneration of the axon tip proceeds from the proximal stump of the injured nerve fibre into the distal nerve and relies on an increase in protein and lipid synthesis in the cell body and an adequate supply of trophic and tropic factors, provided by reactive Schwann cells, macrophages and the extracellular matrix. Axotomised neurons express growth cones on their axon tips and these structures are essential to dictate the direction of axonal outgrowth.

1.2.2.1 Growth cones

Growth cones are dynamic actin-supported motile organelles which extend fine finger-like (filopodia) and web-like (lamellopodia) sensory processes that detect and allow the growth cone to respond to signals in their local environment (Morris and Tiveron 1994) (Figure 1-2). A number of

molecules have been identified that influence growth cone guidance chemotactically and these may be repellent or attractant in nature. These molecules include: netrins (acting through DCC and UNC5 receptors), Ephrins (acting through Ephrin receptor tyrosine kinases) and Slits (acting through Robo receptors). In particular, a large body of research has concentrated on the elucidation of the role of the large semaphorin gene family in axonal guidance (Section 1.2.2.2). Contact guidance is also an important component of growth cone guidance and filopodia/lammelapodia adhere to the basal lamina of Schwann cells, using it as a guide for outgrowth.

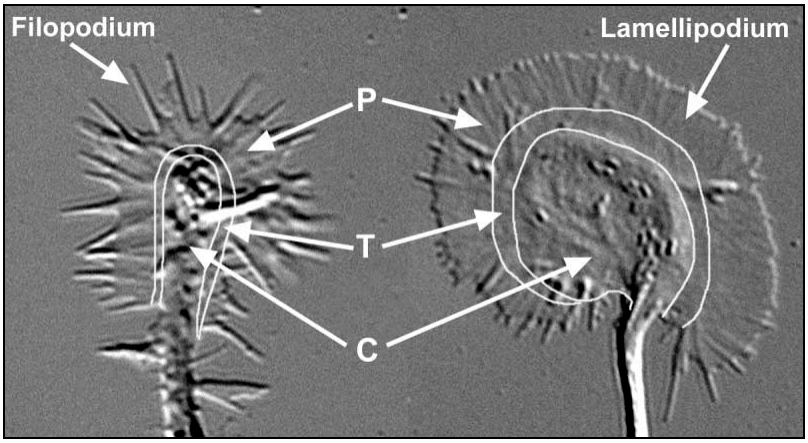

Figure 1-2: Examples of primarily filopodial and primarily lamellopodial growth cones. Growth cones possess functionally defined zones; P: The peripheral domain which primarily consists of an actin based cytoskeleton. This region contains the motile filopodia and lammelopodia; T: the transitional domain is the thin band between the central and peripheral domains and C: the central domain, the region of the growth cone nearest the axon which consists of a microtubule based cytoskeleton and contains many organelles and vesicles (Taken from Dent and Gertler (2003).

Early observations of *Aplysia* axon growth *in vitro* indicated that axonal outgrowth occurs through a cycle of protrusion, engorgement and consolidation (Goldberg and Burmeister 1986) (Figure 1-3). Protrusion relies on the polymerisation of actin filaments, leading to the elongation of filopodia and lamellipodia. Engorgement occurs when microtubules invade the protrusions and populate them with membranous vesicles and organelles. Consolidation, the final stage of the cycle, involves depolymerisation of F-actin in the neck of the growth cone. This allows the axonal membrane to shrink around the microtubules forming a new, cylindrical section of axon shaft. Dent and Gertler (2003) proposed that growth cone repellents and attractants in the local environment can bias one side of a growth cone to pass through the described stages of growth and thus influence the directionality of axon outgrowth. In addition, they presented a model for cytoskeletal regulation of axon outgrowth and guidance involving local stabilization/destabilization of the microtubule array. They suggest that in normal circumstances, protrusion is in balance across the growth cone and thus the growth cone remains in a straight trajectory. However, when an attractant is detected on one side of the growth cone, F-actin-driven protrusion is favoured on that side while retraction is favoured on the contralateral side. Ena/VASP proteins, a conserved family of actin-regulatory

proteins that are found concentrated at filopodial tips, are implicated in translating guidance cues into changes in cytoskeletal dynamics and filopodial formation (Drees and Gertler 2008).

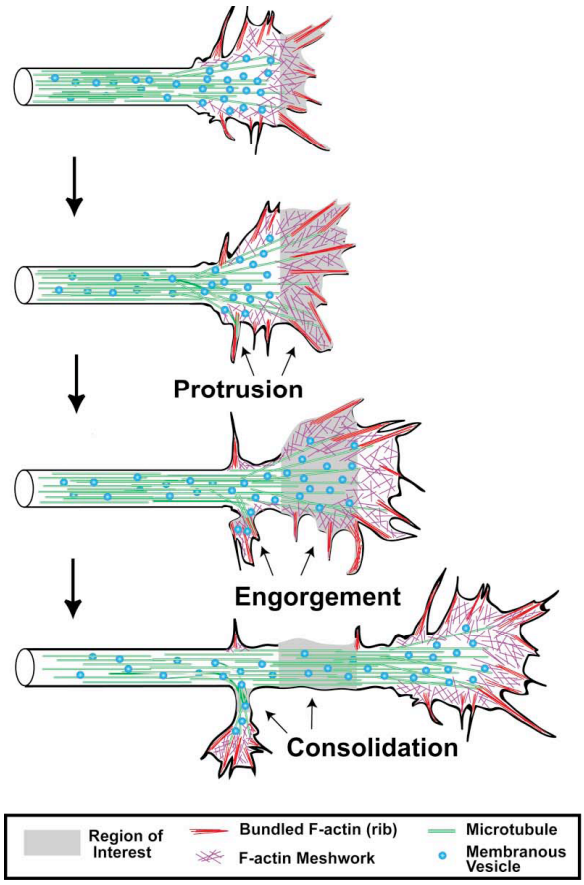

Figure 1-3: Stages of axon growth. Axons undergo a cycle of protusion, engorgement and consolidation whereby polymerisation of the actin meshwork in the lamellopodia of the growth cone results in its fillopodia that then become engorged with microtubules, vesicles and organelles. Depolymerisation of F-actin and membrane shrinkage in the neck of the growth cone is the final step in the cycle leading to axon outgrowth. Taken from Dent and Gertler (2003).

1.2.2.2 Semaphorins in growth cone guidance

The semaphorins comprise a family of secreted or membrane-associated proteins that can signal growth cone repulsion and/or attraction and can thus influence the trajectory of axonal outgrowth (Dodd and Schuchardt 1995; Pasterkamp et al. 2001; Pasterkamp and Verhaagen 2001). The semaphorin family has been categorised according to sequence and structural similarity into eight classes, classes 3-7 being the vertebrate semaphorins (Figure 1-4a). In development, semophorins have a mainly repulsive role in axon guidance and act by altering the axonal cytoskeleton by modification of actin and microtubule dynamics through a neurophilin/plexin/CAM receptor complex or through direct interaction with plexin or integrins (Figure 1-4b) (Rohm *et al.* 2000). Semaphorin 3a, the most studied member of the semaphorin family, has been shown to play a key role in developmental axonal guidance by causing growth cone collapse by

depolymerisation and loss of F-actin (Luo *et al.* 1993) through intracellular collapsin response mediator prioteins (CRMPS) and G-proteins (Nakamura *et al.* 2000; Hotta *et al.* 2005; Rosslenbroich *et al.* 2005; Schmidt and Strittmatter 2007). A role for membrane-bound semaphorin 6a in the appropriate segregation of the CNS and PNS during development has also been suggested (Mauti *et al.* 2007). The role of the semaphorins is not howerver limited to the developing nervous system and there is a sustained expression of semaphorins and their effectors (such as CRMPs) during adulthood (Giger *et al.* 1998; Bretin *et al.* 2005; Sahay *et al.* 2005). In the adult nervous system semaphorins act to prevent abberant axonal sprouting by limiting structural plasticity (de Wit and Verhaagen 2003).

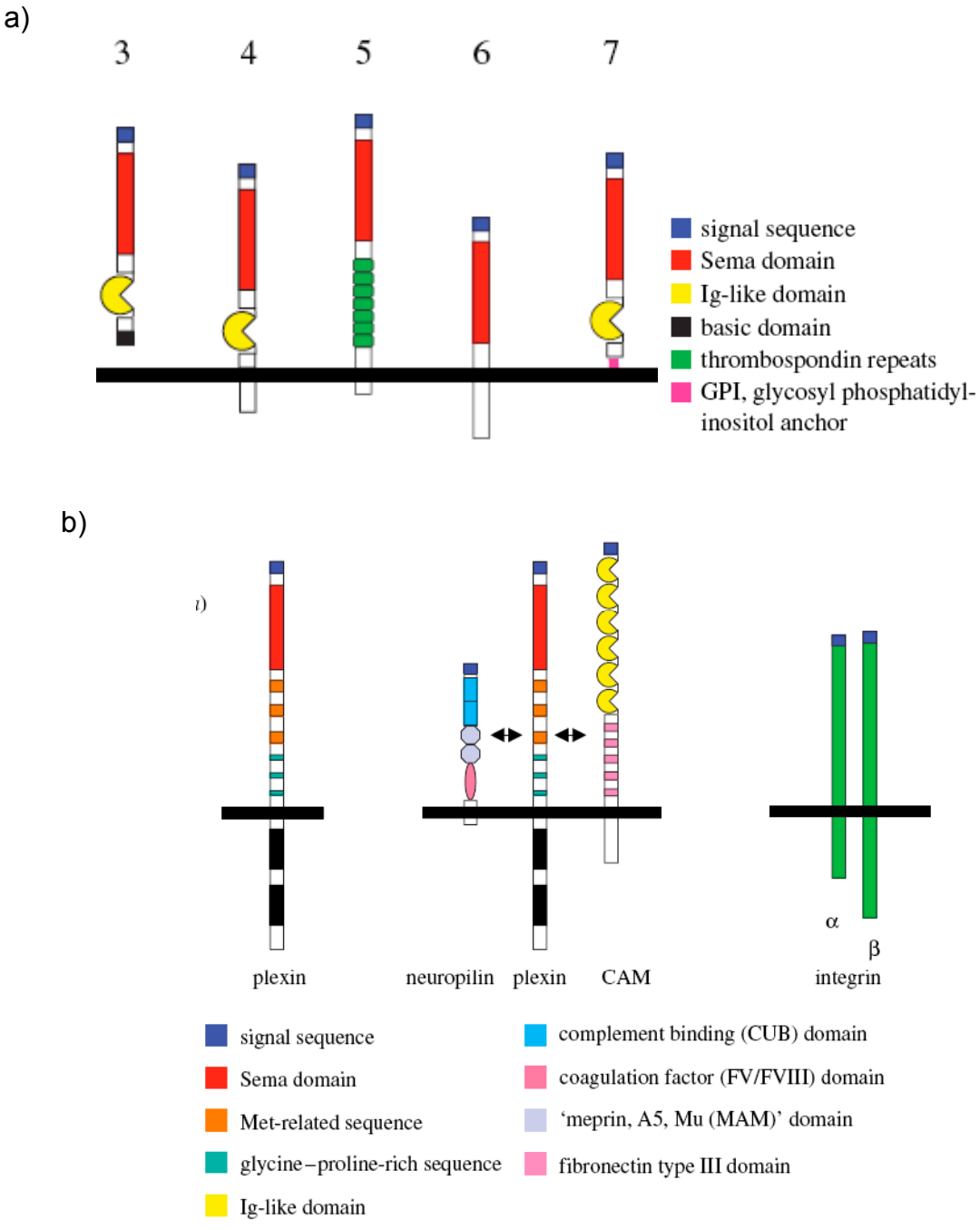

Figure 1-4: The vertebrate semaphorins and their receptors. a) Semaphorins have a conserved N-terminal signal sequence and semaphorin domain. b) Semaphorins classes 4-7 and

semaphorin 3E can interact directly with plexins. c) Semaphorin class 3 signals though a neurophilin/plexin/CAM complex and c) Sema7A requires β1-integrin. Adapted from Pasterkamp and Verhaagen (2006).

1.3 Injury to the CNS

In contrast to PNS damage, injuries to the CNS (brain and spinal cord) are almost always irrevocable and can lead to permanent loss of function. Spinal cord injury has particularly debilitating consequences and affects approximately 40000 people in the UK alone (The Spinal Injuries Association (SIA), 2008. (www.spinal.co.uk)). It is thus the focus of a large body of research directed towards the development of putative therapies to reinstate lost function.

1.3.1 The anatomy of the spinal cord

The spinal cord is the extension of the central nervous system outside the cranium and forms a gateway for transfer of sensory, motor and proprioceptive information between the body and brain. It begins immediately below the brain stem and extends to the first lumbar vertebra where it blends with the *conus medularis* to become a group of nerves resembling a horse's tail (*cauda equina*). Three membranes (Figure 1-5) collectively known as the meninges cover the spinal cord (and also the brain). The innermost membrane, the pia mater, is extremely delicate and closely covers the surface of the spinal cord. A weblike membrane called the arachnoid lies between the pia mater and the tough outermost membrane, the dura mater. The space between the arachnoid and pia meninges (subarachnoid space) is filled with cerebrospinal fluid (CSF), forming a fluid filled sack around the brain and spinal cord.

The spinal cord is housed and protected within the vertebral (spinal column) which has a segmental organisation and consists of 7 cervical, 12 thoracic, 5 lumbar, 5 sacral and 4 coccygeal vertebrae. 31 pairs of spinal nerves exit along the length of the spinal column through the intervertebral foramen (small hollows between each vertebra). The spinal nerves branch to form the peripheral nerves that are responsible for movement and sensation of the extremities and trunk. The origins of the spinal nerves, as they emerge from the spinal cord are called the nerve roots (Figure 1-5). Each spinal nerve is formed by the merging of two roots: the dorsal root; which contains axons entering the spinal cord and has cell bodies in the dorsal root ganglion (DRG), and a ventral root; which contains axons exiting the cord. Figure 1-6 illustrates the segmental organisation of the spine and the relationship between the spinal nerve roots and vertebrae.

The spinal cord itself contains a central core of grey matter which is butterfly shaped in transverse section (Figure 1-5). The grey matter contains the spinal neurons and can broadly be divided into the dorsal (sensory) and the ventral (motor) horns. The sensory neurons (primary afferents) entering the spinal cord through the dorsal roots synapse onto the spinal neurons in the dorsal horn and also project rostrocaudally in axon tracts in the white matter that surrounds the grey

matter (see also section 1.5.2.2 and Figure 1-14). The white matter contains ascending and descending axon tracts which are arranged in columns, the dorsal columns being the principle axon tract through which sensory information is transmitted.

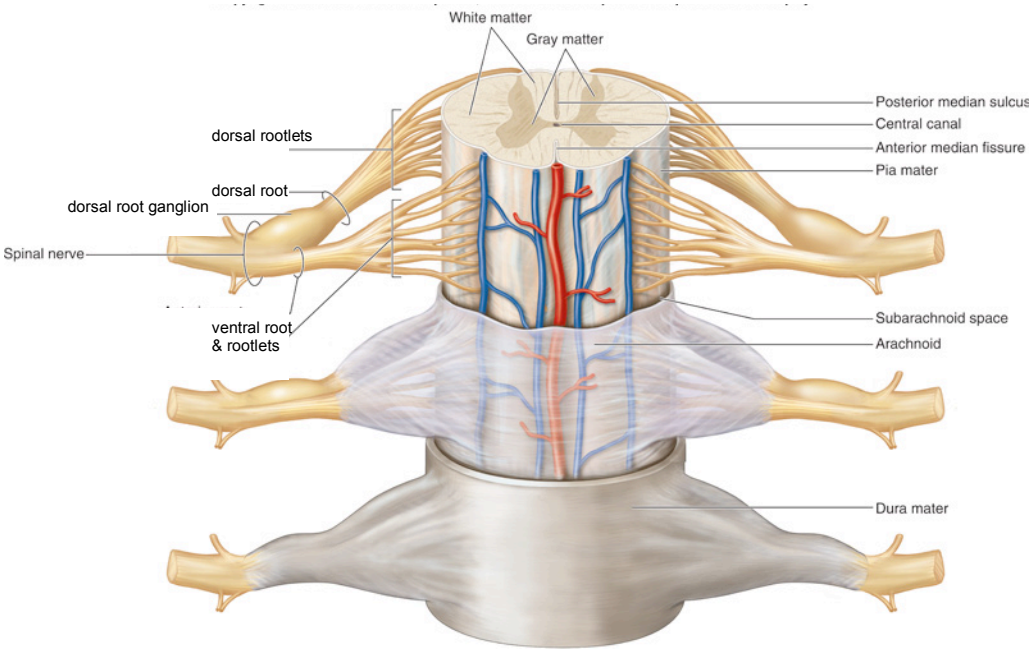

Figure 1-5: Diagramatic representation of the spine in transverse section (lumbar region) viewed from the ventral aspect. Adapted from a diagram published by McGraw-Hill Companies, Inc.

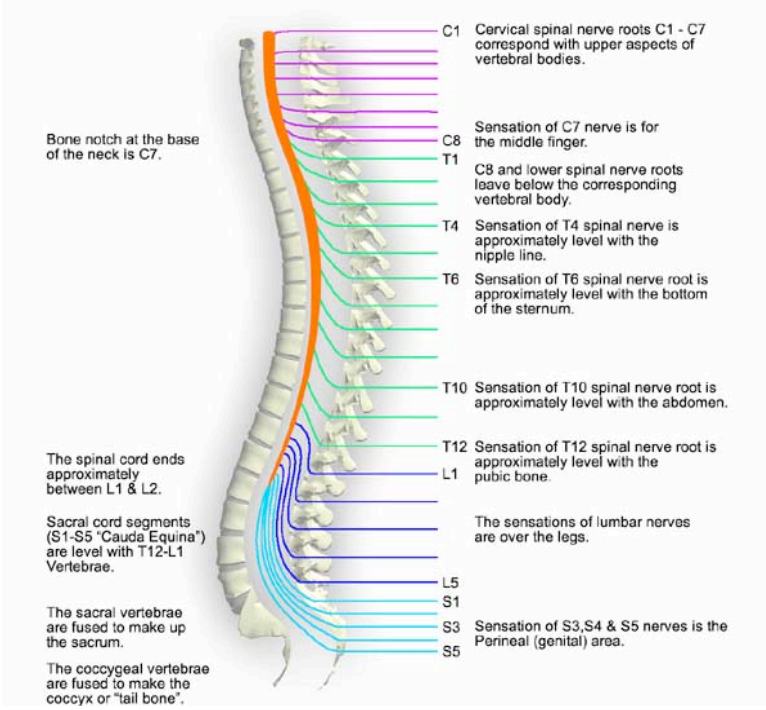

Figure 1-6: The relationship between the spinal nerves and vertebrae. (www.apparalyzed.com).

1.3.2 Spinal cord injuries

Spinal cord injury causes the spinal nerves below the level of the injury to be partially or completely isolated from the brain. This leads to a loss of sensory function and motor paralysis below the level of injury. Depending on the level of the injury, quadriplegia/tetraplegia or paraplegia may occur (Figure 1-7). Quadriplegia/tetraplegia occurs with injury above the first thoracic vertebra and describes paralysis that affects all four limbs. In this type of paralysis there is further discomfort as the abdominal and chest muscles are also affected, resulting in weakened breathing and an inability to clear the chest by coughing. Paraplegia occurs when the level of injury is below the first thoracic spinal nerve and can vary in severity from impairment in leg movement to complete paralysis of the legs and abdomen to nipple level.

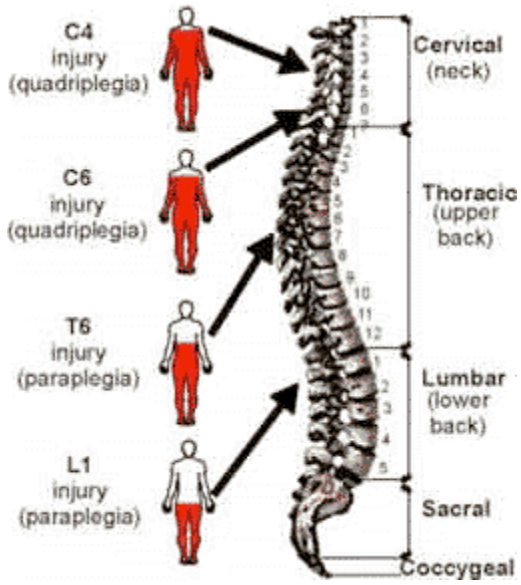

Figure 1-7: Injury outcomes at different levels of spinal cord injury. The area of paralysis is indicted in red.

Injury to the spinal cord is most common at the C5-C7 and T12-L1 levels and may be due to concussion, contusion, laceration, compression or complete transection. Hyperextension and the resultant dorsal column contusion and posterior dislocation of the vertebrae is often seen in motor accidents due to the victim being thrown against the windshield or steering wheel. Compression injuries are frequently seen following jumps or falls in which the individual lands on their feet or buttocks. The force of the impact fractures the vertebrae and compresses the cord, most commonly at the lumbar and lower thoracic level. Traumatic injuries to the spine and brachial plexus can result in avulsion of the dorsal and ventral roots whereby the roots are damaged or are ripped from the spinal cord. Although this is not a direct injury to the spinal cord, this injury, which is commonly caused by motor cycle accidents, often results in indirect spinal cord damage and lost sensory function because of the inability of the sensory fibres contained within the dorsal root to

regenerate across the PNS/CNS border of the dorsal root entry zone (DREZ), despite an initial regenerative response (Zhang *et al.* 2001).

1.4 Why doesn't the CNS regenerate?

Spinal cord injury, along with other CNS injuries such as stroke and optic nerve damage, carries an extremely poor prognosis because of the lack of regeneration in CNS nerves. The investigation of the reasons for this lack of regeneration has found fundamental differences in the CNS response to injury compared to that in the PNS and a number of factors are now known to play an instrumental part in creating an environment that is conducive or inhibitory to neuronal regeneration. This knowledge has led to the development of a number of approaches to promote CNS regeneration *in vivo*.

The profound morphological and metabolic changes in the cell body (chromatolysis) and beneficial inflammatory mechanisms that occur following PNS injury are diminished or absent following an equivalent injury to the CNS (Lieberman 1971); WD and clearance of debris is significantly slower in the CNS and is incomplete (Vargas and Barres 2007). The CNS does however undergo a brief period of regeneration immediately following injury. Cajal (1928) was first to confirm histologically that following injury, the CNS undergoes a phase of abortive sprouting around the injury site whereby the newly formed axons were often hypertrophied, branched and irregular and ended in clubs, points or rings. In addition, he demonstrated growth of CNS cortical axons through pre-degenerated peripheral nerve graft and hypothesised that the failure of CNS regeneration was due to the absence of a number of extrinsic growth promoting and neurotrophic factors that are present in the PNS. Indeed, David and Aguayo (1981) showed that neurons in the adult mammalian CNS were capable of long distance axon regeneration if provided with an appropriate glial environment and a number of extrinsic factors have been identified that contribute to the CNS injury response. Conversely, there is evidence that PNS myelin is not permissive to axonal growth (Bahr and Przyrembel 1995) and manipulation of extrinsic factors is insufficient to promote axonal outgrowth in the CNS (Dusart *et al.* 2005) This, along with the observation that there is variation in intrinsic regenerative potential between PNS and CNS neurons and also within different classes and ages of neurons in the CNS (Chen et al. 1995; Ng and Lozano 1999), suggests that PNS neurons possess intrinsic properties that allow them to regenerate. The failure of CNS axonal regeneration is therefore multifactorial, involving extrinsic and intrinsic factors.

1.4.1 Extrinsic factors and how they are targeted

1.4.1.1 Myelin-associated inhibitors of regeneration

Myelin-associated inhibitors and the formation of a glial scar are two major obstacles to CNS axon regeneration (Figure 1-8) and have been targeted therapeutically (see reviews (Fawcett and Asher 1999; Gurgo *et al.* 2002; Batchelor and Howells 2003; Spencer *et al.* 2003; Profyrus *et al*. 2004)). Myelin-associated inhibitors are localised predominately on the innermost lamella of the myelin sheath (McKerracher and Winton 2002) and are exposed during axonal damage. They are thus the principle obstacles to axonal regeneration in the acute phase of CNS injury. Three such inhibitors have been identified (Figure 1-9); myelin-associated glycoprotein (MAG) (McKerracher *et al.* 1994), oligodendrocyte-myelin glycoprotein (OMgp) (Kottis et al. 2002) and Nogo-A (Prinjha *et al.* 2000), the antigen for IN-1, a monoclonal antibody previously shown to permit some CNS regeneration and functional recovery in rats (Caroni and Schwab 1988; Bregman *et al.* 1995). Myelination is key to limiting plasticity and thus preventing aberrant sprouting within the adult CNS (Schwegler *et al.* 1995). The limited regenerative capacity of the CNS is therefore a necessary consequence of this restricted plasticity. This is supported by the observation that the loss of regenerative capacity in the mammalian CNS is concurrent with myelination (Ghooray and Martin 1993).

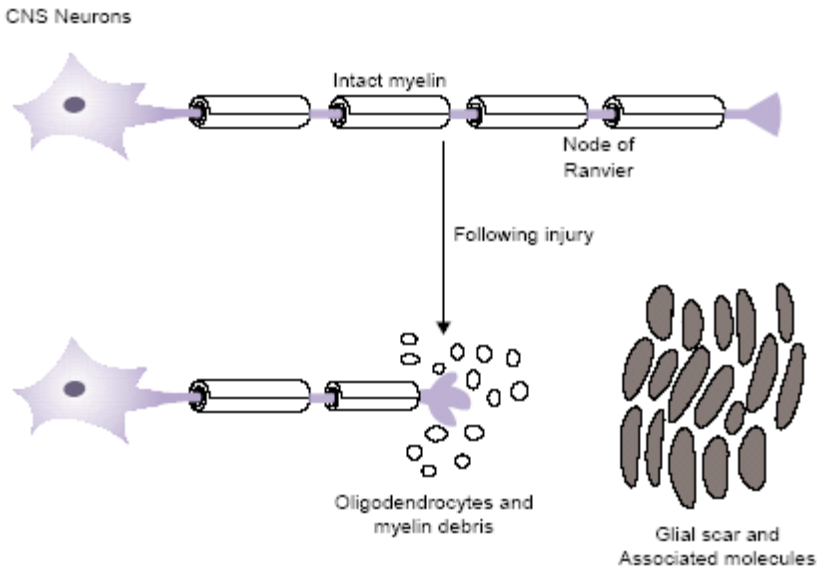

Figure 1-8: Barriers to axonal regeneration- myelin-associated inhibitors of regeneration are exposed on damage to myelin and a glial scar that forms a physical barrier to regeneration is formed. Taken from Spencer *et al.* (2003).

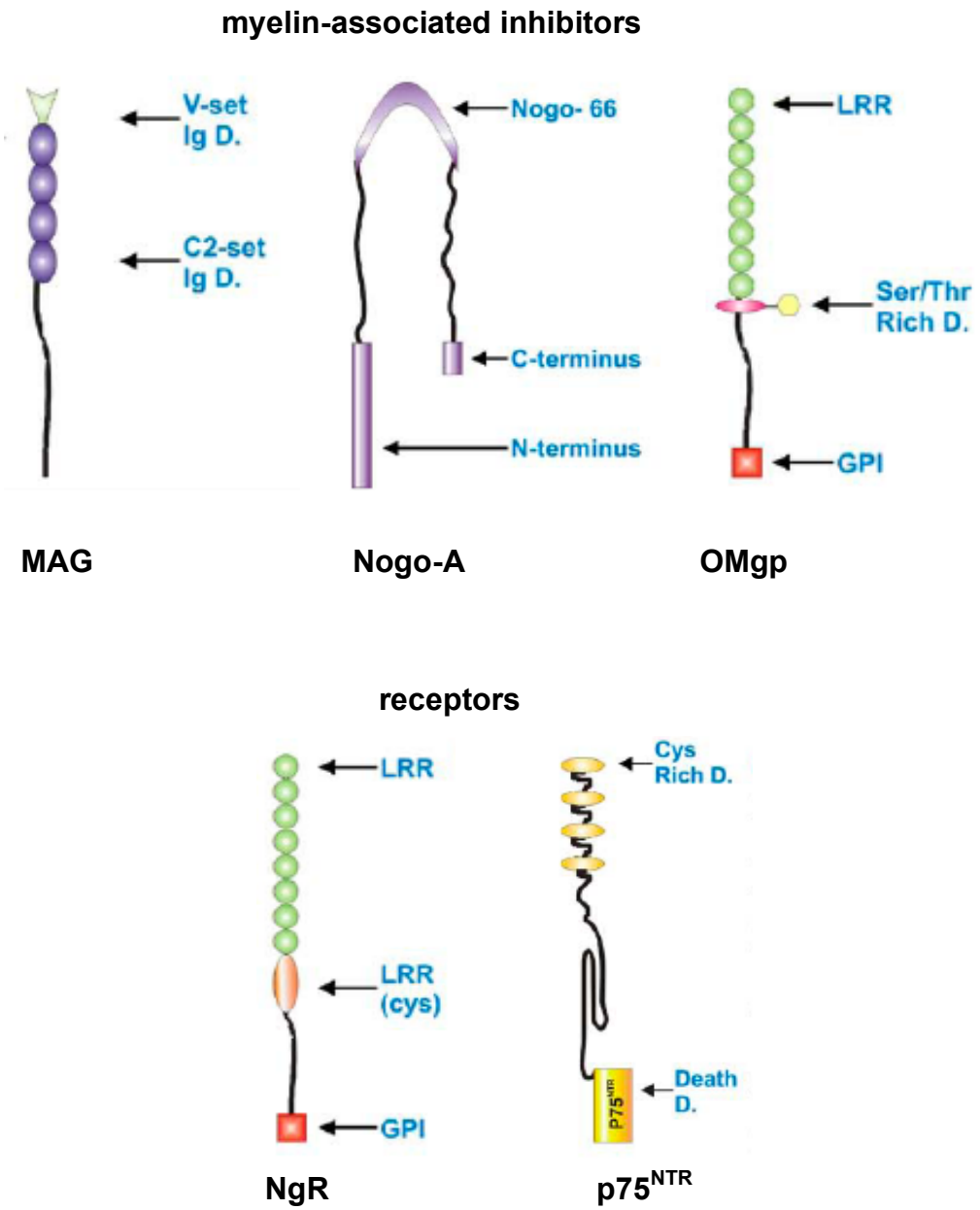

Figure 1-9: Structural features of the myelin associated inhibitors and their receptors. MAG has a large extracellular domain and an intracellular C-terminus**.** Nogo-A has a short extracellular domain (Nogo-66) that can induce growth cone collapse by binding to NgR, its C- and N-terminus domains are internalised. OMgp is a cell adhesion molecule that is linked to the membrane by a GPI-anchor. It has a leucine rich repeat (LRR) domain that binds NgR causing growth cone collapse. $p75^{NTR}$ acts as a co-receptor with the Nogo receptor (NgR) interacting with the C-terminal end of the LRR. Small GTPase adaptor proteins bind the death domain of p75NTR and mediate growth cone collapse via activation of RhoA. (adapted from (Profyrus et al. 2004).

The myelin associated inhibitory molecules are juxtaposed at the myelin-axon interface to the Nogo receptor (NgR), and all three (with exception of the N-terminal region of Nogo-A, the amino-nogo domain, whose receptor is unknown but which appears to function via inhibition of integrin signalling (Hu and Strittmatter 2008), exert their effects via this receptor (Wang *et al.* 2002) (Figure 1-10). NgR, a glycosylphosphatidylinositol (GPI)-linked protein, lacks transmembrane and cytosolic domains and utilises the neurotrophin receptor p75 ($p75^{NTR}$) as a transducing partner (Yamashita *et al.* 2002). Thus, despite distinct structural features, OMgp, the extracellular region of Nogo-A (Nogo-66) and MAG bind the NgR receptor with similar affinities and consequently activate common intracellular signalling pathways. In particular, the Rho signalling pathway has emerged playing a particularly important role in the inhibition of axonal outgrowth by several myelin components.

The Rho family of small GTPases are key regulators of cytoskeletal dynamics and cell motility (Hall 1998). Specific inactivation of RhoA by C3 transferase has been shown to block myelin-induced inhibition of neurite outgrowth and growth cone collapse (Jin and Strittmatter 1997) and to promote axon regeneration *in vivo* (Lehmann *et al.* 1999; Dergham *et al*. 2002). The Rho GTPases cycle between the GTP-bound (active) and guanosine diphosphate (GDP)-bound (inactive) states as regulated by guanine nucleotide exchange factors. Binding of myelin inhibitory factors to the NgR results in activation of Rho GTPases, which ultimately leads to growth cone collapse (Figure 1-10). Elevation of neuronal cAMP levels has been shown to prevent Nogo-A and MAG induced RhoA activation (Bandtlow 2003). Intracellular cAMP levels are raised by a conditioning lesion (see also 1.4.2.1) in the PNS prior to CNS injury (Qiu *et al.* 2002) and such conditioning lesions have been shown to allow regeneration of the axotomised central processes of DRG neurons inside the spinal cord (Neumann and Woolf 1999).

Strategies to encourage CNS regeneration *in vivo* have targeted the myelin-associated inhibitors and their receptors (extrinsic approaches) or their intracellular signalling pathways (intrinsic approaches). As already discussed, the monoclonal antibody IN-1 has been successful in encouraging CNS regeneration by blocking the effects of Nogo-A *in vivo*. Antibodies against the other inhibitory myelin components may therefore be of some therapeutic benefit. However the difficulties in delivery of such antibodies to the CNS has not yet been fully addressed. A vaccine approach whereby the patient's immune system is stimulated to produce antibodies against myelin-associated inhibitors would overcome problems with antibody delivery and has had some degree of success *in vivo* (Huang *et al.* 1999). Antagonistic peptides, such as NEP1-40, that block NgR have also had limited success *in vivo* (GrandPre *et al.* 2002). The identification of the receptor for Amino-Nogo will allow for a more complete blockade of the effects of the myelin-associated inhibitors.

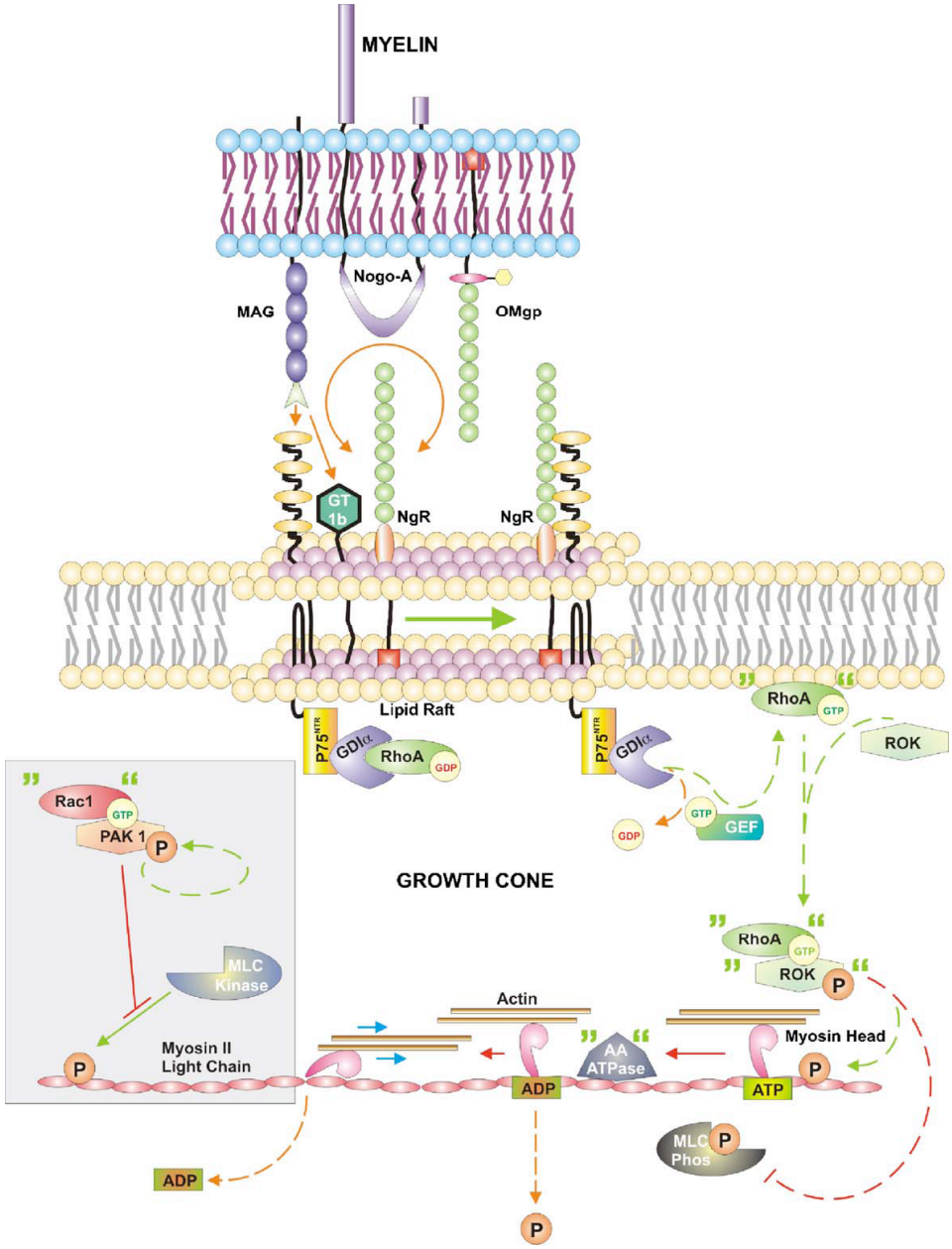

Figure 1-10: Molecular mechanisms of growth cone collapse following myelin-associated inhibitor binding with NgR. Guanine triphosphate exchange factors (GEFs) activate RhoA which then associates with the plasma membrane and binds serine-threonine kinase Rho-kinase (ROK), rendering ROK's kinase active. ROK phosphorylates the regulatory light chain of the major cytoplasmic myosin (myosin II), thus increasing myosin II's activity of actin-activated ATPase. Activation of this ATPase hydrolyses myosin ATP and initiates contraction between myosin within the growth cone and actin filaments of the filopodia. This contraction pulls the actin filaments towards the centre of the growth cone, which culminates in growth cone collapse. Taken from Profyrus *et al.* (2004)

1.4.1.2 Glial scar

The other major barrier to CNS regeneration, the glial scar, is an evolving structure that forms over several days (Buss *et al*. 2004). It is composed of a number of cell types (oligodendrocytes, microglia/macrophages, meningeal cells and oligodendrocyte precursors) but consists mainly of a meshwork of astrocyte processes bound together by tight and gap junctions (Fawcett and Asher 1999). Reactive astrocytes have been shown to be inhibitory to axon growth *in vitro* (Fawcett *et al.* 1989) and this is due to secretion of certain extracellular matrix components of which the chondroitin sulphate proteoglycans (CSPGs) and to a lesser extent, the tenascins, have emerged as being particularly important (Eddleston and Mucke 1993). *In vitro* treatment of reactive astrocytes with Chondroitinase ABC (that removes the chondroitin sulphate GAG chains from CSPG) has been successful in neutralising the inhibitory activity of the CSPGs (Rudge and Silver 1990). Furthermore, recent evidence has suggested that a CSPG (Versican V2) exerts its inhibitory effects on axonal regeneration via the Rho signalling pathway (Sweigreiter *et al.* 2004). There is potential therefore for combined block of inhibitory molecules associated with the scar and those associated with myelin at this common point of signal convergence.

Another approach to overcome the glial scar as a physical barrier to regeneration is the use of cellular substrates to bridge the injury site. Cell grafts of olfactory ensheathing cells (OECs), macrophages, embryonic and bone marrow stem cells and Schwann cells, as well as PNS nerve grafts, have all been investigated. Seemingly one of the most promising of these strategies is the use of OECs, specialised glial cells that guide primary olfactory axons from the neuroepithelium in the nasal cavity to the brain. OECs used in isolation have however had limited success in promoting regeneration across the transplant (Riddell *et al.* 2004; Collazos-Castro *et al.* 2005) although there is electrophysiological evidence that they improve functional recovery after dorsal column transection injury (Toft *et al.* 2007). The potential and limitations for the use of OECs in spinal cord injury have been discussed in a number of recent reviews (Barnett and Riddell 2004; Barnett and Riddell 2007; Radtke *et al.* 2008; Yuan 2008). The limited success of this and other similar strategies again highlights the multifactorial nature of CNS regenerative failure and the need for a multi-faceted approach to promote regeneration *in vivo*.

Neurotrophic factors have also been used in an effort to overcome growth inhibitory effects of molecules associated with the glial scar and myelin (Romero *et al*. 2001; Ramer *at al.* 2002). They include the family of neurotrophins (nerve growth factor (NGF), brain-derived neurotrophic factor (BDNF), neurotrophin-3 (NT-3), NT-4/5 and NT-6), ciliary neurotrophic factor (CNTF) and glial derived neurotrophic factor (GDNF). The neurotrophin family bind specifically to one of three membrane bound *trk* receptor tyrosine kinases and to the p75 neurotrophin receptor (Figure 1-11) and induce axonal extension and dendritic arborisation by acting on cytoskeletal proteins (Chao 2003).

1.4.1.3 Inhibitory molecules in the DREZ

Dorsal root avulsion injury (section 1.3.2) is an intractable injury because sensory fibres are prevented from regenerating across the CNS/PNS interface of the DREZ. Zhang *et al*. (2001) observed that dorsal root axons regenerate as far as the DREZ where they grow no further or turn back towards the ganglion suggesting the presence of repellent molecules in the DREZ. They found two molecules, tenascin-R and chondroitin sulfate proteoglycan 4 (CSPG4 or NG2) to be highly expressed in the DREZ suggesting that these may contribute to the inhibition of regeneration at the DREZ. Ramer *et al*. (2001) have proposed a two-tiered inhibition at the DREZ. The first barrier is astrogliotic and surmountable by treatment with neurotrophins whilst the second barrier is caused by spinal cord degeneration with infiltration of phagocytes and cannot be overcome by neurotrophin treatment. This is supported by another study in which delayed NT-3 treatment was not sufficient to overcome the barrier caused by the protracted myelin clearance in the CNS (McPhail *et al.* 2007). This study suggested facilitation of the elimination of myelin in combination with neurotrophin treatment could constitute an effective therapeutic approach for treatment of dorsal root avulsion and again highlights the multiplicity of the extrinsic barriers to regeneration and the requirement for tailored interventions to overcome them.

1.4.2 Intrinsic determinants of regeneration

Evidence points to there being multiple intrinsic factors involved in the regenerative failure of the CNS. Firstly, attempts to neutralise the inhibitory extrinsic factors within the CNS have not been sufficient to encourage regeneration (Schwab 1993) whilst different types of neuron have been reported to have different responses to injury despite existing in the same environment and hence having exposure to the same extrinsic factors (Dusart *et al.* 2005). Furthermore, intrinsic growth capacity is reduced with age such that embryonic neurons have a greater intrinsic capacity for growth than adult neurons. Finally, it has been demonstrated both *in vivo* (Jacob and McQuarrie 1993; Chong *et al.* 1999; Neumann and Woolf 1999) and *in vitro* (Smith and Skene 1997) that 'conditioning' peripheral nerve lesions increase the ability of the associated primary afferent central processes to regenerate successfully.

1.4.2.1 Clues from conditioning lesions

Injury to peripheral branch neurons elicits a very different cell body response than injury to central branch neurons (Smith and Skene 1997). The expression of regeneration-associated genes (RAGs) such as growth associated proteins (GAP43 and CAP23) and the immediate-early gene c-jun is induced after peripheral nerve injury while their induction is reduced or absent after a central lesion (Chong *et al.* 1994; Broude *et al.* 1997; Andersen and Schreyer 1999) (see also section 1.5.2). The conditioning peripheral nerve lesion acts to encourage central regeneration by priming the cell body with the activation of an intrinsic transcriptional programme within the cell body that marks a switch of function away from synaptic transmission and towards regeneration. In order to

sustain axonal elongation a neuron must synthesize structural components for newly formed processes and activate signal transduction pathways that decode external guidance cues and is associated with dramatic changes in gene expression. The identification of genes associated with the intrinsic regenerative ability of the PNS and the corresponding lack of regeneration in the CNS has thus become the aim of a number of global gene expression studies (section 1.5).

The transcriptional effects of the conditioning lesion are downstream of a primary elevation of intracellular cAMP. cAMP also has a transcription-independent local effect on the growth cone cytoskeleton through type II PKA, which is enriched in filopodia (Han *et al.* 2007). Indeed, intraganglionic injection of cAMP can mimic the effect of a conditioning lesion to increase regeneration of the central branch of lesioned neurons (Neumann *et al.* 2002; Qiu *et al.* 2002). The transcription-dependent effect of cAMP requires activation of the cAMP response element binding protein (CREB) (Gao *et al.* 2004) and leads to the upregulation of, among other genes, arginase I (ArgI), and subsequent increased synthesis of polyamines (Cai *et al.* 2002) (Figure 1-11). It has been shown that increased intracellular cAMP can help axons to overcome the inhibitory molecules associated with myelin and can even convert negative growth cues to positive ones (Song *et al.* 1998; Spencer and Filbin 2004). This demonstrates how the intrinsic state of the neuron can modulate its response to extrinsic factors. CREB may be central to this effect but is however multifunctional and is therefore not an attractive target for therapeutic manipulation. The identification of CREB-regulated transcriptional events could however lead to pharmacological manipulation of the intrinsic regenerative potential of CNS neurons.

The observation that conditioning lesions are less effective in the sensory neurons of LIF null (Cafferty *et al.* 2001) and Il-6 null mice (Cafferty *et al.* 2004) has led to the suggestion that these genes play an important role in the mitigation of the conditioning lesion effect. Both these cytokines signal via the JAK-STAT pathway and activate signal transducer and activator of transcription 3 (STAT3) (Horvath 2004; O'Brien and Nathanson 2007) (Figure 1-11). STAT3 can induce transcription of SPRR1A, a protein known to be involved in growth cone dynamics and that promotes axon outgrowth (Bonilla *et al.* 2002) (see also section 1.5.2.3).

.

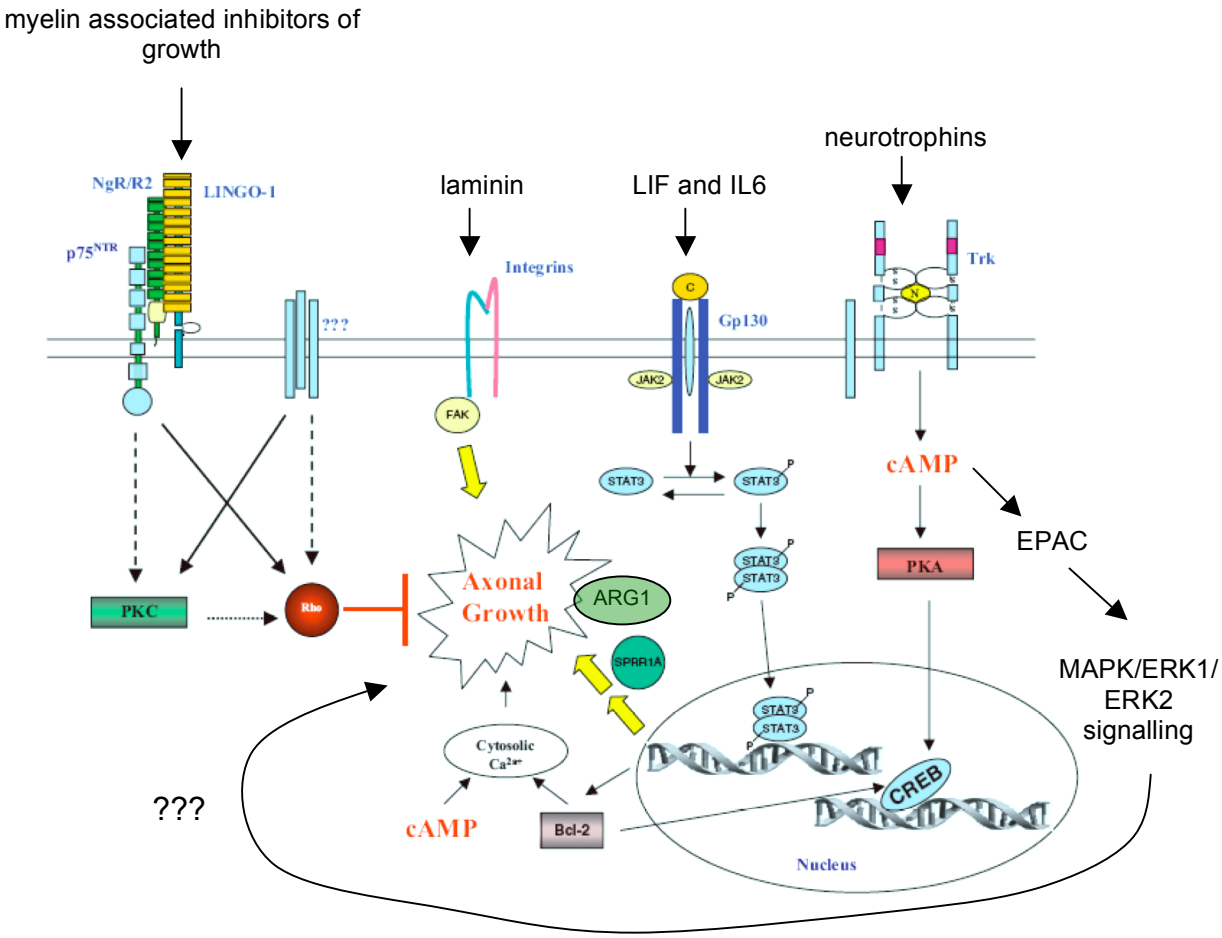

Figure 1-11: Signalling molecules involved in mediating intrinsic regenerative potential. Intrinsic regenerative capacity is conferred by cAMP- CREB and cytokine-STAT3 mediated activation of transcription and production of growth promoting gene products such as ARG1 and SPRR1A which overcome Rho activation by myelin associated inhibitors. The transcription of growth promoting genes can be enhanced by BCL-2 which activates CREB and modulates calcium signalling. Adapted from Teng and Tang (2006)

1.4.2.2 Clues from embryonic neurons

Embryonic CNS neurons have a greater intrinsic capacity for growth than adult CNS neurons and can therefore provide information as to which genes are important in providing a neuron with intrinsic regenerative ability. Loss of regenerative potential is concominant with a dramatic decrease in the expression of Bcl-2 (Chen *et al.* 1997) (Figure 1-11). Furthermore, Bcl-2 overexpression overcomes loss in intrinsic regenerative capacity with development by enhancing Ca^{2+} signalling and activating CREB (Jiao *et al.* 2005). Bcl-2 expression is maintained in the PNS in adulthood further supporting a role for this protooncogene in the regenerative capacity of trhe PNS and the corresponding lack of regeneration in the adult CNS (Merry *et al.* 1994).

Another group of molecules that appear to decline with development are receptors for the adhesive molecules L1/NgCAM, Integrins (Figure 1-11) and cadherins that embryonic neurons use to extend axons in the spinal cord (Blackmore and Letourneau 2006). This raises the possibility that the reduced expression of these receptors contribute to the low-regenerative capacity of adult neurons. Transected peripheral axons undergo adhesive changes and these are essential for their regeneration. Werner *et al*. (2000) demonstrated impaired axonal regeneration in α7 Integrin-deficient mice. α7 Integrin is strongly upregulated in neurons and axons following peripheral but not central nerve injury and has been shown to be involved in the conditioning lesion effect (section 1.4.2.1) by increasing axon responsiveness to laminin (Ekstrom *et al.* 2003). Similarly, L1/NgCAM and its homologue CHL1 are upregulated at 2-5 weeks following sciatic nerve injury while dorsal root transection elicited only transient upregulation of CHL1 and minimal upregulation of L1 (Zhang *et al*. 2000). CHL1 was also strongly upregulated by dorsal root Schwann cells that support regeneration, but not by CNS glia in the DREZ where regeneration is blocked. Taken together, this suggests an important role for adhesion molecules in the creation of an environment that is conducive to axonal regeneration.

That cAMP plays an important role in the intrinsic regenerative potential of neurons is further supported by the fact that there is a decline in developing neuronal cAMP which renders adult mammalian CNS neurons more susceptible to myelin associated inhibitors (Fawcett 1992) (see also section 1.4.1.1). The role of CREB in cAMP signalling has already been discussed (see section 1.4.2.1). More recently cAMP has been shown to enhance neurite outgrowth through activation of Rap guanine nucleotide exchange factor (Epac) which can act independently of PKA through the MAPK/ERK1/ERC2 signalling casade (Bos 2003) (Figure 1-11). Epac is developmentally regulated and can enhance neurite outgrowth and growth cone turning *in vitro* (Murray and Shewan 2008). It is therefore an attractive target to increase intrinsic growth ability by overcoming extrinsic inhibitory molecules.

1.5 Genome-wide approaches to investigating neuronal regeneration

The growth programme initiated by peripheral axotomy provides adult DRG neurons with both intrinsic growth capacity and the ability to overcome a hostile environment. In recent years there has been an explosion of research centred on identifying genes that are key to this regenerative response and the corresponding lack of regeneration in the adult CNS. While some researchers have chosen a focused study of the expression of one particular gene or a small set of genes, the birth of DNA microarray technology (section 1.6.2) has allowed researchers to obtain vast quantities of information from a single experiment and hundreds of genes are now known to be differentially expressed in nerves following various experimental models of PNS (Araki *et al.* 2001; Costigan *et al.* 2002; Schmitt *et al.* 2003) and CNS (Tachibana *et al*. 2002; Di Giovanni *et al.* 2003; Schmitt *et al.* 2003; Aimone *et al.* 2004; Kury *et al*. 2004; Velardo *et al*. 2004) injury. These

studies have examined gene expression changes at the lesion site or in the neuronal cell body itself.

1.5.1 Gene expression changes at the lesion site

1.5.1.1 CNS lesion site studies

The majority of microarray studies that have addressed the mammalian CNS response to injury have examined gene changes at the spinal cord lesion zone (Carmel *et al.* 2001; Song *et al.* 2001; Nesic *et al.* 2002; Tachibana *et al.* 2002; Bareyre and Schwab 2003; Di Giovanni *et al.* 2003; Liu *et al.* 2003; Aimone *et al.* 2004; Resnick *et al.* 2004; Zhang *et al.* 2004; De Biase *et al.* 2005; Di Giovanni *et al.* 2005; Hashimoto *et al.* 2005; Xiao *et al.* 2005; Schmitt *et al.* 2006). These studies, with the exception of a couple, (Resnick *et al.* 2004; Schmitt *et al.* 2006), have concentrated on acute changes occurring within hours to a few days of the injury.

The gene changes observed at the lesion site following a primary injury to the spinal cord are consistent with a number of vascular, metabolic, biochemical and cellular alterations that together form the pathophysiology or secondary injury of SCI. Immediately after injury (within 6 hours), there is downregulation of ion channels (K+, Na+ and Ca2+) and transporters (GABA and glutamate) involved in cell excitability (Carmel *et al.* 2001; Song *et al.* 2001; Tachibana *et al.* 2002; Di Giovanni *et al.* 2003). In addition, there is a strong upregulation of interleukins and other inflammation-related factors (Carmel *et al.* 2001; Di Giovanni *et al.* 2003) reflecting recruitment of peripherally derived immune cells to the lesion zone (Schnell *et al.* 1999; Bethea and Dietrich 2002). At high concentrations pro-inflammatory molecules can lead to the activation of transcription factors that lead to cell death. Indeed, there is a strong induction of transcription factors involved in cell damage and death in the acute stage of SCI (Song *et al.* 2001). (Song *et al.* 2001) also reported an elevation in immediate early gene expression with c-jun showing a particularly dramatic upregulation.

Studies that have examined gene expression changes at 12-72 hours after SCI have shown that many of the changes seen in the acute stage after SCI are sustained or augmented. In addition, there is downregulation of synaptic molecules and cytoskeletal proteins (Carmel *et al.* 2001) reflecting the compromised functional integrity of the spinal cord at this time point and suggesting impaired synaptic function. There is however elevated expression of growth factors such as VGF, BDNF and IGF (Song *et al.* 2001, Carmel *et al.* 2001) suggesting that the spinal cord makes an attempt at regeneration.

Less is known from microarray studies about gene expression in the lesion zone during the chronic phase of SCI. There are however phenomena, such as neuropathic pain, that develop some weeks to months following injury suggesting that biochemical and functional changes are still taking place at this late time point after injury (Hulsebosch *et al.* 2000). In support of this (Resnick

et al. 2004) noted changes occurring at the molecular level at 42 days following SCI in rat. Among these changes was a reduction in myelin-associated glycoprotein (MAG), a change that was not seen during the acute phase of SCI. A more recent study by the same authors suggests that the gene expression in chronic SCI varies between rat stains which show differing potential for functional recovery after SCI (Schmitt *et al.* 2006) providing evidence for a link between intrinsic genetic background and regenerative capacity.

1.5.1.2 PNS lesion site studies

Following peripheral nerve injury changes occur at the lesion site that allow axonal regeneration (Section 1.2.2). An important aspect of this is the proliferation of Schwann cells in the distal nerve segment. In order to identify genes involved in Schwann cell activation (Araki *et al.* 2001) examined gene changes in the distal stumps of sciatic nerve lesioned rats at several time points 3 hours to 56 days post-lesion. They identified four distinct groups of genes that clustered together according to their temporal regulation, each cluster potentially representing a different biological process. One cluster corresponded to early induction of IEGs. Another group of genes that were induced early and peaked around 7 days contained gene associated with macrophage infiltration and proliferation (KI67 and MAC1). A third cluster of genes was induced at around 3 days and peaked 7-14 days post-injury. The cluster contained genes such as GFRα1 which is known to be expressed by Schwann cells during Wallerian degeneration and to be negatively regulated by axon contact (Taniuchi *et al.* 1988) suggesting that regenerating axons contact the distal segment at 7-14 days post injury. The final cluster of genes, containing neurotrophic and growth factors such as BDNF and GDNF, was induced at 7 days post-lesion and peaked at 14 days consistent with phenotypic changes in Schwann cells to promote neurite outgrowth.

(Kubo *et al.* 2002) examined changes in the distal stump 7 days after sciatic injury in mice, a time point at which many genes had been shown to peak (Araki *et al.* 2001). They showed a number of similarities and differences in gene regulation at the PNS lesion zone from that seen in the CNS, the main difference being the absence of the induction of proinflammatory mediators in the PNS lesion zone. This revealed important differences between peripheral and central immune responses after injury that may influence potential to regenerate.

1.5.2 The cell body response to injury

1.5.2.1 How is injury signalled to the cell body?

The cell body of a neuron is often some distance from the site of nerve injury yet the neuron responds to injury to its axon with changes in gene expression. Injury is signalled in three ways (Figure 1-12). Immediately after damage to the axon the first indication of injury is a rapid burst of action potentials called ‘injury discharge’ that propagates to the cell body (Berdan *et al.* 1993)

(Figure 1-12a). From hours to days after injury there are 'positive signals' that are conveyed to the cell body by retrograde transport. These are *de novo* activated proteins emanating from the injury site (Figure 1-12c). In addition to these positive signals, termination of normal trophic support constitutes a 'negative signal' to the cell body (Figure 1-12b) (Ambron and Walters 1996; Perlson *et al.* 2004).

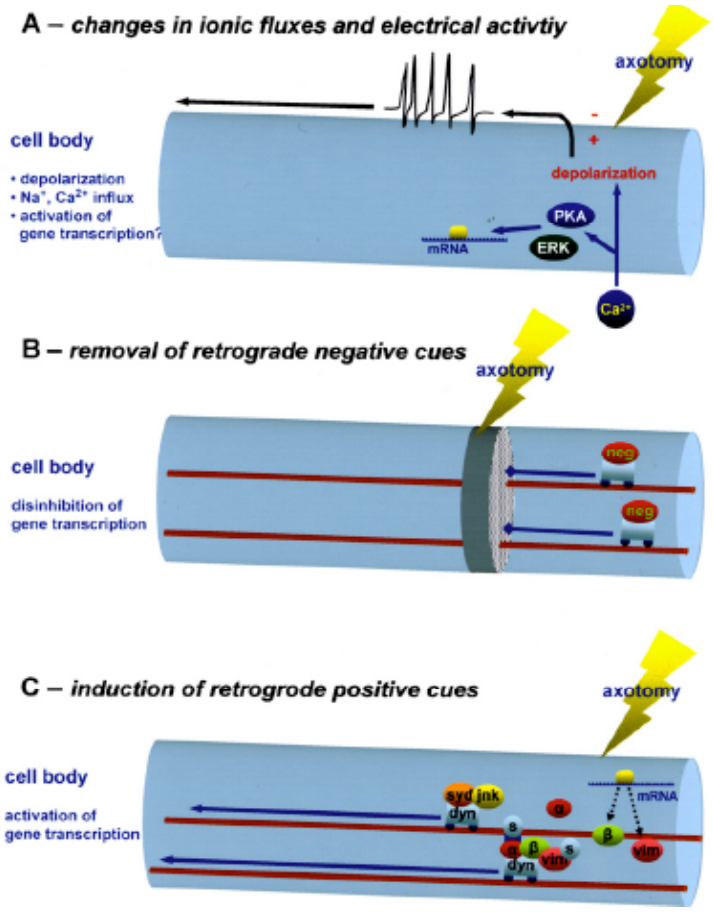

Figure 1-12a-c: Retrograde signalling of axonal injury. Injury is initially signalled by rapid bursts of action potentials. Termination of normal trophic support causes disinhibition of gene transcription whilst locally translated positive cues cause activation of gene transcription. **Taken from Rossi *et al*. (2007).**

1.5.2.2 Studying the cell body response using the dorsal root ganglion neuron

The dorsal root ganglion neuron (DRGN) is a pseudounipolar neuron that has an axon that bifurcates from a cell body contained within the DRG (Figure 1-13). Peripheral branch DRG axons form the peripheral nerves and serve as sensory receptors in various organs while the central branch DRG axons course though the dorsal root and make synaptic connections on neurons, largely within the dorsal horn, and also project rostrocaudally in axon tracts in the dorsal columns. Central axotomy thus deprives the DRG cell of a different set of target-defined interactions than does peripheral axotomy. In addition, while the peripheral branch generally regenerates and

reforms functional connectivity with its innervating organs, the central branch sprouts through the dorsal root but is growth arrested at the CNS-dorsal root junction (dorsal root entry zone (Quaglia *et al.* 2008). If the injury is within the CNS at the level of the dorsal columns, attempts to regenerate are abortive. This presents the opportunity to explore, in the same nerve cell body, gene expression associated with regeneration of the peripheral and central branches and also that associated with blocked or abortive regeneration.

To date, most of the microarray studies examining gene expression changes in the DRG have examined changes associated with sciatic or spinal nerve injury. Only one (Stam *et al.* 2007) has been comparative in nature, comparing gene expression after injury to the dorsal root with that after sciatic nerve crush. To the best of my knowledge, there have been no published microarray studies of gene expression changes in the DRG after spinal cord injury.

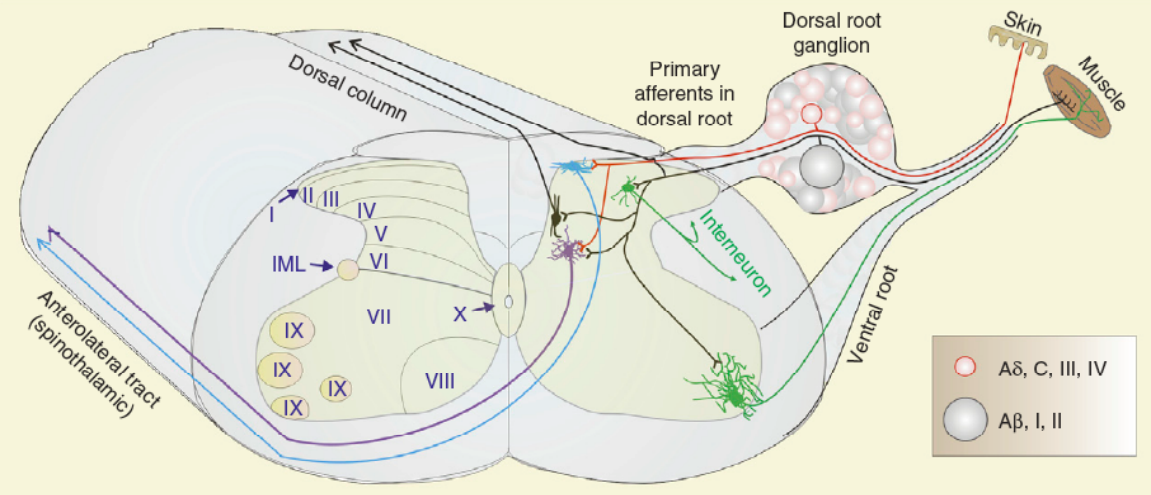

Figure 1-13: Schematic diagram illustrating the primary sensory neurons located within the dorsal root ganglion. Laminae I-VI (marked on the left of the diagram) constitute that dorsal horn and many of the sensory neurons entering from the dorsal root terminate here while others form ascending sensory pathways in the dorsal columns. Taken from Hochman (2007).

1.5.2.3 The neuronal response to sciatic and spinal nerve injury

Much of what we know about the neuronal response to peripheral nerve injury comes from studies that aim to elucidate the molecular mechanisms of neuropathic pain rather than the mechanisms of regeneration *per se*. Studies that have examined gene expression changes in the DRG accompanying neuropathic pain caused by spinal nerve ligation (Wang *et al.* 2002; Valder *et al.* 2003) have found changes in immediate early genes, in ion channels and signalling molecules associated with excitability of neurons and in genes indicative of neuroinflammation.

Costigan *et al*. (2002) used triplicate microarrays to examine changes in gene expression in the L4 and L5 dorsal root ganglion of rats 3 days following sciatic nerve transection by comparing expression levels with non-injured DRGs. The microarray data were validated using northern blots,

quantitative slot blots and *in situ* hybridisation. While only a small number of genes were validated, the authors gave a conservative estimate of 240 regulated genes and functional classification of these genes indicated an up-regulation of genes expressed by immune and inflammatory cells and a down-regulation of those genes involved in neurotransmission. This is consistent with the notion that peripheral nerve injury initiates an inflammatory response in the cells of the DRG, migration of inflammatory cells into the DRG and a phenotypic switch away from neurotransmission.

Bonilla *et al*. (2002) examined global gene expression changes in the DRG 1 week after sciatic nerve transection in the mouse. They found the highest level of upregulation in the muscle stretch sensor protein, small proline-rich repeat protein 1A (SPRR1A) and this was verified by Northern blot. SPRR1A is expressed in sensory and motor fibres and the authors show that it colocalises with F-actin axonal growth cones, consistent with a role in axonal outgrowth by modification of actin dynamics. Indeed, they showed that acute overexpression of SPRR1A can promote axonal outgrowth of adult neurons and can increase axonal outgrowth of embryonic neurons on inhibitory substrates whilst blockade of SPRR1A expression decreases adult outgrowth of adult neurons. This demonstrates the potential for promoting axonal outgrowth through manipulation of proteins that affect F-actin driven growth cone dynamics.

In a more recent study using chips covering a higher proportion of the mouse genome (Tanabe *et al.* 2003) performed a more complete survey of DRG gene expression changes 1 week following sciatic nerve transection in the mouse. They identified a novel regeneration-associated gene, fibroblast growth factor-inducible 14 (FN14) and showed that this induces neurite outgrowth, filopodial and lamellopodial formation and growth cone formation in PC12 cells. Furthermore, they show that FN14 interacts with the Rho family GTPase Rac1. The Rho family of GTPases are known to have a role in modulating F-actin structures (Hall 1998) and hence influence growth cone motility. This suggests that, like SPRR1A, FN14 may act upon F-actin structures in the growth cone to enhance neurite extension. It also demonstrates that there are multiple components active at the level of the growth cone.

A comparison of these three sciatic nerve studies reveals eleven consistently regulated genes; neuropeptides (NPY and GAL), cytoskeletal proteins (GAP43 and SPRR1A), calcium signalling (calcium channel alpha-2-delta subunit), development (SOX11), cell death (GADD45, annexin-1 (ANXA1), HSP27, cytochrome P450 1bl1 (CYP1B1)) and extracellular matrix (MMP9). All these genes may play an important role in the regenerative response of the PNS to injury. The microarray studies thus far have however only covered a small proportion of the mouse or rat genome and as such many putative regeneration associated genes could be still undiscovered.

1.5.2.4 The neuronal response to dorsal root axotomy

Wong and Oblinger (1990) presented the first information regarding changes in mRNA levels in mammalian DRG cells in response to dorsal root axotomy and showed that these cells are capable of mounting a specific molecular response to central axotomy. Their study also documented differences between the response of DRG cells to central and peripheral axotomy with a focus on

the cytoskeletal proteins β-tubulin and neurofilament protein NF-1. Peripheral crush produced a change in NF-1 and β-tubulin expression that was greater in magnitude and of longer duration than central crush. In addition, β-tubulin mRNA levels were down-regulated at 8 weeks following dorsal root crush, by which time the DRG axons had failed to reconnect to their original targets. In contrast, β-tubulin mRNA levels had returned to control levels 8 weeks after sciatic nerve crush following reconnection with appropriate target cells. β-tubulin expression therefore appears to be regulated by signals generated by or at the end of the axon. NF-1 did not show this pattern of regulation, initially decreasing in the large DRG neurons and then increasing to control levels during 4-8 weeks after both CNS and PNS nerve crush. This suggests that the aberrant contact of dorsal root axons on astroglial cells in the DREZ generates sufficient signals to enable NF-1 gene expression but not that of β-tubulin to recover. This study also demonstrated the importance of the interaction between axons and their targets in the regulation of cytoskeletal gene expression.

1.5.2.5 Comparative studies

The first microarray study of the DRG response to more than one injury type was conducted by (Stam *et al.* 2007) who identified transcriptional factors involved in successful regeneration by comparing gene expression changes in the DRG at a number of timepoints 2 hours-14 days after a sciatic nerve or dorsal root crush. They showed that injuries to the peripheral or central branch lead to very different transcriptional responses in the DRG, differences that are evident from as early as 6 hours. At this time point dorsal root fibres will not yet be under inhibitory influence at the DREZ suggesting that the intrinsic differences in the central and peripheral branch response are not purely due to the inhibitory factors at the DREZ that act upon the dorsal root. Furthermore, the authors identify the muscle stretch sensor Ankrd1 as a novel candidate transcriptional regulator of neuroregeneration and show that knock-down of this gene results in decreased adult DRG neuron outgrowth *in vitro.* They hypothesise the involvement of multiple stretch-sensitive proteins in regenerating neurons as other muscle stretch sensor proteins such as SPRR1A (Bonilla *et al.* 2002) have been identified as mediators of axonal outgrowth by past studies.

1.5.2.6 The neuronal response to CNS lesions

As yet, there have been no genome-wide studies of the DRG response to injuries within the spinal cord. There have however been two studies of the neuronal response to a postcomissural fornix (an axon bundle located in the brain with cell bodies in an area called the subiculum) transection in rat. Abankwa *et al*. (2002) examined gene expression changes in the subiculum following a fornix transection at three timepoints corresponding to the degenerative, spontaneous sprouting and abortive phases (1 day, 7 days and 3 weeks, respectively) of the CNS response to injury. They found dramatic differences in the transcriptional programmes that are illicited at the three time points and even found some genes to be antagonistically regulated between the time points corresponding to degeneration and spontaneous outgrowth. Three genes were particularly highly induced during the sprouting phase. One such gene, gastric inhibitory peptide (GIP) is known to enhance intracellular cAMP production (Usdin *et al.* 1993) and may thus stimulate the short regenerative phase of the CNS injury response by cAMP-mediated processes (Section 1.4.2.1).

The other two genes that showed high induction during axon outgrowth but not during the degerative and abortive phases were transcription factors EAR2/NRSF6 and CDP2/Cux. EAR2 belongs to a family of nuclear receptors that are widely expressed during neuronal development (Qiu *et al.* 1994) and members of this family have been shown to induce GAP43 (Neuman *et al.* 1995) and enhance axon outgrowth (Adam *et al.* 2000). CDP2 is thought to be involved in the Notch signalling pathway (de Celis and Bray 1997) working antagonistically on the positive feedback mechanisms that act on Notch. Activation of the Notch pathway results in inhibition of neurite growth (Franklin *et al.* 1999; Sestan *et al.* 1999) and as such CDP2 may act to remove this inhibition, promoting regenerative sprouting.

In their more recent study (Kury *et al.* 2004) compared gene expression in the subiculum 3 weeks after fornix axotomy with gene expression changes in the lesion site to identify gene expression changes associated with axonal regenerative failure. The lesion site showed upregulation of multiple inhibitory factors whilst the subiculum showed upregulation of genes that can be associated with axonal growth or synaptic potential suggesting a residual potential for regeneration that is repressed by inhibitory signals from the lesion zone. Evidence from these studies therefore suggests that the CNS retains some intrinsic ability for regeneration but that regenerative attempts may be thwarted by inhibitory factors originating from the lesion.

1.6 Experimental rationale

Injuries to the spinal cord and dorsal root avulsion injury result in functional deficits because of the limited ability of the CNS to regenerate. We wished to investigate the intrinsic factors that are involved in successful/unsuccessful regeneration and identify putative regeneration-associated genes by performing a genome-wide screen of gene expression in regenerating and non-regenerating conditions using microarrays. Injuries to the sciatic (Carroll *et al*. 1997; Yang *et al.* 2004), facial (Werner *et al*. 2000) and spinal nerves (Gaudet *et al.* 2004) have been utilised as models in order to investigate neuronal regeneration in the PNS while injuries to the dorsal column, dorsal root, inner ear hair cells (Morest and Cotanche 2004) and optic nerves (Werner *et al.* 2000) have been used as models of CNS injury. Our study takes advantage of the unique features of the dorsal root ganglion neuron (section 1.5.2) to compare gene expression in regenerating and non-regenerating conditions.

1.6.1 The injury models used in this study

Sciatic nerve transection (Figure 1-15a) has been commonly used as the peripheral injury in the DRG model as it can be accessed at the mid-thigh level and thus requires a fairly simple surgical procedure (Broude *et al.* 1997; Gallinat *et al.* 1998; Antunes Bras *et al.* 1999; Fan *et al.* 2001; Bloechlinger *et al.* 2004.). The DRG response to this injury is therefore fairly well characterised.

This injury was used as the basis of a pilot microarray experiment to optimise experimental parameters before the larger main microarray experiment in which a spinal nerve injury is used as the PNS injury model (Figure 1-15b). Spinal nerve crush is a more difficult procedure to conduct than sciatic nerve lesion but has the advantage of affecting only the DRG from which it has originated and is more likely to affect all the cells within a given DRG. This contrasts sciatic nerve injury, which does not affect all the neurons in any one DRG. For the CNS injury model, dorsal root injury (where there is regeneration (Figure 1-15c) then blocked regeneration at the dorsal root entry zone (Figure 1-15d) and dorsal column injury (Figure 1-15d) (where regeneration is blocked) was employed. Several comparisons could therefore be made by examination of DRGs from a combination of the two types of CNS lesion, spinal nerve lesion and control animals. The crush lesion was favoured over complete transection in the case of the spinal nerve and dorsal root lesions in order to preserve the basal lamina and stimulate a stronger regenerative response. A transection injury using an optimised wire knife technique that produces a consistent lesion without disruption of the overlying blood vessels was used to produce the dorsal column lesion.

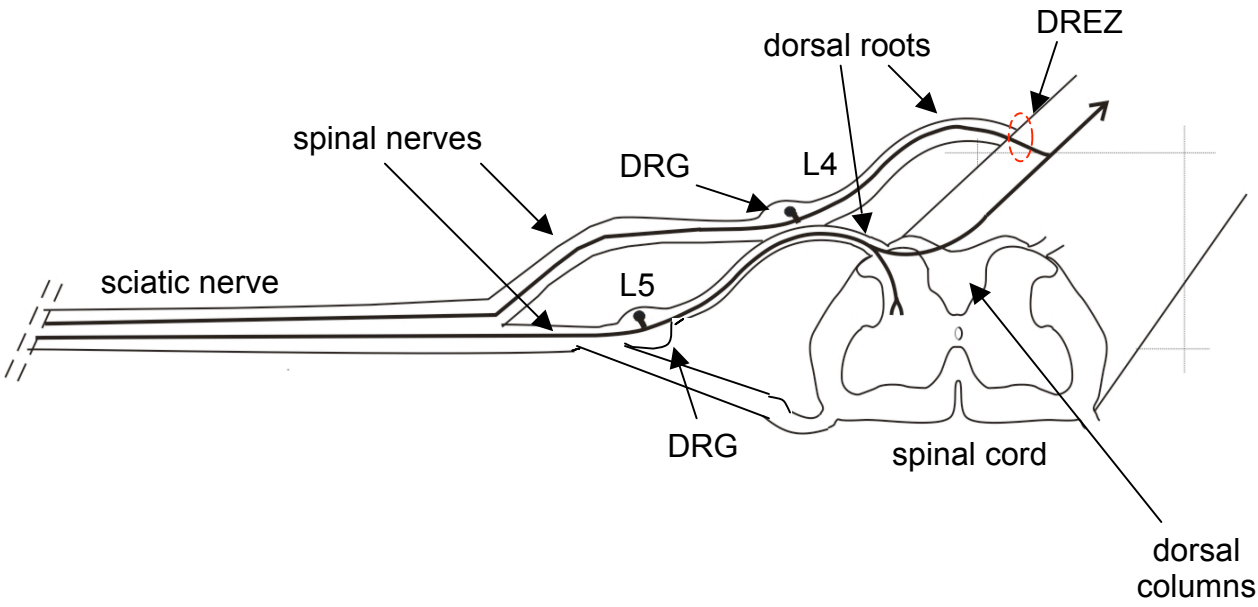

Figure 1-14: Schematic diagram of the spinal cord in cross section with anatomical features relevant to the injury models labelled (not to scale). The parallel dotted lines show the position of cross section for Figure 1-15 b-c.

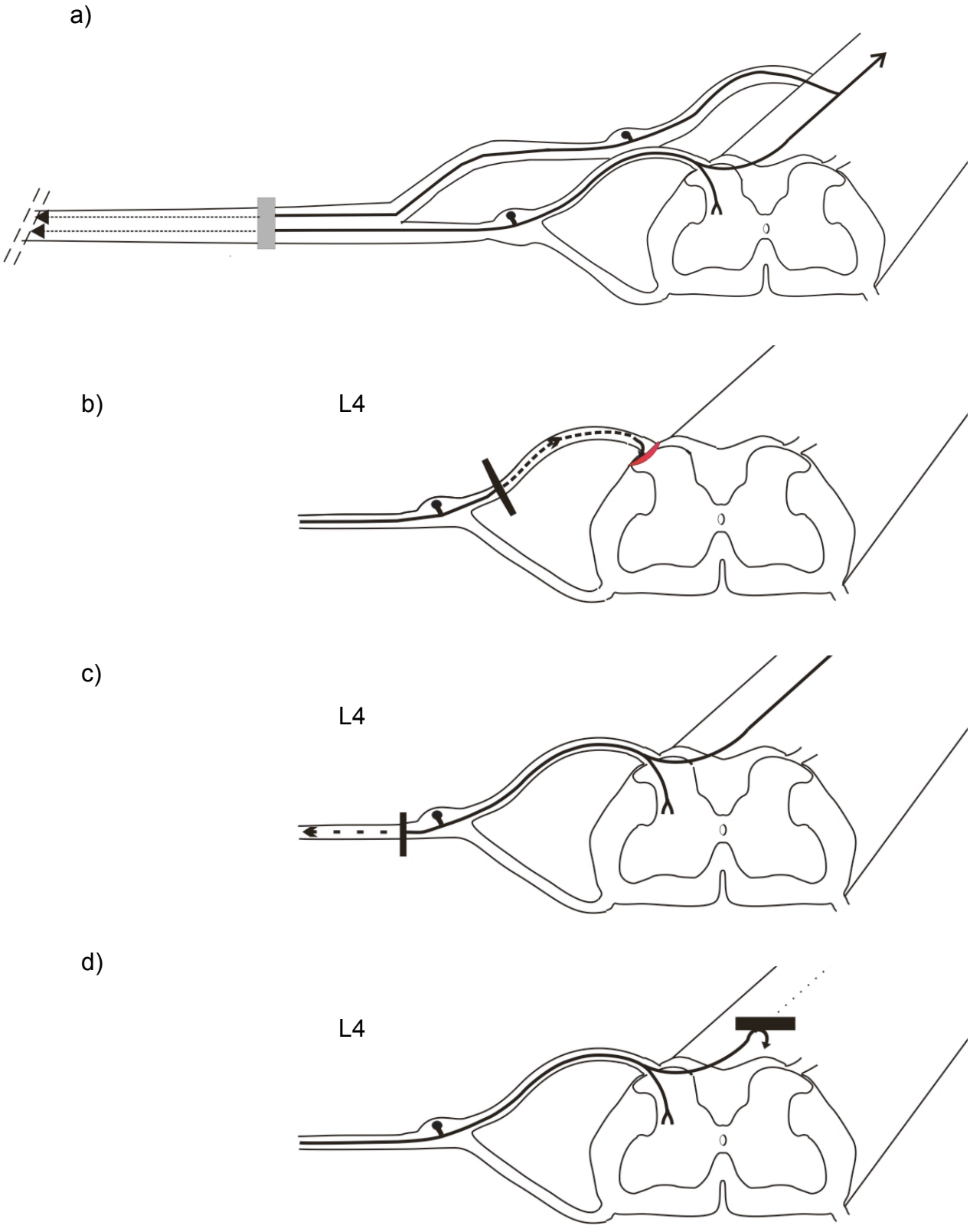

Figure 1-15: Schematic diagram illustrating the position of injury models used in the study. a) sciatic nerve transection (regeneration), b) dorsal root crush (DREZ marked in red) (regeneration until the point of CNS entry at the DREZ where it is blocked), c) spinal nerve crush (regeneration) d) dorsal column transection (abortive regeneration). Dark dotted lines represent axon outgrowth. See **Figure 1-14** for anatomical labelling.

1.6.2 Microarray technology

1.6.2.1 The principle of microarrays

DNA microarray technology, pioneered by Affymetrix Inc. (Santa Clara, CA), and first described in a seminal paper in Science in 1991 (Fodor *et al.* 1991), is a powerful and relatively new molecular genetics technique that allows the expression analysis of a large number of genes simultaneously. DNA microarrays consist of a small membrane or glass slide onto which thousands of DNA probes are attached at high density and at precise and fixed locations. There are three main types of microarray available; filter arrays and spotted glass slides (both of which can be produced in academic facilities to produce custom arrays), and *in situ* synthesised oligonucleotide arrays (produced commercially using photolithographic masks). The choice of microarray will depend on the aims of the experiment in question, budget and available facilities. For example, custom arrays can be less costly and may be favoured in situations where the number of genes of interest has been narrowed. However, although expensive, commercially produced arrays carry many advantages. Commercial arrays are manufactured with built-in process controls at each synthesis step thus ensuring they produce accurate and reproducible results. In addition, most commercially available arrays form part of an integrated system of microarray chips, reagents, scanning instruments and data analysis software. Furthermore, evidence from a number of studies has suggested that the Affymetrix GeneChip, the choice of array for the current project, performs more reliably compared to custom made and other commercially available arrays (Li *et al*. 2002; Park *et al*. 2004).

In sample preparation for microarray experiments, mRNAs from the sample of interest are used as templates to generate fluorescently labelled cDNA. Incubation of the microarray with this fluorescently labelled cDNA causes hybridisation of the cDNA to complementary DNA sequences on the microarray and fluorescence emission at defined regions when excited by a laser scanner. Where the sample yields limiting amounts of RNA, it may be necessary to increase the fluorescence signal by amplification processes, which include the binding of highly branched molecules (dendrimers) carrying fluorescent tags to each hybridised molecule. Alternatively, the sample may be amplified by means of polymerase chain reaction (PCR) or linear amplification (Livesey 2003). It is also generally accepted that the minimum number of replicates per experiment for statistical reliability should be at least three and this is now the usual minimum standard demanded for journal publications (Lee *et al*. 2000) and was the number of replicates used for each of the conditions in this study.

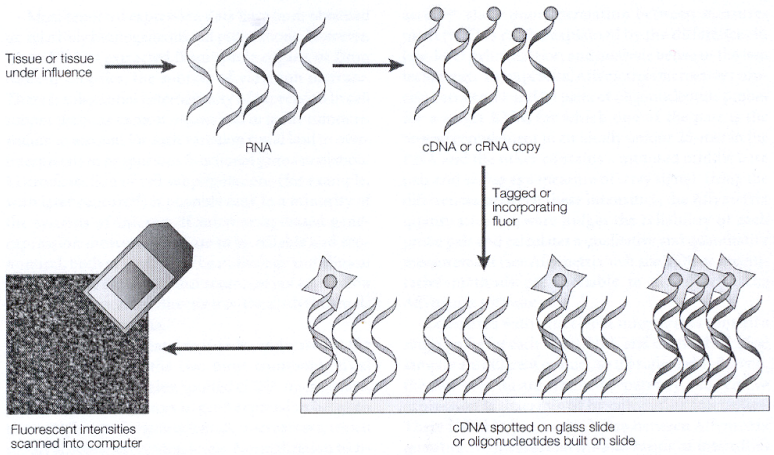

Figure 1-16: Schematic diagram summarising the steps of a microarray experiment.

1.6.2.2 Validation of microarrays

Validation of microarray data is a necessary step in microarray data quality control as array results can be influenced by each step of the complex assay, from array manufacture to sample preparation and analysis (Rajeevan *et al.* 2001; Chuaqui *et al*. 2002). Validation can be achieved via an *in silico* or laboratory-based analysis. The *in silico* method compares microarray results with information from literature or from public and private expression databases. Laboratory-based methods provide an independent means of validating array results and commonly used techniques include: semi-quantitative reverse transcription PCR (RT-PCR), quantitative RT-PCR, northern blot, ribonuclease protection assay and *in situ* hybridisation or immunohistochemistry for tissue microarrays. Real-Time PCR was utilised in the validation step for the current project, being rapid, relatively inexpensive and requiring minimal starting template (Rajeevan *et al*. 2001).

1.7 Conclusions and aims

Axonal injury initiates a transcriptional response within the cells of the DRG leading to a temporally orchestrated gene expression programme. This project aimed to identify putative regeneration associated genes that are expressed at a late timepoint post-injury using more comprehensive microarrays than previously used that cover the majority of the rat genome. Implementation of a combination of injury models allowed for a more thorough investigation of the DRG injury response and allowed us to better evaluate when gene redundancy may account for the differences observed. Indeed, this is the first microarray study that addresses the neuronal response after dorsal column transection injury. It is hoped that the data provided by this study will gain further insight into the signalling processes associated with regeneration, thus allowing potential methods of increasing the intrinsic growth state of injured CNS neurons to be identified.

1.7.1 Chapter summaries

The aims and objectives of the project were:

- To optimise tissue collection and processing protocols for microarray and qRT-PCR by completing and validating a pilot microarray experiment (Chapter 3)

- To determine appropriate time points at which to harvest DRGs after dorsal root and spinal nerve crush (Chapter 4).

- To compare and contrast gene expression changes in regenerating and non-regenerating conditions using various analysis methods (Chapter 5).

    - Do axotomised CNS neurons respond to remote injury by altering their gene expression programmes?
    - Do such genetic programmes include regeneration associated genes, perhaps re-activating developmental processes?
    - What are the intrinsic differences between injured peripheral and central neurons?

- To validate using qRT-PCR a number of genes which demonstrate an interesting pattern of regulation in the microarrays or have been implicated in regeneration previously (Chapter 6).

2 Materials and Methods

2.1 Solutions used for *in vivo* work

4% Paraformaldehyde solution

4% w/v paraformaldehyde in 0.1M phosphate buffer

Mammalian ringer

130 mM NaCl, 4 mM KCl, 1 mM $CaCl_2$, 1 mM $MgSO_4$, 1 mM NaH_2PO_4, 18 mM glucose, 20 mM HEPES-Tris in DEPC-treated water, pH 7.4.

Phosphate buffered saline (PBS)

0.08 % w/v NaCl, 0.002% w/v KCl, 0.0144% w/v Na_2HPO_4, 0.0024% w/v KH_2PO_4 in DEPC-treated water, pH 7.4.

0.1% Toluidine Blue stain

0.1% w/v toluidine blue in DEPC-treated water

2.2 Injury Models

2.2.1 Pre-operative Medication and Anaesthesia

Adult male Sprague Dawley rats (Harlan, Loughborough, UK) were used in all the operations described below. Animals were housed in groups of 2-3 in standard solid bottomed cages with woodchip bedding and had free access to food and water. Anaesthesia was induced with 4% halothane and maintained with 1.5-2.5% (as appropriate) halothane in oxygen delivered via a mask following transfer to the operating table. Depth of anaesthesia was assessed by monitoring pedal withdrawal reflexes. Rectal temperature was monitored and regulated via a homeothermic heating blanket connected to a rectal thermister. Pre-operative medication consisted of antibiotics (Amfipen, 0.3ml 100 mg/ml, Intervet, UK) and analgesics (Vetergesic, 0.05 mg/kg, Alstoe Ltd., UK) administered subcutaneously. The incision area was shaved and swabbed with ethanol. Dr J S Riddell carried out all operations using sterile precautions and in accordance with the UK Animals (Scientific Procedures) Act 1986.

2.2.2 Post-operative care

Animals were monitored visually during recovery on a fleece covered heat mat. Animals were offered chocolate mousse to encourage appetite and administered with a further dose of analgesic

(Vetergesic, 0.05 mg/kg) on the morning following the surgery. Saline (0.2-0.4 ml/0.1 kg) was administered 2-3 times daily for up to 3 days following surgery via the oral or subcutaneous route to compensate for fluid loss during surgery.

2.2.3 Sciatic Nerve Transection

The left sciatic nerve was exposed at mid thigh level and a tight ligature (6/0 silk) was placed around the nerve. The nerve was transected distal to this ligature and a 1 cm length was removed. The wound was sutured in two layers and the rat was allowed to recover. The animal's hind legs were examined daily for signs of autophagia (nibbling of own toes). Animals exhibiting autophagia were euthanased humanely.

2.2.4 Dorsal Root Crush

The lumbar spinal cord was exposed by a hemi laminectomy at the L4 vertebral level. The bone was thinned using a dental drill then removed using bone rongeurs to expose the L4 DRG and proximal roots and the dura was opened. The L4 dorsal root was identified and a loop of 10/0 suture was placed loosely around the root to allow post mortem confirmation of its identity (Figure 2-1 a). The root was then crushed ~5 mm proximally to the DRG with watchmaker's forceps (Figure 2-1 b). The dura was closed with 10/0 suture and the overlying tissues were sutured in layers with 3/0 vicryl.

2.2.5 Spinal Nerve Crush

The lumbar spine was exposed and the lateral processes at the L4 vertebral level were removed using bone ronguers. The L4 spinal nerve was identified and crushed using watchmaker's forceps (~6 mm distal to the DRG) for approximately 20 seconds until translucent. A loose ligature of 6/0 silk was placed around the nerve at the lesion site and the overlying tissues were sutured in layers with 3/0 vicryl.

2.2.6 Lumbar Dorsal Column Transection

The lumbar spinal cord was exposed by laminectomy at the L1/rostral T13 vertebral junction. The T13 vertebra was clamped to immobilise the vertebrae. The dorsal columns were then lesioned at the border between the L3 and L4 spinal segments using a wire knife (David Kopf Instruments, Tujunga, USA). The knife within its cannula was inserted through a small slit made in the dura with a fine hypodermic needle at the dorsal root entrance zone on left side of the cord. The cannula was lowered into the cord to a depth of approximately 950um (Figure 2-2a) and the knife was protruded to form an arc of approximately 1.5 mm inside diameter, encompassing the dorsal columns (Figure 2-2b). A glass rod (1 mm diameter) was then positioned at the surface of the dorsal columns and the wire knife was raised until it pressed firmly against the rod (Figure 2-2c).

The wireknife was then retracted and withdrawn (Figure 2-2d). A 10/0 ligature was stitched into the dura at the lesion site to allow confirmation at post mortem that the lesion was at the L3/L4 border. The tissues were then sutured in layers and the animal was allowed to recover.

2.2.7 Sham operations

In the case of a sham operation, animals underwent all stages of the operation (including, where appropriate, removal of bone, cutting of dura and placement of marking ligature) but did not receive a lesion.

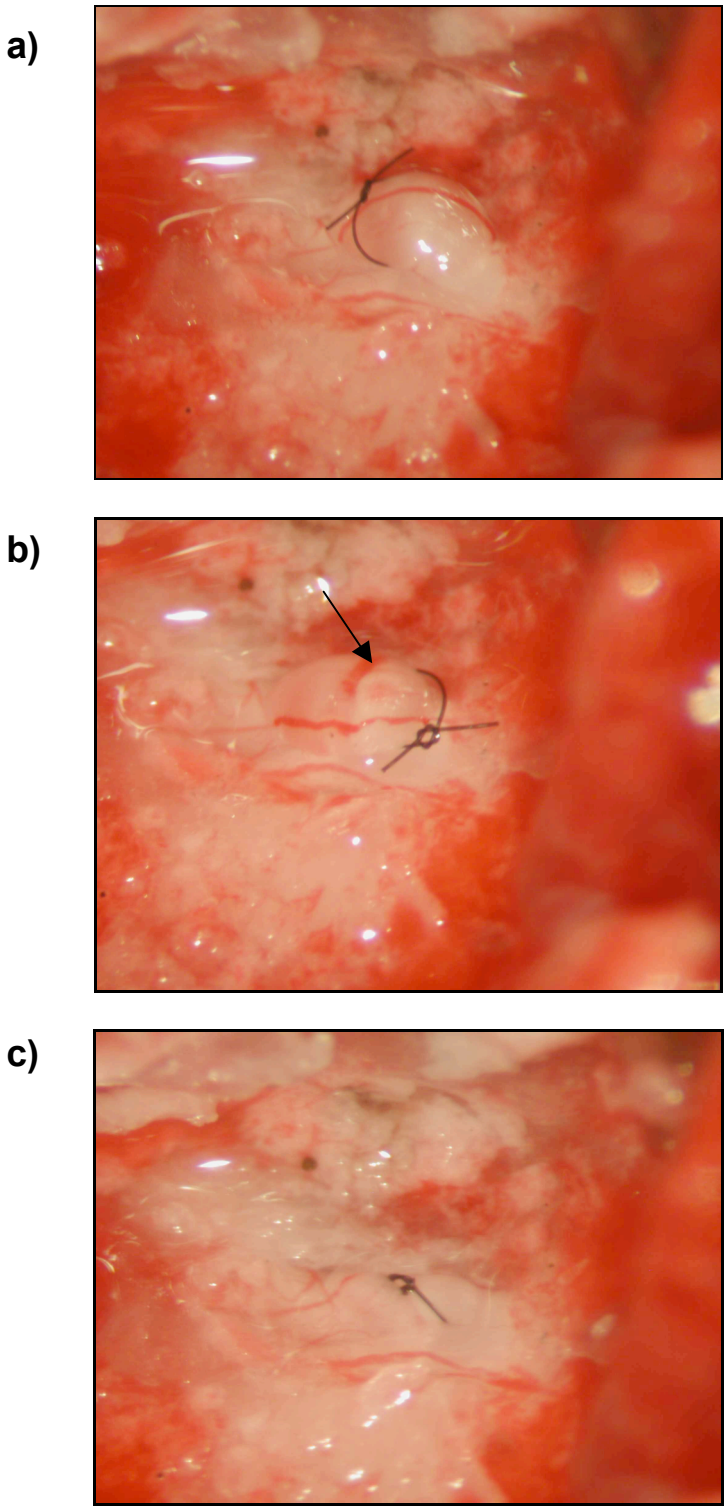

Figure 2-1: Dorsal root crush. a) The L4 dorsal root is exposed and a loose ligature is tied around it. b) The root is crushed using watchmaker's forceps (the crush is marked by an arrow). c) The dura is closed with 10/0 suture.

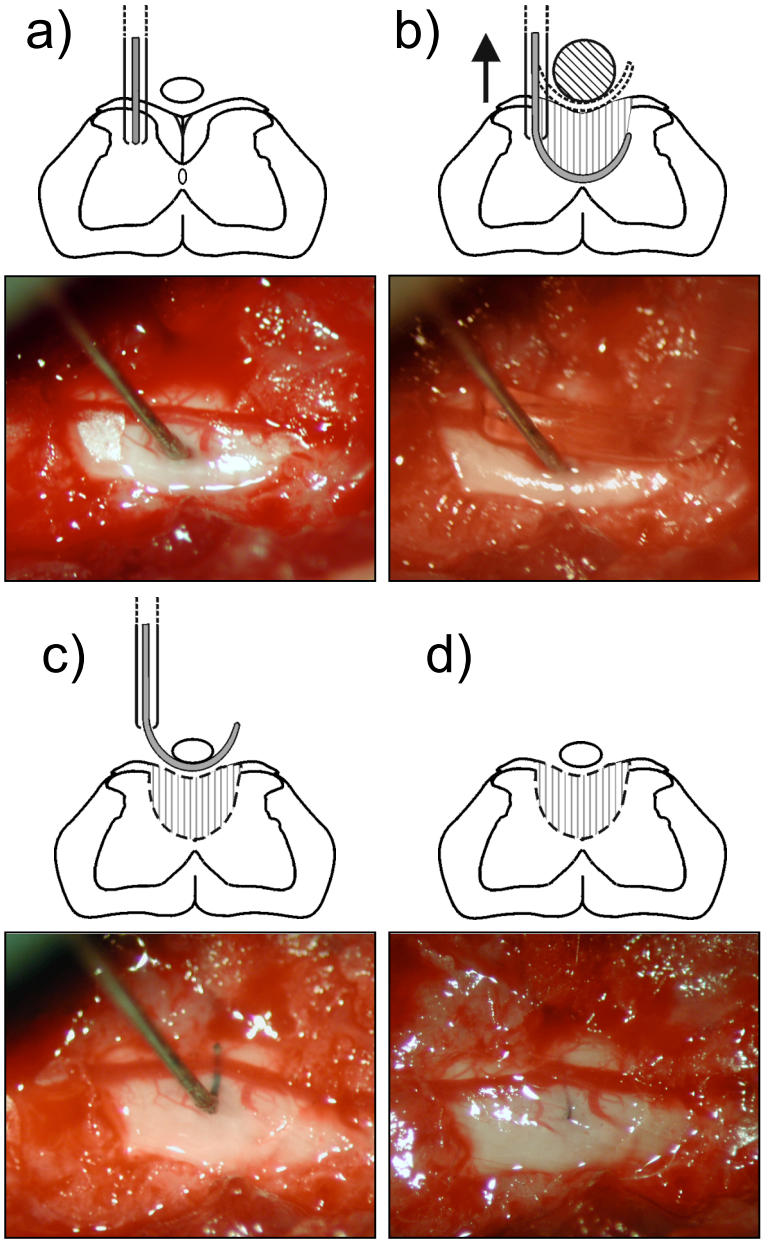

Figure 2-2: Lumbar dorsal column transection. a) A wire knife within a cannula is inserted through a small slit in the dura. b) The wire knife is protracted under the dorsal columns. c) The wire knife is raised, cutting through the dorsal columns, until it is pressed against a glass rod. d) The wire knife is retracted and withdrawn.

2.3 Neuroanatomy

2.3.1 Spinal Nerve Injection of biotin dextran amine (BDA)

The left sciatic nerve was exposed and the tract tracer biotin dextran amine (BDA; 10,000MW, product no. D-1956, Molecular probes) was injected into the nerve in a sterile operation under halothane anaesthesia. A solution of 20% BDA dissolved in 0.1 M phosphate buffer (PB) with 2% (v/v) fast green dye (to detect spillage; R.A Lamb Supplies, UK; product 42053) was injected through a glass pipette with a bevelled tip (internal diameter approximately 45 μm) using a PV30 pneumatic PicoPump (World Precision Instruments). A total of approximately 3-4 μl of BDA was injected over ~4 mins (approx 1 μl/min) using repeated 40 ms pressure pulses. Wounds were closed in layers with 3/0 vicryl and post-operative analgesia administered.

2.3.2 Sciatic Nerve Injection of cholera toxin B (CTB)

The left sciatic nerve was exposed and approximately 3-4 μl 1% CTB (List Biological Laboratories) dissolved in 0.1 M PB with 2% (v/v) fast green was injected into the sciatic nerve as proximally as possible and approximately level with the sural nerve branch using a PV830 pneumatic PicoPump (World Precision Instruments) as in Section 2.3.1. The overlying muscles and skin were sutured in layers with 3/0 vicryl and post-operative analgesia was administered.

2.3.3 Histological processing

Animals were deeply anaesthetised with intraperitoneal sodium pentobarbital (200 mg/ml Euthatal, Vericone Ltd, UK) and perfused through the left ventricle with 50 ml mammalian ringer's solution followed by 500 ml 4% paraformaldehyde in mammalian ringer 0.1M, pH 7.4.

The animal was dissected to expose the lumbar spinal cord, L4 and L5 dorsal roots, ganglia and spinal nerves and sciatic nerves and where appropriate, the position of the lesion was confirmed by virtue of a loose 10/0 ligature placed at the lesion site at the time of surgery. The L4 and L5 ganglia were removed for inspection in the CTB experiment. In addition to the DRGs, the L4 and L5 dorsal roots, L4 spinal nerve, sciatic nerve and L4 and L5 spinal cord segments were removed for the BDA experiment. The tissue was post-fixed overnight with 30% sucrose added to the fixative solution and then transferred to 30% sucrose in phosphate buffered saline (PBS).

Blocks corresponding to the L4 spinal segment were cut into 70 μm transverse sections while the L4 and L5 DRG and 3 mm lengths of dorsal root and spinal/sciatic nerve were cut into 70 μm longitudinal sections on a freezing microtome. Sections were immersed in 50% ethanol for 30 minutes to improve antibody penetration and then incubated in primary antibodies (Table 2-1).

Sections were subsequently incubated for 2-4 hours in secondary antibodies (Table 2-1). All antibodies were diluted in PBS with 0.3% triton X-100 (Sigma) to aid tissue penetration. Sections were mounted on plain slides in Vectashield (Vector Labs, UK) and stored at -20°C.

Table 2-1: Primary and secondary antibodies used in histological processing (Colours indicate colour of fluorescence emitted).

PRIMARY ANTIBODIES	SECONDARY ANTIBODIES
Mouse anti-neurofilament (NF200: 1:1000, clone N52, Sigma)	Donkey anti-mouse IgG conjugated to rhodamine (RRX 1:100, Jackson Immuoresearch Laboratories Inc.)
Rabbit anti-CGRP (calcitonin gene-related peptide)	Donkey anti-rabbit IgG conjugated to cyanine5 (Cy5; 1:100, Jackson Immunoresearch Laboratories Inc.)
Goat anti-CTB	Donkey anti-goat IgG conjugated to FITC (RRX 1:100, Jackson Immunoresearch Laboratories Inc.)
	Streptavidin conjugated to DTAF to detect BDA (1:1000, Jackson Immunoresearch Laboratories Inc.)

2.3.4 Microscopy

Sections were initially examined on a Nikon Eclipse E600 epi-fluorescence microscope through dry (x10 and x20) objectives. Selected sections were serially scanned at 2 μm intervals through dry objectives on a Bio-Rad MRC 1024 confocal microscope equipped with a Krypton-Argon laser (Bio-Rad, Hemel-Hempstead, UK). Projections of confocal image stacks were formed using Confocal Assistant software (Todd Clark Brelje, University of Minnesota).

2.4 Removal of DRGs for Microarray

Animals were deeply anaesthetised with intraperitoneal sodium pentobarbital (200 mg/ml Euthatal, Vericone Ltd, UK) and perfused through the left ventricle for 30 seconds with freshly prepared, ice-cold mammalian ringer's solution (this flushes out the blood which can hinder dissection and which is a potential source of tissue contamination) and rapidly dissected to expose the lumbar spinal cord, dorsal roots and DRGs. Where appropriate, the location of the lesion was confirmed by visual inspection, under a dissecting microscope, of the position of a loose ligature placed at the lesion site at the time of surgery. DRGs were freed carefully from surrounding tissues, and removed into ice-cold saline with their corresponding roots and spinal nerve (Figure 2-3). DRGs were trimmed to remove roots, spinal nerve and any excess tissue surrounding the DRG, transferred individually into screwcap tubes and flash frozen in liquid nitrogen. The removal of the L4 and L5 DRGs from both sides of one animal took typically, under 15 minutes.

a)

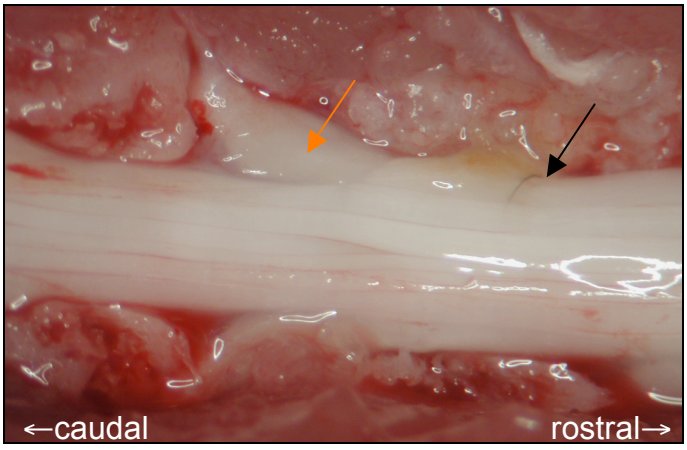

b)

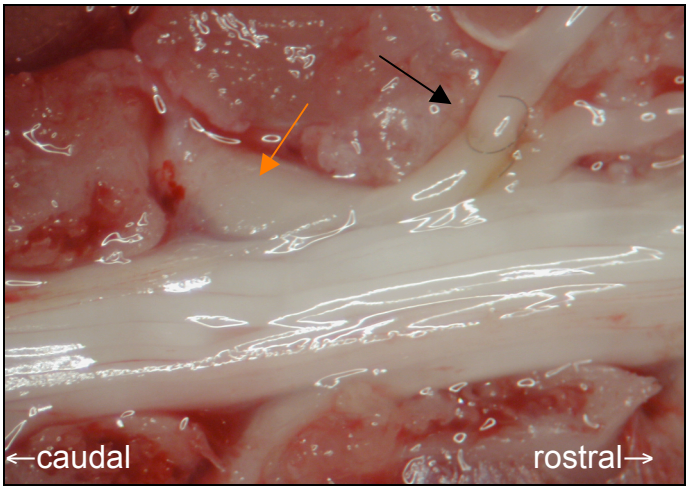

c)

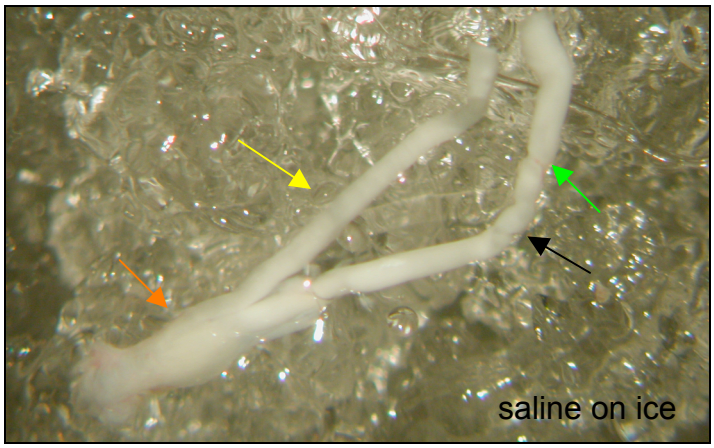

Figure 2-3: Removal of DRG for microarray. In this case, from a dorsal root lesioned animal. a) L4 DRG (orange arrows) and intact ventral root. The position of the crush is marked by a loose ligature (black arrows). b) The L4 dorsal root is cut before the DRG is freed carefully from the surrounding tissue. c) The L4 DRG, dorsal and ventral roots (green and yellow arrows, respectively) are removed to ice cold saline for trimming before being flash frozen in liquid nitrogen.

2.5 Human patient material

DRGs from three patients who had suffered a dorsal root avulsion injury were removed by Mr Timothy Hems during brachial plexus surgery. DRGs were subject to histopathological examination in order to confirm the identity and extent of damage and remaining tissue was frozen in liquid nitrogen. Samples were stored at -80°C in the Department of Neuropathology at the Southern General Hospital, Glasgow before transfer in liquid nitrogen and storage at -80°C in our lab until use.

2.6 Electrophysiology

2.6.1 Surgical Preparation

Male Sprague Dawley rats that had previously undergone a left L4 spinal nerve crush (5-8 mm distal to DRG) were anaesthetised in halothane gas and maintained with sodium pentobarbitone (10mg/kg i.v), given as required. The trachea, left jugular vein and left carotid artery were cannulated to enable artificial respiration, the administration of drugs and solutions, and the recording of systemic blood pressure, respectively. Body temperature was maintained at 38ºC by an electric heating mat with feedback control from a rectal probe thermistor. Mean blood pressure was always greater that 80 mm Hg and pCO2 was maintained within 4-4.5%.

The left sciatic nerve was exposed as far proximally (40mm from crush) and distally (66 mm from crush) as possible and freed from surrounding connective tissue along its length. A laminectomy (L3-L5 segments) was performed to expose the spinal cord and the cauda equina at the level of the L4 and L5 dorsal root ganglia. Once preparative surgery was complete, the rat was administered the neuromuscular blocker Pancuronium (Faulding Pharmaceuticals PLC, Warwickshire, U.K.; 0.1mg i.v at 40 minute intervals) to prevent movement artefacts and was artificially ventilated. The depth of anaesthesia was then monitored and maintained such that no precipitate changes in blood pressure were observed on the application of a noxious stimulus. The animal was transferred to a rigid spinal frame and supported by clamping the L2 and L6 vertebrae. The exposed tissues were bathed in paraffin oil to prevent short- circuiting of the electrodes and drying out of tissues. Surgical preparation and positioning of electrodes was performed by Dr Dugald Scott.

2.6.2 Orthodromic Mapping

The sciatic nerve was placed on cathodes placed proximally and stimulated supramaximally (1mA-10mA) at 2 mm intervals down its exposed length (24-62 mm from crush- see table) and monopolar recordings were made from the L4 and L5 dorsal roots using a silver wire electrode. Loose ligatures were placed at the recording sites on the L4 and L5 dorsal roots and at the most

distal point at which a response could still be detected upon stimulation. Recordings were amplified and filtered and displayed on an oscilloscope during the experiment. Between 10 and 20 responses to each stimulus were recorded and averaged with use of CED 1401+ interface and Signal software (Cambridge Electronic Design, Cambridge, UK). The amplitudes and latencies of the CAPs recorded at each location were measured off-line using Signal software (Figure 2-4). Following the experiment the animal was overdosed with anaesthetic and perfused transcardially with 3% PFA. The L4 and L5 dorsal roots, DRGs and sciatic nerve were removed carefully and the distance between the crush site and the stimulation sites was noted to allow calculation of conduction velocities (CV) using Equation 1.

Equation 1: Calculation of conduction velocity.

$$CV = \text{distance} \div \text{latency}$$

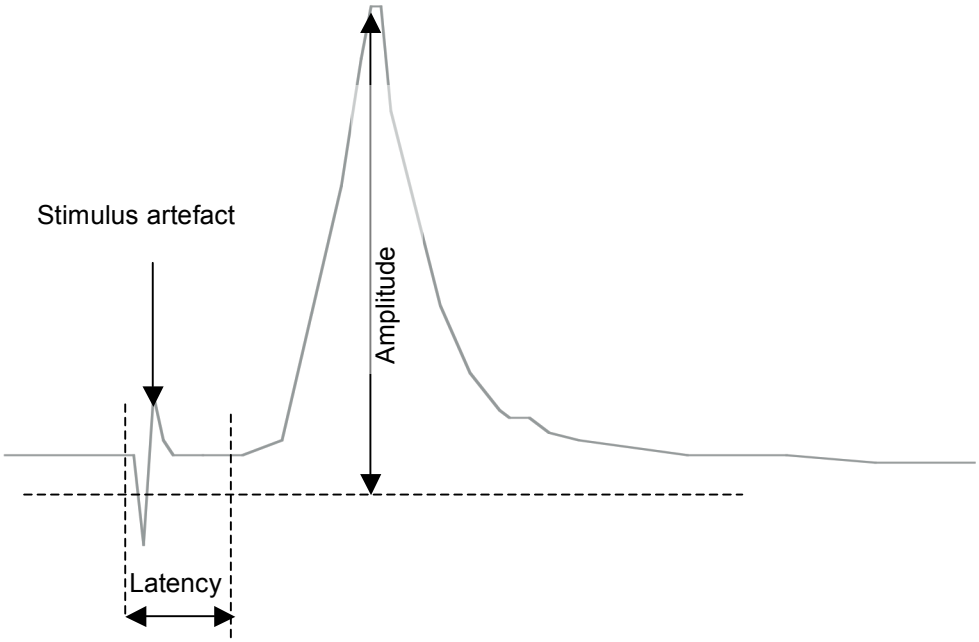

Figure 2-4: Schematic diagram of a CAP illustrating the points from which the latency and amplitude parameters are measured in Signal.

2.7 Materials and general molecular methods

2.7.1 Solutions

2% agarose gel: 2% agarose (w/v) in 1XTBE

0.1% Diethyl pyrocarbonate (DEPC) (v/v) in dH_2O, mixed thoroughly, left overnight at room temperature and autoclaved.

70% ethanol: 70% absolute ethanol (v/v) in dH_2O

Ethidium bromide: Stock solution (10 mg/ml in H_2O). Working solution (200 ng/ml).

1XTAE: 0.04 M Tris base, 0.04 M acetic acid, 0.001 M EDTA, pH 8.0.

1XTBE: 0.09 M Tris base, 0.09 M boric acid, 0.001 M EDTA, pH 8.0.

2.8 RNA analysis

2.8.1 Precautions for RNA handling

All RNA handling was carried out in a laboratory dedicated to RNA work and using a dedicated set of pipettes. Care was taken to minimise RNase and DNase contamination by use of DEPC treated and autoclaved plastics and DNAse/RNAse free pipette tips (Greiner Bio-one). Total RNA samples were stored at -80°C and freeze/thawing was minimised to avoid RNA degradation.

2.8.2 Disruption and homogenisation of rat DRG

Frozen tissue was weighed (DRGs weighed 9-14 mg) and transferred to a volume (350 or 600 ul) of either Trizol (Invitrogen) or buffer RLT (Qiagen) in bead filled tubes (Lysing matrix D,) and simultaneously disrupted and homogenised in a Ribolyser™ cell disrupter (Hybaid) (3x 20s runs, 6000g). Homogenates were frozen on dry ice and stored at -70°C until use.

2.8.3 Disruption and homogenisation of fibrous tissues

Fibrous tissues (20-30 mg) such as skeletal muscle and heart were homogenised as in section 2.8.2 then transferred to an eppendorf and incubated with 10 μl proteinase K (Qiagen) for 10 mins at 56°C. The homogenates were then centrifuged at 10000g for 3 mins to pellet cellular debris and the supernatant was removed and stored at -70°C until use.

2.8.4 Isolation of total RNA

2.8.4.1 Tissue homogenised in Trizol

Following thawing at room temperature, 200 μl chloroform was added to each of the Trizol homogenates which were then shaken vigorously and incubated at room temperature for 10 mins. Following incubation on ice for 2 mins and centrifugation (10,000 g) for 15 mins, the aqueous layer was removed to a fresh eppendorf. Another 400 μl chloroform was added to the aqueous layer and the incubation and centrifugation steps were repeated. The aqueous layer was again removed to a fresh eppendorf and RNA isolation proceeded according to manufacturer's guidelines for isolation of total RNA from animal tissue using the RNeasy mini kit (Qiagen). RNA was eluted in a volume of 20-50 μl.

2.8.4.2 Tissue homogenised in buffer RLT

Homogenates were thawed at room temperature and RNA was isolated using the RNeasy micro kit (Qiagen) according to the manufacturer's protocol for isolation of total RNA from animal tissue. The optional on-column DNase digestion was used. RNA was eluted in a volume of 14 μl.

2.8.5 Laser capture microdissection (LCM)

2.8.5.1 Poly-L-lysine coating of sides

Plain glass slides were dipped in Poly-L-lysine solution (Sigma) freshly diluted 1:10 in DEPC H_2O and processed according to manufacturer's guidelines.

2.8.5.2 Preparation of fresh-frozen sections

DRGs were removed from storage at -70°C and allowed to equilibrate in a cryostat at -20°C for 10-15 mins prior to mounting. The DRG was mounted on a chuck with Cryomatrix (Shandon). 10 μm serial longitudinal sections were cut with a cryostat and thaw mounted onto uncoated or poly-L-

lysine (Sigma) coated glass slides (Section 2.8.5.1). The sections were allowed to dry and then stored at -70°C.

2.8.5.3 Toluidine blue staining of frozen sections

Slides of serial DRG sections were transferred directly from -70°C storage to ice cold acetone for 3 minutes. 1% Toluidine blue stain was dropped onto slides and sections were left to stain for 3 minutes. Slides then underwent 2x 30 s washes in DEPC treated water before dehydration in a series of ethanol rinses of 30 s each (70%, 95% then 100%) and finally a 2 min xylene rinse. Slides were then air dried and placed in a slide box with silica gel desiccant for use in LCM within 1 hour.

2.8.5.4 Capture of cells

Cells were laser dissected from DRG using the Pix-Cell II LCM (Arcturis) and collected on HS CapSure caps. Capture was performed using a laser power of 70-100 mW, a spot size of 10 μm and a duration of 750 ms. Sensory cells were identified based on morphology (large, light staining) and ~2000 were captured onto each cap. RNA was prepared using the Qiagen RNeasy micro kit according to the manufacturer's protocol.

2.8.6 Assessment of RNA quality using the Bioanalyzer

Quality of total RNA for microarray analysis was assessed using the Agilent 2100 Bioanalyzer (Agilent Technologies). 1μl total RNA was used to generate an electropherogram (Figure 2-5) that allowed an estimate of RNA concentration and ribosomal ratio to be obtained. High quality RNA showed the following features on a electropherogram:

- clear 18S and 28S rRNA peaks
- A low small RNAs (5S, transfer RNA and miRNA) presence relative to the rRNA peaks
- A flat base line in the fast-migrating region
- A flat inter-rRNA peak regions
- A return to the baseline after the ribosomal RNA peaks

In addition to visual inspection of the electropherogram, integrated software generated an RNA integrity number (RIN) by analysis of the entire electrophoretic trace. This number provides a *de facto* standard for RNA integrity with an RIN >7 indicating a sample of sufficient quality for microarray. All our RNA samples from whole, buffer RLT homogenised DRG fulfilled this minimum RIN criterion.

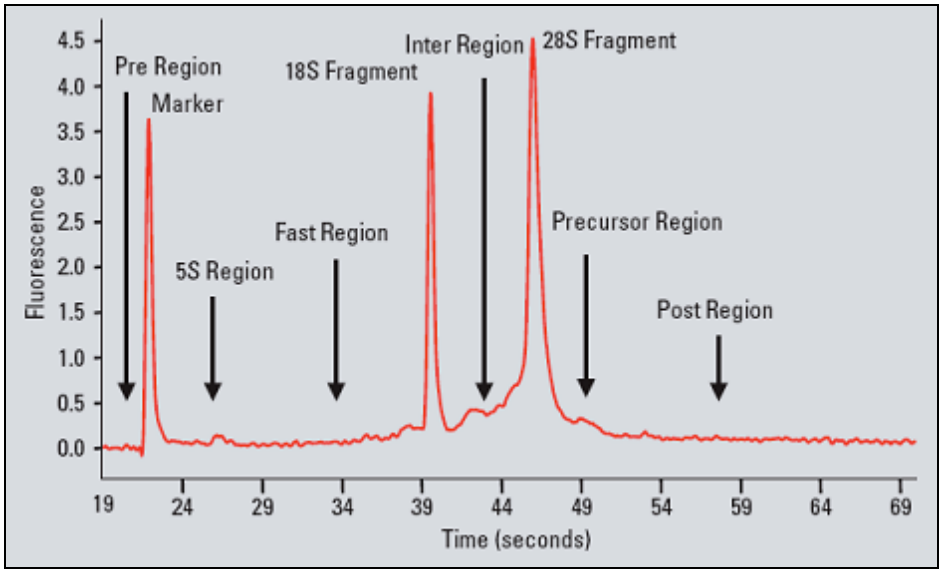

Figure 2-5: Features of a total RNA bioanalyzer electropherogram.

2.8.7 Assessment of RNA quality and quantity using the Nanodrop

Total RNA was quantified by an ND-1000 Spectrophotometer (ND-1000 spectrophotometer; Nanodrop Technologies, Wilmington, DE) using the nucleic acid function which uses the absorbance at 260 nm to calculate concentration using Beer's law. The ratio of absorbance at 260 nm and 280 nm was used to assess purity of the RNA with a ratio of ~2 indicating sample purity. The 260/280 ratios for RNA samples were all in the acceptable range of 1.8-2.1.

2.8.8 Assessment of RNA quality using gel electrophoresis

When yields of RNA were adequate, gel electrophoresis was used to assess RNA quality. 1 μg total RNA and 1Kb+ ladder was loaded onto a 1 % (w/v) TAE agarose gel with ethidium bromide to a final concentration of 0.25 μM. Gels were electrophoresed for 20-30 minutes in Sub Cell-GT electrophoresis tanks (Biorad) at 40-120 volts at room temperature using power packs (PowerPAC-300, Biorad). Agarose gels were visualised under UV light (260 nm) using the UVP Dual Density transilluminator and photographed with the UVP ImageStore 7500 system.

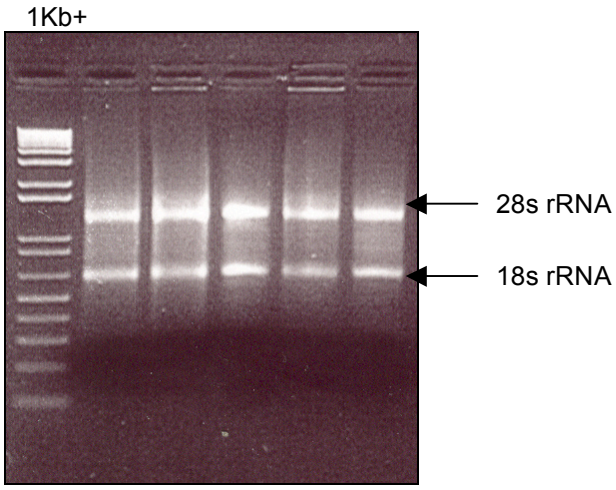

Figure 2-6: Example of an RNA gel with total RNA extracted from different tissues. 1 μg total RNA was loaded in each well.

2.8.9 Complementary DNA (cDNA) synthesis

2.8.9.1 Random Prime method

500 ng-1 μg total RNA was treated with DNase I (Invitrogen) according to the manufacturer's instructions before being reverse transcribed by Superscript® II (Invitrogen) in a total volume of 20 μl according to the manufacturer's recommendations.

2.8.9.2 Quantitect reverse transcription kit

500 ng total RNA was used in cDNA synthesis according to the manufacturer's instructions (Qiagen). This method incorporates an initial DNase digestion step to eliminate contaminating gDNA.

2.8.9.3 Reverse transcriptase negative (RT-) controls

Where RT- controls were included, total RNA was subject to conditions as described in section 2.8.9.1 or section 2.8.9.2 above but RT was substituted with an equivalent volume of RNase- free H_2O.

2.8.9.4 cDNA storage

cDNA samples were diluted 1 in 20 and stored at –80°C. The cDNA was stored in 12 ul aliquots (sufficient for triplicate reactions) to minimise freeze-thaw degradation.

2.8.10 Reverse transcriptase polymerase chain reaction (RT-PCR)

2.8.10.1 Primer design

Primers for standard RT-PCR were designed using the Primer3 website (http://fokker.wi.mit.edu/primer3/input.htm). Default parameters were used for primer picking except for the T_M parameters which were set to as follows: minimum 50°C, maximum 66°C, optimum 55°C and a maximum of 1°C difference between primers. Primer sequences were subject to a BLAST against the nr database. Primers with significant similarities to regions other than the target sequence and in close proximity to one another were re-designed to reduce the possibility of non-specific amplification. Primers were purchased from Sigma-Genosys.

Table 2-2: Primers used in RT-PCR

GENE	EXONS	FORWARD PRIMER SEQUENCE (5' TO 3')	REVERSE PRIMER SEQUENCE (5' TO 3')	PRODUCT SIZE (BP)	T_A (°C)
MX2	3/4	GAGAGGAGTGGAAAGGCAAAGT	GGTCAATCAGAGTCAGGTCTGG	171	66
ECEL1	1/2	GACATGCGTGAGATCGAGAGG	TTCTCTCTGGCAGGGTGAGC	253	61
TGM1	7/8	GCAGAGTTGAAGTTGGTGACAG	TACCTACGCACCGGCTATTC	119	58
NPTX1	4/5	CAAGCTGCCCTTTGTAATCAAC	GGTCCCAGATGTTGAAATGG	250	65
SEMA6A	12/13	GGCCATATGAGAATCACACT	GGCACCTTTATCACACAAGT	244	58

2.8.10.2 Reagents and cycling conditions

PCR optimisations were performed in a Biometra Tgradient machine. Standard PCRs were carried out on a GeneAmp PCR system 9700 (Applied Biosystems).

PCR was carried out in thin-walled 0.2 ml PCR tubes (ABgene) in a volume of 10 μl using 1xThermo-Start PCR master Mix (ABgene) with 1 μM of each primer. For reverse transcriptase PCR (RT-PCR) cDNA was synthesised as in section 2.8.9.1 and 1 μl was added to each reaction. The thermal cycling conditions were; 95°C for 15 minutes, (95°C for 30 seconds, T_A°C for 30 seconds, 72°C for 30 seconds) x 30 cycles, 72°C for 10 mins and 4°C hold.

2.8.10.3 Gel electrophoresis

qRT-PCR products were resolved with a 1Kb+ ladder on 2% (W/V) TBE agarose gels (section 2.7.1) with ethidium bromide to a final concentration of 0.25 μM. Gels were electrophoresed and visualised as in section 2.8.8.

2.9 Microarray experiment

2.9.1 Design

2.9.1.1 Pilot experiment

The pilot experiment consisted of a well-studied injury model (sciatic nerve transection), naïve and sham control. The design of the experiment is described in chapter 3.

2.9.1.2 Main Experiment

The microarray consisted of four experimental conditions (spinal nerve crush, 2 and 6 week dorsal root crush and dorsal column transection) and a naïve control. The design if the experiment is described in chapter 5. Equal masses of total RNA from the L4 DRGs of three animals was pooled and used to generate biotin labelled cDNAs for each of 15 chips (3 chips/condition).

2.9.2 Hybridisation

Total RNA of RIN of >7 was prepared according to the Affymetrix standard (pilot experiment) or Affymetrix small sample protocol (main experiment) and hybridised to Affymetrix 230_A chips (pilot experiment) or Affymetrix 230 2.0 rat arrays (main experiment). The Affymetrix small sample protocol consists of two rounds of amplification (TwoRA) and is a well-established T7-based method for the preparation of biotin-labelled cRNA targets from nanogram amounts of RNA. Hybridisation was performed by Dr Jing Wang of the Sir Henry Wellcome Functional Genomics Unit (SHWFGU), Glasgow.

2.9.3 Statistical Analysis

2.9.3.1 FunAlyse Pipeline Analysis (Performed by the SHWFGU)

2.9.3.1.1 Low Level Normalisation

The Robust Multichip Average (RMA) method of normalisation (Irizarry *et al.* 2003) was implemented through the Affy module of the Bioconductor microarray analysis suite. RMA

performs probe specific background correction to compensate for non-specific binding using PM distribution rather than PM-MM values, probe-level multichip quantile normalisation to normalise PM distributions across all chips and robust probe-set summary of the log-normalised probe-level data by median polishing.

2.9.3.1.2 Identification of differentially expressed genes using Rank Products analysis

Identification of differentially expressed genes was achieved using the RankProducts (RP) approach (Breitling *et al.* 2004). RP sorts all the genes in a data set according to their expression changes and assigns statistical confidence levels to each change in the form of false discovery rates (FDRs) with a 5% FDR corresponding to a p value of 0.05. This method is more powerful than many other techniques used to find differentially expressed genes (such as significance of microarrays (SAM)) (Breitling *et al.* 2004) and is particularly useful for small and noisy data sets.

2.9.3.1.3 Identification of differentially expressed genes using Genespring

Affymetrix cel. files were imported into Genespring GX 7.3 (Agilent technologies) and normalised using RMA. Data was then filtered by error to remove genes that have a large spread around the mean and are thus less likely to be reliable. If it assumed that the data follow a normal distribution, then 68% of the values lie within one SD of the mean and 97% of the values lie within two SD of the mean. A stringent standard deviation filter was set to select genes whose values were within 1 standard deviation of the mean in 5 out of 5 conditions.

An expression filter was applied to remove non-changing genes. To remove genes with a smaller than 2-fold change in all conditions parameters were set thus; min=0.667 max=1.334 in 5 out of 5 conditions. To remove genes with a smaller than 1.5-fold change parameters were set to; min=0.8 and max=1.2 in 5 out of 5 conditions.

A search was carried out for Affymetrix control genes (find gene seach term 'AFFX'). The 57 control genes that were found were also removed from the list of genes used in further analyses.

2.9.3.1.4 Functional interpretation of microarray data

Functional interpretation of the data was aided by Iterative Group Analysis (iGA), a method for identification of differentially expressed functional gene classes (Breitling *et al.* 2004). iGA provides biological summary of the physiological processes affected in a particular experiment whilst providing statistical confidence levels.

2.9.3.2 Ingenuity Pathways Analysis

Data were analysed through the use of Ingenuity Pathways Analysis (IPA) (Ingenuity® Systems, www.ingenuity.com).

2.9.3.2.1 Network Generation

A data set of genes (differentially expressed in each of the injury models relative to control) containing gene identifiers and corresponding expression fold changes and FDRs were uploaded into the application. Each gene identifier was mapped to its corresponding gene object in the Ingenuity Pathways Knowledge Base. A FDR cut-off of 5% was set to identify genes whose expression was significantly differentially regulated. These genes, called focus genes, were overlaid onto a global molecular network developed from information contained in the Ingenuity Pathways Knowledge Base. Networks of these focus genes were then algorithmically generated based on their connectivity.

2.9.3.2.2 Functional analysis

Functional Analysis identified the biological functions that were most significant to the data set. Genes from the dataset that met the FDR cut-off of 5% and were associated with biological functions in the Ingenuity Pathways Knowledge Base were considered for the analysis. Fischer's exact test was used to calculate a p-value determining the probability that each biological function assigned to that data set is due to chance alone.

2.9.3.2.3 Canonical Pathway Analysis

Canonical pathways analysis identified the pathways from the Ingenuity Pathways Analysis library of canonical pathways that were most significant to the data set. Genes from the data set that met the FDR cut-off of 5% and were associated with a canonical pathway was measured in 2 ways: 1) A ratio of the number of genes from the data set that map to the pathway divided by the total number of genes that map to the canonical pathway is displayed. 2) Fischer's exact test was used to calculate a p-value determining the probability that the association between the genes in the dataset and the canonical pathway is explained by chance alone.

2.10 Quantitative Real time PCR (qRT-PCR)

2.10.1 SYBR Green I chemistry

In qRT-PCR, the quantity of amplification product is measured during every PCR cycle. SYBR green I, a minor groove binding dye, was used for the quantitative detection of the amplification product. Figure 2-7 illustrates the principle of qRT-PCR using SYBR Green I chemistry. The fluorescence measured at the end of every extension phase can be plotted as an amplification graph (Figure 2-8) and the cycle at which the fluorescence rises above threshold (threshold cycle, Ct) is related to the starting template amount. Since the quantity of DNA doubles every cycle during the exponential phase, relative amounts of DNA can be calculated e.g. a sample whose Ct is 2 cycles earlier than another has 2^2=4 times more template.

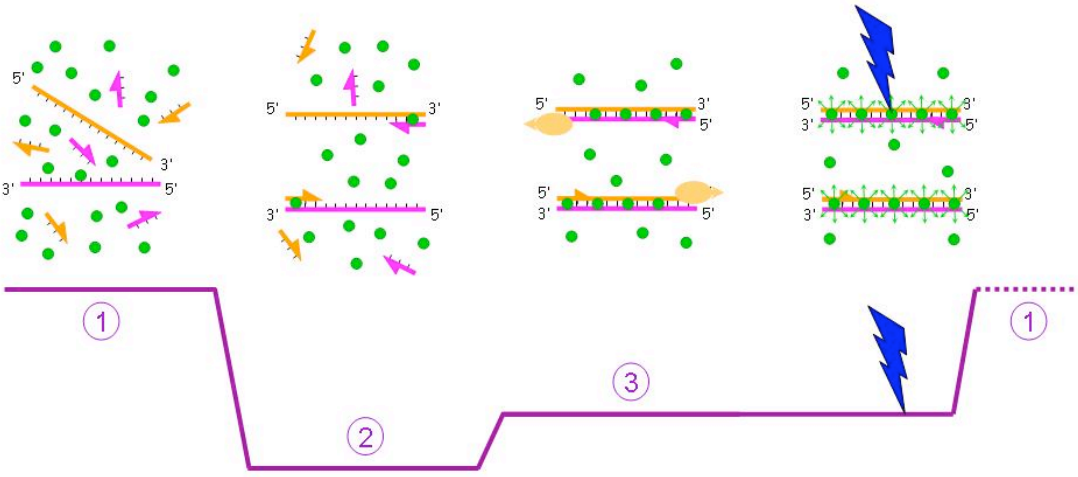

Figure 2-7: Schematic diagram illustrating SYBR Green I chemistry. During the denaturation (stage 1) and annealing (stage 2) process, the SYBR Green I molecule does not bind the single-stranded DNA and consequently does not fluoresce. Upon primer extension (stage 3), the DNA target is now present as a double-stranded template which now binds SYBR Green I. This causes the bound SYBR Green I to fluoresce (blue lightning symbol) The cycle is repeated and the fluorescence is 'read' at the end of each extension reaction with the total amount of fluorescence being proportional to the concentration of the amplified product.

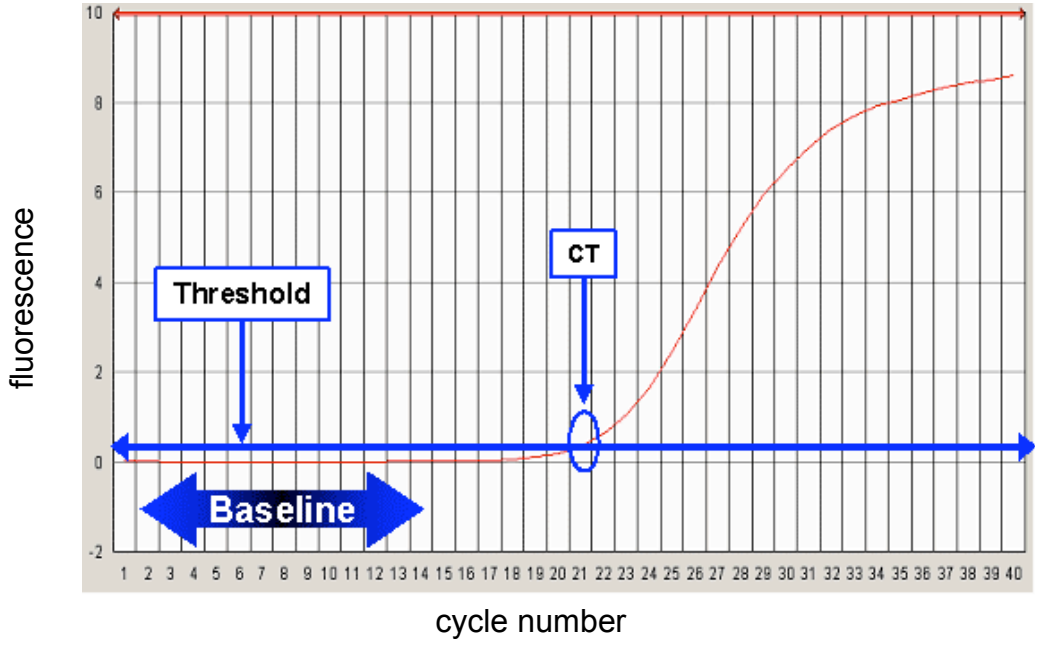

Figure 2-8: Diagram illustrating the features of an amplification plot. Threshold and cycle threshold (Ct) are shown.

2.10.2 Two-step qRT-PCR

Real-time RT-PCR was performed using the DNA Engine Opticon-2 (MJ Research Inc, Boston. MA). Real-time fluorescence detection was performed in 96-well plates using Quantitect SYBR Green PCR mastermix (Qiagen). Samples were assayed in triplicate. Each 20-µl reaction contained

cDNA (equivalent to 5 ng RNA) and a final concentration of 1x Quantitect primer assay (Qiagen) and 1x Quantitect SYBR green master mix. After the initial 15-min. incubation at 95°C for activation of the Hot Start Taq DNA polymerase, all templates were amplified for 45 cycles using the following protocol: denaturation for 15 s at 94°C, primer annealing for 30 s at 55°C, and elongation for 30 s at 72°C. Fluorescence data were acquired at the end of each elongation phase. After the amplification program, melting curves were generated by measuring the fluorescence as the temperature was raised from 60°C to 90°C in 1°C increments to verify specificity of fluorescence detection. Specificity of amplification products was further verified by gel electrophoresis and ethidium bromide staining (Section 2.8.10.3). Threshold cycle (Ct) values were determined by automated threshold analysis (3x S.D. of the global minimum across all primers and samples in a plate). Positive (no template reaction) controls were run in triplicate and included in each PCR assay. Negative (no RT) controls were deemed unnecessary for the majority of the assays as Quantitect Primer assays are designed, where possible, to span exon/exon boundaries to prevent coamplification of genomic DNA (gDNA). Negative controls were included for YWAZ, ATP5B and BDNF as these assays co-amplify gDNA. In addition, a plate calibrator (described in section 2.10.4.2) was run in triplicate on each plate.

Table 2-3: Qiagen primer assays used in qRT-PCR. * Number of exons according to Ensembl Transcript. ** Indicates a primer assay that may potentially amplify gDNA.

TARGET GENE SYMBOL	QIAGEN CATALOG NUMBER	*EXONS AMPLIFIED	PRODUCT SIZE (BP)
Sema6a	QT01603791	8/9	98
Top1	QT00193718	10/11	87
B2m	QT00176295	1/2	61
Canx	QT00177975	12/13	92
Ywhaz **	QT01083992	---	97
Atp5b **	QT00434385	---	104
Ankrd1	QT01083845	5/6	69
Bdnf **	QT00375998	---	143
Notch4	QT01626415	12/13	126
Gapdh	QT00199633	1/3	149
Ptpn5	QT01081458	8/10	120
Atf3	QT00183883	3/4	76
Wisp2	QT00189840	3/4	101
Igf1	QT00996247	3/4	118
Tfpi2	QT00183190	3/4	86
Tgm1	QT00178948	8/9	94

2.10.3 Assessment of Experimental Precision

2.10.3.1 Intra and inter-run precision

To quantify inter-run variation, two identical runs were carried out using the same cDNA template, reagents and RT-PCR conditions on two different days. Each run consisted of 15 replicates of the same cDNA sample. A master mix of reagents was aliquoted into each well such that each well contained 5 ng cDNA (RNA equivalents) in a total volume of 20 μl. As qRT-PCR data are

logarithmic Ct values were first linearised (using 2^{-CT}) and CV_{exp} (CV=SD/mean x100) was calculated for both runs to give the intra-run variation. The difference between these CVs gave the inter-run variation.

2.10.3.2 Operator precision

Operator precision was assessed by a third run consisting of 15 replicates of the same template cDNA as above. The cDNA was added separately to each well and run under the same conditions as before. Again, the Ct values were linearised and the CV_{exp} (CV= SD/mean x 100) for the run was calculated. Operator associated variation was calculated as (mean CV_{exp} Run 1 and Run 2) – CV_{exp} Run 3).

2.10.4 Analysis of qRT-PCR data

2.10.4.1 Validation of reference genes: geNorm and NormFinder.

6 housekeeping genes were assessed for stability and hence, suitability for use as reference genes in the sciatic nerve transection injury paradigm. The three most stable of these genes were used in conjunction in generation of a normalisation factor in qRT-PCR analysis software REST-MCS (Section 2.10.4.5).

Briefly, geNorm (Vandesompele *et al.* 2002) calculates the gene expression stability value M for a reference gene as the pairwise variation *V* of that gene with all other reference genes tested. Stepwise exclusion of the least stable gene (with the highest M value) allows ranking of the tested genes according to their expression stability and thus the most stable genes can be identified. Since co-regulated genes lead to stable expression ratios, care was taken that the genes chosen for consideration as reference genes were not co-regulated.

Like geNorm, NormFinder (Andersen *et al.* 2004) ranks a panel of potential reference genes on the basis of their stability but uses a model-based approach to estimate expression variation instead of a pairwise comparison approach. NormFinder assigns a stability value to each gene having first estimated both intra- and inter-group variation. This stability value represents a practical measure of the systematic error that will be introduced if the gene were to be used.

2.10.4.2 Plate to plate calibrator

As the samples for any one gene were split between 3- 5 plates, a plate to plate calibrator was included in each run as a quality control measure (Godfrey and Kelly 2005). The calibrator was a

cDNA sample from RNA originating from several different tissues (DRG, heart, liver, spleen and spinal cord dissected from rats used for other purposes) that was amplified in triplicate on each plate. Ct values obtained for the calibrator sample were relatively invariant with differences between plates of typically <0.8 cycles. Where CVs could be calculated (in the case of genes run over 4 or 5 plates) they were in the range of 0.6072-1.042%.

2.10.4.3 Identification of outliers

Within triplicates, an outlier was defined as having a Ct >0.5 cycles different from the other Cts in the triplicate. These triplicate outliers were removed before calculation of the triplicate means from the remaining 2 values.

Within group outliers were identified by subjecting the triplicate mean Ct values to a Grubb's test (http://www.graphpad.com/quickcalcs/Grubbs1.cfm) (Burns *et al.* 2005). Significant outliers ($p \leq 0.05$) were eliminated before further analysis.

2.10.4.4 Calculation of well-well reaction efficiencies with LinRegPCR

Raw fluorescence data for each qRT-PCR run was exported as Excel spreadsheets from MJR Opticon Software and analysed using LinRegPCR software tool (Ramakers *et al.* 2003). LinRegPCR calculates reaction efficiencies by linear regression on the Log(fluorescence)/cycle number data and allows assay-specific PCR efficiency to be determined. Subsequent data analysis is therefore not based on the erroneous assumption of 100% reaction efficiency and the need for standard curves is removed.

2.10.4.5 Relative expression quantification using Relative Expression Software Tool (REST-MCS)

Mean triplicate Ct values were analysed in REST-MCS relative expression software (Pfaffl *et al.* 2002). REST-MCS employs a non-parametric method to assess the statistical differences between experimental groups. It calculates P values on the basis of the pair-wise fixed reallocation randomisation test which jointly reallocates the Ct values for reference and target genes to control and sample groups then calculates the resulting expression ratios on the basis of the mean values. In the course of each test 2000 such randomisations are performed. The method avoids the reduction in power that is encountered when using parametric tests and avoids assumptions about data distribution that may be encountered in non-parametric tests that employ measurements of rank (Pfaffl *et al.* 2002). The software also takes into account gene-specific reaction efficiencies. Mean reaction efficiencies were therefore calculated from the well reaction efficiencies calculated by LinRegPCR (section 2.10.4.4) and these gene-specific reaction efficiencies were integrated into the REST-MCS analysis.

3 Pilot microarray experiment, analysis and qRT-PCR validation

3.1 Introduction and aims

A conditioning lesion to the peripheral branch of a DRG neuron facilitates regenerative sprouting after a lesion to the central branch (Neumann and Woolf 1999) (see also section 1.4.2.1). This is thought to be due to a priming effect whereby intracellular cAMP is elevated within the nerve cell body (Neumann *et al.* 2002) and the slow component of axonal transport that carries cytomatrix proteins to the site of injury is accelerated (Jacob and McQuarrie 1991; McQuarrie and Jacob 1991). Additionally, it has been shown that sciatic nerve transection, a well-studied conditioning lesion, induces changes in gene expression within the cells of the DRG (Costigan *et al.* 2002). It is therefore likely that the priming effect of a conditioning lesion is partly due to a regeneration-permissive transcriptional programme being activated within the nerve cell bodies in the DRG.

Here we aimed to optimise parameters for a large microarray experiment by conducting an experiment to examine gene changes at 8 days following sciatic nerve transection using microarray technology. Use of such a well-studied injury model allowed us to confirm that our experimental methods could yield biologically valid results that are consistent with other experiments of this type. In addition, it allowed optimisation of various technical aspects of the experiment such as tissue collection and homogenisation, RNA extraction, cDNA synthesis and qRT-PCR. In addition, laser capture micro-dissection (LCM) was explored as a method to obtain a homogenous population of DRG cells as an alternative to extracting RNA from whole DRG.

3.2 The microarray

The left (ipsilateral) L4 and L5 DRGs from 6 rats (310-380 g) that had undergone a left sciatic nerve transection 8 days before (section 2.2.3) were homogenised in pairs in Trizol (section 2.8.2) and total RNA extracted (section 2.8.4.1). L4 and L5 DRGs from 4 naïve control animals and a further 2 sham control rats (250-360g) were also processed. Figure 3-1 illustrates the design of the pilot microarray experiment. Briefly, RNA from 2 rats was pooled and biotinylated cDNA was synthesized, fragmented and hybridized to RAE 230A GeneChips (Affymetrix, Santa Clara, CA). Three chips were used for each condition according to MIAME guidelines (Brazma *et al.* 2001). Tissue collection and processing for 5 of the 6 chips was completed before my arrival by a final year undergraduate project student, Miss Virginia Bound. I observed surgery and completed tissue collection and processing for the third in the triplicate of sciatic transection chips (chip F). It should be noted that chip F was hybridized separately and at a later date than the other 5 chips.

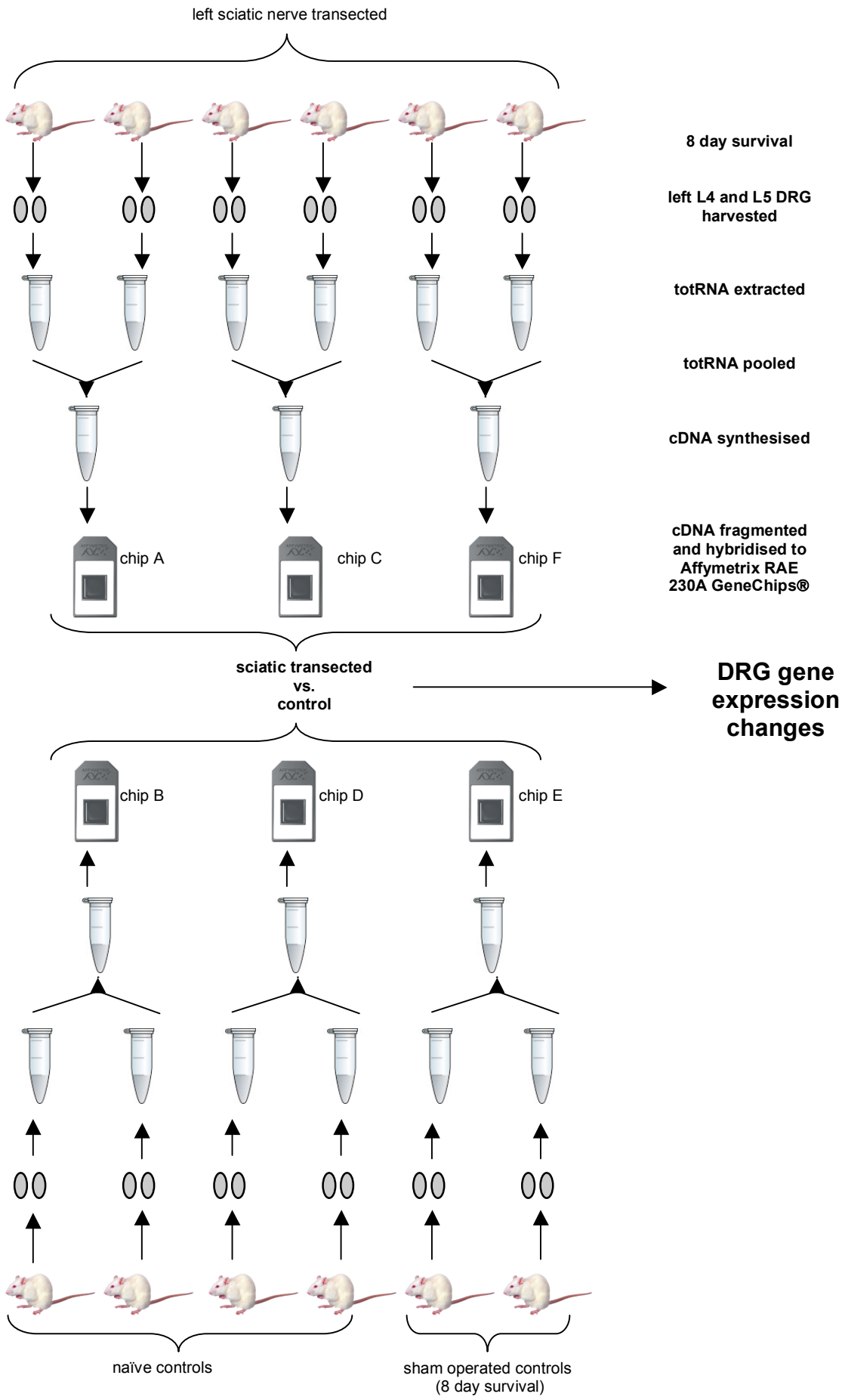

Figure 3-1: Schematic diagram illustrating the design of the pilot microarray experiment that investigated gene changes in the DRG 8 days after a sciatic nerve transection injury.

3.2.1 Low level analysis for QC

3.2.1.1 Internal controls

Internal controls provide a measure of RNA sample quality by showing the 3'/5' ratios for a set of specific probe sets. Ratios of greater than 3 can indicate sample degradation. The 6 chips in this pilot microarray showed elevated 3'/5' ratios for the hexokinase control in all but chip F (Table 3-1). Since this chip was hybridized separately from the other chips it is possible that the difference in internal controls for this chip could be due to differences in the extraction of the RNA and in the RNA/cDNA handling.

Table 3-1: RNA sample quality assessed by 3'/5' ratios in probe sets for internal controls. Hexokinase shows elevated 3'/5' ratios in all but chip F.

CHIP	BETA-ACTIN	GAPDH	HEXOKINASE
A	2.030334	1.1738755	3.6950305
B	2.070120	1.2229369	4.1672587
C	1.871972	1.2387062	3.2658498
D	1.787989	1.1488721	3.531362
E	2.020886	1.3364604	3.7674406
F	2.815433	2.1557865	2.5883071

3.2.1.2 Hybridisation controls

Affymetrix chips have integral hybridisation controls to allow assessment of hybridisation quality. Hybridisation controls are composed of a mixture of biotin-labelled cRNA transcripts (bioB (1.5 pM), bioC (5 pM), bioD (25 pM) and cre (100 pM)). This mixture was spiked into the hybridisation cocktail. BioB is at the level of assay sensitivity and should thus be present 50% of the time while bioC, bioD and cre should appear in increasing concentrations.

Figure 3-2 shows the hybridisation control profiles for all 6 chips. All the hybridisation controls are present in increasing concentrations on all the chips. There is a close clustering of profiles for all chips apart from chip F. The separation is unsurprising as chip F was hybridized at a later time-point than the other chips that were hybridized together. All the profiles are however roughly parallel to each other suggesting a high quality, uniform hybridization across chips.

3.2.1.3 Principal components analysis

Principal component analysis (PCA) is a decomposition technique that can be used to check data quality. It allows projection of complex data sets onto an easily visualized, 2-dimensional or 3-dimensional space. Replicates within a condition should cluster together and separately from arrays in other conditions. Principal components are numbered according to their decreasing significance. Principal components 1 and 2 for the pilot microarray experiment are illustrated in Figure 3-3. Control chips cluster together indicating a similarity in gene behaviour on these chips. Chip F separates from the other experimental chips suggesting that this chip differs in its global gene expression from the other chips in the triplicate.

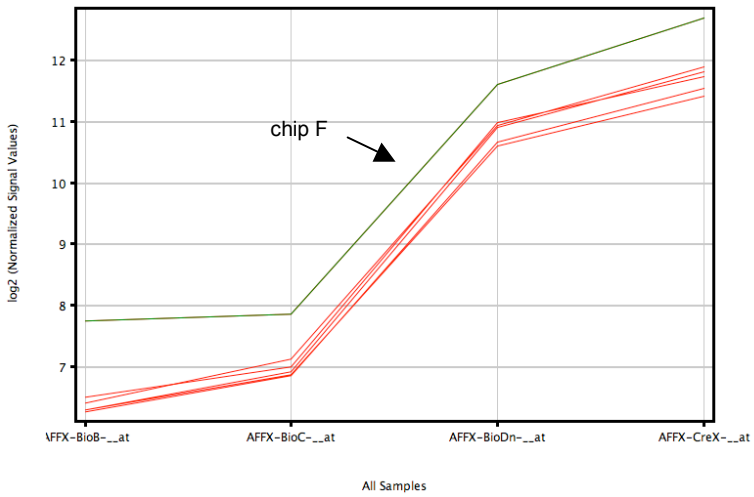

Figure 3-2: Hybridisation control profiles. The x axis represents the hybridisation controls present at 1.5, 5, 25 and 100 pM, respectively. The log of the normalised signal values is plotted on the Y-axis.

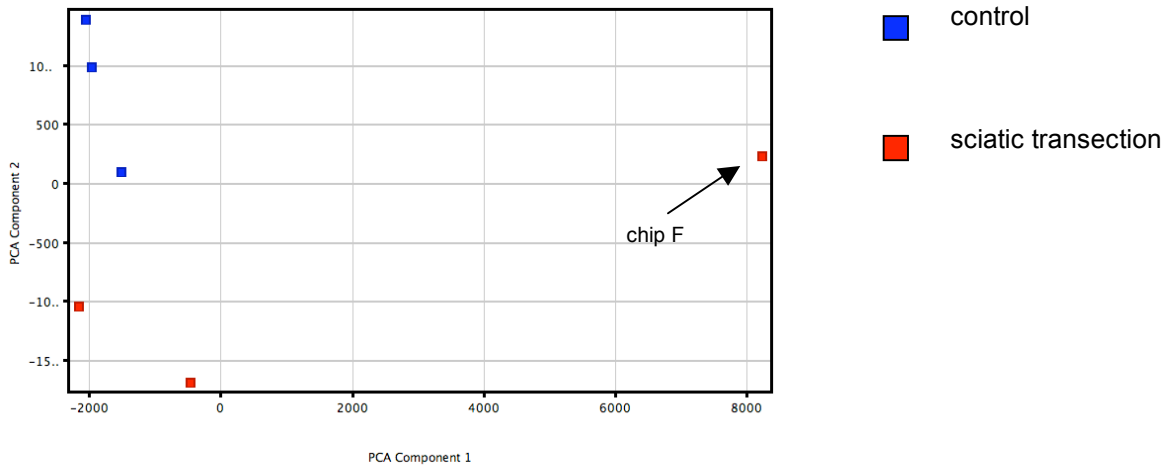

Figure 3-3: Principal components analysis (PCA) for pilot experiment chips: PCA Component 1 is plotted against PCA component 2.

3.2.2 Differentially expressed genes

Rank products analysis (section 2.9.3.1.2) was used to identify genes that were up or downregulated 8 days after sciatic nerve transection. Table 3-2 presents the descriptive statistics for this analysis while Figure 3-4 illustrates the proportion of probes that were up and downregulated. At the 5% level there are roughly 50% more downregulated genes than upregulated genes. There are however more dramatic fold changes to be seen amongst the upregulated genes with neuropeptide Y (NPY) showing a massive 45-fold upregulation. Table 3-3 and **Table 3-4** below show the top 20 up and downregulated genes. A list of ranked genes to 1% FDR is presented in appendix A while ranked genes to 50% FDR are presented on the accompanying CD.

Table 3-2: Pilot microarray descriptive statistics.

HIGHEST FOLD CHANGES		UPREGULATED GENES		DOWNREGULATED GENES	
Up	Down	1% FDR	5% FDR	1% FDR	5% FDR
45.88	-3.60	44	86	57	138

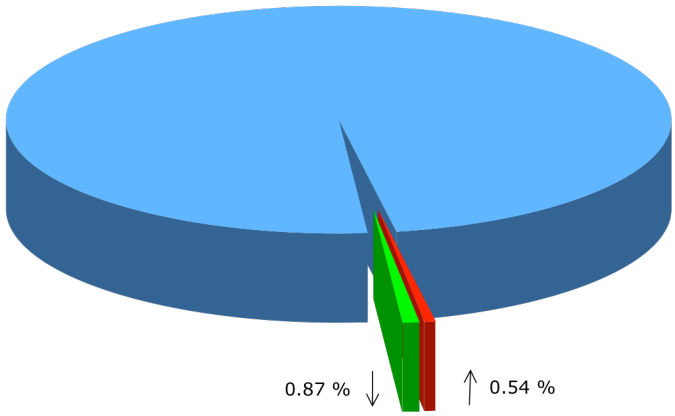

Figure 3-4: Pie chart showing the percentage of probe sets regulated within 5% FDR. The chips contained 15924 probes sets covering 15700 genes. The proportion of upregulated probe sets is denoted by the red slice while the green slice indicates downregulated probe set.

Table 3-3: Top 20 genes upregulated after sciatic nerve transection ranked by fold change

PROBESET ID	GENE SYMBOL	GENE NAME	ACC. NO.	FC	FDR
1387154_at	Npy	neuropeptide Y	NM_012614	45.88	0.00
1377146_at	Vip	vasoactive intestinal polypeptide	AI412212	28.51	0.00
1369268_at	Atf3	activating transcription factor 3	NM_012912	14.32	0.00
1387088_at	Gal	Galanin	NM_033237	12.00	0.00
1398243_at	Vsnl1	Visinin-like 1	NM_057144	8.71	0.00
1368238_at	Pap (Reg2)	pancreatitis-associated protein	NM_053289	8.82	0.00
1371248_at	Sprr1a	small proline-rich protein 1A (predicted)	BI286387	7.15	0.00
1376601_at	Sema6a	Similar to semaphorin 6A1; semaphorin 6A-1	BF397526	6.35	0.00
1368224_at	Spin2c	Serine protease inhibitor	NM_031531	6.62	0.00
1387396_at	Hamp	hepcidin antimicrobial peptide	NM_053469	5.80	0.00
1369202_at	Mx2	myxovirus (influenza virus) resistance 2	NM_017028	5.35	0.00
1377334_at	RT1-Ba	RT1 class II, locus Ba	BG378249	4.80	0.00
1388451_at	Cacna2d1	V-dependant calcium channel	AA817802	3.76	0.00
1370883_at	RT1-Da	Antigen processing and presentation	Y00480	4.03	0.07
1368947_at	Gadd45a	growth arrest and DNA-damage-inducible 45 alpha	NM_024127	4.12	0.07
1368266_at	Arg1	arginase 1	NM_017134	3.69	0.06
1370315_a_at	Stmn4	stathmin-like 4	AF026530	3.56	0.06
1371450_at	Sox11	SRY-box containing gene 11	BE117330	3.02	0.11
1367973_at	Ccl2	chemokine (C-C motif) ligand 2	NM_031530	3.20	0.11
1372734_at	Smagp	small cell adhesion glycoprotein	AI408095	3.44	0.10

Table 3-4: Top 20 genes downregulated 8 days after sciatic nerve transection ranked by fold change

PROBESET ID	GENESYMBOL	GENE NAME	ACC. NO.	FC	FDR
1368751_at	Kcns3	potassium voltage-gated channel, delayed-rectifier, subfamily S, member 3	NM_031778	-3.60	0.00
1393933_at	RGD:1310938	sortilin-related receptor, L(DLR class) A repeats-containing (predicted)	AW144823	-3.25	0.00
1371108_a_at	Atp1a1	ATPase, Na+/K+ transporting, alpha 1 polypeptide	M74494	-3.82	0.00
1374046_at	Hs3st2	Heparin sulfate (glucosamine)-3-0 sulfotransferase 2	BG376092	-3.03	0.00
1368506_at	Rgs4	regulator of G-protein signaling 4	U27767	-3.37	0.00
1368821_at	Fstl1	follistatin-like 1	BI290885	-3.23	0.00
1370556_at	Vamp1	Vesicle-associated membrane protein	M24104	-3.06	0.00
1370517_at	Nptx1	neuronal pentraxin 1	U18772	-2.88	0.00
1377457_a_at	Sorl1	sortilin-related receptor, L(DLR class) A repeats-containing (predicted)	AA850618	-2.8	0.00
1377095_at	LOC287847	similar to ataxin 2-binding protein 1 isoform 1	BG380409	-2.91	0.00
1369390_a_at	Dpp6	dipeptidylpeptidase 6	NM_022850	-2.82	0.00
1371077_at	Htr3b	5-hydroxytryptamine (serotonin) receptor 3b	AI575989	-2.63	0.00
1369428_a_at	Htr3a	5-hydroxytryptamine (serotonin) receptor 3a	U28430	-2.65	0.00
1371211_a_at	Nrg1	neuregulin 1	U02315	-2.78	0.00
1369001_at	Chrna3	cholinergic receptor, nicotinic, alpha polypeptide 3	NM_052805	-2.57	0.00
1388000_at	Slc24a2	solute carrier family 24 (sodium/potassium/calcium exchanger), member 2	AF021923	-2.65	0.00
1369116_a_at	Calca	calcitonin/calcitonin-related polypeptide, alpha	NM_017338	-2.5	0.00
1370572_at	Gpr149	G protein-coupled receptor 149	AY030276	-2.43	0.00
1375242_at	Cadm1	Cell adhesion molecule 1	BI296440	-2.39	0.05
1384132_at	RGD:1310999	immunoglobulin superfamily, member 4A (predicted)	H31111	-2.63	0.05

3.2.3 Comparison with past studies

A number of studies have examined gene changes in the DRG after sciatic nerve transection. A comparison of our data with past studies was performed whereby the microarray data was searched (by gene symbol and all known gene symbol aliases) for the presence of genes whose regulation is already known. Studies included in the comparison have examined gene changes in the DRG at various time points after sciatic nerve transection in rodents using various techniques. The results of this comparison are presented in Table 3-5. On the whole, the microarray showed good concordance with past studies and where a gene was identified as regulated, the direction of change was, in general, the same as previously reported (see genes highlighted in bold). Only one gene showed regulation in the opposite direction to previously reported (ROBO2, highlighted in red). A number of genes that have been previously reported as regulated after sciatic nerve injury were unchanged at the 50% FDR level in our microarray. These were mainly encoding G protein coupled receptors that are in low abundance. Whilst this may indicate a problem with sensitivity of the microarray, it is possible that these genes are simply not regulated at this relatively late time point after injury. There is also evidence that the mRNA for a number of proteins, such as the κ-opioid receptor, undergoes axonal transport and local translation (Willis *et al.* 2005; Bi *et al.* 2006; Bi *et al.* 2007) and as such would only be detected as increased in the DRG at a very early timepoint after injury.

Table 3-5: Comparison of microarray and known regulation data for genes whose expression within the DRG following nerve injury has been studied previously. Genes that show the same regulation in our microarray as past studies are highlighted in bold. Where information is unavailable cells are shaded in grey. NC= no change (for past studies) or no change within 50% FDR (for our pilot microrray), A= absent on all chips.

CATEGORY	GENE SYMBOL	KNOWN REGULATION	(Costigan *et al.* 2002) 3 days post-lesion	FC	FDR
G protein coupled receptors	ADRA2A	Up (Birder and Perl 1999; Shi et al. 2000)	A	NC	---
	ADRA2C	**Down (Shi et al. 2000)**	**A**	**-1.25**	**48.66**
	AGTR1	Up (Gallinat et al. 1998)	A	NC	---
	AGTR2	Up (Gallinat et al. 1998)	A	NC	---
	BDKRB1	Up (Levy and Zochodne 2000)	-1.6	NC	---
	BDKRB2	Up (Levy and Zochodne 2000)	A	NC	---
	CCKBR	Up (Zhang et al. 1993; Antunes Bras et al. 1999)	-1.1	NC	---
	GALR1	Down (Xu *et al.* 1996; Zhang *et al.* 1998)	A	NC	---
	GALR2	Down (Sten Shi *et al.* 1997; Zhang *et al.* 1998)	A	NC	---
	NPY1R	Down (Zhang *et al.* 1994; Landry *et al.* 2000)	-1.3	NC	---
	OPRM1	Down (Zhang *et al.* 1998)	-3.2	NC	---
	OPRD1	Down (Zhang *et al.* 1998)	A	NC	---
Ligand gated ion channel receptors	**GABRA2**	**NC (Fukuoka *et al.* 1998)**	**-1.6**	**NC**	**---**
	GABRG2	down (Bradbury *et al.* 1998)	-1.5	NC	---
	P2RX3	**Down (Bradbury *et al.* 1998; Yiangou *et al.* 2000)**	**-1.1**	**-1.73**	**15.02**
	TRPV1	**Down (Michael and Priestley 1999)**	**-1.8**	**-2.07**	**1.41**
Receptor tyrosine kinases	**NGFR**	**Down (Krekoski *et al.* 1996)**	**A**	**-1.73**	**9.43**

Table 3-5 continued.

	GFRA1	**Up (Bennett *et al.* 2000)**	**2.00**	**2.42**	**1.1**
	GFRA2	**Down (Bennett *et al.* 2000)**	**-1.7**	**-1.31**	**34.82**
	TRKA	**Down (Kashiba *et al.* 1998; Bergman *et al.* 1999)**	**-1.3**	**-2.23**	**0.91**
Cytokine/growth factors/neuropeptides	BDNF	Up (Cho *et al.* 1997; Kashiba and Senba 1999)	1.6	NC	---
	CALCB	**Down (Noguchi *et al.* 1990)**	**-1.6**	**-1.51**	**19.98**
	CALCA	**Down (Noguchi *et al.* 1990)**	**-1.6**	**-1.64**	**7.31**
	CCK	Up (Verge *et al.* 1993)	A	NC	---
	FGF2	Up (Ji *et al.* 1995)	A	NC	---
	GAL	**Up (Hokfelt *et al.* 1994; Tanabe *et al.* 2003)**	**28.8**	**12**	**0**
	IL1B	Up (Murphy *et al.* 1995)	1.1	NC	---
	IL6	**Up (Murphy *et al.* 1995)**	**A**	**1.81**	**8.21**
	NPY	**Up (Hokfelt *et al.* 1994; Tanabe *et al.* 2003)**	**9.7**	**45.88**	**0**
	ADCYAP1	**Up (Jongsma *et al.* 2000)**	**3.5**	**2.88**	**0.25**
	SST	**Down (Alvares and Fitzgerald 1999)**	**-1.5**	**-1.82**	**4.28**
	TAC1	**Down (Noguchi *et al.* 1990; Zhang *et al.* 1995; Alvares and Fitzgerald 1999)**	**-2.2**	**-1.78**	**6.83**
	TNF	Up (Murphy *et al.* 1995)	A	NC	---
	DAP	Down (Mulder *et al.* 1997)	-4.7	NC	---
	REG2 (PAP)	**Up (Livesey *et al.* 1997)**	**18.5**	**8.82**	**0**
	ROBO2	Up (Bloechlinger *et al.* 2004; Yi *et al.* 2006)		-1.53	16.61
	SLIT1	Up (Yi *et al.* 2006)		NC	---
	STAT3	Up (Qiu *et al.* 2005)		NC	---
	PACAP	**Up (Pettersson *et al.* 2004)**		**2.88**	**0.25**
	NTS	Up (Tanabe *et al.* 2003)		A	
Receptor- associated proteins	**RBP1**	**Up (Karchewski *et al.* 2004)**		**1.55**	**18.7**
Ion channels	BNC1	Up (Waxman *et al.* 1994) (Dib-Hajj *et al.* 1996)	1.4	NC	---
	KCNA7, KCNA2	Down (Ishikawa *et al.* 1999; Park *et al.* 2003)	-1.1	NC	----
	KCNA4	**Down (Park *et al.* 2003)**		**-1.37**	**22.76**
	KCND2	Down (Park *et al.* 2003)		NC	---
	SCN10A	**Down (Dib-Hajj *et al.* 1996; Okuse *et al.* 1997) (Sleeper *et al.* 2000)**	**-1.9**	**-1.96**	**1.71**
	CACNA2D1	**Up (Luo *et al.* 2001)**	**3.4**	**2.46**	**1.84**
	NaN alpha subunit	Down (Dib-Hajj *et al.* 1998; Sleeper *et al.* 2000)	-2.1	??	
	TRPC1	**NC (Wu *et al.* 2008)**		**NC**	**---**
	TRPC3	**NC (Wu *et al.* 2008)**		**-1.48**	**22.53**
	TRPC4	Up (Wu *et al.* 2008)		NC	---
	TRPC6	**NC (Wu *et al.* 2008)**		**NC**	**---**
	TRPC7	**NC (Wu *et al.* 2008)**		**NC**	**---**
Cell cytoskeleton	ACTB	Up (Lund and McQuarrie 1996)	-1.1	NC	---
	GAP43	**Up (Chong *et al.* 1994)**	**1.8**	**2.77**	**0.08**
	GFAP	**Up (Woodham *et al.* 1989)**	**3.8**	**2.06**	**2.74**
	NEFH	**Down (Oblinger *et al.* 1989; Wong and Oblinger 1990)**	**-1.2**	**-1.35**	**33.85**
	NEFM	**Down (Oblinger *et al.* 1989; Wong and Oblinger 1990)**	**-1.1**	**-1.39**	**31.98**
	NEFL	**Down (Oblinger *et al.* 1989; Wong and Oblinger 1990)**	**1**	**-1.42**	**23.95**
	PRPH	Up (Wong and Oblinger 1990; Chadan *et al.* 1994)	-1.1	NC	---
	TUB	**Up (Moskowitz *et al.* 1993; Jiang *et al.* 1994)**	**-1.3**	**1.9**	**8.22**
	LASP1?	Up (Newton *et al.* 2000)	4	NC	---
	SPRR1A	**Up (De Leon *et al.* 1995)**	**3.6**	**7.15**	**0**
	MYO10	Up (Tanabe *et al.* 2003)		NC	---
	ITGA6	Up (Wallquist *et al.* 2004)		NC	---

Table 3-5 continued.

Transcription factors	ITGA7	Up (Wallquist *et al*. 2004)		NC	---
	ITGB1	**Up (Wallquist *et al.* 2004)**		**1.51**	**31.61**
	ATF3	**Up (Tsujino *et al.* 2000; Tanabe *et al.* 2003)**	**11.4**	**14.32**	**0**
	c-jun	**Up (Herdegen *et al.* 1992; De Leon *et al.* 1995; Kenney and Kocsis 1997)**	**7.3**	**2.68**	**0.26**
	jun-D	Up (Herdegen *et al.* 1992; De Leon *et al.* 1995; Kenney and Kocsis 1997)	A	NC	---
	SOX11	**Up (Tanabe *et al.* 2003)**		**1.68**	**15.74**
	RGS3	**Down (Costigan *et al.* 2003)**		**-1.88**	**4.22**
	RGS4	**Down (Costigan *et al.* 2003)**		**-3.37**	**0**
	TNFRSF12A (FN14)	Up (Tanabe *et al*. 2003)		NC	---
Cell surface/extracellular matrix	AEG	Up (Newton *et al.* 2000)	7.5	NC	---
	ITGA7	Up (Werner *et al*. 2000)	1.5	NC	---
	NCAM	Up (Daniloff *et al.* 1986)	A	NC	---
	L1CAM	**NC (Zhang *et al.* 2000)**	**1.2**	**NC**	**---**
	NRP1	Up (Gavazzi *et al*. 2000)	-1.2	NC	---
	NINJ1	Up (Araki and Milbrandt 1996)	1	NC	---
	CSPG4	**NC (Rezajooi *et al.* 2004)**		**NC**	**---**
	GPC1	Up (Bloechlinger *et al.* 2004)		NC	---
Transmembrane proteins	FLRT3	Up (Tanabe *et al*. 2003)		NC	---
Enzymes	NOS1	Up (Shi *et al*. 1998; Gonzalez-Hernandez and Rustioni 1999)	A	NC	----
	RHOA	Up (Cheng *et al*. 2008)		NC	---
	ECEL1	**Up (Kato *et al.* 2002; Kiryu-Seo 2006)**		**2.42**	**1**
Chaperone proteins	TOR1A	Up (Zhao *et al.* 2008)		NC	---
Cell death/survival	**BAX alpha**	**NC (Gillardon *et al.* 1994; Gillardon *et al.* 1996)**	**1**	**NC**	**---**
	BCL2	Down (Gillardon *et al.* 1994; Alberi *et al.* 1996)	-1.1	NC	---
	SOD2	**Up (Fernandes and Tetzlaff 2001)**	**1.1**	**1.51**	**29.6**
	HSP27	**Up (Tandrup *et al.* 2000)**	**2.9**	**1.8**	**9.22**
	SOD	**NC (Fernandes and Tetzlaff 2001)**	**1**	**NC**	**---**
Metabolism	**FABP**	**Up (De Leon *et al.* 1996)**	**1.5**	**1.64**	**18.68**
	PPI	**NC (Tandrup *et al.* 2000)**	**-1.1**	**NC**	**---**
Immune and inflammation	**C1QA**	**Up (Tanabe *et al.* 2003)**		**2.39**	**1.67**
Vesicular transport proteins	**SLC17A7**	**Down (Brumovsky *et al.* 2007)**		**-1.29**	**41.45**
	SLC17A6	Down (Brumovsky *et al.* 2007)		NC	---

3.2.4 Functional analysis of differentially expressed genes

Iterative group analysis (IGA) (section 2.9.3.1.4) was used to aid in the functional interpretation of the pilot microarray data. Ontological analyses such as this simplify microarray data by identifying the ontological groups that are most changed in a data set. The top represented up and down regulated ontological groups are presented in Table 3-6 and Table 3-7. IGA can operate in a 'classic' mode whereby multiple probe sets for one gene can contribute or in a 'representative' mode, whereby only one probeset per gene is included in the analysis. I have chosen to present data from IGA analysis in the latter mode as it avoids overrepresentation of ontological groups because of genes with more than one probe set.

Table 3-6: Top upregulated groups as determined by IGA (representative mode).

TOP CHANGED GROUPS	NO. OF GROUP MEMBERS	NO. OF CHANGED MEMBERS	P VALUE	% MEMBERS CHANGED	GENES INVOLVED
1664 - G-protein-coupled receptor binding	14	3	3.6e-06	21.43	Npy Gal Ccl2
42613 - MHC class II protein complex	4	3	5.9e-06	75.00	RT1-Ba RT1-Bb RGD:735096
IPR000971 - Globin	8	3	1.1e-04	37.50	Hba-a1 LOC287167 Hbb
IPR000375 - Dynamin central region	6	2	1.3e-04	33.33	Mx2 Mx1
IPR003130 - Dynamin GTPase effector	6	2	1.3e-04	33.33	Mx2 Mx1
IPR000353 - Class II histocompatibility antigen, beta chain, beta-1 domain	2	2	1.3e-04	100.00	RT1-Bb RGD:735096
5525 – GTP binding	78	5	1.5e-04	6.41	Mx2 Rhoq Mx1 RGD:621810 Rasd1
IPR000532 - Glucagon/GIP/secretin/VIP	6	2	1.6e-04	33.33	RGD:621647 Adcyap1
5833 - hemoglobin complex	2	2	1.7e-04	100.00	Hba-a1 Hbb
IPR001401 - Dynamin	7	2	1.8e-04	28.57	Mx2 Mx1
6956 - complement activation	10	3	2.1e-04	30.00	C1qb C3 C4a

Table 3-7: Top downregulated groups as determined by IGA (representative mode)

TOP CHANGED GROUPS	NO. OF GROUP MEMBERS	NO. OF CHANGED MEMBERS	P VALUE	% MEMBERS CHANGED	GENES INVOLVED
5261 - cation channel activity	30	8	2.2e-09	26.67	Kcns3 Kcnd3 Grik1 RGD:628841 RGD:3629 Kcns1 Kcnb1 Kcnc2
IPR003131 - K+ channel tetramerisation	23	7	7.5e-09	30.43	Kcns3 Kcnd3 Kcns1 Kcnv1 Kcna1 Kcnb1 Kcnc2
IPR005821 - Ion transport protein	76	9	8.7e-09	11.84	Kcns3 Kcnd3 Scn1a Scn11a RGD:3629 Kcns1 Kcnv1 Kcna1 Kcnb1
6812 - cation transport	53	7	2.0e-07	13.21	Kcns3 Kcnd3 Scn1a Scn11a RGD:3629 Kcns1 Kcnb1
IPR006202 - Neurotransmitter-gated ion-channel ligand binding domain	36	4	6.0e-06	11.11	Htr3b Htr3a Chrna3 Glrb
IPR010526 - Sodium ion transport-associated	10	3	2.4e-05	30.00	Scn1a Scn11a RGD:3629
Calcium_regulation_in_cardiac_cells - GenMAPP	96	7	5.0e-05	7.29	Rgs4 RGD:628732 Rgs10 Gnai1 Rgs3 Atp2b3 Gnaq
IPR001990 - Chromogranin/secretogranin	4	2	1.6e-04	50.00	Scg2 Chga

3.3 qRT-PCR validation of microarray results

Changes observed in the microarray for selected genes were validated by qRT-PCR on separate samples from those used in the microarray (n=6/group (transected, sham ctrl. and naïve ctrl.) using SYBR green chemistry (see section 2.10.1). The inclusion of sham controls allowed us to test the hypothesis that the changes were a result of the transection injury and not a non-specific response to surgery and/or anaesthesia. Genes chosen for validation are described in section 3.3.3.

3.3.1 Validation of qRT-PCR reference genes

qRT-PCR data was normalised against stably expressed reference genes, the purpose of normalisation being to correct for non-specific variation, such as differences in cDNA quantity and quality which can affect efficiency of the PCR reaction. There have however been several reports of variation in supposedly stable housekeeping genes (Schmittgen and Zakrajsek 2000; Selvey *et al.* 2001) and it has been demonstrated that errors of up to 20-fold can be generated through normalization to a single housekeeping gene (Vandesompele *et al.* 2002). Consequently, normalization to a single reference gene is thought to be insufficient and it is recommended that potential reference genes are validated for stability when subject to the specific experimental manipulations in question (Thellin *et al.* 1999; Dheda *et al.* 2004). A panel of 6 housekeeping genes; 18s rRNA, GAPDH, TOP1, B2M, RPL13 and UBC were therefore assessed with Genorm (Vandesompele *et al.* 2002) and NormFinder (Andersen *et al.* 2004) to validate their stability in the sciatic nerve transection injury paradigm and hence their suitability for use as reference genes for relative quantification. The genes were chosen from separate functional pathways (with guidance from Primer Design Ltd.) in order to minimise the possibility of co-regulation. Both Genorm and NormFinder found the most stable three genes to be GAPDH, TOP1 and B2M in both transected vs. naïve and transected vs. sham samples (Figure 3-5 and Figure 3-6) and these genes were used to calculate a composite normalisation factor for analysis of subsequent experiments.

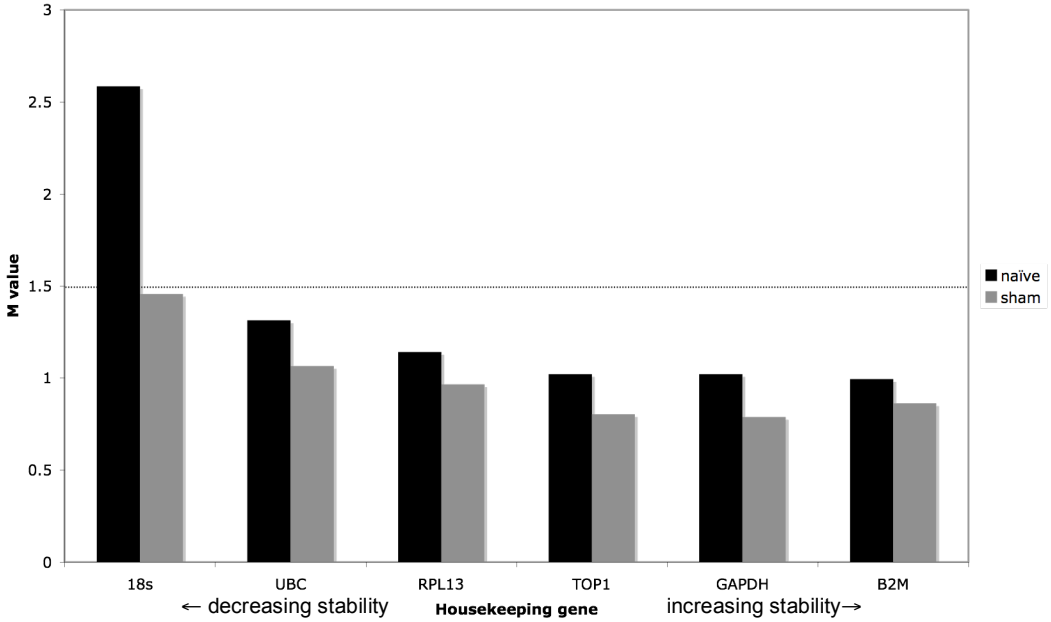

Figure 3-5: Genorm analysis of HKG stability. TOP1, GAPDH and B2M were most stable in transected vs. naive and transected vs. sham conditions. A low M value represents high stability with an M value of >1.5 indicating a gene that is unsuitable for use a reference gene (Vandesompele et al. 2002).

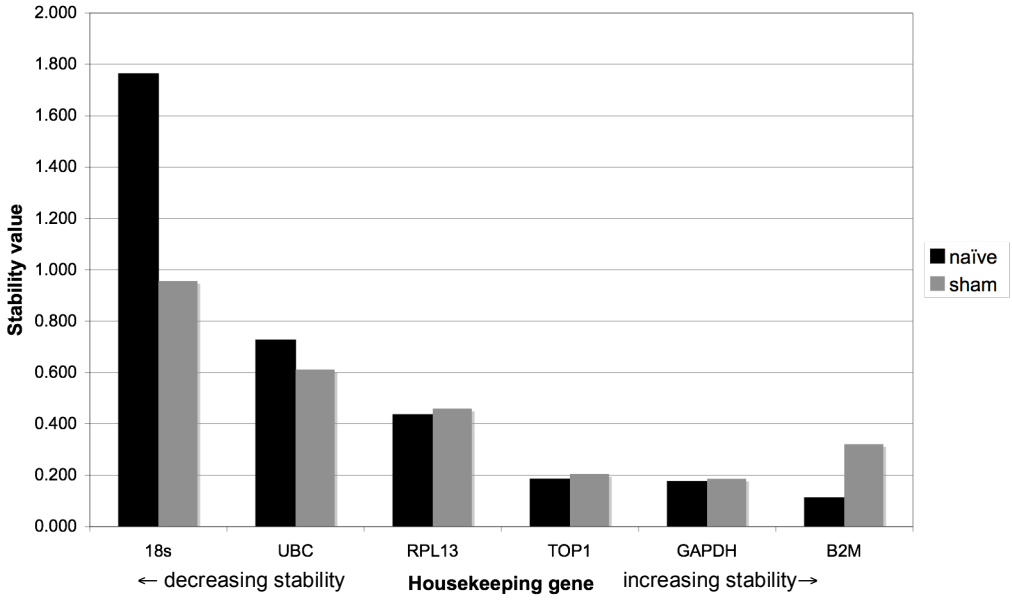

Figure 3-6: Normfinder analysis of HKG stability. TOP1, GAPDH and B2M were most stable in transected vs. naive and transected vs. sham conditions.

3.3.2 PCR efficiency testing using raw fluorescence data

LinReg-PCR (Ramakers *et al.* 2003) was used to calculate well-to-well reaction efficiencies from the amplification of target genes. Raw fluorescence data from each well were analysed and gene-specific PCR efficiencies calculated using 4-6 fluorescence data points within the log-linear phase with a correlation coefficient of r>0.99. Figure 3-7 illustrates the calculation of well-to-well reaction efficiencies for one gene.

The average PCR efficiencies obtained from LinReg-PCR for each of the reference and target genes are recorded in Table 3-8. These PCR efficiencies are significantly lower than those assumed by the $2^{-\Delta\Delta Ct}$ quantification method (one sample t-test, two tailed, $p<0.0001$). This is consistent with previous findings that indicate that the $2^{-\Delta\Delta Ct}$ method tends to overestimate reaction efficiencies (Ramakers *et al.* 2003) and thus may lead to erroneous gene expression data. Assay-specific reaction efficiencies were therefore used in subsequent data analysis with REST-MCS, a software tool that allows estimation of up and down-regulation for gene expression studies (Pfaffl *et al*. 2002) (section 3.3.3). All primer sets appeared to be functioning with similar mean efficiency (70-85 %).

Table 3-8: Mean gene specific reaction efficiencies and standard deviations as calculated by LinRegPCR.

GENE	MEAN REACTION EFFICIENCY	STANDARD DEVIATION
GAPDH	1.793	0.289
TOP1	1.713	0.185
B2M	1.789	0.258
NPTX1	1.733	0.162
ATF3	1.794	0.159
ECEL1	1.743	0.159
MX2	1.709	0.165
SEMA6A	1.848	0.200
TGM1	1.757	0.195

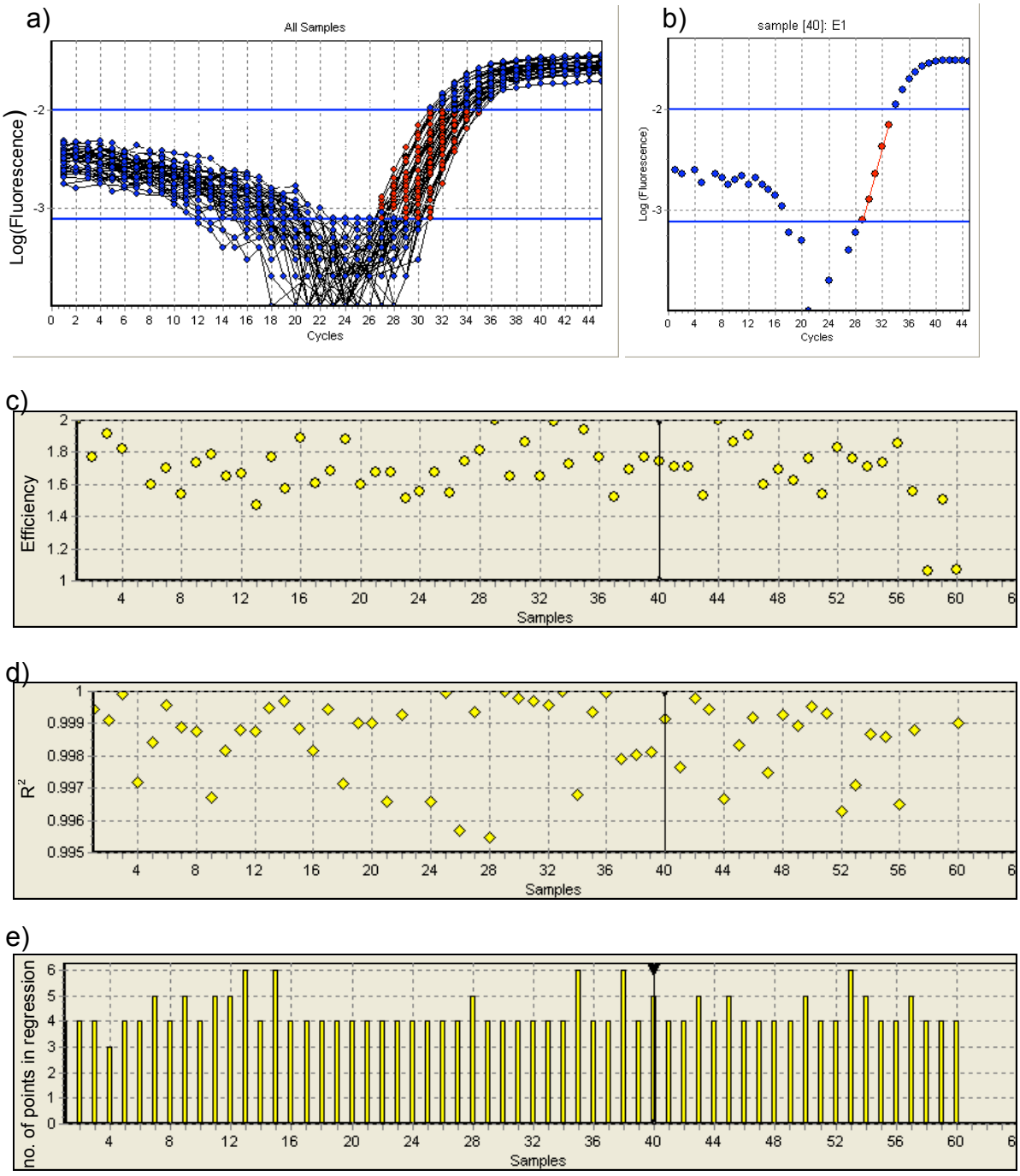

Figure 3-7: Example of determination of PCR efficiency using LinReg-PCR tool. a) Amplification plots generated from raw fluorescence data from a group of 60 samples and b) for a single sample, highlighting the points used for the linear regression c) Calculated efficiencies, d) R^2 values and e) number of points included in linear regression calculation for each sample.

3.3.3 Quantification of relative gene expression levels using REST-MCS

Figure 3-9 compares microarray and qRT-PCR expression data of the 6 genes chosen for validation. The expression of 5 of these genes in spinal cord, skeletal muscle, heart, spleen, lung and kidney was also investigated using standard RT-PCR (section 2.8.10) (Figure 3-8). The qRT-PCR results for each gene are described in the ensuing sections (3.3.3.1 to 3.3.3.6). Gene positions are for rat and according to *Ensembl* release 49.

3.3.3.1 Endothelin converting enzyme-like 1 (ECEL1)

ECEL1 (or DINE) has been mapped to position 85,939,300 - 85,945,981 on chromosome 9 in rat. It is a CNS-specific metallopeptidase and this is supported by RT-PCR that shows its expression only in CNS tissue (Figure 3-8). It undergoes an extreme transcriptional response to a variety of injury types both in the central and peripheral NS and in response to LIF and NGF deprivation (Kato *et al.* 2002). It is upregulated mainly in small-sized DRG cells after sciatic nerve transection where it has a similar regulatory pattern to galanin and as such has been suggested to share a common transcriptional machinery and neuroprotective role with this gene (Kato *et al.* 2002; Kiryu-Seo 2006). It has been shown that ECEL1 can be regulated by interaction of ATF3, c-JUN and STAT3 with the general transcription factor SP1 (Kiryu-Seo *et al.* 2008). ECEL1 (probe set 1368923_at) had a 2.42 fold-change in the microarray (FDR=1%). qRT-PCR confirmed this upregulation and this was significant for both the transection vs. naive ctrl. ($p=0.001$) and transection vs. sham ctrl. ($p= 0.001$) comparisons. There was no significant difference in expression of this gene between the naïve and sham ctrl. ($p=0.716$).

3.3.3.2 Activating transcription factor 3 (ATF3)

ATF3 (also known as LRFI and LRF1) maps to position 107,191,622 - 107,223,850 on chromosome 13 and has been previously associated with neuronal injury (Tsujino *et al.* 2000; Kataoka *et al.* 2007). It has been suggested that this gene contributes to neurite outgrowth by orchestrating gene expression in the injured neuron (Seijffers *et al.* 2006). There is also evidence of an antiapoptotic role for the gene (Francis *et al.* 2004; Hamdi *et al.* 2008). ATF3 (probe set 1369268_at) showed a large upregulation in the microarray (14.32-fold, FDR<0.01%). qRT-PCR detected a similar degree of upregulation in this gene in both the transection vs. naïve and transection vs. sham comparisons ($p=0.001$ in both cases). Again, sham and naïve controls showed no significant difference in expression of this gene ($p=0.851$).

3.3.3.3 Interferon-induced GTP-binding protein (MX2)

MX2 is located on chromosome 11, position 37,548,833 - 37,611,797. It is expressed upon interferon treatment when it localizes to the cytoplasm and has an antiviral role (Jin *et al.* 1999); (Stark *et al.* 1998). There is however support for MX2 also having an inflammatory role within the CNS as its expression has been shown to be concurrent with astrocytosis and microglial activation in rodent brain (Stobart *et al.* 2007). RT-PCR indicates that MX2 is expressed constitutively in normal spleen and lung as previously reported (Asano *et al.* 2003), also in kidney, skeletal muscle and spinal cord but not in heart (Figure 3-8). MX2 (probe set 1369202_at) was upregulated 5.35-fold (FDR<0.01%) in the microarray and dominated the IGA ontological analysis. qRT-PCR confirmed this upregulation in comparisons of transection with both the control groups and was significant for the transection vs. sham comparison (p=0.007) although the transection vs. naïve comparison misses significance (p=0.074). There was however no significant difference between the sham and naïve groups (p=0.973).

3.3.3.4 Neuronal pentraxin 1 (NPTX1)

NPTX1, mapped to position 108,918,661 - 108,927,625 on chromosome 10, has been reported to be localized exclusively to the nervous system where it may mediate the uptake of synaptic material (Omeis *et al.* 1996). This is contrary to the results of the standard RT-PCR that suggested a fairly ubiquitous expression in all tissues examined apart from spinal cord (Figure 3-8). NPTX1 is also thought to be involved in extracellular matrix reorganization and its expression was shown to be increased following a treatment that led to decreased collagen content in the male reproductive tract (Yasuhara *et al.* 2008). NPTX1 (probe set 1370517_at) was downregulated in the microarray (-2.88-fold, FDR<0.01%). qRT-PCR analysis of this gene also showed downregulation in this gene in comparisons with both the naïve and sham ctrl groups although insignificant (p=0.414 and p=0.743, respectively). These changes were however significant before normalization (p=0.005 for transection vs. naïve and p=0.046 for transection vs. sham). There was no significant difference between the two ctrl. groups (p=0.743).

3.3.3.5 Semaphorin 6A (SEMA6A)

SEMA6A, mapped to chromosome 18, position 41,545,337 - 41,666,255, is one of the less well characterized members of the large semaphorin family of axonal guidance molecules (see also section 1.2.2.2). As well as its role in axon guidance, SEMA6A is expressed in the cytoskeleton in association with beta-actin and has thus been suggested to have a role in modulating tubulin isotype composition (Prislei *et al.* 2008). During spinal cord development SEMA6A expression is localized to the cells at the PNS/CNS interface and is thought to be necessary for prevention of the emigration of motoneurons out of the ventral spinal cord and for correct segregation of the dorsal roots (Bron *et al.* 2007; Mauti *et al.* 2007). RT-PCR did however suggest a fairly ubiquitous expression of the gene in all the tissues examined (Figure 3-8). SEMA6A (probe set 1376601_at) exhibited a fairly large upregulation in the microarray (6.35 fold, FDR<0.01%). This change was validated in the transection vs. sham comparison (p=0.004) and was of a similar magnitude.

Upregulation of this gene was also seen in the transection vs. naïve comparison although this was insignificant (p=0.162). No significant difference was found between the control groups (p= 0.422).

3.3.3.6 Transglutaminase 1 (TGM1)

TGM1 (also known as TGR) is located on chromosome 15, position 33,846,335 - 33,859,759 where it encodes a cross-linking enzyme. Its expression has been most well characterised in keratinocytes where mutations in this gene cause a skin disorder called lamellar ichthyosis (Boeshans *et al.* 2007). RT-PCR provided evidence for a ubiquitous expression of this gene in all tissues examined with highest expression in heart, spleen and lung (Figure 3-8). There is evidence for a role for this gene in axonal regeneration as TGM1 promotes axonal elongation at the surface of retinal ganglion cells after optic nerve injury (Sugitani *et al.* 2006). TGM1 (probe set 1370051_at) showed a 2.83 fold change in the microarray (FDR 0.36%). qRT-PCR validated this change with significant upregulation of this gene seen in both the transected vs. naïve and transected vs. sham comparisons (p=0.002 and p=0.003, respectively). There was no significant difference between the sham and naïve groups (p=0.922).

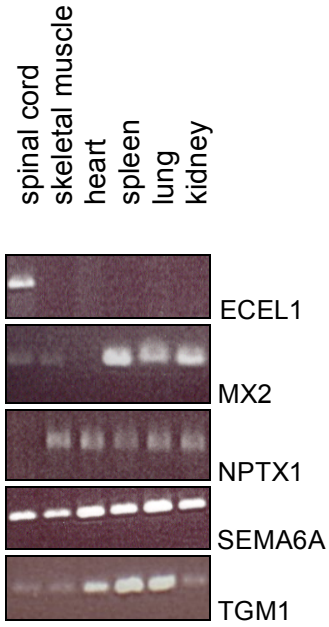

Figure 3-8: Expression of selected genes in normal rat tissues. 2 μl PCR product was loaded in each well of a 2% agarose gel.

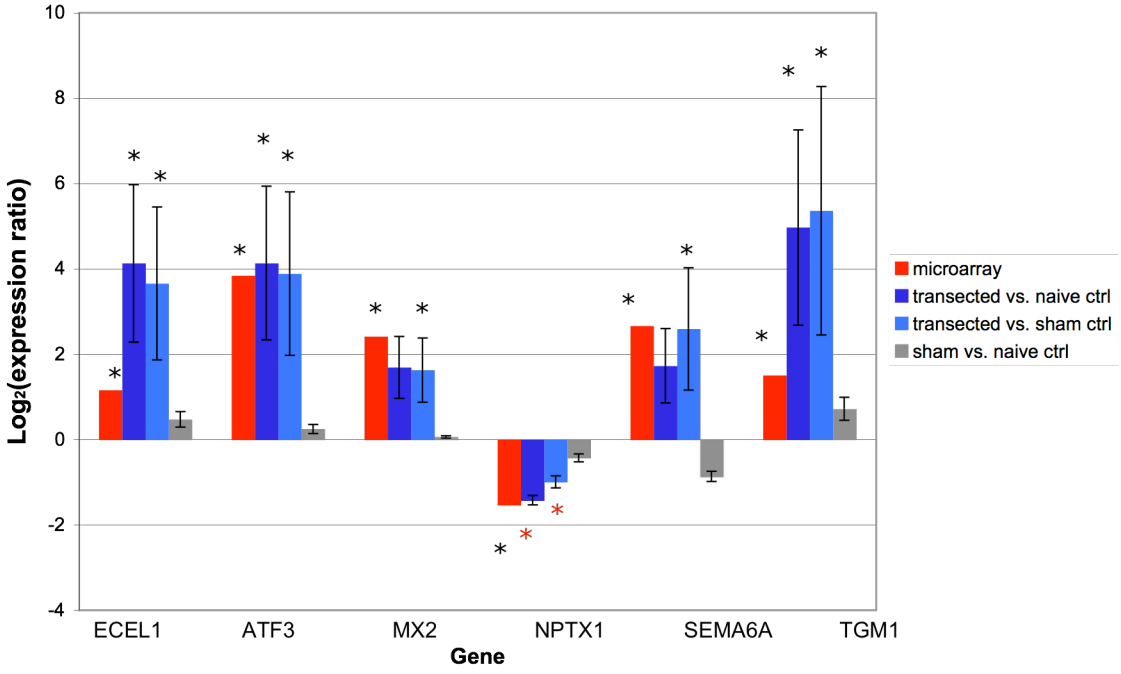

Figure 3-9: Validation of microarray by qRT-PCR. Log_2expression ratio (± S.E.M, n=5-6). *= p<0.01 for the plotted qRT-PCR comparison or FDR <5% in the case of the microarray experiment. *=p<0.05 before normalization to housekeeping genes.

3.3.4 Correlation between fold changes determined by microarray and qRT-PCR

Microarray fold changes for each gene were plotted against the fold changes obtained by qRT-PCR for the qRT-PCR. Although direction of change was the same in the qRT-PCR as the micrarray, fold changes tended to be greater in the qRT-PCR leading to a weak correlation (R= 0.267 and R=0.460, p>0.05 (d.f=4) when microarray was compared to qRT-PCR using naïve and sham ctrl, respectively). This is consistent with past studies that have shown qRT-PCR to provide larger fold change estimates than microarray due to greater sensitivity of the assay. In addition, it has been demonstrated that microarray fold change estimates arising from RMA normalized data are significantly lower than nominal fold changes calculated from spiked in controls (Cope *et al.* 2004).

a)

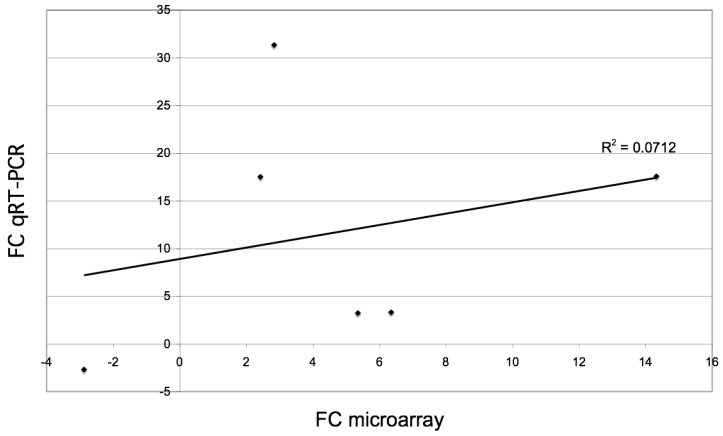

b)

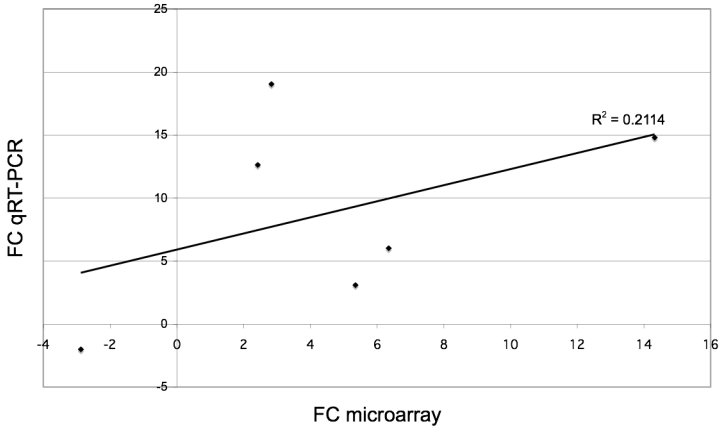

Figure 3-10: Correlation between qRT-PCR and microarray fold change data. a) microarray vs. qRT-PCR with naive ctrl, b) microarray vs. qRT-PCR with sham ctrl.

3.4 Further optimisation of experimental parameters

3.4.1 Laser capture microdissection

The DRG is a heterogeneous tissue containing schwann cells, satellite cells, fibroblasts, inflammatory cells and vascular endothelium/smooth muscle cells, as well as the sensory neuron cell bodies that are of interest to this study. LCM was investigated as a method to obtain a homogeneous population of sensory cells from which RNA could be extracted for microarray purposes, the advantage of a pure population of sensory cells being that gene expression changes in these cells of interest will be neither exaggerated nor obscured by changes in other cell types.

Sensory nerve cells were successfully captured from thin, toluidine-blue stained DRG sections mounted on poly-L-lysine coated slides following unsuccessful attempts to capture cells from plain slides (Figure 3-11). Approximately 2000 cells were captured onto each cap and subjected to lysis and subsequent total RNA isolation (Section 2.8.5.4).

Total RNA yield/2000 cells ranged from 0-50 ng and was thus insufficient quantity for use in microarray experiments using the Affymetrix standard protocol. Whilst there have been reports in previous studies of LCM successfully producing material for microarray experiments (Luo *et al.* 1999) this hasn't been without the subsequent use of several rounds of T7 amplification (Eberwine method). The small sample protocol for Affymetrix requires >100 ng of good quality RNA as starting material. Although this quantity of RNA may have been achievable with the use of additional animals, the high 260/280 ratios (2.35- 3.21) of the RNA originating from laser captured cells suggested the presence of degraded RNA and it can be envisioned that RNA damage may have occured in the DRG sections during staining, fixing, dehydration or use of the laser itself. Since high quality, intact RNA is key to the quality of microarray experiments, LCM was pursued no further and whole DRG were again used in the main microarray experiment.

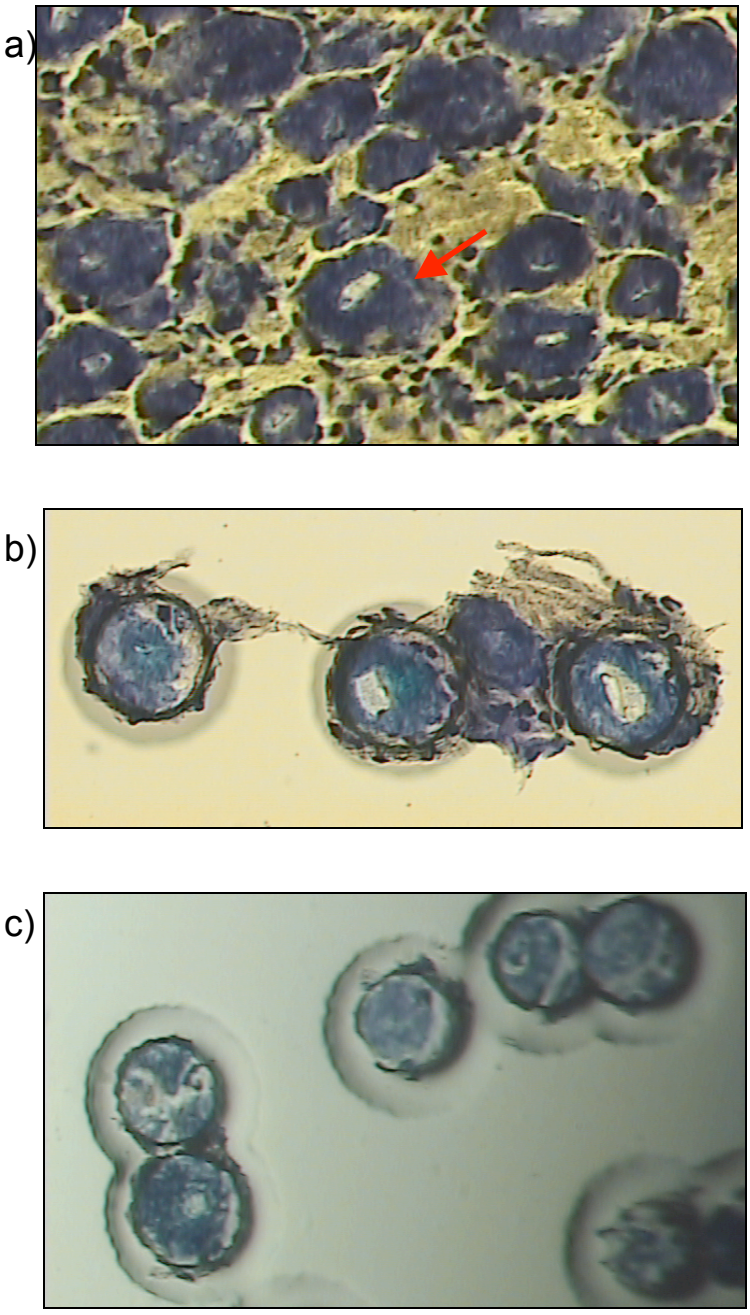

Figure 3-11: Laser capture microdissection of DRG cells. a) Toluidine blue stained DRG section. DRG cells captured from sections mounted on b) plain slides and c) Poly-L-Lysine coated slides. The arrow in a) indicates a cell of correct morphology for capture.

3.4.2 Homogenisation in buffer RLT improves RNA integrity

RNA extraction for the pilot microarray had been carried out using TriReagent as a lysis buffer. RNA obtained using this method showed an unusual bioanalyser profile, showing only one peak and also only one band when run on an agarose gel. An alternative method of RNA extraction using buffer RLT (Qiagen) was investigated and this appeared to improve RNA integrity (Figure 3-12). All subsequent homogenisations for the main microarray experiment were therefore carried out in buffer RLT and total RNA obtained had an RIN of >7 (Schroeder *et al.* 2006).

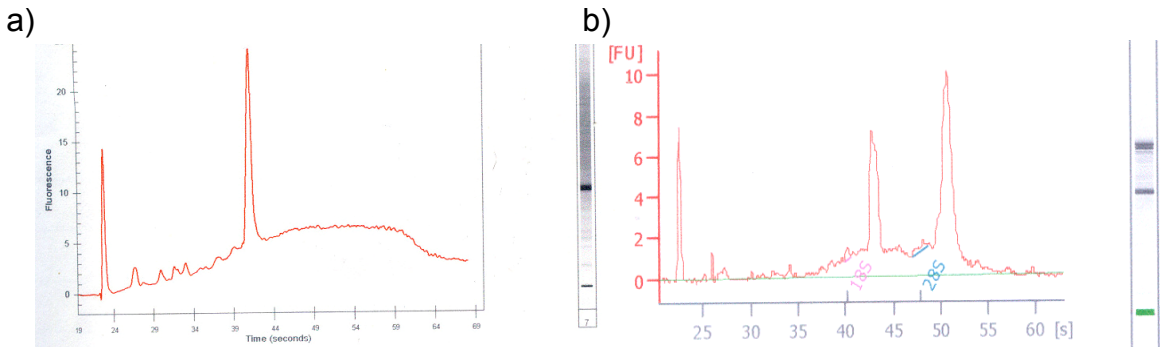

Figure 3-12: Typical bioanalyser traces for RNA extracted after a) trizol homogenisation and b) buffer RLT homogenisation. Trizol homogenized RNA shows an absence of the 28s peak.

3.5 Discussion and summary

Sciatic nerve transection elicits changes in the regulation of hundreds of genes in the DRG (Costigan *et al.* 2002; Tanabe *et al.* 2003). The pilot microarray was successful in detecting gene expression changes in the DRG at 8 days following a sciatic nerve transection (~1.5 % of probes, <5%FDR) and many of these changes were consistent with those already reported in past studies (Table 3-5) providing *in silico* validation of the data in addition to the qRT-PCR validation.

3.5.1 Sample and experiment quality

RNA quality is of paramount importance to microarray experiments and our method of rapid isolation and freezing of DRGs in liquid nitrogen after perfusion of the rat with ice cold mammalian ringer yielded good quality RNA as indicated by high RINs. An alternative method of DRG isolation has since come to light that may further improve RNA quality and could be considered for future projects. (LeDoux *et al.* 2006) perfusion fixed rats with RNAlater before isolation of DRGs. This avoids the potential for introduction of RNases during the perfusion step and eliminates the need for freezing of tissue, hence reducing freeze-thaw degradation of RNA.

Although LCM was investigated as a method to obtain a pure population of sensory nerve cells for the main microarray it was decided that whole DRG would again be used allowing higher quality total RNA to be obtained with a reduction in animal numbers. In addition, it can be argued that the inflammatory response after injury of non-neuronal cells within the DRG is inextricably linked to regeneration and therefore gene responses in these cells are also of interest to this study. Indeed, it has been suggested that inflammation near the nerve cell body enhances axon outgrowth and that axotomy-induced mitosis of glial satellite cells is a mechanism by which conditioning lesions facilitate regeneration after a subsequent injury to the central branch (Lu and Richardson 1991). Microarray analysis of whole DRG has value in that it gives an overall picture of gene expression changes in the neuronal cells and also the non-neuronal cells in close proximity to them. Further investigation of individual genes and their gene products using *in situ* hybridisation and immunohistochemistry will allow their spatial expression within the DRG to be disseminated.

Quality control assessment of the microarray data suggested that experimental chip F showed slightly different sample quality (Table 3-1), hybridization profile (Figure 3-2) and distribution of gene changes (Figure 3-3) than the ctrl chips and more importantly, the other two chips in the sciatic transection triplicate. The other chips were hybridized separately from chip F, and using material collected and processed by a different experimenter than chip F, highlighting the importance of consistency in the preparation of material for microarray and also the importance of hybridizing all chips for one experiment together using chips from a single batch. Whilst there is argument to exclude chip F from the analyses, bioinformatics advice was sought and the decision was taken to include this final chip. In addition, RP lists generated with and without inclusion of this chip did not differ greatly in the genes regulated at <5% FDR.

3.5.2 Consistency with past studies and biological validity

3.5.2.1 Expression of regeneration and pain associated genes

The microarray yielded data that was consistent with past studies of the DRG response to sciatic nerve injury. It is known that the sciatic nerve undergoes a regenerative response to injury and is associated with neuropathic pain. Gene regulation reflected this with changes in expression of several known regeneration- associated genes (RAGs) and neurotrophic factors and in neuropeptides known to modulate pain transmission. Among the top upregulated genes (Table 3-3) were genes previously implicated in axonal regeneration (ARG1, SPRR1A and ATF3) or neuronal development. ARG1 (3.69-fold upregulated) and SPRR1A (7.15-fold upregulated) have been shown to be downstream effectors of the cAMP-mediated conditioning lesion effect (see also section 1.4.2.1). ATF3 showed a 14.32-fold upregulation which was confirmed by qRT-PCR (Figure 3-9) and is an attractive candidate RAG as not only is it upregulated in all DRG cells after a peripheral but not a central axonal injury (Tsujino *et al.* 2000), but it also enhances neurite outgrowth in culture (Pearson *et al.* 2003; Seijffers *et al.* 2006). Furthermore, in mice overexpressing ATF3 the rate of peripheral nerve regeneration was increased to an extent comparable to a conditioning lesion although overexpression was not sufficient to overcome the inhibitory effects of myelin to promote regeneration in the spinal cord *in vivo* (Seijffers *et al.* 2007). The upregulation of growth associated genes such as SPRR1A in these ATF3 overexpressing mice also suggests that ATF3 can regulate expression of regeneration enhancing genes and thus increases the intrinsic growth state of neurons. The neurotrophic factor PAP (REG2) (upregulated 8.82-fold in our study) is upregulated in axons and DRG cells after sciatic nerve injury and is thought to have a mitogenic effect on Schwann cells and a proregenerative effect on sensory and motor neurons (Livesey *et al.* 1997). More recently (Averill *et al.* 2002) showed REG2 to have a dynamic expression in DRG neurons after injury, with expression moving from small to large size DRG cells.

Expression of genes with a putative neuroprotective role was also increased. GADD45a, which showed a 4.12-fold upregulation in our study, is not constitutively expressed in adult or embryonic DRG neurons but has been previously shown to be upregulated after peripheral nerve injury but not after dorsal rhizotomy (Costigan *et al.* 2002; Befort *et al.* 2003). The function of this gene is unclear but its upregulation after various lesions has led to the suggestion that it has a role in neuroprotection after injury (Jin *et al.* 1996; Uberti *et al.* 2002).

Also among the top upregulated genes were genes involved in nervous system development, consistent with the theory that regeneration may in part recapitulate developmental gene expression. The transcription factor SOX11, 3.02-fold upregulated in our microarray, has been shown to be upregulated after sciatic nerve injury (Tanabe *et al.* 2003) and is expressed during neuronal development although its role in regeneration is not well characterised (Uwanogho *et al.* 1995; Jankowski *et al.* 2006; Kim *et al.* 2008). SEMA6A, a member of the large semaphorin family of axon guidance molecules expressed in development and thought to limit plasticity in the adult

CNS was 6.35-fold upregulated. While it may seem paradoxical that a molecule that limits plasticity in the CNS is re-expressed during axonal regeneration in the PNS, a new role for this molecule in modulating microtubule dynamics has been suggested (Prislei *et al.* 2008) and it is conceivable that the upregulation of SEMA6A could therefore reflect a need for microtubule remodeling during axonal outgrowth.

Another gene involved in microtubule modulation was also upregulated. The expression of microtubule disassembly molecules such as stathmins has been shown to be upregulated during regeneration (Iwata *et al.* 2002) and STMN4, upregulated 3.56-fold in our microarray, has been previously shown to be upregulated following optic nerve axotomy (Nakazawa *et al.* 2005). Stathmins have a role in tubulin regulation (Jourdain *et al.* 2004; Ravelli *et al.* 2004) and stathmin deficient mice develop axonopathy indicating that stathmin is important for maintenance of axonal integrity (Liedtke *et al.* 2002).

Also consistent with past studies, the neuropeptides VIP, GAL and NPY, known to contribute to the mechanisms of neuropathic pain, were among the top upregulated genes (Ma and Bisby 1998). These neuropeptides are thought to be upregulated by the activation of c-jun, which is also upregulated following sciatic nerve injury (Son *et al.* 2007). Galanin (GAL) showed a 12-fold upregulation after axotomy as has already been reported (Kashiba *et al.* 1994; Sun and Zigmond 1996; Sun and Zigmond 1996; Ma and Bisby 1999). GAL has been shown to have a complex role in the modulation of pain with facilitatory and inhibitory effects (reviewed in (Xu *et al.* 2000) as well as a role in nerve regeneration and knock-out mice have significantly reduced axonal regeneration after sciatic nerve injury (Holmes *et al.* 2000). The IL-6 and LIF cytokines positively regulate Gal expression suggesting an involvement of the JAK/STAT (Figure 1-11) pathway in its regulation (Thompson *et al.* 1998). Besides neuropeptides, upregulation was also seen in the chemokine CCL2 (3.2-fold upregulation). Mice overexpressing CCL2 have enhanced nociceptive responses suggesting that this gene has a role in modulation of pain (Menetski *et al.* 2007).

Many of the downregulated genes have also been reported in past studies of this type. RGS4 encodes a GTPase boosting protein that is expressed constitutively at high levels in adult sensory DRG neurons and is downregulated by axotomy (Costigan *et al.* 2003). This downregulation is therefore likely to cause an increase in G-protein coupled receptor sensitivity and RGS4 has been upregulated in sciatic nerve ligation and is thought to contribute to neuropathic pain via attenuation of opioid signaling via G protein coupled receptors (Garnier *et al.* 2003).

There was also a generalized depression in the expression of various ion channels and neurotransmitter receptors suggesting a transcriptional switch away from neurotransmission following injury. The downregulation of voltage-gated potassium channels dominated the IGA ontological analysis (Table 3-7) and the delayed rectifier, subfamily S, member 3 (KCNS3) was the top ranked downregulated gene according to RPA (**Table 3-4**). This has been previously reported following chronic constriction (Kim *et al.* 2002) and transection (Park *et al.* 2003) of the sciatic nerve. This reduction of K+ current is thought to contribute to the electrical abnormalities in primary sensory neurons that are involved in the generation and maintenance of neuropathic pain and

allodynia. There was also downregulation of serotonin receptors and although 5-HT3 receptor expression has been shown to be downregulated in motor neurons of the spinal cord after sciatic nerve lesion (Rende *et al.* 1999), there have been to my knowledge no reports of how type 3 serotonin receptor are regulated in the DRG after injury. 5-HT3a and 3b are constitutively expressed on small medium and large size DRG neurons (Morales *et al.* 2001; Nicholson *et al.* 2003) and decreased expression of these receptors is likely to result in a reduction in the excitability of afferent neurons.

3.5.2.2 Immunological and inflammatory gene changes

The DRG is known to undergo inflammatory and immunological changes as a result of peripheral nerve injury, such as infiltration of macrophage and lymphocytes (Hu and McLachlan 2002). Inflammation is thought to both enhance regeneration (Lu and Richardson 1991; Golz *et al.* 2006) and contribute to neuropathic pain (Znaor *et al.* 2007). We would therefore expect there to be upregulation of genes involved in inflammation and immune response. Indeed, ontological analysis (Table 3-6) shows upregulation of genes involved in activation of complement and presentation of antigens. The presence of Mx2 and Mx1 which dominate the ontological analysis and which are interferon-inducible genes (Asano *et al.* 2003) provides indirect evidence for there being activation of interferon-expressing glia (Cameron *et al.* 2003). Additionally, Reg-2, mentioned above and upregulated in our microarray has been shown to be upregulated when inflammation is induced in DRGs (Averill *et al.* 2008).

3.5.3 qRT-PCR successfully validated microarray gene expression changes

Six genes were selected and confirmed as being regulated thus further validating the microarray and optimising the qRT-PCR assay for use later in the project. Furthermore, to our knowledge, this is the first report of the thorough evaluation of housekeeping genes for use as reference genes in the sciatic nerve transection experimental paradigm. The importance of the use of appropriate reference genes in relative quantification of qRT-PCR has already been discussed (section 3.3.1) and given that this injury model is widely used in studies of neuropathic pain and neuronal regeneration it is of significant value that a set of stably expressed HKGs is established. The combined use of TOP1, GAPDH and B2M for normalization of qRT-PCR data in future studies of this kind is recommended.

For the six validated genes there was no significant difference between their expression in the sham operated and naïve controls suggesting that their regulation was a genuine response to transection injury and not due to non-specific effects of surgery. All genes, with the exception of NPTX1 were significantly increased after transection in both the microarray and qRT-PCR and may therefore contribute to the regenerative response of the sciatic to injury. The downregulation of

NPTX1 after sciatic injury may represent removal of a plasticity-limiting factor or simply downregulation of an unneeded synaptic protein.

Whole DRG were used in the microarray and thus we cannot be certain as to which cells expressed these genes, however, MX2 is most likely to be induced as part of an inflammatory response to injury through the proliferation of non-neuronal astrocytic and glial cells that exist in the DRG as its expression is concominant with microglial activation (Stobart *et al.* 2007). Further investigation using *in situ* hybridization techniques on DRG sections could elucidate the locus of the gene expression changes.

3.5.3.1 Summary

In summary, the pilot microarray generated data that was both biologically valid as well as consistent with past studies of sciatic nerve transection. LCM was investigated but did not provide RNA of a sufficient quantity or quality for use in our main experiment. Finally, qRT-PCR with an n of 5-6 successfully validated changes in six genes that were regulated in the microarray experiment and identified suitable reference genes for future use in experiments of this kind.

4 Determination of time points to study regeneration

4.1 Introduction and Aims

In order that putative regeneration-associated genes could be identified from our microarray study, a key prerequisite was that neuronal regeneration was occurring at our chosen time points. Examination of past studies of nerve regeneration following peripheral nerve injury in the rat revealed a confusing range of estimates of regenerative rate (2.5- 5 mm/day) (McQuarrie 1975; Forman and Berenberg 1978; Forman *et al.,* 1979; Bisby 1985; Danielsen *et al.,* 1986; Mandys *et al.,* 1991; Verdu and Navarro 1997; Kamijo *et al.,* 2003; Lozeron *et al.,* 2004) In addition, whilst a large number of studies have focussed on regeneration following sciatic nerve crush or transection injury, few have examined regeneration following the spinal nerve and dorsal root crush injuries that are relevant to this study. We aimed therefore, to obtain our own estimate of the rate of neuronal regeneration in the rat following dorsal root and spinal nerve crush to allow us to choose a time point at which fibres are actively regenerating (i.e. have not reached distal targets in the hind limb in the sciatic nerve or have not reached the dorsal root entry zone (DREZ) in the case of the dorsal root). We also wished to choose a later time point for the dorsal root by which time its fibres will have reached the DREZ and ceased to regenerate. We hoped that this would allow comparison of gene expression during regeneration and at a time when regeneration is blocked in the dorsal root. To determine these time points we employed two main approaches; a tract tracing approach using Cholera Toxin B (CTB) or Biotin Dextran Amine (BDA) and an electrophysiological approach.

4.2 Tract tracing with CTB

4.2.1 Introduction

Cholera toxin subunit B (CTB) is commonly used as a tool for the retrograde and anterograde labelling of neurons. CTB binds via the pentasaccharide chain of the ganglioside G_{M1} and is thus selectively taken up by and transported in the large diameter myelinated neurons that express this ganglioside. The sciatic nerve contains the afferents of the L4 and L5 DRGs. Therefore, it was expected that in an intact animal, injection of CTB into the proximal sciatic nerve would cause labelling of the large diameter cells of the L4 and L5 DRGs. In contrast, it was expected that for a certain time period following a complete spinal nerve crush, no CTB labelling would be seen in the corresponding DRG, indicating that the nerve had yet to reinnervate distal targets and was thus still regenerating.

Male SD rats (244-284 g) underwent a spinal nerve crush 5-8 mm distal to the DRG (section 2.2.5) and a second operation two weeks (n=3) or one week (n=3) later to inject CTB into the proximal sciatic nerve (section 2.3.2). CTB labelling in the L4 and L5 DRGs was examined using indirect

immunofluorescence three days following CTB injection. CTB labelling in the L4 and L5 DRGs was also examined after CTB injection in control rats (n=3) that had not undergone a crush injury. Again, three days was allowed for transport of the CTB following its injection into the proximal sciatic nerve. The animals were then perfused with fixative and tissues removed for histological processing (section 2.3.3). Labelling of longitudinal DRG sections with anti-NF200 and anti-CGRP allowed visualisation of myelinated and unmyelinated fibres respectively and identification of cell types containing CTB.

4.2.2 Three days is adequate for CTB transport and DRG labelling

Three days following CTB injection into the proximal sciatic nerve of normal nerve intact animals, CTB labelling was detected mainly in the large diameter cells of the L4 and L5 DRGs (Figure 4-1). As expected, CTB staining mainly co-localised with NF200 fluorescence but not CGRP indicating that CTB was transported in the large, NF200 expressing myelinated axons.

4.2.3 Absence of CTB labelling in spinal nerve crushed animals confirms efficacy of crush injury.

1 week following L4 spinal nerve crush and CTB injection into the distal sciatic nerve (~52mm distal to crush site), CTB labelling was present within the L5 DRG. CTB labelling was absent within the L4 DRG (Figure 4-2), confirming to the extent possible using this approach, that the crush was indeed complete.

4.2.4 CTB tract tracing may overestimate rate of regeneration after spinal nerve crush

2 weeks following L4 spinal nerve crush and CTB injection into the distal sciatic nerve (~52mm distal to crush site) it was expected that there would be an absence of CTB labelling within the L4 DRG (based on an estimate that peripheral nerves regenerate at a rate of 1mm/day) and CTB labelling within the L5 DRG (the internal control). CTB labelling was however observed in the large diameter cells of both the L4 and L5 DRGs. Additionally, CTB labelling was observed within small diameter cells in the L4 DRG and is presumed to be a consequence of G_{M1} ganglioside expression in damaged small unmyelinated fibres (Figure 4-3).

The high level of labelling within the L4 was surprising, and suggested a faster rate of regeneration (>3.7 mm/day) than estimates from some previous studies. However, it is likely that CTB may have diffused proximally encountering regenerating fibres further up the nerve and hence overestimating regenerative rate (Shehab *et al.,* 2003), led to investigation of another tract tracer approach using BDA.

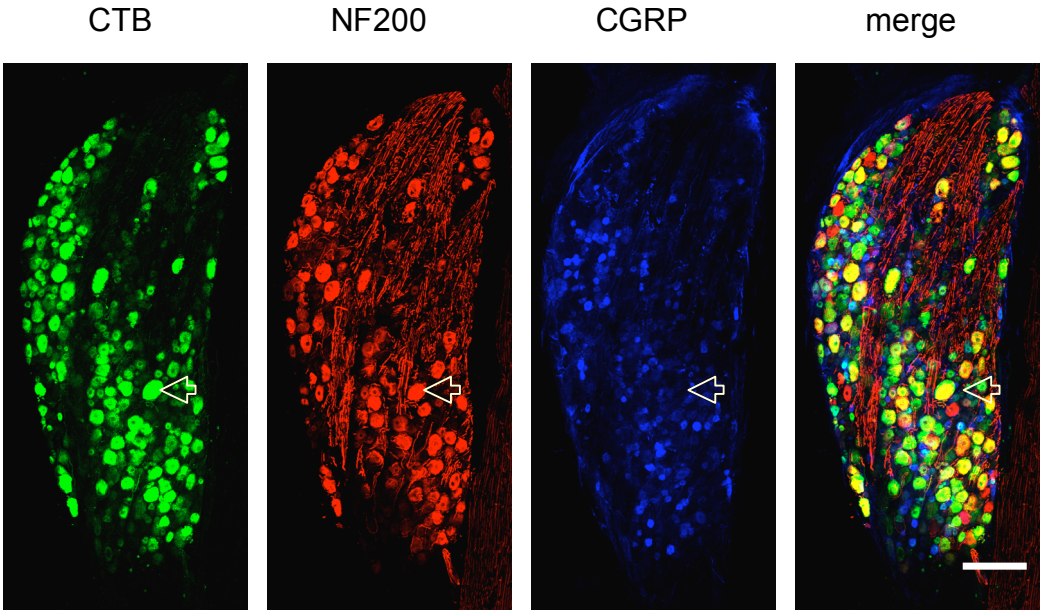

Figure 4-1: CTB, NF200 and CGRP labelling within an L4 DRG of an intact control animal. Yellow cells within the merged image indicate where CTB staining is colocalised with NF200 (arrow indicates an example). Scale bar = 100 μm.

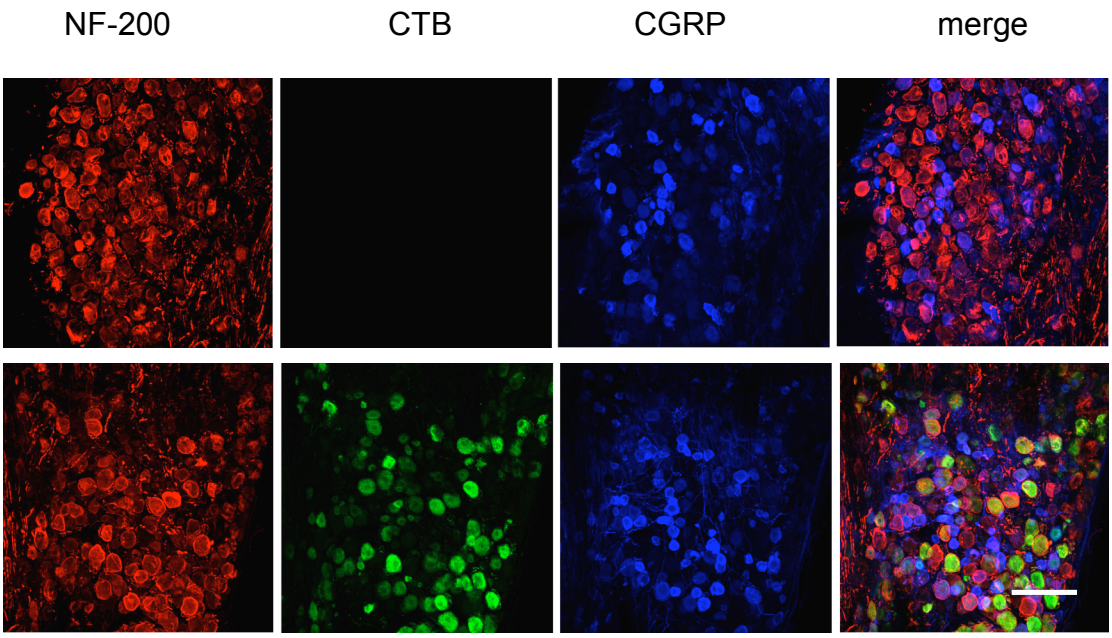

Figure 4-2: CTB labelling of DRG cells 1 week post- L4 spinal nerve crush. CTB was injected at 52 mm from the crush site. There was an absence of CTB labelling in the L4 DRG (top panel). CTB labelling in L5 DRG of same animal (bottom panel) acts as a positive control indicating that CTB has had adequate time to travel the length of the nerve. The absence of CTB labelling in the L4 DRG therefore indicates a complete crush of all L4 spinal nerve fibres. Scale bar = 200 μm.

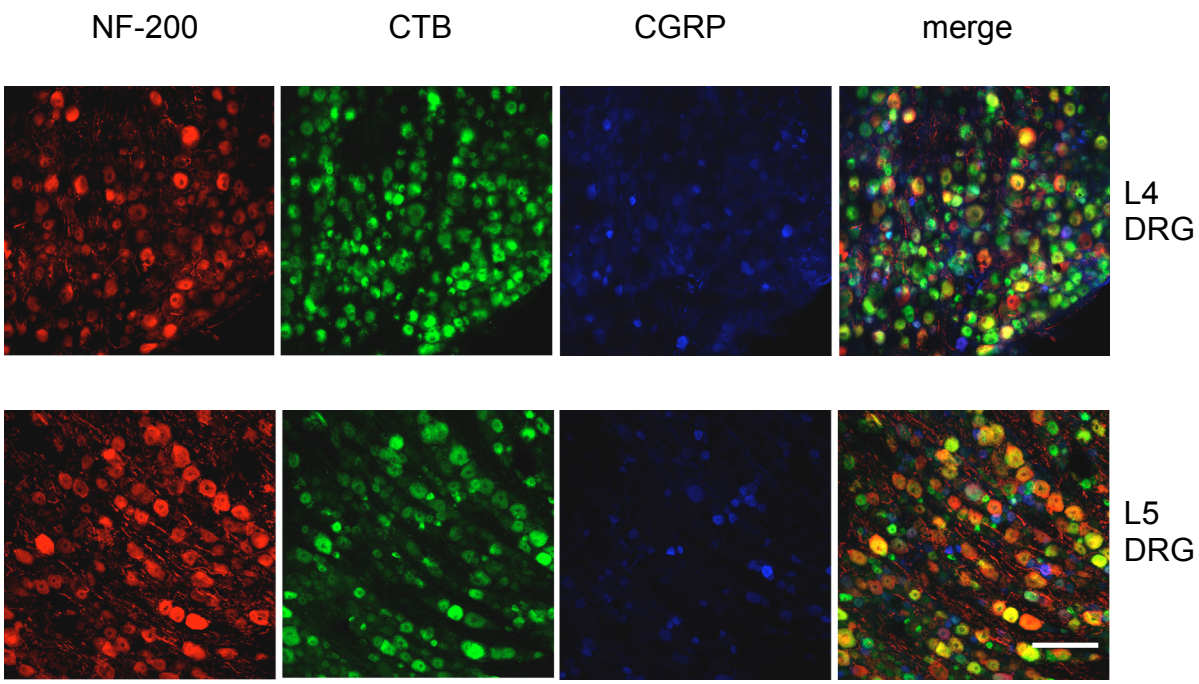

Figure 4-3: CTB labelling in DRG cells 2 weeks following spinal nerve crush. CTB was injected at 52 mm from crush site. CTB labelling is present in both the L4 DRG (top panel) and the L5 DRG that served as an internal control (bottom panel). Scale bar = 200 μm.

4.3 Tract tracing with BDA

4.3.1 Introduction and Aims

The results from the experiments using CTB to determine the rate of regeneration within the spinal/sciatic nerve following spinal nerve crush suggested that the rate of regeneration was at least 3.7 mm/day. This supported the findings of Lozeron et al. (2004), who, using a retrograde tracer method, showed that the axonal growth rate for unmyelinated and myelinated sensory fibres following sciatic nerve crush was 3.7 mm/day. However, neither this study nor our experiment could show to what extent the result was attributed to distal diffusion of the tracer within the nerve fascicle, as has been reported previously (Shehab *et al.,* 2003).

To test the findings of the CTB experiments, we used Biotin Dextran Amine (BDA) to visualise the progress of the regenerating nerve fibres. BDA (10kD) is a neuroanatomical tracer that is taken up endocytically by intact nerves and diffuses laterally within the plane of the cell membrane in a predominantly anterograde direction. These transport properties mean that unlike CTB, that undergoes vesicular transport and which produces a granular appearance within the cell soma, BDA produces a much smoother labelling of the complete nerve fibre. BDA is however transported more slowly than CTB and it was therefore necessary to check that BDA's transport rate was sufficient (at least 3.7 mm/day) to test the findings of the previous experiments.

Male SD rats (263-316 g, n=2) underwent an operation to inject BDA into the L4 spinal nerve (section 2.2.5) and perfused with fixative seven days later. BDA progress both centrally and peripherally was examined by indirect immunofluorescence (section 2.3.3). BDA labelling was then used to assess L4 dorsal regeneration at the proposed microarray time points 2 weeks (n=2) and 6 weeks (n=2) after a dorsal root crush injury (section 2.2.4). In each case BDA was injected seven days prior to sacrifice to allow adequate time for transport of the tracer.

4.3.2 Seven days is sufficient for BDA to label the whole dorsal root in a control animal

At 7 days post-BDA injection, BDA labelling was observed along the entire length of the L4 dorsal root (20 mm) and within the L4 segment of the spinal cord suggesting that the tracer would be useful in tracking the progress of regenerating fibres within the dorsal root. Labelling could be seen within the left dorsal horn and also within the motor neurons in the left ventral horn suggesting that the injection had successfully labelled the majority of fibres, both sensory and motor (Figure 4-4)

4.3.3 BDA transport rate and quality of labelling is insufficient to track regeneration following spinal nerve crush

Poorer BDA labelling was observed in the sciatic nerve up until ~24mm from the injection site within the sciatic nerve suggesting that BDA travels through the spinal/sciatic nerve at a rate of approximately 3.43 mm/day. BDA was therefore unsuitable to trace the progress of a regenerating peripheral nerve as the results from the CTB experiments suggested that nerve fibres within the sciatic nerve regenerate at a rate of >3.7 mm/day following spinal nerve crush.

4.3.4 Dorsal root fibres have not yet reached the DREZ two weeks post-dorsal root crush.

At 2 weeks following L4 dorsal root crush, BDA labelled nerve fibres could be observed along the majority of the dorsal root but not in the dorsal rootlets at the DREZ (Figure 4-5 top panels). This suggested that at 2 weeks following dorsal root crush, the nerve fibres are yet to reach the DREZ and are thus still regenerating and confirmed 2 weeks as a suitable early time point for our study.

4.3.5 Dorsal root fibres have reached the DREZ six weeks post-dorsal root crush

At 6 weeks post dorsal root crush, more extensive BDA labelling was observed along the whole length of the dorsal root and also in the dorsal rootlet at the entry to the spinal cord (Figure 4-5 bottom panels). This suggested that the fibres had regenerated as far as the DREZ and, as such, 6 weeks was a suitable late time point at which to examine genes involved in arrested regeneration.

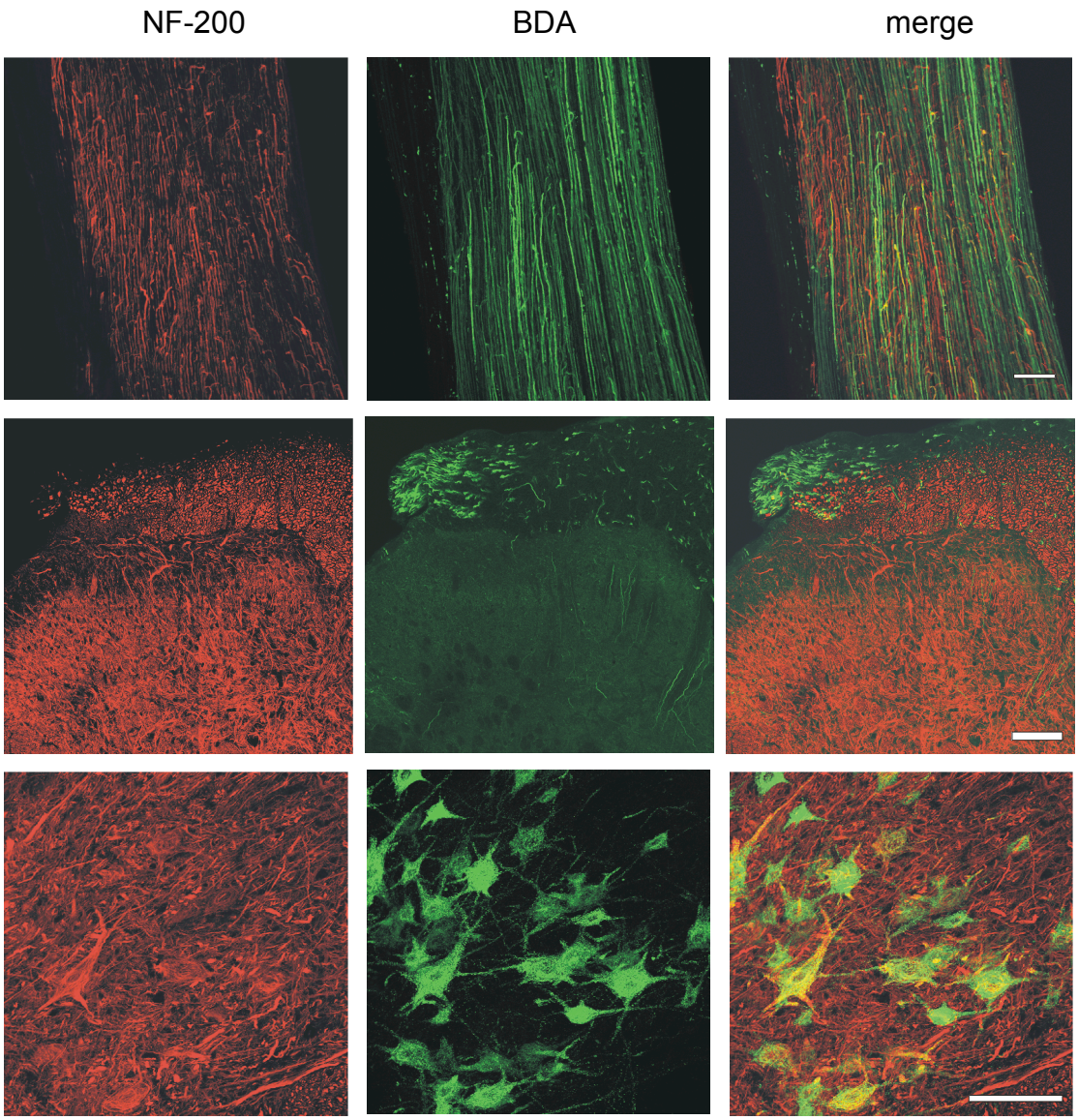

Figure 4-4: BDA labelling in the dorsal root and spinal cord of a control animal 7 days after injection. Labelling could be seen in the L4 dorsal root (top panel), dorsal rootlet and in sensory fibres entering the dorsal horn of the spinal cord (middle panel) and motor neurons in the ventral horn (bottom panel) indicating efficacy of the injection. Scale bars = 100 μm.

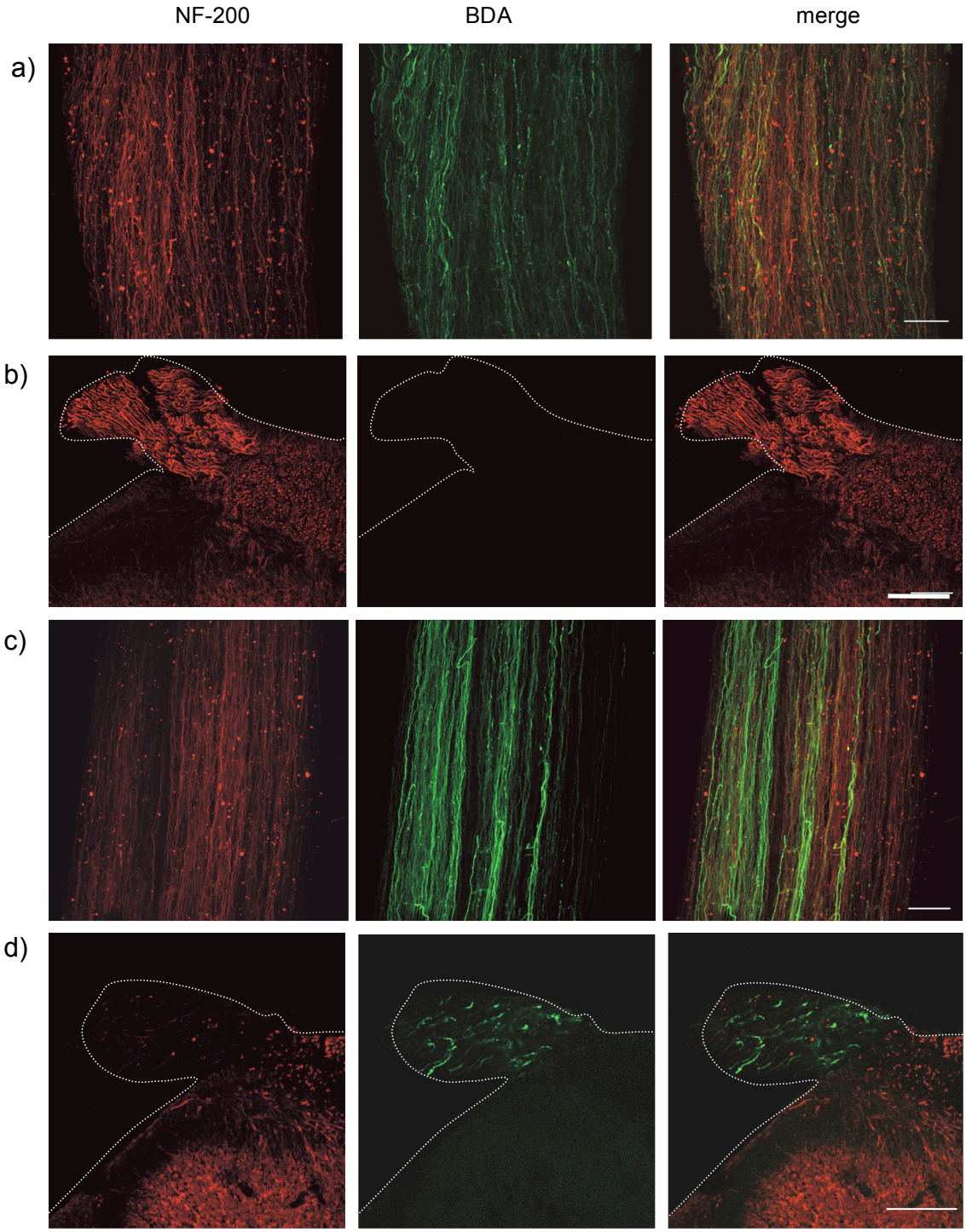

Figure 4-5: BDA labelling in dorsal root and rootlet at 2 (a and b) and 6 (c and d) weeks after dorsal root crush. Panels a and c show a longitudinal section of dorsal root that corresponds to the 3 mm block which ended ~ 2 mm away from the DREZ. Panels b and d show in transverse section the dorsal rootlet still attached to the dorsal horn of the spinal cord (Scale bars= 100 μm).

4.4 Electrophysiological investigation of peripheral nerve regeneration

4.4.1 Introduction and aims

Evidence from some past studies and our CTB tract tracer experiment has suggested that peripheral nerves regenerate at a much faster rate than classic estimates and observations by surgeons of regeneration in human patients suggest (up to 5 mm/day as opposed to 1 mm/day). However, many experiments that have aimed to estimate the rate of peripheral nerve regeneration have provided the rate of growth of the fastest growing lead nerve fibres which may not necessarily be in the majority. In addition, differences in choice of experimental method may account for the discrepancies in growth rate estimates obtained. For example, those experiments that use tract tracers do not necessarily take into consideration diffusion of the tracer within the nerve fascicle and thus may overestimate nerve growth rates. Experiments that utilise the pinch reflex test measure the regenerative rate of unmyelinated and finely myelinated afferents and not large myelinated motor and sensory axons, the latter of which are the focus of this study. For the purposes of our microarray experiment we wished to evaluate the rate at which the *majority* of large myelinated sensory nerve fibres regenerate. In order to answer this question, we carried out orthodromic electrophysiology experiments to determine the extent of regeneration at three timepoints following an L4 spinal nerve crush.

4.4.2 Experimental Rationale

In a control animal stimulation of the sciatic nerve will provoke a response (detectible as a C.A.P) in the L4 and L5 dorsal roots that are upstream from the spinal nerves that contribute to the sciatic. Following an L4 spinal nerve crush, it was expected that stimulation to the sciatic would only provoke a response in the L4 dorsal root if the nerve fibres originating from the L4 spinal nerve had regenerated as least as far as the stimulation site. A response should however be detectible in the L5 dorsal root as the fibres downstream from this root are uninterrupted. We therefore assessed progress of regeneration in five male SD rats (305-410 g) that had under-gone an L4 spinal nerve crush (section 2.2.5) at 4 (n=2), 6 (n=2) or 8 (n=1) weeks previously. The sciatic nerve was stimulated at increasing distances from the spinal nerve crush and recordings were made from the L4 and L5 dorsal roots, with the latter acting as an internal control (section 2.6) (Figure 4-6).

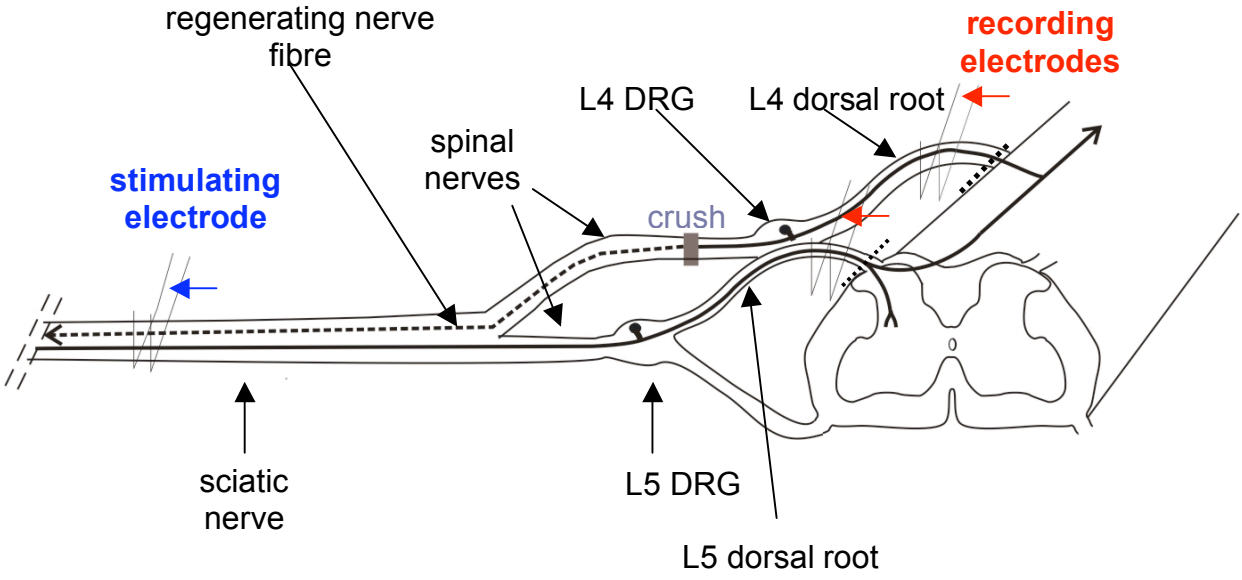

Figure 4-6: Schematic diagram illustrating the setup for electrophysiology (not to scale). The dorsal roots are cut and mounted on silver biolar recording electrodes. The sciatic nerve is mounted on a stimulating electrode and stimulated at 2 mm intervals distally to proximally.

4.4.3 Results and discussion

4.4.3.1 Interpretational caveats and stimulus spread

Interpretation of the data from this experiment was complicated by a number of factors. There was a large degree of biological variation between animals in the amplitude of the response of the L5 dorsal root (internal control). This made comparison of the results from separate experiments difficult. This was partly overcome by expressing the L4 dorsal root response amplitude as a percentage of the amplitude of the L5 control in each case (Figure 4-9a). This approach is however hampered by the fact that the regenerating L4 fibres are less excitable than the normal L5 fibres and thus often require higher stimulus intensities for activation. Such high stimulus intensities can result in the phenomena of anodal block in the L5 fibres, decreasing their response amplitude. High stimulus intensity also carries the risk of causing stimulus spread and hence artefactual responses within the crushed nerve. In a test for stimulus spread in which the nerve was crushed and stimulated distally at increasing intensity, C.A.Ps could only be detected 1mm proximal to the crush when the nerve was stimulated at over 4mA (Figure 4-7). Therefore to eliminate as far as possible stimulus spread and anodal block, records at 2mA stimulus intensity were used for further analysis.

Figure 4-8 illustrates some representative C.A.Ps at selected distances along the sciatic nerve. Compound action potentials (C.A.P.s) were always recorded in the L5 dorsal root and were of a higher amplitude than those recorded in the L4 dorsal root. This contrasts with what we would expect to see in a normal animal. The sciatic nerve has a higher contribution from the L4 spinal nerve than the L5 spinal nerve and we would thus expect to detect a higher response amplitude in the L4 DR than in the L5 DR. This test is therefore conservative for our purposes in that it is likely to *overestimate* the proportion of nerve fibres that have regenerated to any given point.

4.4.3.2 Regeneration proceeds at <1.43 mm/day following a spinal nerve crush

At 4 weeks post-injury, a small number of fibres have reached the most proximal stimulation site as indicated by a small C.A.P (40 mm) but not the most distal stimulation site (60 mm). This indicates that the majority of fibres are regenerating at <1.43 mm/day. At 6 weeks post crush only a very small C.A.P could be detected at the most distal stimulation site indicating again that most of the fibres are regenerating at <1.43 mm/day. By 8 weeks a large C.A.P could be detected at the distal stimulation site, and as this position corresponded to the point at which fibres entered the muscle, this suggested that a substantial proportion of fibres may be reinnervating target tissues at this time point. At 4 weeks post-crush the C.A.P.s recorded in the L4 dorsal root are of a considerably smaller amplitude and area (Figure 4-9 a & b) than those recorded in the L5 dorsal root such that by the most distal recording point they are hardly detectible. In addition, those fibres that have reached the most distal recording point have a much higher response latency (Figure 4-10). This may be due to differences in the electrical properties of regenerating nerve fibres due to immature ion channels etc. At 8 weeks post crush, there appears to be less difference in amplitude between the L4 and L5 C.A.Ps and in latency of response. In addition, conduction velocities calculated from the regenerating nerve at 8 weeks are significantly higher than those calculated for 4 and 6 weeks $p<0.05$ (1 way ANOVA) (Figure 4-11) suggesting that a large proportion of fully functional axons had reached the most distal stimulation site.

These data suggested that 4 weeks was a suitable time point at which to study regeneration in the sciatic nerve as little or no fibres were likely to have reached their distal targets. This was also the case for the 6 week time point. At 8 weeks however nerve fibres may be reconnecting with target tissues and thus ceasing to regenerate. We chose 6 weeks as our peripheral branch time point as it allowed us to draw a direct comparison between it and the 6 week dorsal root crush injury. The data also suggested that CTB tract tracing provided an overestimation of regenerative rate in the sciatic nerve.

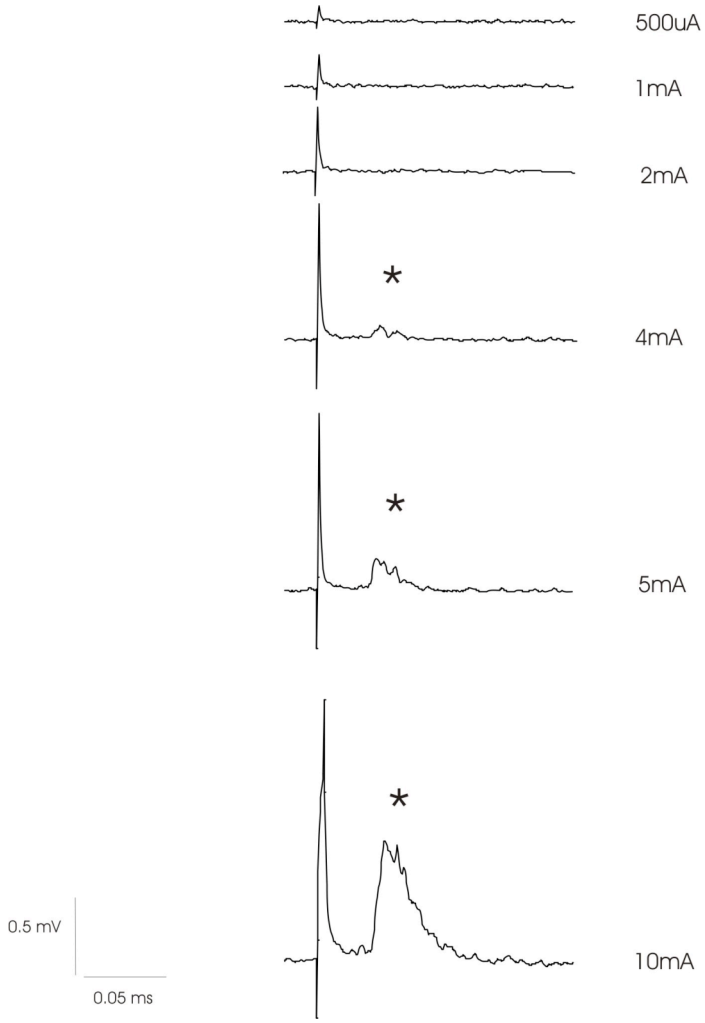

Figure 4-7: Stimulus spread in the sciatic nerve occurs at ≥4mA stimulus intensity. The sciatic nerve was crushed and stimulated at increasing intensity just distal to the crush. Recordings were made at 1 mm proximal to the crush and stimulus spread (indicated by the presence of a C.A.P) could be detected at >4mA stimulus intensity. * indicates presence of C.A.P.

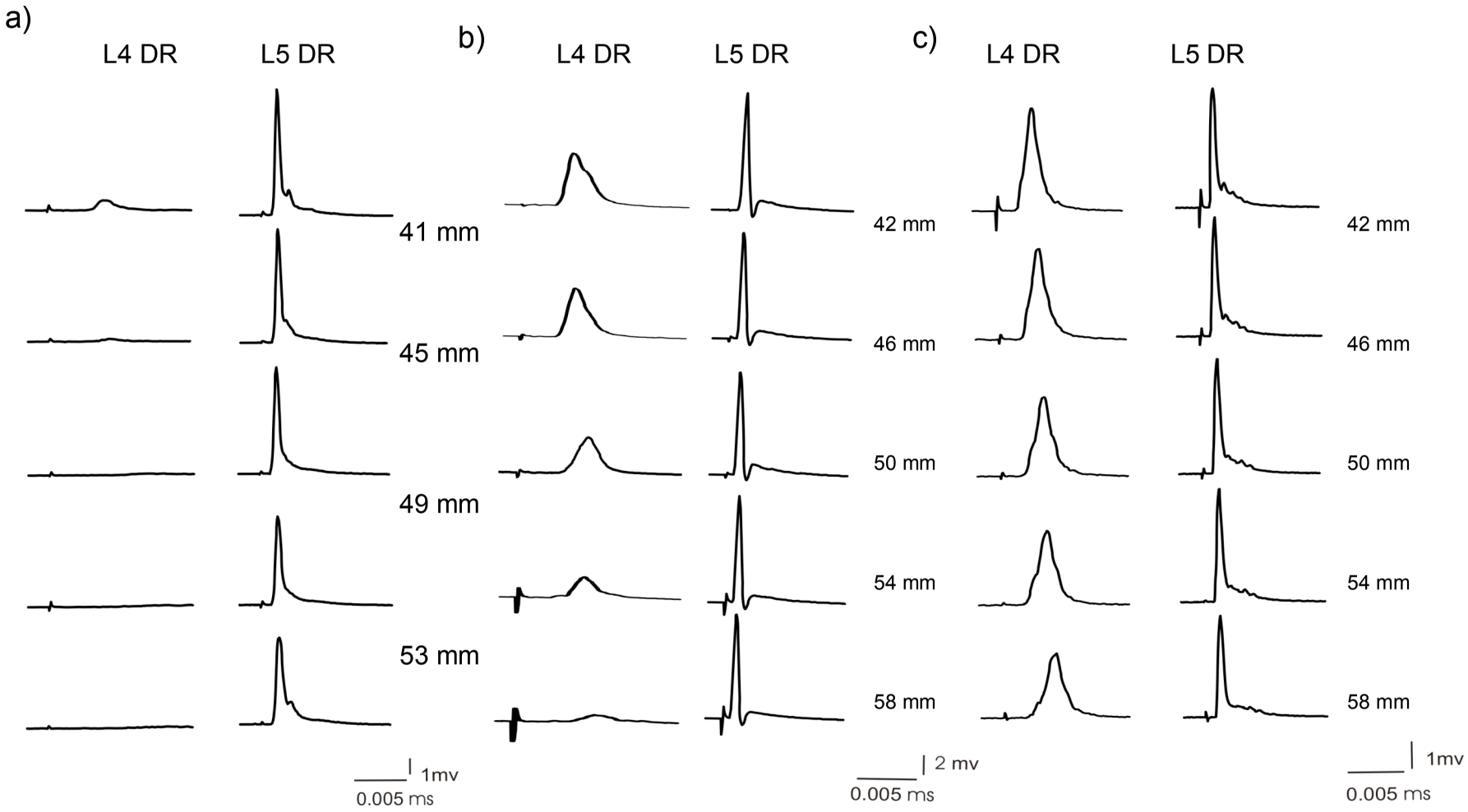

Figure 4-8: Representative C.A.Ps recorded from L4 and L5 dorsal roots following sciatic nerve stimulation at a) 4, b) 6 and c) 8 weeks following spinal nerve crush.

a)

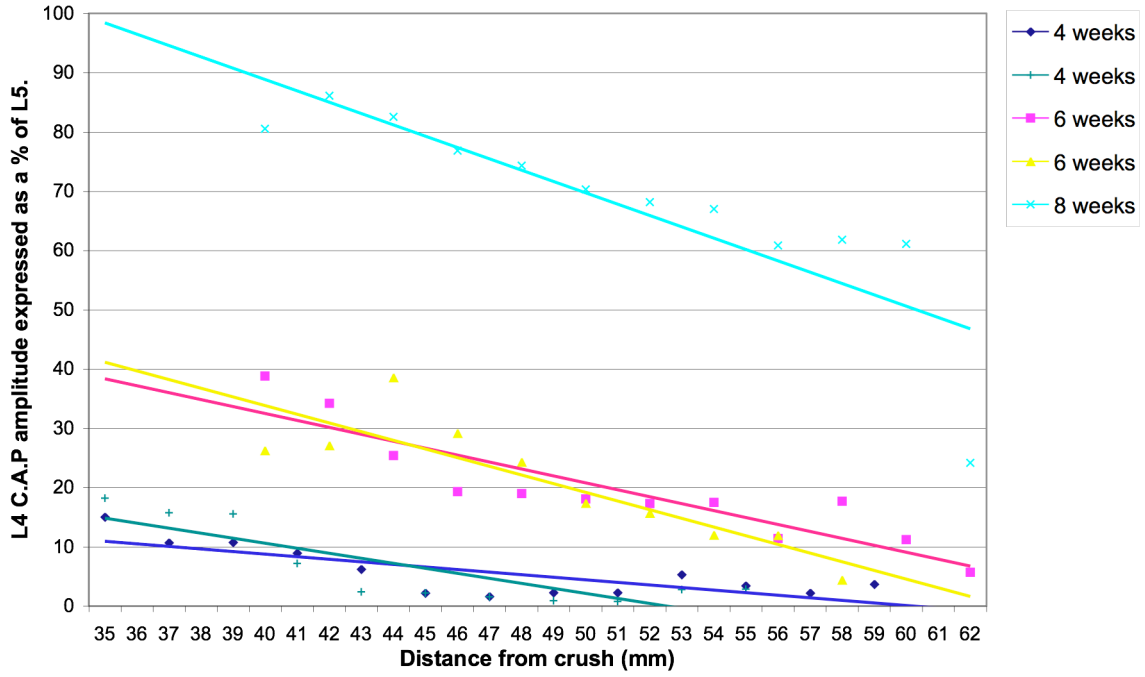

b)

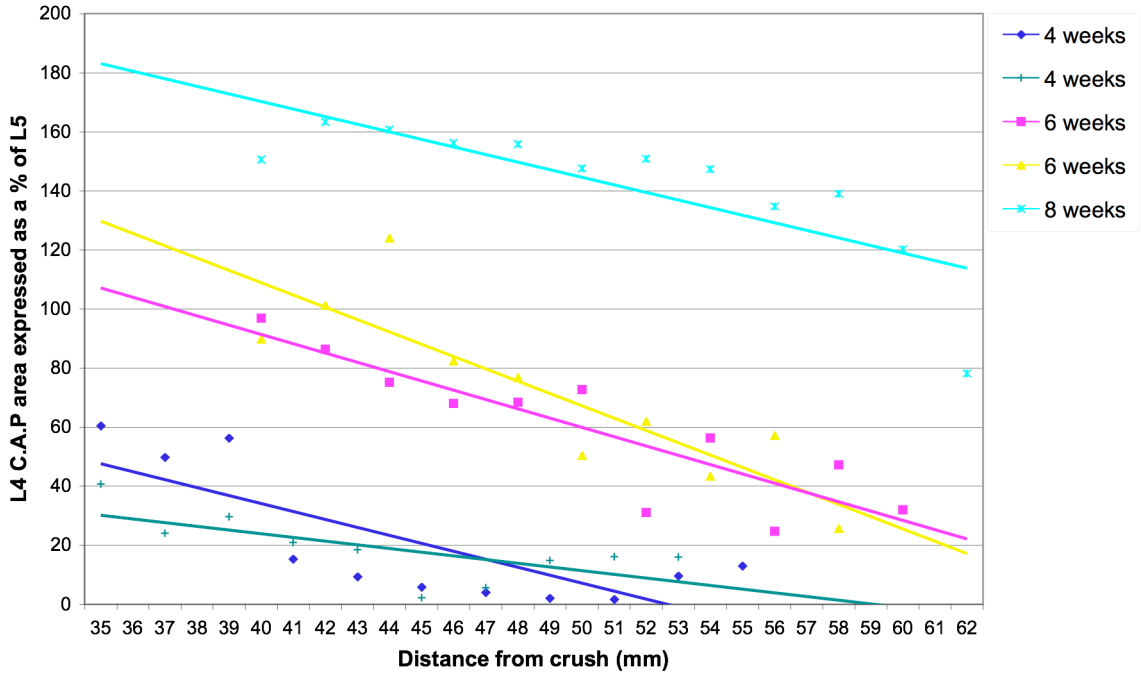

Figure 4-9a) Amplitude and b) Area of C.A.Ps recorded in the L4 dorsal root 4, 6 and 8 weeks post L4 spinal nerve crush expressed as a % of the response in the L5 dorsal root (internal control). Each line represents data from a single animal.

a)

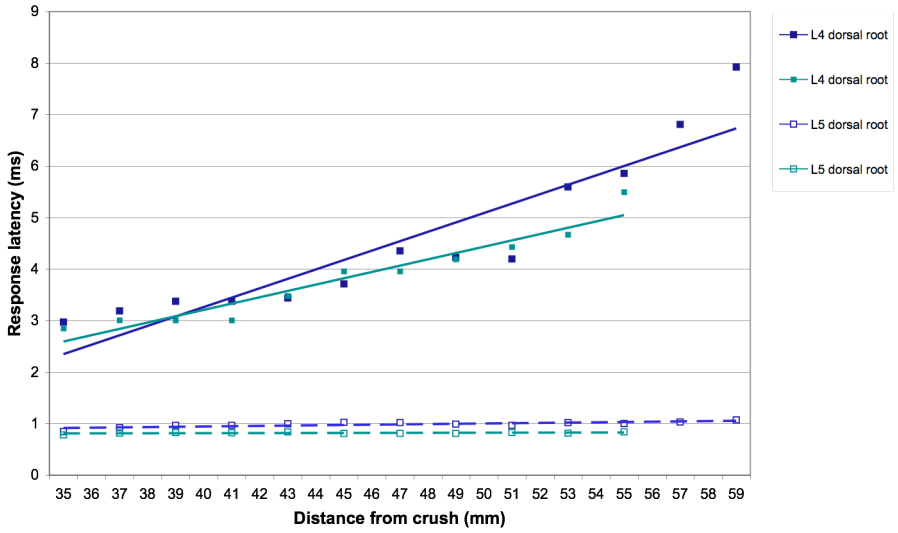

b)

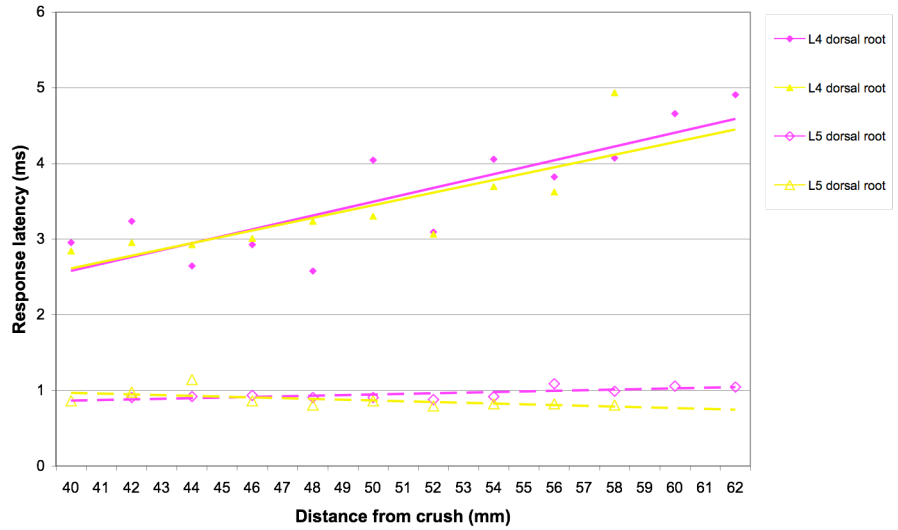

c)

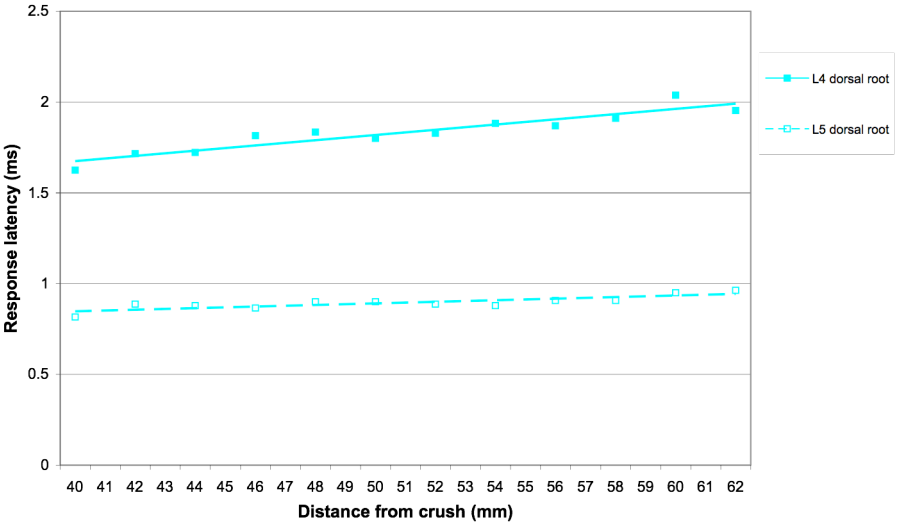

Figure 4-10: Latency to responses recorded from L4 and L5 dorsal roots at a) 4 weeks, b) 6 weeks and c) 8 weeks post- L4 spinal nerve crush. Each line represents data from a single animal.

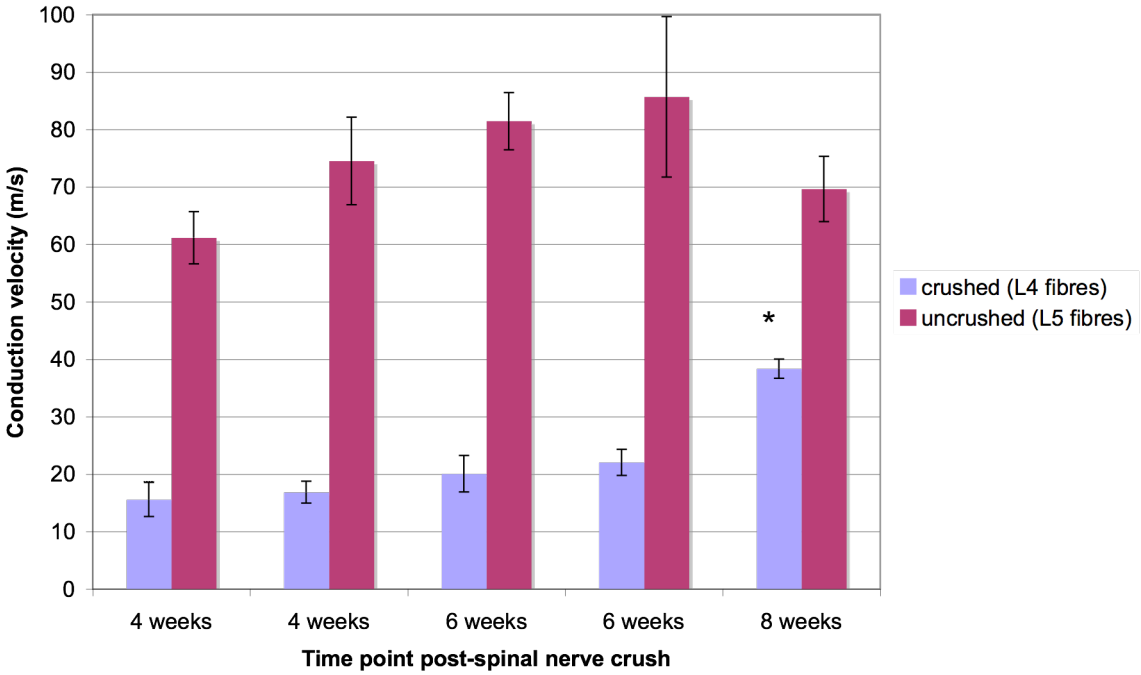

Figure 4-11: Conduction velocity of L4 and L5 nerve fibres 4, 6 and 8 weeks post- spinal nerve crush (± S.D). Conduction velocities measured at 8 weeks post spinal nerve crush were significantly greater than those measured at both 4 ($p<0.05$) and 6 weeks ($p<0.05$) (1-way ANOVA). Each pair of columns represents data from one animal. Conduction velocities were calculated from each point at which a response could be detected and the mean calculated.

4.5 Chapter summary

Anatomical and electrophysiological studies allowed us to determine suitable time points for our microarray experiment. Evidence from BDA tract tracing suggests that at 2 weeks following DR crush, nerve fibres are yet to reach the DREZ and are thus still regenerating whilst at 6 weeks they have reached the point of CNS entry. Evidence from electrophysiology suggests that at 6 weeks post L4 spinal nerve crush, the majority of fibres within the sciatic nerve have not reached distal targets in the hind limb and are thus still regenerating. The time points for our microarray were thus confirmed as 2 and 6 weeks post dorsal root crush and 6 weeks post spinal nerve crush.

5 Microarray analysis of DRG gene expression after axonal injury

5.1 Introduction and Aims

We aimed to identify putative regeneration-associated genes using a microarray approach. Having identified appropriate time points to harvest DRGs after dorsal root and spinal nerve crush (Chapter 4), gene expression changes in the DRG after injuries in which regeneration is expected to occur (2DR and 6SN) were compared with that after injuries where regeneration is blocked or abortive (6DR and 2DC respectively).

The first part of this chapter deals with quality control issues and low-level statistical analysis of the microarray experiments. The remainder of the chapter tackles the more difficult task of making sense of the data in a biological context. Two main approaches to higher-level analysis was taken. Firstly, an ontology-based approach whereby the whole of each data set was interrogated and interpreted according to existing ontological information using IGA and IPA analyses. There was a particular focus on genes involved in the development of the nervous system and in embryological development in general as these may constitute plasticity-related genes that could have a role in remodelling in the damaged CNS. Simple filtering and sorting of the data on the fold change and/or FDR criterion using Venn diagrams and Excel spreadsheets followed by a focussed search of literature and gene databases, allowed a second, question-led investigation of the data. The main question that informed this investigation was: What features do the regenerating conditions have in common that are not shared by the non-regenerating conditions? Secondary to this, this study has relevance to studies of neuropathic pain. Regulated genes were therefore investigated with the various mechanisms of pain generation in mind.

5.2 The microarray

The left L4 DRG was harvested from rats that had undergone a left spinal nerve crush (section 2.2.5) (n=9) or a dorsal column transection (section 2.2.6) (n=9) at 6 or 2 weeks, respectively. DRGs were also harvested 2 and 6 weeks after a dorsal root crush (n=9/group) and from a naïve control group that had not undergone any surgery (n=9). Total RNA was extracted (section 2.8.4.2) and for each condition RNA from 3 animals was pooled before synthesis of biotinylated cDNA and hybridisation to Affymetrix® chips. Each condition was replicated on three chips, each of which containing material from 3 animals. Figure 5-1 illustrates the design of the experiment.

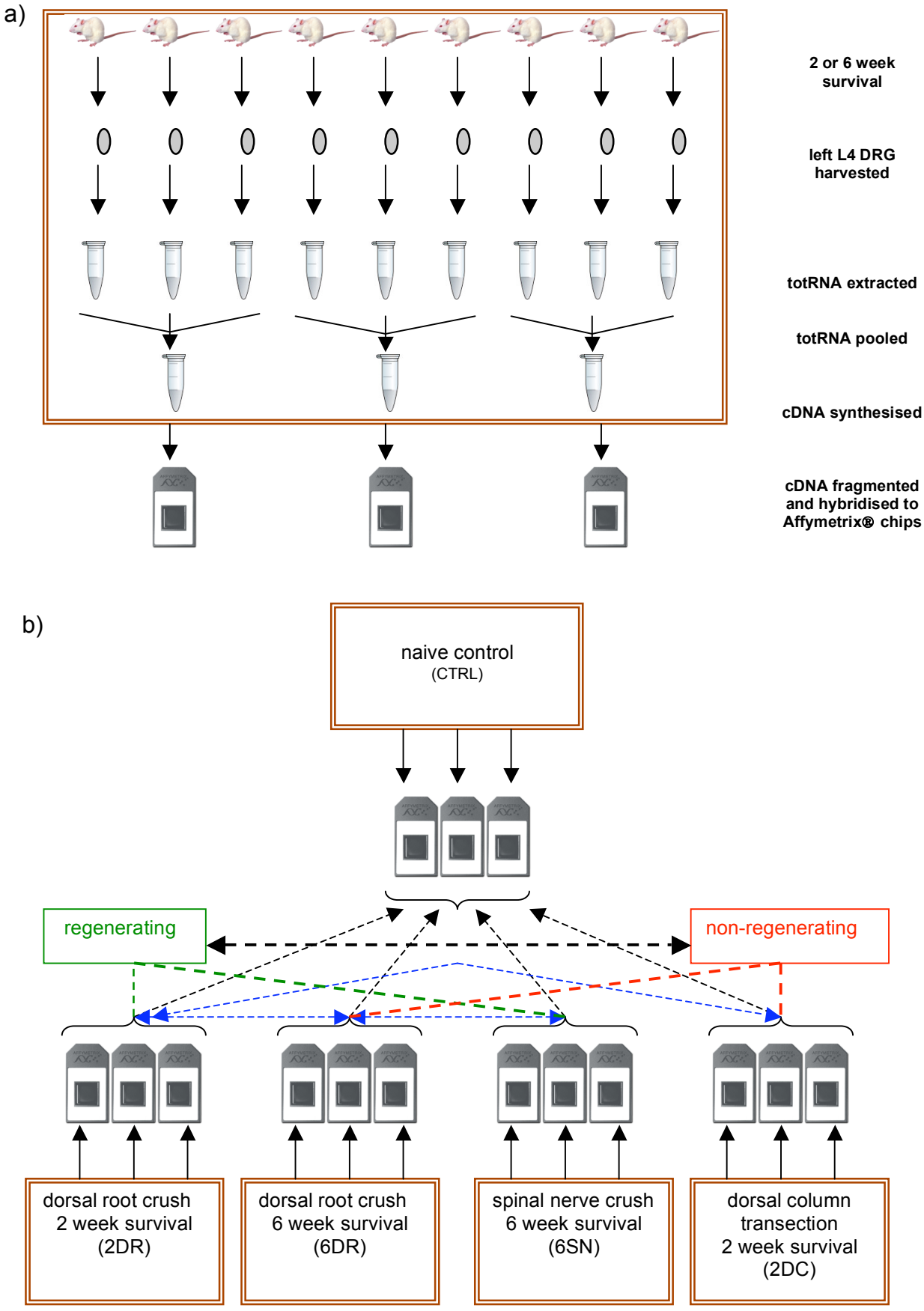

Figure 5-1: Schematic diagram illustrating microarray design. a) Generalised scheme that applies to each of the conditions. b) Illustration of conditions and the main comparisons that are possible.

5.3 Low level analysis: results and discussion

5.3.1 Quality control on samples assessed by Genespring

5.3.1.1 Internal controls

Internal controls provide a measure of RNA sample quality by showing the 3'/5' ratios for a set of specific probe sets. Ratios of greater than 3 can indicate sample degradation. The 9 chips in our main microarray experiment showed ratios of less than 3 for 2 out of the 3 internal controls. Given that the total RNA showed little indication of degradation with high RNA integrity numbers it is likely that the elevated ratios for beta-actin are due to the use of the small sample amplification protocol that may have lead to the generation of targets skewed to the 3' end.

Table 5-1: RNA sample quality assessed by internal controls. 3'/5' ratios of greater than 3 suggest sample degradation. Beta-Actin shows elevated 3'/5' ratios.

SampleName	AFFX_Rat_beta-actin__at	AFFX_Rat_GAPDH__at	AFFX_Rat_Hexokinase__at
AB1Rat2302Ctr1.CEL	6.574168	2.1081595	1.5266877
AB1Rat2302Ctr2.CEL	7.211664	2.1251173	2.0593991
AB1Rat2302Ctr3.CEL	8.782671	2.5493276	1.9934335
AB1Rat23022DR1.CEL	7.887351	2.2793832	1.2011455
AB1Rat23022DR2.CEL	8.723589	2.5174458	1.8035073
AB1Rat23022DR3.CEL	7.63474	2.315108	2.10843
AB1Rat23026DR1.CEL	7.600569	2.239223	1.386011
AB1Rat23026DR2.CEL	9.780514	2.503572	2.0285718
AB1Rat23026DR3.CEL	7.7443085	2.2594118	2.0353477
AB1Rat2302SN1.CEL	8.346943	2.3500707	1.6174058
AB1Rat2302SN2.CEL	9.464098	2.2478232	1.9174759
AB1Rat2302SN3.CEL	10.202974	2.4288597	1.9611225
AB1Rat2302DC1.CEL	8.620907	2.1460145	1.2512201
AB1Rat2302DC2.CEL	8.996834	2.3592603	1.8738096
AB1Rat2302DC3.CEL	9.088102	2.420578	2.6035702

5.3.1.2 Hybridisation controls

Affymetrix chips have integral hybridisation controls to allow assessment of hybridisation quality (described in section 3.2.1.2). Figure 5-2 shows the hybridisation control profiles for all 15 chips. All the hybridisation controls are present in increasing concentrations in all the chips. This, along with the close clustering of the hybridisation profiles, indicates a high quality, uniform hybridisation across chips.

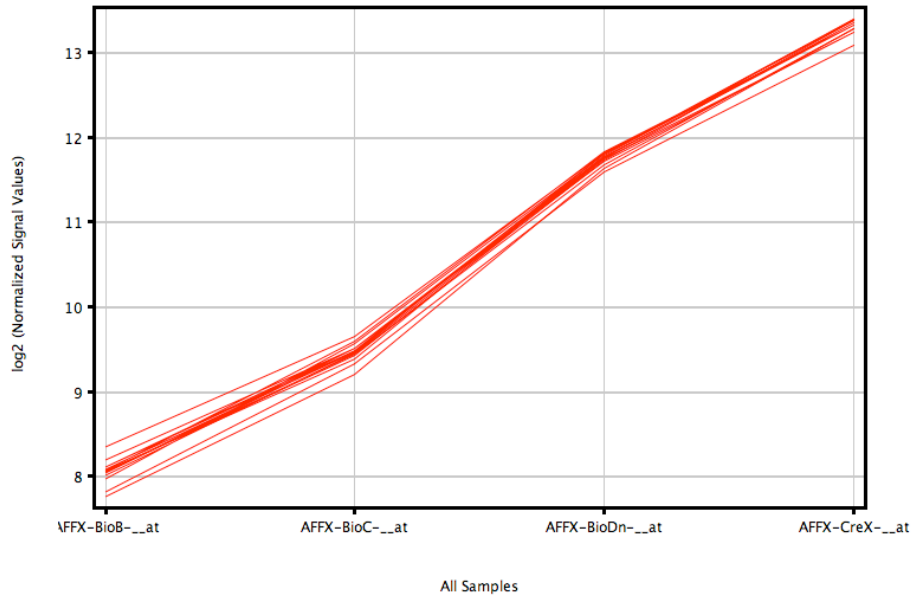

Figure 5-2: Hybridisation control profiles for all chips. The x axis represents the hybridisation controls present at 1.5, 5, 25 and 100 pm, respectively. The log of the normalised signal values is plotted on the Y-axis. All hybridisation controls were present in increasing concentrations in all chips.

5.3.1.3 Principal component analysis scores

Principal component analysis (PCA) is a decomposition technique that can be used to check data quality. Replicates within a condition should cluster together and separately from arrays in other conditions. Principal components are numbered according to their decreasing significance. Figure 5-3 illustrates the principal components for the main microarray experiment coloured by condition, time point and regenerative state. In general, replicates within each of the injury conditions cluster together and ctrl separates from all the conditions. However, 2DR, 6DR and SN do not have a high degree of separation from one another. The 2DC condition separates from all the other conditions and control. The regenerating conditions appear to roughly cluster while the non-regenerating conditions do not and samples do not cluster according to time point. This perhaps suggests that the regenerative state of a neuron is more important than the time since injury in dictating its transcriptional status and that mixed regenerating conditions share more in common than mixed non-regenerating conditions.

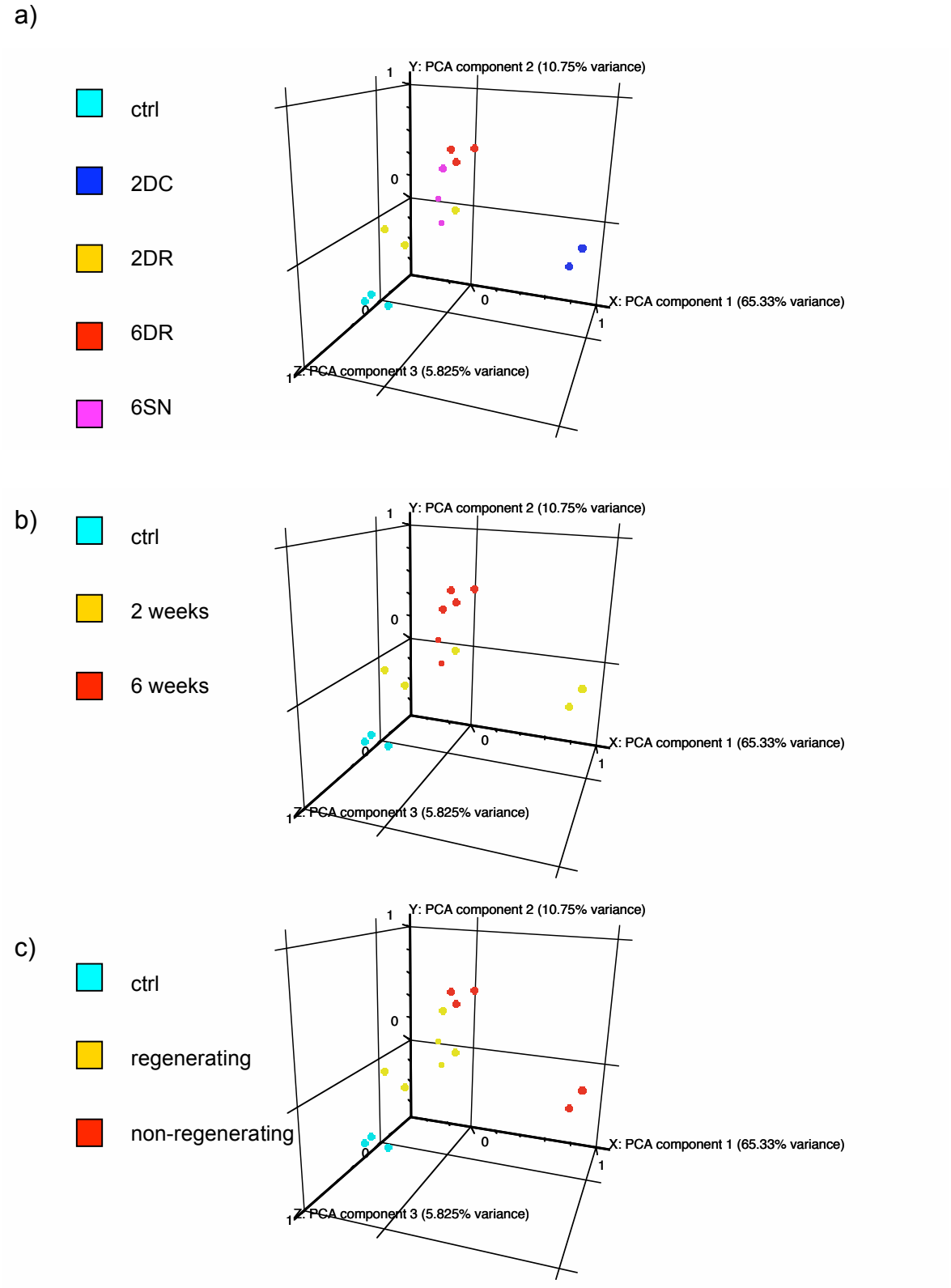

Figure 5-3: Principal components analysis of main microarray experiment. Replicates are coloured by a) conditions, b) time point and c) regenerative state.

5.3.1.4 Across-array correlation analysis

Calculation of a correlation coefficient for each pair of arrays can give a measure of how arrays correlate with each other. Arrays within a condition should correlate highly with each other. On the whole, arrays were well correlated (R^2=0.989-1). The dorsal column chips showed the least correlation with chips from other conditions and out of all the conditions correlated least well with the control chips. This suggests that dorsal column injury elicits a transcriptional programme that is distinct from that elicited by the other injuries.

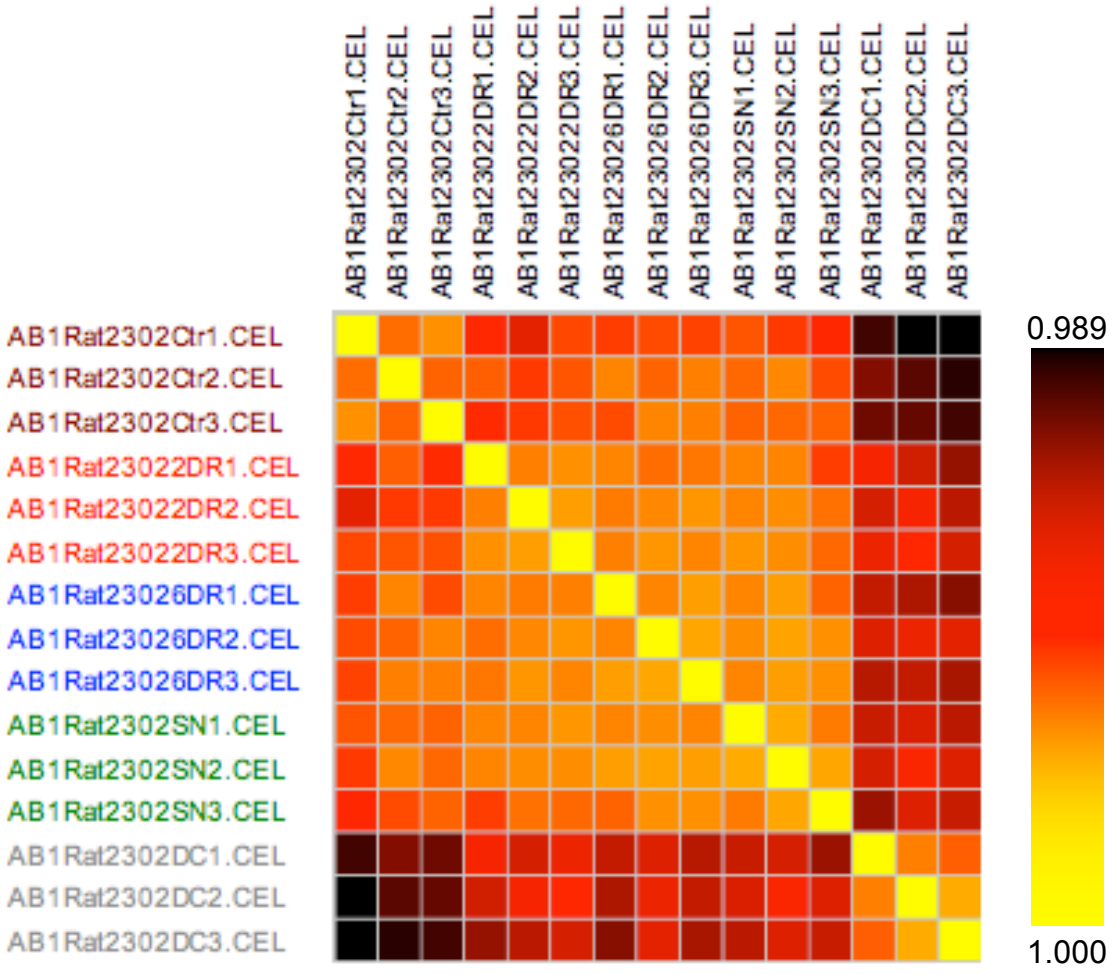

Figure 5-4: Heatmap showing across-array correlations illustrating lack of correlation between dorsal column injury and other conditions. Each chip is compared to every other chip. A perfect correlation of 1 can be seen when chips are compared to self whilst the lowest correlation is seen between DC chips and chips from other conditions.

5.4 Identification of differentially expressed genes

Two approaches were taken to identify differentially expressed genes, Rank Product Analysis (RPA), which allows a cut-off for significant regulation to be set according to false discovery rate (FDR) and, for comparison, ANOVA, which was implemented in Genespring. Use of Genespring also enabled enhanced visualisation of the data using volcano plots.

5.4.1 Rank products analysis

Rank products analysis is described in section 2.9.3.1.2. Each condition was compared to control as well as to every other condition. The descriptive statistics from this analysis are presented in Table 5-2 and Figure 5-5 illustrates the percentage of probe sets changed after each injury. Dorsal column transection elicited many more changes in gene expression than the other injuries and unlike other injuries, more genes were downregulated than upregulated. In addition, when each condition was compared to every other condition, comparisons with the dorsal column transection injury yielded the highest number of gene differences. This again indicates that dorsal column injury elicits a transcriptional programme within the DRG that is distinct to that initiated by either spinal nerve or dorsal root crush. This is consistent with the principle components and correlation analyses that showed a separation of dorsal column transection from these injuries (sections 5.3.1.3 and 5.3.1.4). The top 20 up and downregulated genes for each condition compared to control are presented in Table 5-3 to Table 5-10. Regulated genes (<1% FDR) are presented in appendix A, while a full list of regulated genes (<50% FDR) is presented on the accompanying CD.

Table 5-2: Descriptive statistics for all microarray comparisons.

COMPARISON	LARGEST FOLD CHANGE		NO. GENES UPREGULATED		NO. GENES DOWNREGULATED	
	Up	Down	1% FDR	5% FDR	1% FDR	5% FDR
2DR vs. ctrl	13.64	-2.44	172	403	34	146
6DR vs. ctrl	2.67	-14.12	44	150	30	84
6SN vs. ctrl	3.26	-8.89	72	222	25	90
2DC vs. ctrl	87.59	-9.97	208	502	279	627
6DR vs. 2DR	2.63	-15.89	12	39	74	163
6DR vs. 6SN	1.87	-2.77	11	63	20	69
6DR vs. 2DC	4.32	-81.94	204	483	160	321
2DR vs. 6SN	16.58	-2.68	43	106	12	56
2DR vs. 2DC	4.31	-91.65	188	441	144	254
6SN vs. 2DC	4.02	-84.02	231	544	169	292

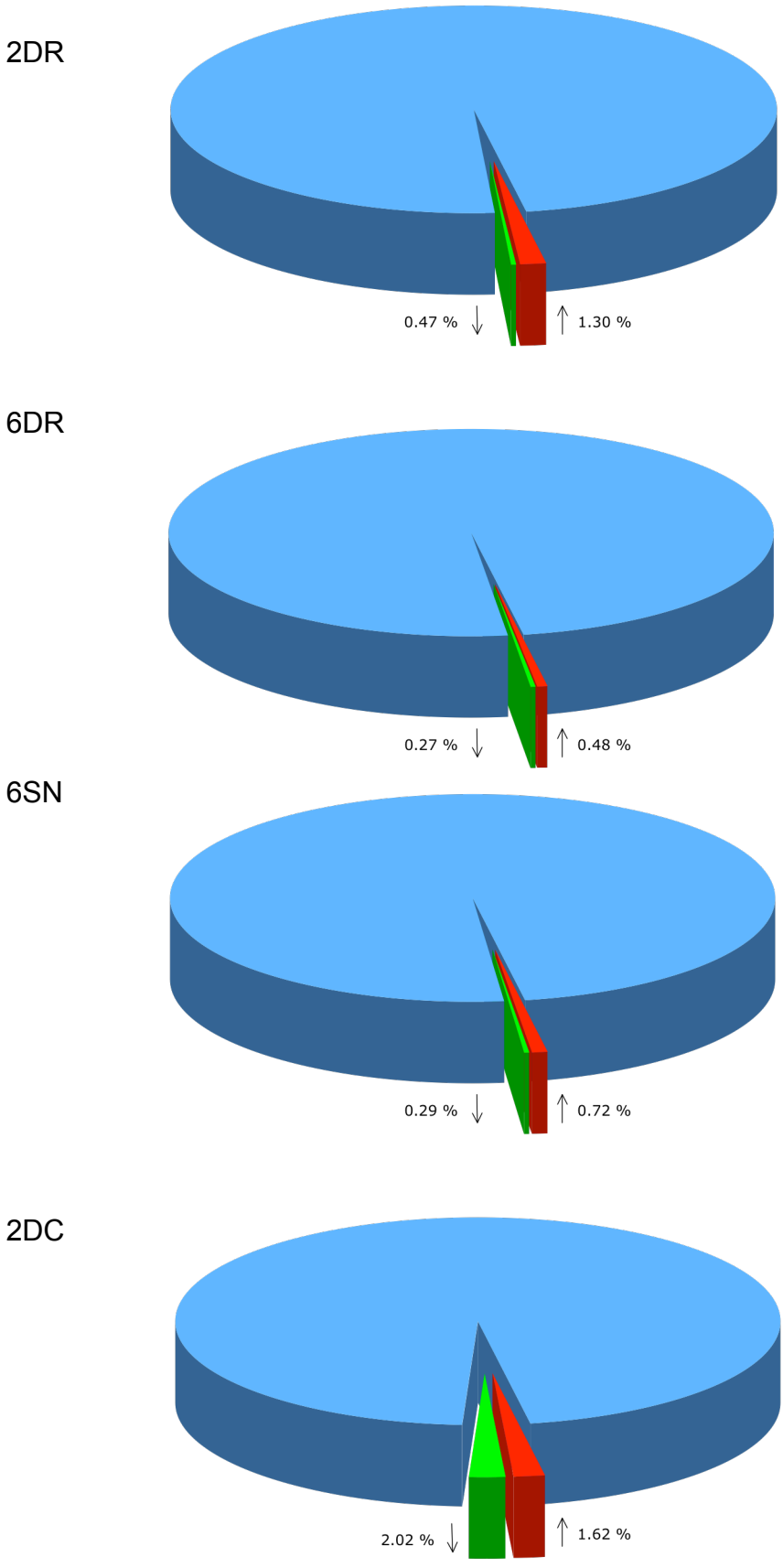

Figure 5-5: Pie charts showing the percentage of all probe sets regulated within 5% FDR for each condition. The chips contained 31000 probe sets covering 28700 genes. The red slice denotes the proportion of upregulated probe sets while the green slice indicates downregulated probe sets for each injury vs. naïve control.

Table 5-3: Top 20 genes identified by RPA as upregulated 2 weeks after dorsal root crush

PROBESET ID	GENE SYMBOL	GENE NAME	ACC. NO.	FC	FDR
1368238_at	Pap	pancreatitis-associated protein	NM_053289	13.64	0
1387930_at	Reg3a	regenerating islet-derived 3 alpha	L10229	4.55	0
1368187_at	Gpnmb	glycoprotein (transmembrane) nmb	NM_133298	3.71	0
1387154_at	Npy	neuropeptide Y	NM_012614	3.18	0
1368677_at	Bdnf	brain derived neurotrophic factor	NM_012513	2.86	0
1368359_a_at	Vgf	VGF nerve growth factor inducible	NM_030997	2.83	0
1375010_at	Cd68	CD68 antigen	AI177761	2.53	0
1384063_at	Cthrc1	collagen triple helix repeat containing 1	AA958001	2.49	0
1395126_at	Msr2_predicted	macrophage scavenger receptor 2 (predicted)	AI011393	2.45	0
1369268_at	Atf3	activating transcription factor 3	NM_012912	2.45	0
1373386_at	Gjb2	gap junction membrane channel protein beta 2	AI179953	2.49	0
1390119_at	Sfrp2	secreted frizzled-related protein 2	BF396602	2.41	0
1376750_at	Thbs2	thrombospondin 2	AA963477	2.32	0
1385751_at	Thbs2	thrombospondin 2	BF408413	2.38	0
1377092_at	Socs3	suppressor of cytokine signaling 3	BF389682	2.33	0
1368224_at	Serpina3n	serine (or cysteine) peptidase inhibitor, clade A, member 3N	NM_031531	2.34	0
1392965_a_at	Smoc2_predicted	SPARC related modular calcium binding 2 (predicted)	AI028877	2.25	0
1385248_a_at	Ogn_predicted	osteoglycin (predicted)	AA997590	2.25	0
1370892_at	C4a /// C4-2	complement component 4a /// complement component 4, gene 2	BI285347	2.27	0
1367973_at	Ccl2	chemokine (C-C motif) ligand 2	NM_031530	2.33	0

Table 5-4: Top 20 genes identified by RPA as downregulated 2 weeks after dorsal root crush

Probeset id	Gene Symbol	Gene name	Acc. NO	FC	FDR
1387133_at	Calb2	calbindin 2	NM_053988	-2.44	0
1394297_at	Hoxd1_predicted	homeo box D1 (predicted)	BG670107	-2.31	0
1390881_at	Abra	actin-binding Rho activating protein	AI172339	-2.25	0
1370900_at	Myh4	myosin, heavy polypeptide 4, skeletal muscle	BM391169	-9.32	0.25
1367962_at	Actn3	actinin alpha 3	NM_133424	-7.31	0.4
1384269_at	Mterf	mitochondrial transcription termination factor	BF386887	-1.77	0.5
1377163_at	Inhbb	inhibin beta-B	BM385741	-1.74	0.57
1372195_at	Tnnc2	troponin C type 2 (fast)	BG663128	-6.72	0.5
1370033_at	Mlc3	fast myosin alkali light chain	NM_020104	-5.55	0.44
1391575_at	Hapln4	Hyaluronan and proteoglycan link protein 4	BG380566	-1.67	0.4
1380306_at	---	Transcribed locus	AW435415	-1.96	0.36
1367626_at	Ckm	creatine kinase, muscle	NM_012530	-5.3	0.42
1391305_at	---	---	AI576233	-1.62	0.46
1387787_at	Myl2	myosin, light polypeptide 2	NM_012605	-5.11	0.43
1368585_at	Cart	cocaine and amphetamine regulated transcript	NM_017110	-1.66	0.53
1395714_at	---	---	AT005664	-1.53	0.5
1388349_at	Ckm	creatine kinase, muscle	AA799557	-1.75	0.71
1367762_at	Sst	somatostatin	NM_012659	-1.58	0.67
1371247_at	Ap2a1_predicted /// Ptov1 /// Med25_predicted	Adaptor protein complex AP-2, alpha 1 subunit (predicted) /// Prostate tumor over expressed gene 1 /// Mediator of RNA polymerase II transcription, subunit 25 homolog (yeast) (predicted)	BF521859	-4.33	0.68
1370198_at	Trdn	triadin	AJ243304	-2.86	0.65

Table 5-5: Top 20 genes identified by RPA as upregulated 6 weeks after dorsal root crush

PROBESET ID	GENE SYMBOL	GENE NAME	ACC. NO.	FC	FDR
1387902_a_at	LOC500180 /// LOC500183	similar to IG KAPPA CHAIN V-V REGION K2 PRECURSOR /// similar to NGF-binding Ig light chain	L22655	2.67	0
1371447_at	Plac8_predicted	placenta-specific 8 (predicted)	BG378630	1.98	0
1368187_at	Gpnmb	glycoprotein (transmembrane) nmb	NM_133298	2.11	0
1371245_a_at	LOC689064	similar to Hemoglobin beta-2 subunit	BI287300	1.94	0
1390798_at	Ptprc	protein tyrosine phosphatase, receptor type, C	BF288130	1.87	0
1373386_at	Gjb2	gap junction membrane channel protein beta 2	AI179953	2.05	0
1367553_x_at	Hbb	hemoglobin beta chain complex	NM_033234	1.81	0
1371102_x_at	MGC72973	beta-glo	X05080	1.8	0
1387125_at	S100a9	S100 calcium binding protein A9 (calgranulin B)	NM_053587	2.29	0
1388602_at	Cfd	complement factor D (adipsin)	AI237358	1.87	0
1369705_at	Xtrp3	X transporter protein 3	AI169634	2.03	0
1370967_at	Cldn10_predicted	Claudin 10 (predicted)	BG374683	1.71	0.08
1382083_at	Coch_predicted	coagulation factor C homolog (Limulus polyphemus) (predicted)	BF287593	1.82	0.15
1391446_at	Ms4a1_predicted	membrane-spanning 4-domains, subfamily A, member 1 (predicted)	AA817742	1.68	0.29
1374334_at	Igha_mapped	immunoglobulin heavy chain (alpha polypeptide)	AI412189	1.87	0.27
1382305_at	Zfp364_predicted	Zinc finger protein 364 (predicted)	AI236814	1.65	0.25
1368422_at	Meox2	Mesenchyme homeobox 2	NM_017149	1.7	0.24
1395126_at	Msr2_predicted	macrophage scavenger receptor 2 (predicted)	AI011393	1.71	0.28
1367985_at	Alas2	Aminolevulinic acid synthase 2	NM_013197	1.65	0.26
1397999_at	Irs2	Insulin receptor substrate 2	BF386502	1.61	0.5

Table 5-6: Top 20 genes identified by RPA as downregulated 6 weeks after dorsal root crush

#GENE NAME	GENE SYMBOL	GENE TITLE	ACC. NO.	FC	FDR
1387133_at	Calb2	calbindin 2	NM_053988	-1.86	0
1367962_at	Actn3	actinin alpha 3	NM_133424	-9.27	0
1387787_at	Myl2	myosin, light polypeptide 2	NM_012605	-8.39	0
1370033_at	Mlc3	fast myosin alkali light chain	NM_020104	-9.08	0
1384269_at	Mterf	mitochondrial transcription termination factor	BF386887	-1.72	0
1370900_at	Myh4	myosin, heavy polypeptide 4, skeletal muscle	BM391169	-14.12	0
1377106_at	---	Transcribed locus	AW533050	-5.94	0
1372195_at	Tnnc2	troponin C type 2 (fast)	BG663128	-8.73	0
1378252_at	Chodl_predicted	Chondrolectin (predicted)	AI029745	-1.66	0
1370971_at	Myh1 /// LOC691644	myosin, heavy polypeptide 1, skeletal muscle, adult	BI277545	-6.99	0
1388604_at	LOC679341 /// LOC686019	similar to Calsequestrin-1 precursor	BI276959	-3.1	0
1369928_at	Acta1	actin, alpha 1, skeletal muscle	NM_019212	-4.79	0.08
1367626_at	Ckm	creatine kinase, muscle	NM_012530	-6.48	0.08
1387414_at	Duox2	dual oxidase 2	NM_024141	-1.58	0.07
1390881_at	Abra	actin-binding Rho activating protein	AI172339	-1.66	0.4
1370198_at	Trdn	Triadin	AJ243304	-3.15	0.38
1390355_at	Ryr1	ryanodine receptor 1, skeletal muscle	AI575442	-2.21	0.41
1368554_at	Pnlip	pancreatic lipase	NM_013161	-1.58	0.39
1395327_at	---	Transcribed locus, weakly similar to XP_580018.1	AW522341	-3.09	0.37
1371247_at	Ap2a1_predicted /// Ptov1 /// Med25_predicted	Adaptor protein complex AP-2, alpha 1 subunit (predicted) /// Prostate tumor over expressed gene 1 /// Mediator of RNA polymerase II transcription, subunit 25 homolog (yeast) (predicted)	BF521859	-5.61	0.45

Table 5-7: Top 20 genes identified by RPA as upregulated 6 weeks after spinal nerve crush

PROBESET ID.	GENE SYMBOL	GENE NAME	ACC. NO.	FC	FDR
1387125_at	S100a9	S100 calcium binding protein A9 (calgranulin B)	NM_053587	3.26	0
1371245_a_at	LOC689064	similar to Hemoglobin beta-2 subunit	BI287300	2.88	0
1367553_x_at	Hbb	hemoglobin beta chain complex	NM_033234	2.58	0
1370913_at	Best5	Best5 protein	AI409634	2.57	0
1368494_at	S100a8	S100 calcium binding protein A8 (calgranulin A)	NM_053822	2.85	0
1371102_x_at	MGC72973	beta-glo	X05080	2.51	0
1382031_at	---	Transcribed locus	AA859079	2.38	0.14
1370240_x_at	Hba-a1 /// LOC360504	hemoglobin alpha, adult chain 1	AI179404	2.32	0.12
1367985_at	Alas2	aminolevulinic acid synthase 2	NM_013197	2.34	0.11
1368021_at	Adh1	alcohol dehydrogenase 1 (class I)	NM_130780	2.23	0.1
1370239_at	Hba-a1 /// LOC360504	hemoglobin alpha, adult chain 1 /// hemoglobin alpha 2 chain	AI179404	2.28	0.09
1375519_at	LOC287167	globin, alpha	AI237401	2.26	0.08
1371447_at	Plac8_predicted	placenta-specific 8 (predicted)	BG378630	2.1	0.08
1388142_at	Cspg2	chondroitin sulfate proteoglycan 2	AA850991	2.05	0.14
1385248_a_at	Ogn_predicted	osteoglycin (predicted)	AA997590	2.38	0.13
1370791_at	Hgfac	Hepatocyte growth factor activator	U16683	2.46	0.12
1385229_at	Pcdh20_predicted	protocadherin 20 (predicted)	AW524146	2.42	0.18
1388608_x_at	Hba-a1 /// LOC360504	hemoglobin alpha, adult chain 1 /// hemoglobin alpha 2 chain	AI577319	2.07	0.17
1387943_at	Defa	defensin, alpha 5, Paneth cell-specific	U16686	2.19	0.16
1374334_at	Igha_mapped	immunoglobulin heavy chain (alpha polypeptide)	AI412189	2.21	0.2

Table 5-8 Top 20 genes identified by RPA as downregulated 6 weeks after spinal nerve crush

PROBESET ID	GENE SYMBOL	GENE NAME	ACC. NO.	FC	FDR
1367962_at	Actn3	actinin alpha 3	NM_133424	-6.41	2
1377106_at	---	Transcribed locus	AW533050	-5.79	1
1370900_at	Myh4	myosin, heavy polypeptide 4	BM391169	-6.6	0.67
1372195_at	Tnnc2	troponin C type 2 (fast)	BG663128	-6.89	0.5
1370033_at	Mlc3	fast myosin alkali light chain	NM_020104	-5.94	0.4
1383827_at	Tlk1_predicted	tousled-like kinase 1 (predicted)	AI059119	-1.61	0.5
1387787_at	Myl2	myosin, light polypeptide 2	NM_012605	-6.72	0.43
1370971_at	Myh1 /// LOC691644	myosin, heavy polypeptide 1	BI277545	-5.37	0.62
1370198_at	Trdn	triadin	AJ243304	-3.27	0.56
1384717_at	---	---	AA894199	-1.55	0.7
1367626_at	Ckm	creatine kinase, muscle	NM_012530	-5.08	0.64
1370550_at	Lsamp	limbic system-associated membrane protein	U31554	-1.5	0.75
1388604_at	LOC679341/// LOC686019	similar to Calsequestrin-1 precursor	BI276959	-2.82	0.69
1385491_at	RGD1560435_predicted	similar to KIAA1183 protein (predicted)	BF403514	-1.71	0.64
1371247_at	Ap2a1_predicted /// Ptov1 /// Med25_predicted	Adaptor protein complex AP-2, alpha 1 subunit /// Prostate tumor over expressed gene 1 /// Mediator of RNA polymerase II transcription, subunit 25 homolog (yeast)	BF521859	-5.01	0.6
1369928_at	Acta1	actin, alpha 1, skeletal muscle	NM_019212	-4.4	0.62
1399073_at	Otub1_predicted	OTU domain, ubiquitin aldehyde binding 1	BI274378	-1.55	0.65
1387133_at	Calb2	calbindin 2	NM_053988	-1.48	0.61
1374677_at	LOC684425	similar to Adenylosuccinate synthetase isozyme 1	AI577508	-3.21	0.68
1368108_at	Atp2a1	ATPase, Ca++ transporting, cardiac muscle, fast twitch 1	NM_058213	-4.04	0.75

Table 5-9: Top 20 genes identified by RPA as upregulated 2 weeks after dorsal column transection

PROBESET ID	GENE SYMBOL	GENE NAME	ACC. NO.	FC	FDR
1377146_at	Vip	vasoactive intestinal polypeptide	AI412212	87.59	0
1387154_at	Npy	neuropeptide Y	NM_012614	29.13	0
1368238_at	Pap (Reg2)	pancreatitis-associated protein	NM_053289	13.01	0
1369268_at	Atf3	activating transcription factor 3	NM_012912	11.13	0
1398243_at	Vsnl1	Visinin-like 1	NM_057144	9.65	0
1384035_at	LOC685277 /// LOC686794	similar to liver-specific bHLH-Zip transcription factor	AW536030	7.67	0
1387088_at	Gal	galanin	NM_033237	6.14	0
1368266_at	Arg1	arginase 1	NM_017134	5.87	0
1392863_at	Flrt3_predicted	fibronectin leucine rich transmembrane protein 3	AA817953	5.69	0
1393573_at	Pde6b_predicted	phosphodiesterase 6B, cGMP, rod receptor, beta polypeptide	AI575628	5.23	0
1381070_at	Synpr	Synaptoporin	AI233106	4.99	0
1371450_at	Sox11	SRY (sex determining region Y)-box11	BE117330	5.03	0
1383210_at	Sox11	SRY (sex determining region Y)-box11	BF554576	4.95	0
1375661_at	Sox11	SRY (sex determining region Y)-box11	BE104180	4.76	0
1371248_at	SPRR1A	similar to Cornifin A (Small proline-rich protein 1A)	BI286387	4.8	0
1382868_at	Sema6a_predicted	semaphorin 6A	BM387083	4.33	0
1378057_at	Flrt3_predicted	fibronectin leucine rich transmembrane protein 3	BE103354	4.24	0
1392862_at	Sema6a_predicted	semaphorin 6A	AA859389	4.25	0
1378700_at	---	Transcribed locus	BF403674	3.85	0
1376601_at	Sema6a_predicted	semaphorin 6A	BF397526	3.85	0

Table 5-10: Top 20 genes identified by RPA as downregulated 2 weeks after dorsal column transection

PROBESET ID	GENE SYMBOL	GENE NAME	ACC. NO.	FC	FDR
1387133_at	Calb2	calbindin 2	NM_053988	-4.94	0
1388349_at	Ckmt2	Creatine kinase, muscle	AA799557	-5.16	0
1374787_at	Vgkc	V-gated potassium channel	BI282169	-4.04	0
1377163_at	Inhbb	inhibin beta-B /// inhibin beta-B	BM385741	-3.81	0
1376980_at	Htr2c	5-hydroxytryptamine	BF285539	-3.72	0
1391575_at	Hapln4	Hyaluronon and proteoglycan link	BG380566	-3.49	0
1382914_at	Adra1a	Alpha1 adrenergic receptor	AA924097	-3.36	0
1370900_at	Myh4	myosin, heavy polypeptide 4, skeletal muscle	BM391169	-9.97	0
1368407_at	Hpse	heparanase	NM_022605	-3.09	0
1374035_at	Rem2	rad and gem-related GTP	BI296482	-3.08	0
1385731_at	Cntn3	Contactin3	BE113552	-3.07	0
1390530_at	---	Transcribed locus	AI169239	-3.14	0
1387065_at	Plcd4	phospholipase C, delta 4	NM_080688	-2.95	0
1371077_at	Htr3b	5-hydroxytryptamine (serotonin) receptor 3b	AI575989	-2.92	0
1394297_at	Hoxd1_predicted	homeo box D1 (predicted)	BG670107	-3.03	0
1396366_at	Chd12	cadherin 12	BF409020	-3.07	0
1370214_at	Pvalb	parvalbumin	AI175539	-2.83	0
1391563_at	RGD1565148_predicted	similar to melanoma associated antigen (mutated) 1-like 1 (predicted)	AA963184	-2.95	0
1384269_at	Mterf	Mitochondrial transcription term. factor	BF386887	-2.93	0
1377106_at	---	Transcribed locus	AW533050	-6.9	0

5.4.2 ANOVA (Genespring)

Following normalisation and filtering of probe-level raw data (from Affymetrix cel. files) (section 2.9.3.1.3) differentially expressed genes were also identified using 1-way ANOVA in Genespring (Agilent). Volcano plots generated by Genespring illustrate the distribution of fold changes in each of the injury models and genes that are changed significantly ($p<0.05$, uncorrected) and have a fold change >1.5 are coloured in red. The number of differentially expressed genes identified by ANOVA in Genespring and by RPA is compared in Table 5-11. ANOVA identifies approximately twice the number of differentially expressed genes than RPA indicating that the latter method of analysis is more conservative and is less likely to generate false positives. The number of genes changed at $p<0.05$ and greater than 1.5-fold is detailed in the final column of Table 5-11. The numbers of genes generated using these two filters together are considerably smaller than those generated by rank products at 5% FDR. This reflects the fact that many of the genes identified by rank products are less than 1.5-fold regulated, even at 5% FDR and also illustrates how the criterion used to choose differentially expressed genes can dramatically affect the outcome of a microarray experiment.

Table 5-11: Comparison of numbers of differentially expressed genes identified by Rank products and ANOVA.

COMPARISON	NO. DIFFERENTIALLY EXPRESSED GENES AT:		
	5% FDR (RANK PRODUCTS)	P<0.05 (ANOVA)	P<0.05 (ANOVA) and over 1.5-fold changed
2DR vs. ctrl	549	1011	218
6SN vs. ctrl	312	573	69
6DR vs. ctrl.	231	466	41
2DC vs. ctrl.	1129	2303	1016
6DR vs. 2DR	202	403	52
2DR vs. 6SN	162	473	36
6DR vs. 6SN	132	240	15
6DR vs. 2DC	802	1936	619
2DR vs. 2DC	695	1827	491
6SN vs. 2DC	836	1836	632

a) 2DR (218 genes)

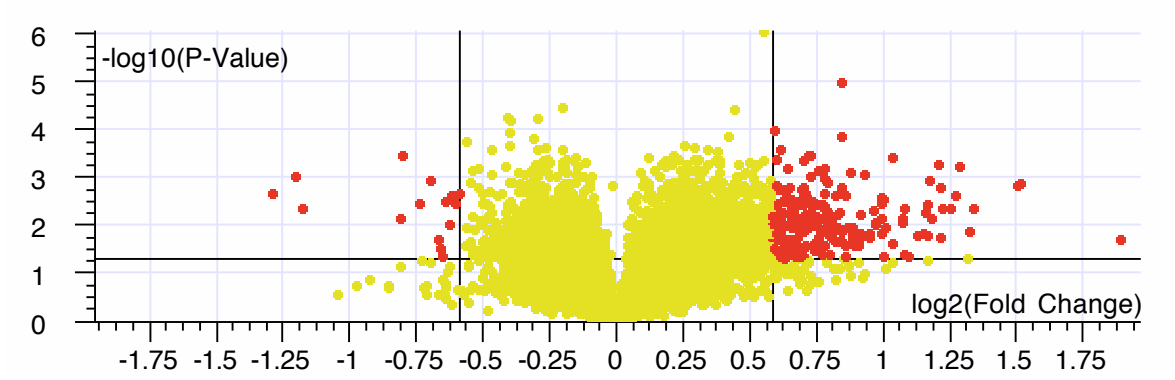

b) 6DR (41 genes)

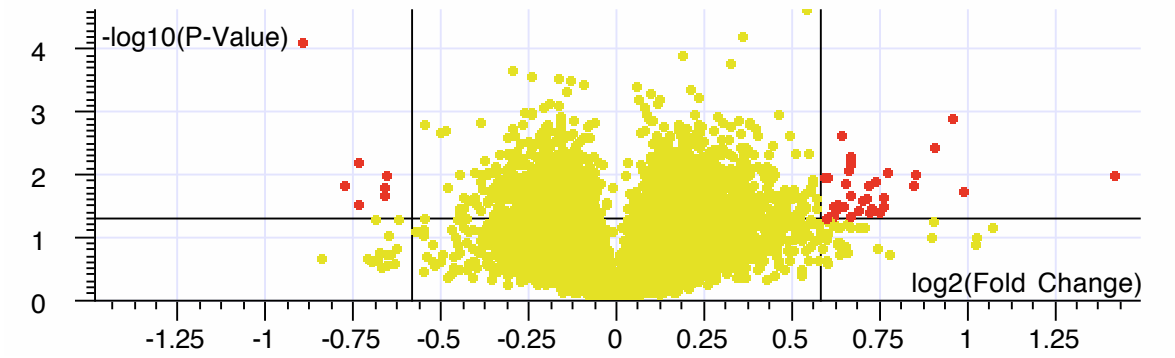

c) 6SN (69 genes)

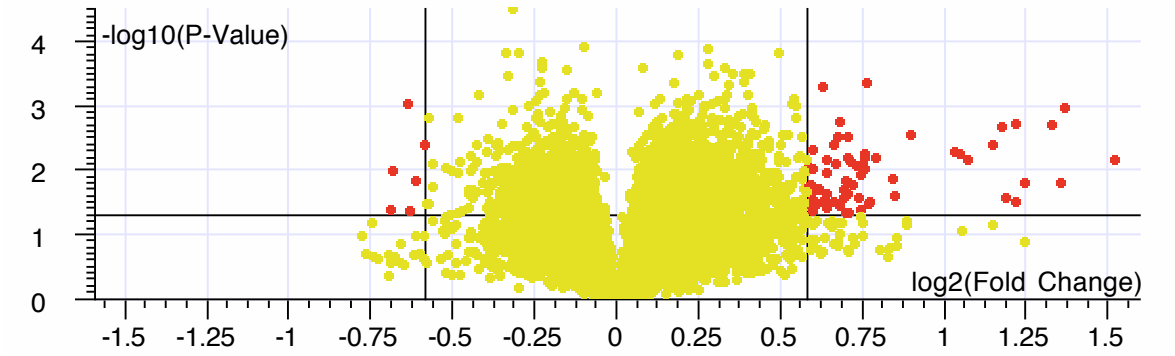

d) 2DC (1016 genes)

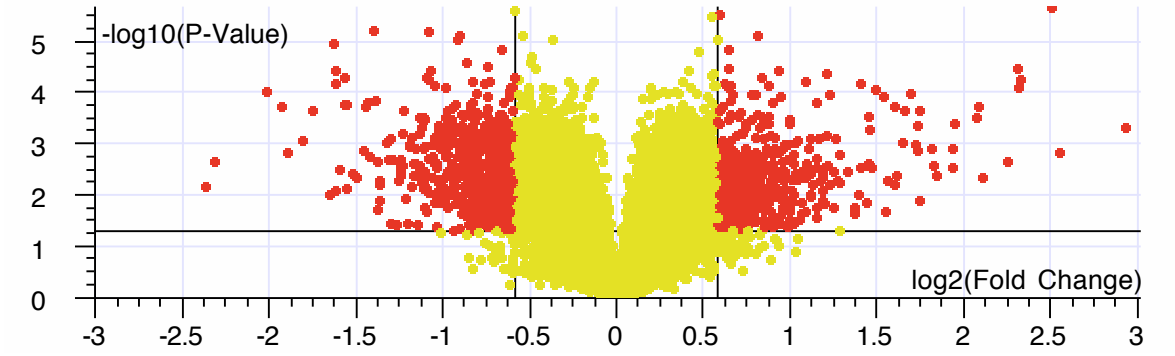

Figure 5-6: Volcano plots displaying mean fold differences for each probe set in the a) 2w DR crush, b) 6w DR crush, c) SN crush and d) DC transection relative to control as a function of P value. Genes showing greater than 1.5-fold differential expression with p values <0.05 are depicted with red dots. Other genes are represented with yellow dots. The vertical line represents a 1.5-fold difference in gene expression whereas the horizontal line corresponds to a P value of 0.05. The data was first filtered on error to remove genes with high variability within conditions (leaving 31028 out of 31099 genes).

5.5 Ontological analysis

Ontological analysis was used to extract the main transcriptional themes associated with each condition. Again for comparison, two different analysis methods were used, Iterative Group Analysis (IGA) that relies on 'GO' classifications, and Ingenuity Pathways Analysis (IPA), which relies upon a recently curated information database based on peer-reviewed papers. IPA also includes a number of visualisation tools that aid in the interpretation of the analysis. Genes that were ranked by false discovery rate using RPA were used in both the ontological analyses methods.

5.5.1 Iterative group analysis (IGA)

IGA was described in (section 2.9.3.1.4). The top changed ontological groups identified by IGA for each condition compared to control and sorted by p-value are presented in Table 5-12 to Table 5-19.

Table 5-12: Top upregulated ontological groups identified by IGA 2 weeks after dorsal root crush

TOP CHANGED GROUPS	NO. GROUP MEMBERS	NO. CHANGED MEMBERS	P-VALUE CHANGED	% CHANGED	GENES INVOLVED
6953 - acute-phase response	26	5	4.4e-09	19.23	PAP, REG3A, A2M, LBP, FN1
8201 - heparin binding	51	6	2.7e-07	11.76	GPNMB, THBS2, FN1, POSTN, ADAMTS1, THBS4
31012- extracellular matrix	13	4	1.4e-06	30.77	CSPG2, COL15A1, ADAMTS1, COL18A1
5529 - sugar binding	96	7	4.9e-06	7.29	PAP, REG3A, LY49, CSPG2, COLEC12, THBD, CLECSF6
IPR008435 - Corticotropin-releasing factor binding	2	2	2.2e-05	100.00	LOC689064, MGC72973
6956 - complement activation	10	3	4.7e-05	30.00	C4A, C1A, C2
5184 - neuropeptide hormone activity	19	2	4.8e-05	10.53	NPY, VGF
7631 - feeding behavior	24	2	5.2e-05	8.33	NPY, BDNF
IPR000961 - Protein kinase C-terminal domain	3	2	6.7e-05	66.67	LOC689064, MGC72973
IPR002075 - Nuclear transport factor 2 (NTF2)	3	2	6.7e-05	66.67	LOC689064, MGC72973
16023 - cytoplasmic membrane-bound vesicle	30	2	8.2e-05	6.67	GPNMB, BDNF
6817 - phosphate transport	50	5	8.4e-05	10.00	CTRC1, COL15A1, COLEC12, COL5A2, COL3A1
4866 - endopeptidase inhibitor activity	52	3	1.3e-04	5.77	SERPINA3N, C4A, A2M
16049 - cell growth	29	4	1.4e-04	13.79	CSRP2, TNN, XM2, EMP1

Table 5-13: Top downregulated ontological groups identified by IGA 2 weeks after dorsal root crush

TOP CHANGED GROUPS	NO. GROUP MEMBERS	NO. CHANGED MEMBERS	P-VALUE CHANGED	% CHANGED	GENES INVOLVED
Striated_muscle_contraction – GenMAPP	26	7	3.6e-11	26.92	ACTN3, MYL2, TPM1, TTN, TNNI2, MYH1, MYBPC1
6941 - striated muscle contraction	22	7	2.5e-10	31.82	MYH4, MYH1, MYBPC1, PGAM2, KBTBD10, SMPX, LOC691644
8307 - structural constituent of muscle	23	7	5.1e-10	30.43	ACTN3, MLC3, MYL2, TPM1, MYBPC2, ASPH, PDLIM3
6936 - muscle contraction	64	6	2.4e-08	9.38	ACTN3, TRDN, ACTA1, TPM1, MYBPC1, MYBPC2
3774 - motor activity	74	5	1.2e-06	6.76	MYH4, MLC3, MYL2, ACTA1, MYH1
16459 – myosin	35	4	1.8e-06	11.43	MYH4, MLC3, MYL2, MYH1
5863 - striated muscle thick filament	16	4	5.4e-06	25.00	MYH4, MYH1, MYBPC1, LOC691644
6937 – regulation of muscle contraction	18	3	8.8e-06	16.67	TNNC2, ATP2A1, TPM1
7517 - muscle development	62	4	1.9e-05	6.45	MLC3, CHODL, ACTA1, MYL1
5865 - striated muscle thin filament	4	2	2.1e-05	50.00	ACTN3, ACTA1
5859 - muscle myosin	10	3	5.0e-05	30.00	MLC3, MYH1, LOC691644
16529 - sarcoplasmic reticulum	8	2	5.5e-05	25.00	TRDN, ATP2A1
45214 - sarcomere organization	6	2	8.4e-05	33.33	ABRA, TTN
5232 - serotonin-activated cation-selective channel activity	2	2	9.1e-05	100.00	HTR3A, HTR3B

Table 5-14: Top upregulated ontological groups identified by IGA 6 weeks after dorsal root crush

TOP CHANGED GROUPS	NO. GROUP MEMBERS	NO. CHANGED MEMBERS	P-VALUE CHANGED	% MEMBERS CHANGED	GENES INVOLVED
5833 - hemoglobin complex	7	3	3.4e-07	42.86	HBB, MGC72973, HBA-A1
IPR008435 - Corticotropin-releasing factor binding	2	2	4.0e-07	100.00	LOC689064, MGC72973
5344 - oxygen transporter activity	8	3	5.4e-07	37.50	HBB, MGC72973, HBA-A1
6956 - complement activation	10	4	8.4e-07	40.00	C4A, C1S, C3, CFB
15671 - oxygen transport	10	3	1.2e-06	30.00	HBB, MGC72973, HBA-A1
IPR000961 - Protein kinase C-terminal domain	3	2	1.2e-06	66.67	LOC689064, MGC72973
IPR002075 - Nuclear transport factor 2 (NTF2)	3	2	1.2e-06	66.67	LOC689064, MGC72973
6957 - complement activation, alternative pathway	6	3	1.0e-05	50.00	CFD, C3, CFB
45087 - innate immune response	27	4	1.4e-05	14.81	CFD, C4A, C1S, C3
19825 - oxygen binding	31	3	4.2e-05	9.68	HBB, MGC72973, HBA-A1
3823 - antigen binding	24	4	6.9e-05	16.67	LOC500180, IGHA, RGD1359202, RT1-BB
50766 - positive regulation of phagocytosis	12	3	6.9e-05	25.00	C3, FCGR2B, FCGR3

Table 5-15: Top downregulated ontological groups identified by IGA 6 weeks after dorsal root crush

TOP CHANGED GROUPS	NO. MEMBERS	NO. CHANGED MEMBERS	P-VALUE CHANGED	% MEMBERS CHANGED	GENES INVOLVED
Striated_muscle_contraction - GenMAPP	26	7	5.3e-11	26.92	ACTN3, MYL2, MYL1, TNNI2, TPM1, TTN, MYBPC1
8307 - structural constituent of muscle	23	9	6.7e-11	39.13	ACTN3, MYL2, MLC3, TPM1, MYBPC2, MYH6, ACTN2, MYOM1, PDLIM3
6941 - striated muscle contraction	22	8	7.8e-11	36.36	MYH4, MYH1, PGAM2, KTBD10, MYBPC1, LOC691644, MYH6, MYH8
5863 - striated muscle thick filament	16	7	9.5e-11	43.75	MYH4, MYH1, MYBPC1, LOC691644, MYH6, MYOM1, MYH8
6936 - muscle contraction	64	9	4.4e-10	14.06	ACTN3, ACTA1, TRDN, TPM1, MYBPC2, CHRNE, MYBPC1, TMOD4, ACTN2
3774 - motor activity	73	5	1.9e-09	6.85	MYL2, MLC3, MYH4, MYH1, ACTA1
16459 - myosin	34	4	6.8e-09	11.76	MYL2, MLC3, MYH4, MYH1
7517 - muscle development	62	4	1.5e-07	6.45	MLC3, CHODL, MYH1, ACTA1
5859 - muscle myosin	10	4	3.3e-07	40.00	MLC3, MYH1, LOC691644, MYH6
5865 - striated muscle thin filament	4	3	1.1e-06	75.00	ACTN3, ACTA1, ACTN2
6937 - regulation of muscle contraction	18	4	3.4e-06	22.22	TNNC2, ATP2A1, TPM1, HSPB6
146 - microfilament motor activity	11	3	4.2e-05	27.27	MYH1, LOC691644, MYH6
45214 - sarcomere organization	6	2	1.1e-04	33.33	ABRA, TTN
16529 - sarcoplasmic reticulum	8	2	1.1e-04	25.00	TRDN, ATP2A1

Table 5-16: Top upregulated ontological groups identified by IGA 6 weeks after spinal nerve crush

TOP CHANGED GROUPS	NO. GROUP MEMBERS	NO. CHANGED MEMBERS	P-VALUE CHANGED	% MEMBERS CHANGED	GENES INVOLVED
5201 - extracellular matrix structural constituent	59	9	1.3e-09	15.25	FN1, COL9A1, COL1A1, FBN1, COL3A1, COL1A2, COL5A2, TFPI2, COL6A1
5833 - hemoglobin complex	7	3	6.8e-09	42.86	HBB, MGC72973, HBA-A1
6817 - phosphate transport	51	8	7.6e-09	15.69	COL9A1, COL1A1, CTHRC1, COL6A3, COL3A1, COL1A2, COL5A2, COL6A1
5344 - oxygen transporter activity	8	3	1.1e-08	37.50	HBB, MGC72973, HBA-A1
15671 - oxygen transport	10	3	2.3e-08	30.00	HBB, MGC72973, HBA-A1
5581 - collagen	17	5	2.0e-07	29.41	COL1A1, COL3A1, COL1A2, COL5A2, COL6A1
IPR008435 - Corticotropin-releasing factor binding	2	2	2.8e-07	100.00	LOC689064, MGC72973
IPR002075 - Nuclear transport factor 2 (NTF2)	3	2	8.5e-07	66.67	LOC689064, MGC72973
IPR000961 - Protein kinase C-terminal domain	3	2	8.5e-07	66.67	LOC689064, MGC72973
19825 - oxygen binding	31	3	8.6e-07	9.68	HBB, MGC72973, HBA-A1
Inflammatory_Response_Pathway - GenMAPP	30	4	3.5e-05	13.33	FN1, COL1A1, COL3A1, COL1A2
5584 - collagen type I	2	2	3.9e-05	100.00	COL1A1, COL1A2
45087 - innate immune response	27	3	9.2e-05	11.11	MX2, CFD, C1S
30278 - regulation of ossification	6	2	9.2e-05	33.33	BEST5, GDF10

Table 5-17: Top downregulated ontological groups identified by IGA 6 weeks after spinal nerve crush

TOP CHANGED GROUPS	NO. GROUP MEMBERS	NO. CHANGED MEMBERS	P-VALUE CHANGED	% MEMBERS CHANGED	GENES INVOLVED
Striated_muscle_contraction - GenMAPP	26	6	3.9e-11	23.08	ACTN3, MYL2, MYH1, TPM1, TTN, TNNI2
6936 - muscle contraction	64	9	2.1e-10	14.06	ACTN3, TRDN, ACTA1, TPM1, MYBPC2, CHME, ASPH, MYBPC1, TMOD4
8307 - structural constituent of muscle	23	6	2.7e-10	26.09	ACTN3, MLC3, MYL2, TPM1, MYBPC2, ASPH
6941 - striated muscle contraction	22	7	3.0e-10	31.82	MYH4, MYH1, KBTBD10, PGAM2, MYBPC1, MYH6, LOC91644
16459 - myosin	35	4	3.8e-09	11.43	MYH4, MLC3, MYL2, MYL1
3774 - motor activity	74	5	2.0e-08	6.76	MYH4, MLC3, MYL2, MYL1, ACTA1
5863 - striated muscle thick filament	16	5	1.1e-07	31.25	MYH4, MYH1, MYBPC1, MYH6, LOC691644
5859 - muscle myosin	10	4	7.1e-07	40.00	MLC3, MYH1, MYH6, LOC691644
6937 - regulation of muscle contraction	18	3	5.8e-06	16.67	TNNC2, ATP2A1, TPM1
5865 - striated muscle thin filament	4	2	8.8e-06	50.00	ACTN3, ACTA1
16529 - sarcoplasmic reticulum	8	2	5.5e-05	25.00	TRDN, ATP2A1
7517 - muscle development	62	3	5.7e-05	4.84	MLC3, MYH1, ACTA1
45214 - sarcomere organization	6	2	7.1e-05	33.33	ABRA, TTN
146 - microfilament motor activity	11	3	7.3e-05	27.27	MYH1, MYH6, LOC691644

Table 5-18: Top upregulated ontological groups identified by IGA 2 weeks after dorsal column transection

TOP CHANGED GROUPS	NO. GROUP MEMBERS	NO. CHANGED MEMBERS	P-VALUE CHANGED	% MEMBERS CHANGED	GENES INVOLVED
19886 - antigen processing, exogenous antigen via MHC class II	9	5	3.2e-10	55.56	RT1-DA, RT1-BA, RT1-DB1, CD74, RT1-BB
42613 - MHC class II protein complex	5	4	2.7e-09	80.00	RT1-DA, RT1-BA, RT1-DB1, RT1-BB
19884 - antigen presentation, exogenous antigen	9	4	6.6e-08	44.44	RT1-DA, RT1-BA, RT1-DB1, RT1-BB
6956 - complement activation	10	4	5.3e-07	40.00	C3, C4A, C1S, C2
6958 - complement activation, classical pathway	20	5	1.0e-06	25.00	C3, C4A, C1S, C2, C1QA
5184 - neuropeptide hormone activity	19	3	3.6e-06	15.79	NPY, GA1, VGF
45087 - innate immune response	27	5	5.0e-06	18.52	C3, C4A, MX2, C1S, C1QA
3823 - antigen binding	24	4	5.2e-06	16.67	RT1-DA, RT1-BA, RT1-DB1, RT1-BB
16064 - humoral defense mechanism (sensu Vertebrata)	13	3	6.2e-06	23.08	CD74, FCGR2B, C4A
Complement and coagulation cascades – KEGG	7	3	1.3e-05	42.86	C3, C1S, C2
Complement_Activation_Classical – GenMAPP	10	3	4.3e-05	30.00	C3, C7, C2
Folate biosynthesis - KEGG	3	2	5.6e-05	66.67	DHFR, GCH
42591 - antigen presentation, exogenous antigen via MHC class II	5	2	6.6e-05	40.00	CD74, FCGR2B
1664 - G-protein-coupled receptor binding	20	2	7.5e-05	10.00	NPY, GAL
51258 - protein polymerization	13	3	1.5e-04	23.08	TUBB6, C7, TUBB2B

Table 5-19: Top downregulated ontological groups identified by IGA 2 weeks after dorsal column transection

TOP CHANGED GROUPS	NO. GROUP MEMBERS	NO. CHANGED MEMBERS	P-VALUE CHANGED	% MEMBERS CHANGED	GENES INVOLVED
5230 – extracellular ligand-gated ion channel activity	38	6	2.6e-10	15.79	HTR3B, GABRA1, CHRNA3, HTR3A, CHRNB4, CHRNE
45211 – postsynaptic membrane	92	8	8.6e-10	8.70	HTR3B, GABRA1, CHRNA3, HTR3A, CHRNB4, CHRNE, SHANK1
5267 - potassium channel activity	65	8	1.8e-08	12.31	KCND3, KCND1, KCND2, KCNC1, KCNS3, CSEN, GRIA2, KCNA4
Striated_muscle_contraction – GenMAPP	26	6	3.4e-08	23.08	ACTN3, MYL2, MYL1, TTN, TPM1, TNNI2
30955 - potassium ion binding	94	9	1.0e-07	9.57	KCND3, KCND1, KCND2, KCNC1, KCNS3, CSEN, KCNA4, SLC24A2, KCNJ6
8076 - voltage-gated potassium channel complex	59	7	1.9e-07	11.86	KCND3, KCND1, KCND2, KCNC1, KCNS3, KCNA4, KCNJ6
8307 – structural constituent of muscle	23	5	1.7e-06	21.74	MLC3, ACTN3, MYL2, TPM1, MYBPC2
6936 - muscle contraction	64	7	1.7e-06	10.94	ACTN3, CHRNE, P2RXL1, ACTA1, TRDN, TPM1, MYBPC2
16459 – myosin	33	4	2.0e-06	12.12	MYH4, MLC3, MYL2, MYH1
5232 - serotonin-activated cation-selective channel activity	2	2	2.6e-06	100.00	HTR3B, HTR3A
15464 – acetylcholine receptor activity	13	3	3.1e-06	23.08	CHRNA3, CHRNB4, CHRNE
3774 - motor activity	72	5	7.9e-06	6.94	MYH4, MLC3, MYL2, MYH1, ACTA1
4890 - GABA-A receptor activity	30	3	2.9e-05	10.00	GABRA1, CHRNA3, CHRNB4
15459 – potassium channel regulator activity	15	3	3.9e-05	20.00	KCNS1, KCNS3, CSEN
7517 – muscle development	62	5	7.4e-05	8.06	NRG1, MLC3, MYH1, ACTA1, CHODL

5.5.2 Ingenuity canonical pathway analysis

The canonical pathways that are affected by the various injury models were analysed using Ingenuity pathways analysis software (IPA) (Ingenuity Systems). In each case, genes regulated within 50% FDR were uploaded to the programme but a 5% FDR cut-off was set for inclusion of a gene in a canonical pathway.

5.5.2.1 Canonical pathways analysis of 2DR data set

In the 2DR injury a total of 2256 of the 3505 inputted transcript IDs (genes regulated within the 50% FDR cut-off) could be mapped in the analysis, 285 of which were within the predefined cut-off of 5% FDR. Of these 285 genes, 271 were align-able with functions/pathways. We defined a deregulation in only two canonical pathways with a p value ≤ 0.05 (Figure 5-7). The affected pathways were 'complement and coagulation cascades' ($p = 8.71E^{-5}$) and 'Il-6 signalling' (p= 0.033). Since any one gene can be mapped to various pathways in this analysis, we identified the differentially upregulated gene A2M (Alpha-2-microglobulin, 2.19 fold change, FDR <0.001 %) as a gene participating in both canonical pathways. Additionally, upregulation of a number of other genes (C2, C3, C1QA, C1R, C1S, C4A, CFH, F3, PROS1, SERPING1 and THBD) were features of the complement and coagulation cascade pathway while upregulation of the immediate-early genes FOS and JUN and the precollagen COL1A contributed to the Il-6 signalling.

5.5.2.2 Canonical pathways analysis of 6DR data set

On analysis of the 6DR data set (1941 transcript IDs) a total of 1285 could be mapped and 120 of 127 genes falling within the 5% FDR cut-off were align-able with functions/pathways. Six significant canonical pathways were identified (Figure 5-7); 'Calcium signallling' ($p = 5.97E^{-10}$), 'Complement and coagulation cascades" ($p = 7.014E^{-8}$), 'Actin cytoskeleton signalling' (p = 0.0001), 'Leukocyte extravasation signalling' (p = 0.0169), 'Il-10 signalling" (p=0.0169) and 'TGF-β signalling" (p = 0.045). The downregulation of ACTA1 (actin alpha 1, 4.79 fold change, FDR=0.08 %) was a major contributor in three of the six identified canonical pathways (calcium signalling, actin signalling and leukocyte extravasation signalling). The downregulation of 13 other genes; ATP2A1, CHRNE, MYH1, MYH2, MYH4, MYL1, RYR1, TNNI, TNNT3, TPM1, TRDN and the upregulation of NFATC1 and TNNT2 were features of the calcium signalling. In the actin cytoskeleton signalling pathway the downregulation of ACTN3, MYH1, MYH2, MYH4, MYL1, TTN and the upregulation of EGFR, LBP were features. The downregulation of ACTN3 and upregulation of CLDN1, CXCL12, CYBB characterise the leukocyte extravasation signalling. The complement and coagulation pathway consisted of 8 upregulated genes; C3, C1S, C4A, CFB, CFD, F3, SERPING1, THBD. The Il-10 signalling pathway consisted of 3 upregulated genes FCGR2B, FOS, LBP while the TGF-β signalling consisted of upregulated genes EGFR and FOS and downregulated INHBB.

5.5.2.3 Canonical pathways analysis of 6SN data set

The 6SN data set (3068 transcript IDs) had a total of 1993 transcript IDs that could be mapped and 154 of 168 of these falling within the 5% FDR cut-off were align-able with functions/pathways. Four significant canonical pathways were identified (Figure 5-7); 'Calcium signalling' ($p = 3.45E^{-5}$), 'Actin cytoskeleton signalling' ($p = 0.0003$), 'Complement and coagulation cascades' ($p = 0.001$) and 'Nitric oxide signalling in the cardiovascular system' ($p = 0.0058$). As in 2DR, the downregulation of ACTA1 was important in defining significant canonical pathways in this analysis, featuring in two out of four of the pathways. Calcium signalling was again characterised by a number of other downregulated genes ASPH, ATPSA1, CALM3, CHRNE, HTR3A, MYH1, MYH4, MYL1, PRKAR2A, RYR1, TN1, TNNT3, TPM1, TRDN along with the upregulation of MYH11, TPM2. Equally, actin cytoskeleton signalling consisted of downregulations of ACTN3, MYH1, MYH4, MYL1, TTN but also upregulations of 6 genes ACTN1, FN1, MYH11, MYLK, PDGFRA, VCL. The complement and coagulation pathway consisted entirely of upregulated genes; C15, C4A, CFD, F3, F5, F13A1, SERPING1, THBD while 'nitric oxide signalling' consisted of downregulated genes ATP2A1, CALM3, HSP90AB1, PRKAR2A and one upregulated gene GUCY1B3.

5.5.2.4 Canonical pathways analysis of 2DC data set

Six significant canonical pathways (Figure 5-7) were identified within the DC data set (6128 transcript IDs, 3892 of which were mapped, 485 of 504 genes falling with 5% FDR were align-able with functions); 'Complement and coagulation cascades' ($p = 0.0012$), 'Calcium signalling' ($p = 0.003$), 'Urea cycle and metabolism of amino groups' ($p = 0.0099$), 'Serotonin receptor signalling' ($p=0.0122$), 'Antigen presentation pathway' ($p = 0.0322$) and 'One carbon pool by folate' ($p = 0.0392$). No one gene could be identified as a main player in multiple pathways. The 14 genes contributing to Complement and coagulation cascades (C2, C3, C1QA, C1QB, C1QC, C1R, C1S, C4A, CFB, CFD, CFH, F3, SERPING1, THBD) were all upregulated whilst genes contributing to the Calcium signalling canonical pathway were mainly downregulated (ACTA1, ASPH, ATP2A1, ATP2B3, CACNA1H, CACNA2D1, CACNG2 CHRNA3, CHRNB4, CHRNE, DSCR1L1, GRIA2, GRIKA2, GRIK1, GRIN1, HTR3A, MYH1, MYH2, MYH4, MYL1, RYR1, TNNI2, TNNT3, TPM1, TRDN and TRPC3) with only three upregulated genes; CAMK2D, CHRNA1 and NFATC1. Urea cycle and metabolism of amino acid was characterised by the downregulation of ASS1, CKM and CKMT1B and the upregulation of ARG1. 'Serotonin receptor signalling' featured downregulation of genes encoding serotonin receptor subunits (HTR3, HTR7, HTR1D, HTR3A and HTR3B) and upregulation of GCH1 and MAOA. The antigen presentation pathway consisted entirely of the upregulated genes CD74, HLA-DMB, HLA-DQA1, HLA-DQB2, HLA-DRA and HLA-DRB1 while 'One carbon pool by folate' consisted only three molecules, one of which was upregulated (DHFR) while the other two were downregulated (DMGDH and GART).

2DR

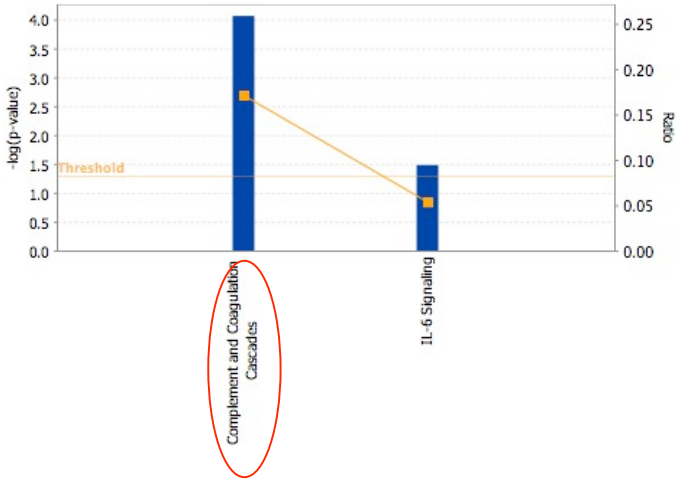

6DR

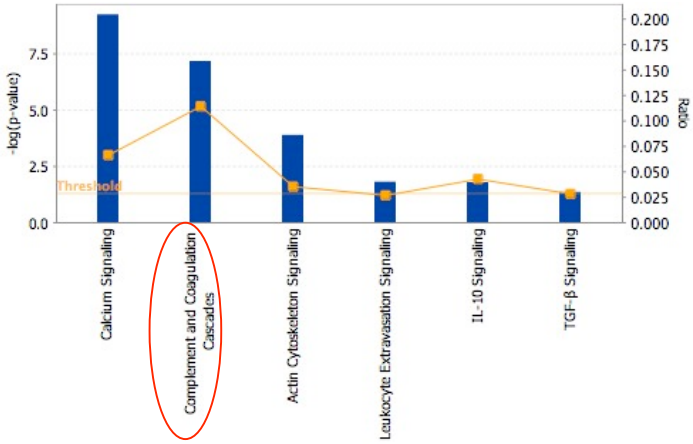

6SN

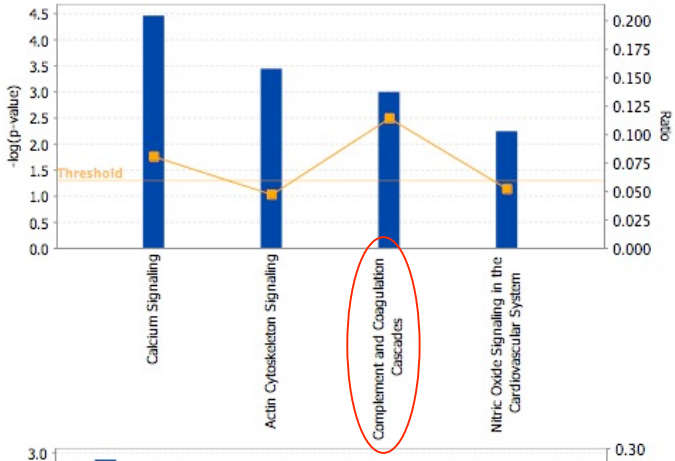

2DC

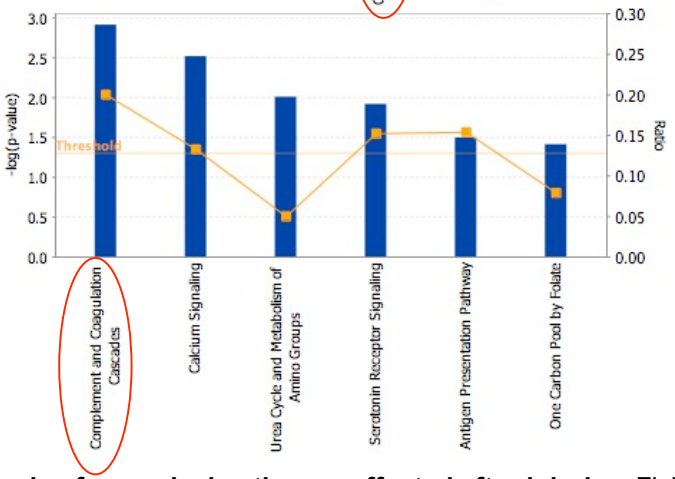

Figure 5-7: IPA analysis of canonical pathways affected after injuries. Fisher's exact test was used to calculate a p value (shown as blue bars) determining the probability that each biological function assigned to the network is due to chance alone. The ratio (shown as yellow squares)

represents the number of differentially expressed genes in a given pathway relative to the total number of genes that make up that canonical pathway. The threshold line is set at p=0.05.

5.5.3 Identification of biologically relevant networks using Ingenuity network generation

To further investigate the global expression response in the DRG to different injuries, and to define how individual regulated genes interact to have a coordinated role in specific pathways, we identified potential networks of interacting genes using IPA's network generation function. The methodology integrates genomic data with mining techniques to predict protein networks that comprise protein-protein interactions and other functional linkages (section 2.9.3.2.1). Each potential network is given a score, which is a probabilistic fit between the networks and a list of biological functions stored in the Ingenuity Pathways Knowledge Base. The score takes into account the number of focus genes (from 5% FDR lists) in the network, and the size of the network, to approximate how relevant it is to the original list of genes. IPA uses a right-tailed Fisher's test to calculate the P value for networks. A score of 10, for example, would mean that there is a $P=10^{-10}$ chance that the genes in that network are associated solely by chance. A score of 3 or greater was therefore considered significant ($p < 0.001$). The scores are used to rank the networks and the top ranked network is presented as a graph indicating the molecular relationships between gene/gene products. Genes or gene products are represented as nodes and the biological relationship between two nodes is represented as an edge (line). All edges are supported by at least one literature reference of direct physical, transcriptional and enzymatic interactions or from canonical information stored in the Ingenuity Pathways Knowledge Base. The colour intensity of the node represents the degree of up (red) or downregulation (green). Nodes are displayed with various shapes that represent the functional class of the gene product. Keys to the network nodes and edges for Figure 5-8 to Figure 5-12 can be found in appendix B. Functional analysis of a network then identified the biological functions/diseases that were most significant to the genes in the network.

5.5.3.1 Networks of genes regulated at 2 weeks after dorsal root crush

We identified 14 networks of potentially interacting genes from the genes regulated at the 5% FDR level 2 weeks post-DR crush; the top 5 networks are provided in Table 5-20. One of the highest ranked networks identified by IPA (Figure 5-8**)** contains genes associated with cell-to-cell signalling and interaction, cellular movement and dermatological diseases while the other (Figure 5-9) contains genes associated with cell morphology, cellular growth and proliferation and carbohydrate metabolism.

Table 5-20: Top 5 networks of genes regulated (all p<0.001) at 2 weeks after dorsal root crush

	NETWORK GENES (FOCUS GENES IN COLOUR)	SCORE	FOCUS GENES	TOP FUNCTIONS
1	ADAMTS1, ATP2A1, C1QA, C1R, C1S, CHGA, CKM, COL18A1, COL1A1, COL1A2, COL2A1, COL3A1, CSPG2, DCN, EGFR, F3, FAP, FBN1, FN1, HLA-DQA1, IGF1, IGFBP5, IGFBP6, LOX, MMP2, NID1, PCOLCE, SERPINA3, SERPING1, SFRP2, SNED1, TFPI2, TNNT3, TWIST1, WISP2	57	35	Cell-To-Cell Signaling and Interaction, Dermatological Diseases and Conditions, Cellular Movement
2	ACP5, ADCYAP1, ATF3, BDNF, CART, CCND2, CDKN1C, DAB2, EGR1, FOS, GPC3, HMGB2, KBTBD10, KCNIP3, LEPR, MYH4, NPY, NRG1, NTS (includes EG:4922), PGAM2, POU3F1, PRRX1, PTGER4, PVR, PVRL3, RAB3A, RBP1, SERPINF1, SFRP4, SOAT1, SST, TGFBI, TGFBR1, TUBB2B, VGF	57	35	Cell Morphology, Cellular Growth and Proliferation, Carbohydrate Metabolism
3	A2M, ANXA1, AXL, C7, CA3, CCL13, CD68, CTSK, CXCL9, CXCL12, CYP1B1, CYP2J2, ERCC1, HRC, ITGAD, ITGAL, JDP2, JUN, LTBP1, MAP3K8, MEOX2, MOG, NFATC1, P2RY2, PCSK1, PKD1, PLA2G4A, PPIC, PTX3, RYR1, RYR2 (includes EG:6262), SMARCA2, THBS2, TRDN, VCAM1	26	22	Cell-To-Cell Signaling and Interaction, Hematological System Development and Function, Immune and Lymphatic System Development and Function
4	ADAMTS4, C5ORF13, CLDN1, CLOCK, COL11A1, COL8A1, COMP, CP, DAPK1, EPB41L1, FBLN1, FKBP5, FN1, GCNT1, GJB2, ITGAE, ITGB6, ITGB8, LOXL2, MGP, MTPN, MYH1, MYLK, MYLPF, NOV, OCLN, PDGFC, PDGFRA, PLEKHC1, TEF, TGFB1, TGFBI, TJP2, TJP3, TPM3	18	17	Cancer, Tumor Morphology, Cell Morphology
5	ASPH, ATP1A3, CHUK, COL5A2, CPT1A, CSRP2, CXCL13, CXCL14, DYRK1A, FGF2, FZD2, GBP4, GDF10, GNA15, GPNMB, HRAS, ID2, KCNC1, KLF5, LOX, MRPL12, NOV, PDLIM5, PGK1, PLOD1, PTEN, PTGS1, SOX4, SPRY1, SPRY2, TMSB10, TOM1, TOP2A, VEGFB, VEGFC	16	16	Cardiovascular System Development and Function, Organismal Development, Cellular Assembly and Organization

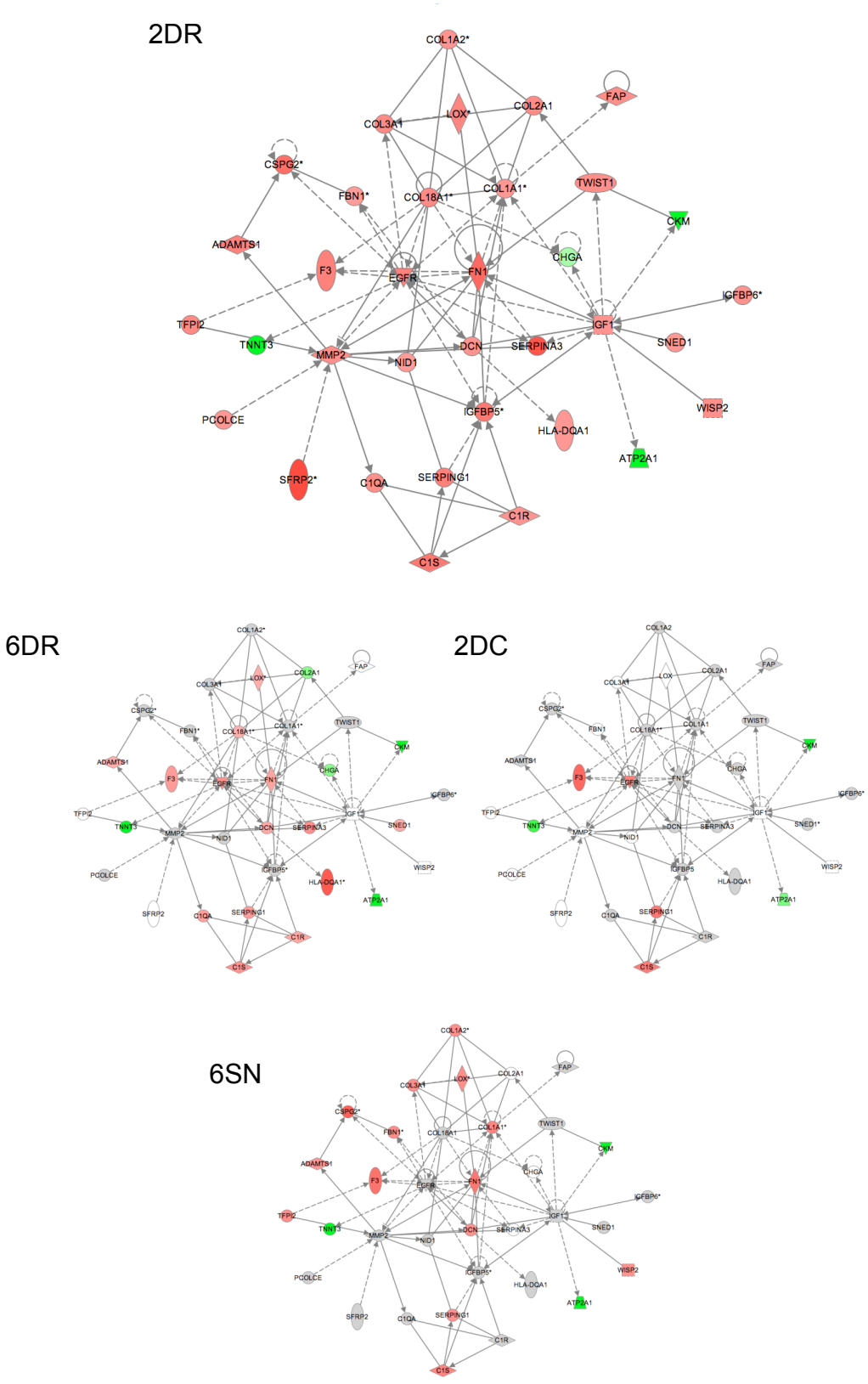

Figure 5-8: Ingenuity pathways analysis identifies a network of genes centred around EGFR, FN1 and IGF1 and that is regulated in the DRG 2 weeks after dorsal root crush relative to naïve control. This is one of the two top regulated networks for this condition (**Table 5-20**). For comparison, the network is also shown overlaid with expression information from the other data sets. Nodes are coloured according to expression (upregulated=red, downregulated=green).

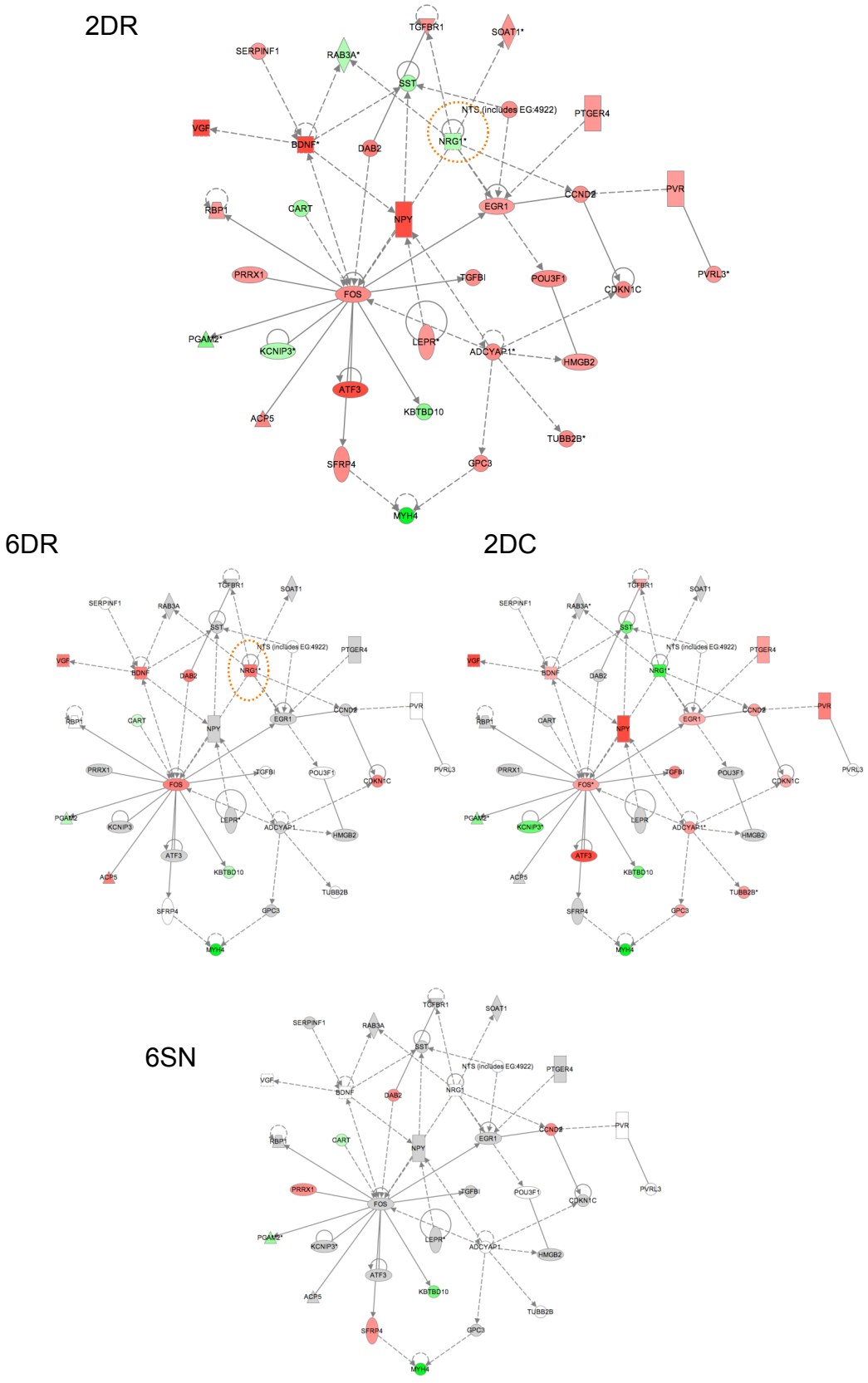

Figure 5-9: Ingenuity pathways analysis identifies a network of genes centred around FOS that is regulated in the DRG 2 weeks after dorsal root crush relative to naïve control. This is one of the top upregulated networks for this data set (Table 5-20). For comparison, the network is also shown overlaid with expression information from the other data sets. Nodes are coloured according to expression (upregulated=red, downregulated=green).

5.5.3.2 Networks of genes regulated at 6 weeks after a dorsal root crush

We identified 6 significant networks from the genes regulated at the 5% level 6 weeks after dorsal root crush. The top 5 networks are described in Table 5-21. The top ranked network (Figure 5-12) contains 33 genes involved in Skeletal and Muscular System Development and Function, Tissue Morphology and Cardiovascular System Development and Function.

Table 5-21: Top 5 networks of genes regulated (all p<0.001) at 6 weeks after a dorsal root crush.

	NETWORK GENES (FOCUS GENES IN COLOUR)	SCORE	FOCUS GENES	TOP FUNCTIONS
1	ACP5, ACTA1, ACTN3, ADIPOQ, AR, BDNF, C3, C1S, C4A, CART, CDKN1C, CFB, CFD, CHRNE, CXCL12, DAB2, EGFR, F3, FOS, GAS5, HBA2, HBB (includes EG:3043), HRC, KBTBD10, LTK, MEOX2, MYOZ1, NRG1, PCK1, PGAM2, RYR1, SERPING1, TNNT3, TRDN, VGF	65	33	Skeletal and Muscular System Development and Function, Tissue Morphology, Cardiovascular System Development and Function
2	ALAS2, ATP2A1, CD40LG, CKB, CKM, CXADR, DDX42, FLOT2, FMO3, FYN, HDLBP, ID2, IGF1, IL15, KRAS, MS4A1, MSC, MYLPF, MYOD1, OGN, PAWR, PDLIM5, RYR1, SLA, SP1, TCF23, TEAD2, THBD, TNNI2, TNNT2, TPM3, WNT11, WT1, YARS, ZFP36L1	24	17	Cellular Growth and Proliferation, Hematological System Development and Function, Immune Response
3	C19ORF10, CCKAR, CD68, CD244, CLDN1, CSNK1A1, CTNNB1, CX3CR1, CYBA, CYBB, DBP, ERBB2, GAD1, GJB2, HIRA, HOXA9, HOXA10, IFNG, JUN, LMO7, MAP3K8, NFATC1, NLK, OCLN, PBXIP1, PCSK1, PKD2 (includes EG:5311), PTCH, PTPRG, RT1-AW2, S100A8, SDPR, TAX1BP3, TJP2, TJP3	21	15	Cancer, Tumor Morphology, Genetic Disorder
4	ACTN1, CEBPA, CFD, COL8A1, CPS1, CPT1A, CYP3A5, ENO3, FABP3, FCAR, FGF19 (includes EG:9965), GFPT1, HK3, LEP, LTC4S, MGP, MTPN, MYF6, MYH1, ORM2, PARD6G, PCTK2, PRKAA1, PTGDS, RAC1, RATNP-3B, S100A8, S100A9, S100G, SC5DL, TGFB1, THBD, TTN, UCP1, VCL	19	14	Cellular Growth and Proliferation, Skeletal and Muscular System Development and Function, Developmental Disorder
5	ALCAM, APLN, CALD1, CHST4, COCH, CP, CXCL13, DDX11, DSTN, FCGR2B, GBP2, GFAP, HK2, HMGN2, HPSE, HTATIP2, KLF10, LBP, LIF, MAP4K2, MBP, MYC, NOS3, ORM2, PRPH, PYGM, QKI, RBP1, RPS13, SLK, SPARC, STEAP4, THBS4, TNF, TPM1	15	14	Connective Tissue Development and Function, Tissue Morphology, Cellular Movement

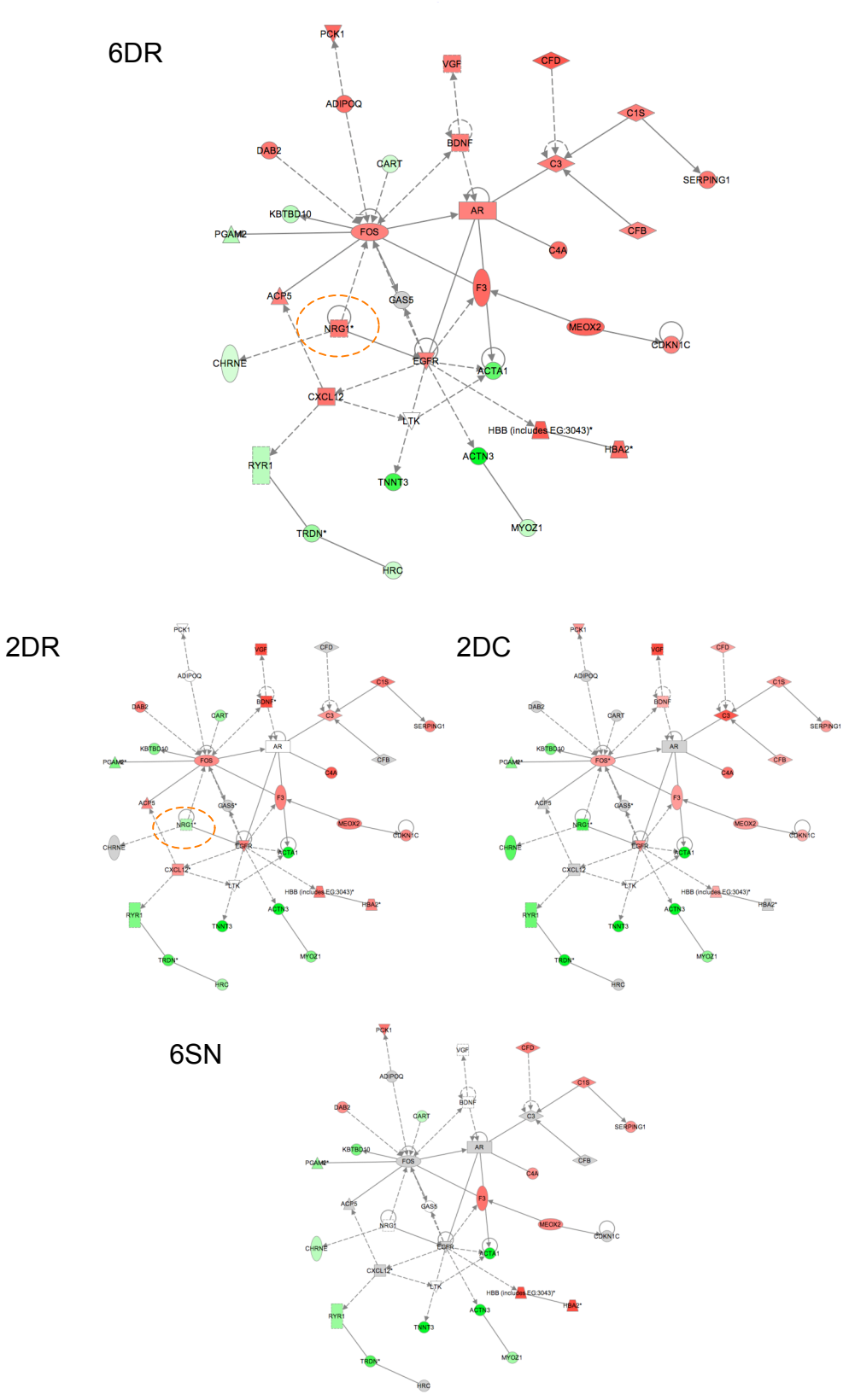

Figure 5-10: Ingenuity pathways analysis identifies a network of genes that is centred around FOS and that is regulated in the DRG 6 weeks after dorsal root crush relative to naïve control. This is the top upregulated network for this data set (Table 5-21) The intensity of the node colour indicates the degree of up (red)- or down (green)- regulation. For comparison, the network is also shown overlaid with expression information from the other data sets.

5.5.3.3 Networks of genes regulated at 6 weeks after a spinal nerve crush

We identified 10 significant networks from the genes regulated at the 5% FDR level at 6 weeks after a spinal nerve crush. The top 5 networks are presented in Table 5-22. The top ranked network (Figure 5-11) contains 26 genes involved in Cellular Movement, Cell-To-Cell Signaling and Interaction and Tissue Development.

Table 5-22: Top 5 networks regulated (all at p<0.001) at 6 weeks after a spinal nerve crush.

	NETWORK GENES (FOCUS GENES IN COLOUR)	SCORE	FOCUS GENES	TOP FUNCTIONS
1	ADAMTS1, ANXA1, Ap1, CAMP, COL1A1, DAB2, DCN, ENTPD1, F3, F5, FBN1, FCGR2B, FN1, IL33, Integrin, ITGB1BP1, MEOX2, MYLPF, OMD, P38 MAPK, Pdgf, PDGF BB, PDGFRA, PI3K, Pkc(s), PPP2R2A, RTK, S100A8, S100A9, TAGLN, TFPI2, Tgf beta, VCAM1, VCAN, WISP2	48	26	Cellular Movement, Cell-To-Cell Signaling and Interaction, Tissue Development
2	ACTA1, Actin, ACTN1, ADH1C (includes EG:126), Akt, AMPD1, ASPH, Calcineurin protein(s), CALM3, Calmodulin, CaMKII, CKM, DBP, F Actin, LMO7, MB, MEF2, MYH1, MYH11, MYL1, MYLK, Myosin, P8, PER2, PER3, Ryr, RYR1, TEF, TNNT3, TPM1, TPM2, TRDN, Tropomyosin, TTN, VCL	45	25	Skeletal and Muscular System Development and Function, Tissue Morphology, Cell Signaling
3	ACTA1, ARID1B, CARTPT, CCNE2 (includes EG:9134), CDH11, CES1 (includes EG:1066), COL6A1, COL6A2, COL6A3, COL6A MAPPED, CTSH, ENO3, ERBB2, FIGF, FOS, GAS1, KBTBD10, KIFC3, LTBP2, LUM, MAP1B, MYH4, NF2, NRP1, PGAM2, PRRX1, SERPINE2, SFRP, SFRP4, SFRP5, SMARCA4, SMARCD1, TNNI2, TNNT3, TPM1	26	17	Genetic Disorder, Skeletal and Muscular Disorders, Cancer
4	ACADVL, ALAS2, ATP2A1, C4A, CD163, CIAA1, CIAA2, CLEC4A, COL10A1, COL1A2, COL3A1, CTSS, dihydrotestosterone, F13A1, G0S2, ganglioside GM4, GPNMB, GPX4, GUCY1B3, H2-Q10, Hsp70, HSP90AB1, HSPA1L, IL13, IL13RA2, IL1B, IL3RA, LOX, MBP, PYGM, RSAD2, S100A8, STAT3, TMF1, UGDH	26	17	Gene Expression, Viral Function, Cell-To-Cell Signaling and Interaction
5	C1q, C1R, C1S, CD74, CD81, CFD, CHRNE, CHRNG, COL15A1, CPT2, CPT1A, CTSC, CTSS, DEFB103A, DEFB4 (includes EG:1673), HLA-DRA, IDH1, IFITM1, IFNK, IGK@, IGKC, malonyl-coenzyme A, MAP3K7IP2, MX1, NCOR1, NID1, NR1D1, NR1D2, OGN, PANK2, RFX5, SERPINE2, SERPING1, STEAP4, TNF	22	15	Immunological Disease, Lipid Metabolism, Small Molecule Biochemistry

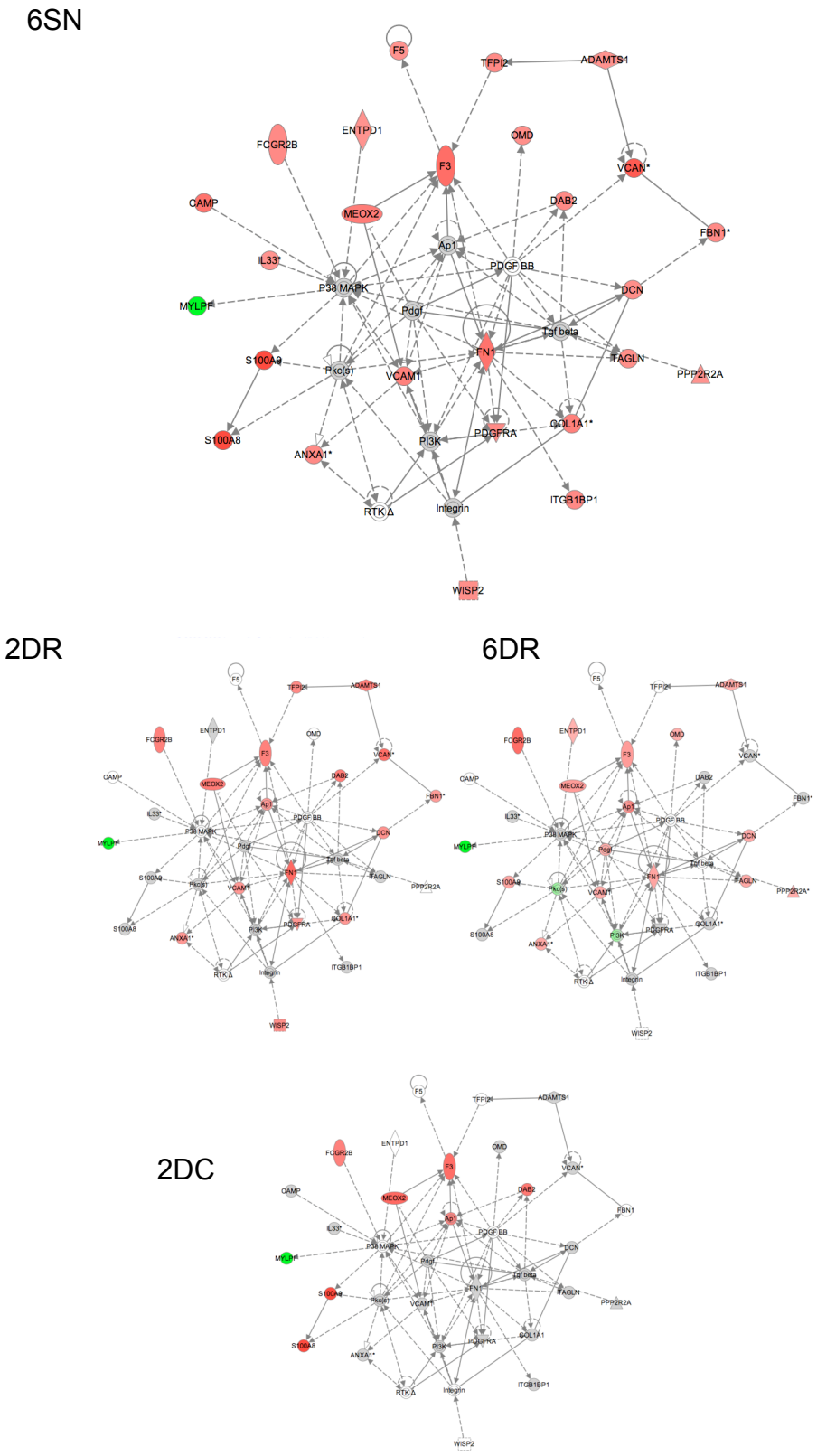

Figure 5-11: Ingenuity pathways analysis identifies a network of genes regulated in the DRG 6 weeks after spinal nerve crush relative to naïve control. This is the top regulated network for this condition (**Table 5-22**). For comparison, the network is also shown overlaid with expression information from the other data sets. Nodes are coloured according to expression (upregulated=red, downregulated=green).

5.5.3.4 Networks of genes regulated at 2 weeks after a dorsal column transection

28 significant networks were identified from the genes regulated at the 5% FDR level 2 weeks after a dorsal column transection. The top ranked network (Figure 5-12) contains 30 focus genes involved in Immune Response, Cell Signaling and Immunological Disease.

Table 5-23: Top 5 networks regulated (all at p<0.001) at 2 weeks after a dorsal column transection.

	NETWORK GENES (FOCUS GENES IN COLOUR)	SCORE	FOCUS GENES	TOP FUNCTIONS
1	ASPH, ATP2A1, C1q, C1QA, C1QB, C1QC, C1R, C1S, CAMK2D, CCKBR, CD63, CD74, CDKN1A, CFH, CTSS, CXADR, DCN, HLA-DMB, HLA-DQA1, HLA-DQB2, HLA-DRA, HLA-DRB1, IRF2, KLF10, MHC Class II, MHC II-β, Phosphoinositide phospholipase C, PLCD1, PLCD4, RACGAP1, RFX4, Ryr, RYR1, TGM1, TRDN	44	30	Immune Response, Cell Signaling, Immunological Disease
2	Ap1, ARRB1, CACYBP, CLDN1, DUSP5, EGFR, F3, FABP7, GABAR-A, GABRA1, GABRA5, GABRB1, GABRG2, GBP2 (includes EG:14469), GJB2, HBD, MEOX2, OCLN, OMD, Pdgf, PDGF BB, Phospholipase C, Pkc(s), PLAC8, PLSCR1, POSTN, PRKCE, PTGER4, RGS2, SLC1A1, STAT5a/b, THBD, UGDH, XDH, ZFP36L1	39	28	Neurological Disease, Developmental Disorder, Psychological Disorders
3	ACTN3, BCL2L2, CHGA, CP, CUGBP2, ERK1/2, FLNC, FOS, FREQ, Gpcr, GTF2F2, HRK, KBTBD10, KCNAB1, KCND3, KCNIP3, Mek1/2, MET, MYH2, MYOT, MYOZ1, Ngf, NMB, NPY, P2RY1, PDGF-AA, PGAM2, PP1/PP2A, PP2A, PPP2R2A, PPP2R5C, SLC40A1, STAT, TGFBI, UCN	37	27	Molecular Transport, Behavior, Carbohydrate Metabolism
4	AEBP1, ASS1, DRD2, ENTPD1, FCGR2B, G alphai, G protein beta gamma, GADD45A, GADD45G, GFRA1, GFRA2, Gi-coupled receptor, GRM4, HTR1D, IL24, KCNJ6, KLF13 (includes EG:51621), Mapk, MYLPF, P2RX3, P2RX5, P2RXL1, P38 MAPK, Pak, Plc beta, PLC gamma, PLEK, PTPN6, PTPRH, RET, RGS3, RGS4, S100A9, SST, TRPV1	37	27	Cell Signaling, Digestive System Development and Function, Organ Morphology
5	C2, C3, C3-Cfb, CASP3, CASP7, Caspase, Caspase 3/7, CD24, CFB, CFD, CYBB, DSP, DUSP1, EMP1, Fibrin, FN1, GZMB, HAPLN1, Igfbp, IGFBP3, INCENP, Integrin, IRF8, LYZ, Mmp, MMP3, MMP16, P2RX7, Rap1, SERPINA3, SERPINI1, SNED1, Sod, TAC1, VIP	35	26	Inflammatory Disease, Connective Tissue Disorders, Skeletal and Muscular Disorders

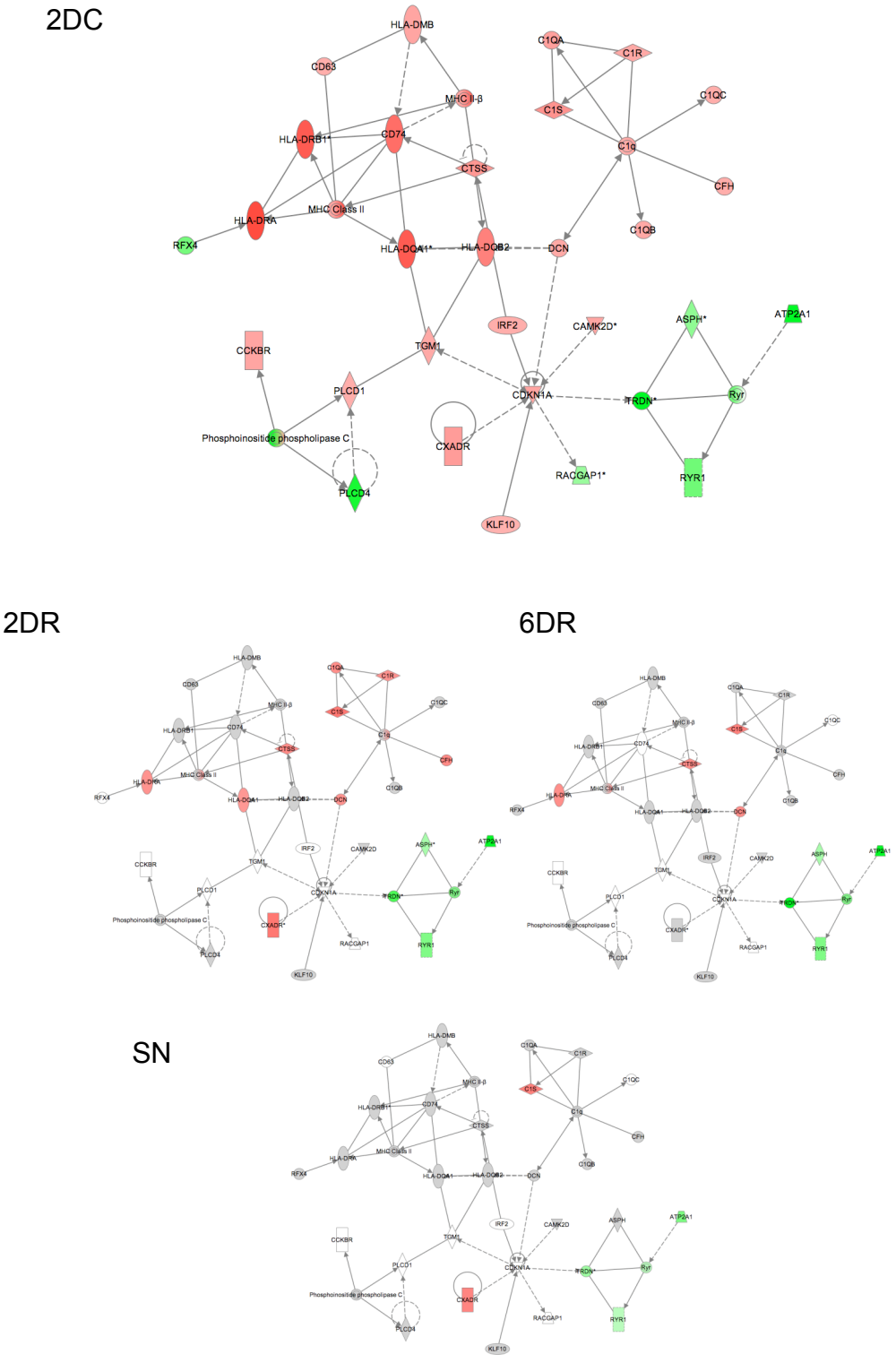

Figure 5-12: Ingenuity pathways analysis identifies a network of genes regulated in the DRG 2 weeks after dorsal column transection relative to naïve control. This is the top regulated network for this data set (**Table 5-23**). For comparison, the network is also shown overlaid with expression information from the other data sets. The nodes are coloured according to expression (upregulated=red, downregulated=green).

5.6 Discussion (for sections 5.4 and 5.5)

5.6.1 Centrally or peripherally axotomised DRG neurons respond to injury by altering their gene expression programmes

All the injury models elicited changes in the expression of genes within the DRG. Whilst there have been previous studies that examine gene changes in the DRG following injury to the spinal nerve or dorsal root, this is the first study that examines changes in the DRG after an injury within the CNS, namely dorsal column transection. This injury elicited the largest changes and changes in more genes than the other injuries. Indeed transection of the dorsal columns elicited a transcriptional response which was more dramatic than that elicited at the same time-point following injury to the dorsal root (Table 5-2). This is perhaps surprising given that transcriptional activation has been shown to diminish as a function of the distance of a lesion from the cell body (Rossi *et al*. 2007). Dorsal column transection also differed from the other injuries in that it caused mainly downregulation of genes as opposed to upregulation. The complete separation of this injury from the other injury models on the basis of principle components analysis and correlation analysis, further suggests that dorsal column transection activates a transcriptional programme that is different to that elicited by injuries out-with the CNS, in either the peripherally or centrally projecting branches of the DRGN. This difference may be attributed to the fact that unlike in dorsal root and spinal nerve crush, dorsal column transected axons retain a supply of target derived factors through their intact central terminals.

5.6.2 Genes regulated after dorsal column transection include known RAGs

The transcriptional response to CNS injury included upregulation of genes that are known to stimulate neurite outgrowth. Some of these were among the top 20 upregulated genes after dorsal column transection (Table 5-9) and included: FLRT3; a cell surface molecule which is expressed in sensory neurons after sciatic nerve injury and which promotes neurite outgrowth *in vitro* (Robinson *et al.* 2004; Tsuji *et al.* 2004); GAL, which has already been reported to be upregulated after dorsal column transection (Zvarova *et al.* 2004) and which been suggested to have a trophic role in regeneration as neuronal outgrowth after a sciatic nerve crush injury is reduced by 35% in Gal-KO mice (Holmes *et al.* 2000); ARG1 and SPRR1A (see section 1.4.2); and ATF3 (see also 3.3.3.2). Indeed, the top upregulated genes showed many overlaps with those regulated after sciatic nerve transection (Chapter 3 table). This can be interpreted in one of two ways. This could suggest that even after the period of spontaneous sprouting (at 6-24 hours (Kerschensteiner *et al.* 2005)) after CNS injury, genes that are conducive to neurite regeneration are upregulated in the DRG. This has relevance to clinical interventions as it suggests that the appropriate transcriptional

programmes for regeneration may still be in place up to 2 weeks after injury and as such provides a window of opportunity for manipulation of the lesion zone. Alternatively, the commonalities that exist between the pilot microarray and dorsal column transection could reflect the fact that these are both transection injuries and differ from the other conditions in that the continuity of the basal lamina is disrupted.

5.6.3 Dorsal column injury triggers changes that are associated with neuropathic pain after peripheral nerve injury

Neuropathic pain is defined as pain initiated or caused by primary lesions or dysfunction in the nervous system. Unlike physiological pain, which is transient, neuropathic pain can be persistent and is associated with changes in the excitability of primary afferent neurons that leads to weakened presynaptic inhibition (Zimmermann 2001). Presynaptic inhibition of primary afferent input is a mechanism by which sensory information from the periphery is filtered. Negative feedback control on activated primary afferents by intraspinal inhibitory neurons results in primary afferent depolarisation (PAD), a mechanism that decreases transmitter from primary afferents and that is known to occur in the main, through activation of ionotrophic GABAergic, glutaminergic and serotonergic receptors. The overall effect is reduced sensory synaptic transmission. These normal inhibitory mechanisms are perturbed in neuropathic pain situations.

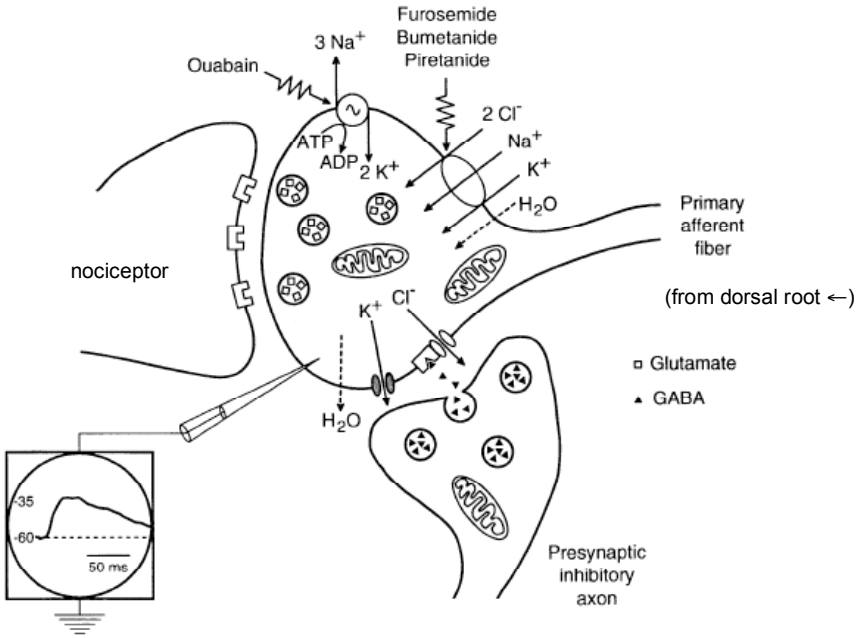

Figure 5-13: Schematic representation of a presynaptic inhibitory axon producing primary afferent depolarisation in a primary afferent fibre. Adapted from Rudomin and Schmidt (1999).

Ontological analysis highlighted another feature of the transcriptional response to dorsal column transection that is also a feature of the response to peripheral nerve injury models of neuropathic pain described by (Wang *et al.* 2002). This was the dramatic downregulation of $GABA_{1A}$ receptors, potassium channels, nicotinic acetycholine receptors, 5HT3 receptors (Table 5-19) and glutamate receptors (Figure 5-14). These changes are associated with increased axonal excitability and neuropathic pain of peripheral nerves or with changes in central pain processing: $GABA_A$ receptor subunits are downregulated in the DRG in the chronic constriction injury (CCI) model of neuropathic pain (Obata *et al.* 2003) and also in chronic pain states (Naik *et al.* 2008); there is loss of functional neuronal nicotinic acetylcholine receptors in DRGs of rats with spinal nerve ligation and neuropathic pain (Dube *et al.* 2005); axotomy of DRG neurons decreases expression of potassium channel subunits leading to a 50-60% decrease in potassium currents and neuronal hyperexcitability (Ishikawa *et al.* 1999; Yang *et al.* 2004) and, 5HT3 receptors are expressed in dorsal horn of the spinal cord where they mediate antinociception (Bardin *et al.* 2000; Sasaki *et al.* 2001). They are also expressed in the DRG (Morales *et al.* 2001). In peripheral nerve injury the downregulation of all these receptors and ion channels in the DRG leads to increased excitability of peripheral nerves and decreased presynaptic inhibition at central terminals. This presynaptic plasticity can modulate neuropathic pain development and maintenance. After dorsal column transection these changes may contribute to the development of chronic spinal pain by causing changes in the effectiveness of transmission in the intact central terminals of the afferent fibres or by modulating the excitability of peripheral branches.

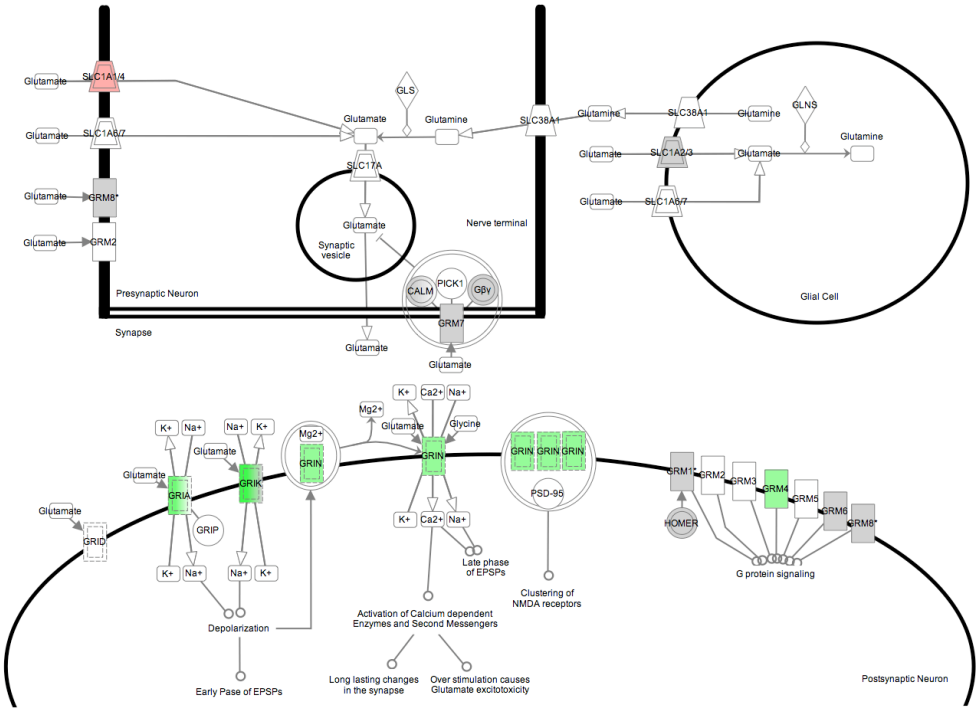

Figure 5-14: Glutamate signalling KEGG pathway illustrating downregulation (green) of glutamate receptors after dorsal column transection.

5.6.4 Dorsal column transection activates MHC class II antigen processing in the DRG

A dominating feature of the IGA analysis for dorsal column transection was activation of genes involved in MHC class II antigen processing (Table 5-18, Figure 5-7 and Figure 5-12). This was specific to this condition and, interestingly, also sciatic nerve transection. DRGs are not protected by the blood brain barrier and are known to undergo invasion by MHC II - expressing macrophages after peripheral nerve lesions (Hu and McLachlan 2002). Macrophage recruitment is stimulated by TNF-α originating from the lesion site which is transported retrogradely, inducing the expression of two monocyte chemoattractants in the DRG (MCP-1 (Tanaka *et al.* 2004) and ICAM-1 (Schafers *et al.* 2002)). It can be envisioned that differences in macrophage recruitment to the DRG and hence levels of MHC II class molecules may result from various types of axon injury if the levels of TNF-alpha that are produced are different. Indeed, recruitment of MHC II+ macrophages has been shown to be greater after a transection injury than after a chronic constriction injury (Hu *et al.* 2007). This may account for the similarities in MHC II activation that we see in the sciatic and dorsal column transection injury models.

5.6.5 Expression of RAGs, neurotrophic factors, growth factors and collagen subunits is depressed in the regeneration arrested dorsal root compared to regenerating dorsal root

At 2 weeks post- dorsal root crush there is the presence of regeneration-associated genes (ATF3, ADAMTS1) and regeneration-promoting neurotrophic factors and growth factors (BDNF and VGF) among the top upregulated genes. This is reflected in the IGA ontological analysis that identifies neuropeptide hormone activity as an important theme at this timepoint (Table 5-3). At 6 weeks after injury these genes no longer appear among the top upregulated genes and there is a general reduction in gene expression changes (Table 5-2).

A striking difference between gene expression in the regenerating and regeneration-arrested dorsal root is the expression of procollagens. IGA identifies ontological groups containing a number of procollagens as significantly upregulated 2 weeks post-dorsal root injury and these are not a feature for the oncological analysis of genes regulated at 6 weeks post injury. IPA network analysis illustrates this difference (Figure 5-15). The fact that the upregulation of procollagens is seen at 6 weeks post- spinal nerve injury suggests that downregulation of these genes at 6 weeks post dorsal root injury is not purely a time dependent effect and may be due to signals encountered at the DREZ. Furthermore, upregulation of procollagens is not a significant feature of the dorsal

column transection injury suggesting that their upregulation is only associated with the regenerating conditions.

In the injured peripheral nerve the secretion of collagen by epineurial fibroblasts is associated with scar formation at the lesion zone and inhibition of regeneration (Siironen *et al.* 1992; Siironen *et al.* 1996; Nath *et al.* 1997). The expression of collagen can be reduced by neutralisation of TGF-beta (Nath *et al.* 1998; Davison *et al.* 1999) suggesting that this growth factor stimulates collagen production. There is less known about collagen production in the DRG itself. DRGs contain non-neuronal cells including fibroblasts (Mudge 1981) and it is possible that it is these cells that are responsible for the regulation of procollagens in our microarray. Macrophage have however been recently shown to express almost every known collagen mRNA (Schnoor *et al.* 2008). The regulation in collagen could therefore be due to resident DRG macrophage or due to infiltration of macrophage. The mechanism and function of this regulation is however unknown. TGF-beta is not significantly upregulated in the DRG in the 2DR and 6SN conditions and as such it can be envisioned that TNF-beta may be retrogradely transported to signal from the lesion zone in a similar manner to TNF-alpha (Section 5.6.4).

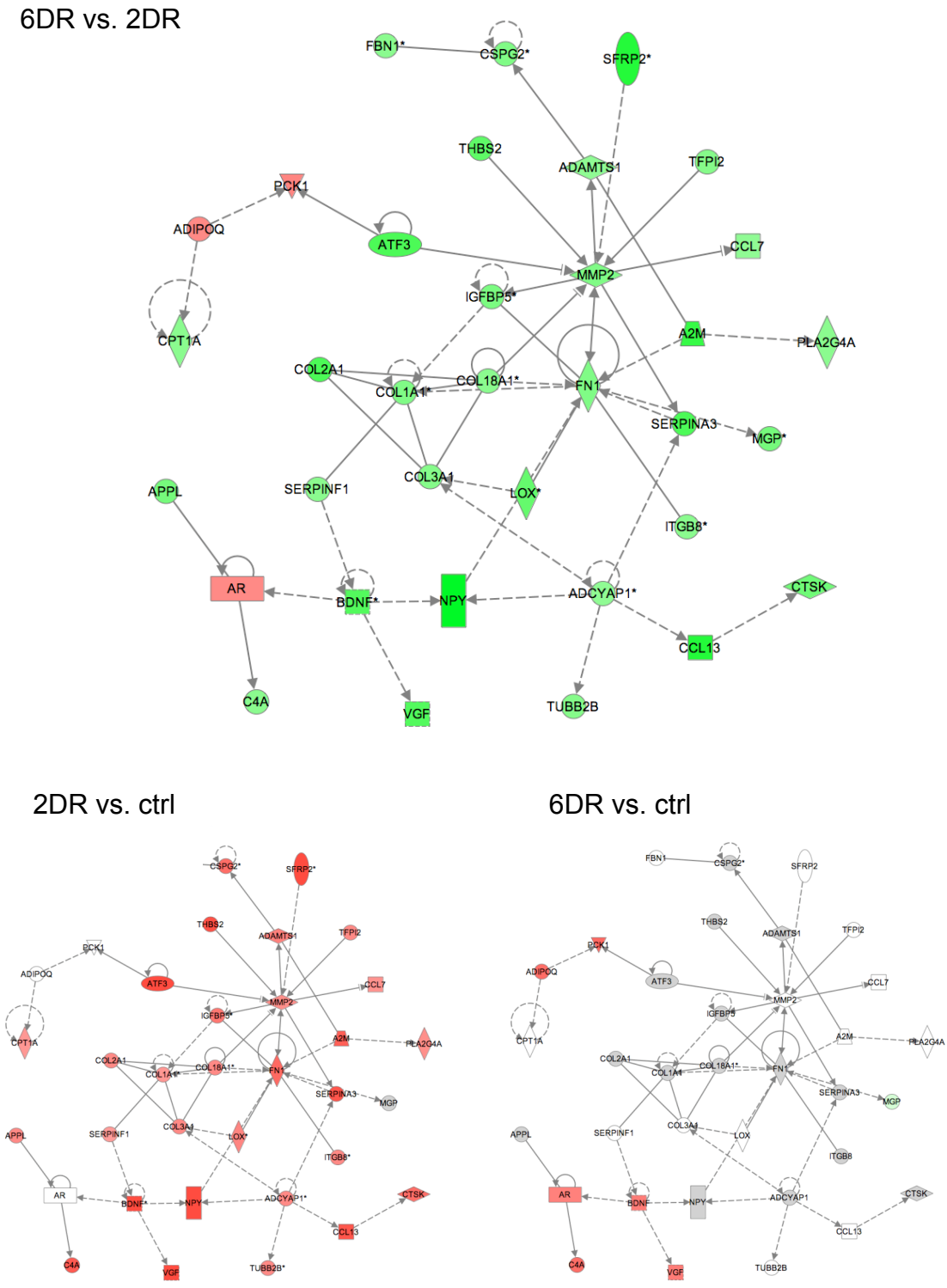

Figure 5-15: IPA identifies a network of genes involved in 'Cellular movement', 'cell-cell signalling and interaction' and 'cell morphology' that is regulated between 2DR and 6DR. The network has a highly significant score of 72 ($p<0.001$). For comparison, the network is also shown overlaid with expression information from the 2DR vs. ctrl and 6DR vs. ctrl data sets. The intensity of the node colour indicates the degree of up (red)- or down (green) regulation. This

network highlights the downregulation of procollagens and growth promoting factors such as BDNF in regeneration-blocked dorsal root fibres.

5.6.6 Activation of complement is a feature of all the conditions

A salient feature of the IGA and IPA canonical pathways analysis for all conditions was the activation of complement within the DRG (**Figure 5-7**). This activation of complement appears to be long lasting as it is a feature at both 2 and 6 weeks after an injury. Complement mediates a large variety of processes including neuronal cell death, cell adhesion and chemotaxis (Morgan and Gasque 1996). Activation of complement can also lead to inflammation with loss of neurons (Speth *et al.* 2002). In addition, mice null for the C5 component of complement have reduced neuropathic pain sensitivity suggesting that complement may have a role in modulation of neuropathic pain. Indeed, increased biosynthesis of complement components by dorsal horn microglia in animal models of neuropathic pain has also been reported (Griffin *et al.* 2007). Complement is also active in the PNS during neuropathic pain states and components of complement have been reported as upregulated in the DRG at 4 weeks after spinal nerve ligation with neuropathic pain (Levin *et al.* 2008). These authors also show that depletion of the complement cascade by treatment with cobra venom factor alleviates neuropathic pain demonstrating a causal link between the two. The mechanism through which components of complement modulate neuropathic pain are currently unknown however inhibitors of microglia have been used to manipulate complement regulation and have potential therapeutic value for treatment of neuropathic pain (Mika 2008). Our finding that central injury also induces complement activation in the DRG has implications for treatment of the chronic pain that is associated with SCI.

5.6.7 All the injuries produce an apparent downregulation of genes involved in the contraction of striated muscle

The downregulation of actin and myosin components that are involved in striated muscle contraction featured in the IGA ontological analysis for all the conditions. This is a previously unreported finding. Some actin and myosin subtypes are found associated with the growth cone and axonal cytoskeleton and IPA canonical pathways analysis suggested that for 6DR and 6SN, the downregulation of these genes was a feature of actin cytoskeleton signalling. Myosin II (MYL2), one of the muscle components found downregulated in this study, is thought to have a role in cytoskeleton disassembly (Medeiros *et al.* 2006; Haviv *et al.* 2008) and actin bundle turnover at the growth cone (Medeiros *et al.* 2006). Indeed, downregulation of this myosin gene has been shown to increase filopodial extension due to decreased rates of actin bundle severing in the growth cone transitional zone (see section 1.2.2.1) (Medeiros *et al.* 2006; Haviv *et al.* 2008). This may explain why this gene is downregulated under injury conditions when there is growth cone activity. It does not however explain the concominant decrease in expression of other muscle components. The expression of these genes on a chip-to-chip basis was therefore investigated using Genespring.

Hierarchical clustering revealed a group of ten muscle genes that clustered closely on the basis of their expression across all chips and that showed an unusual pattern of expression (Figure 5-4). The expression of these genes was extremely variable within chip triplicates; nine of the 10 genes in this cluster showed a very high level of expression on two of the three control chips and elevated expression on one chip out of each of the experimental triplicates. Seven of these genes appeared in at least one of the top 20 downregulated genes lists for each condition however their pattern of expression suggests that their apparent downregulation may be artifactual and due to random error such as varying degrees of contamination from muscle tissue.

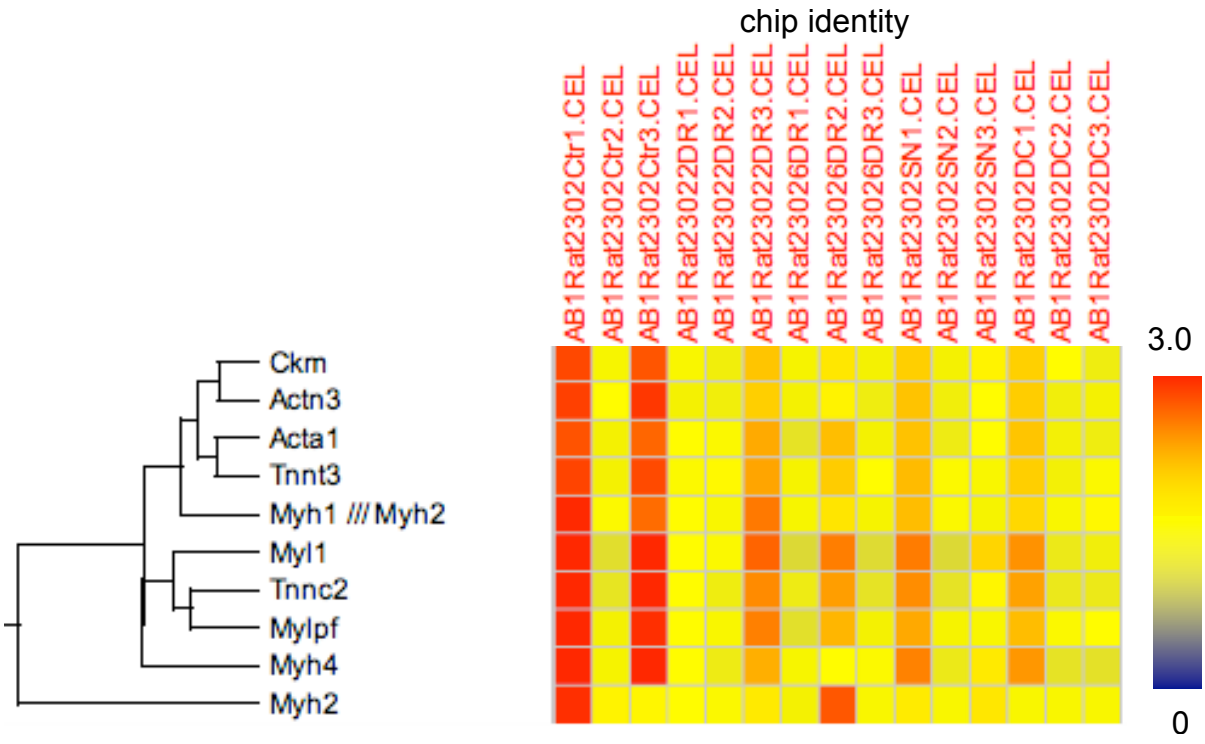

Figure 5-16: Heatmap illustrating across-chip signal intensities of a cluster of muscle related genes. Cells are coloured by normalised signal intensities for each chip.

5.6.8 The top upregulated IPA functional networks for the regenerating conditions show overlaps in a number of genes with putative roles in regeneration

One of the top functional networks identified as regulated at 2 weeks following a dorsal root crush (Figure 5-8) was centred around the epidermal growth factor receptor (EGFR1), fibronectin 1 (FN1) and insulin-like growth factor (IGF1) and was associated with cell-to-cell signalling and cellular movement. The involvement of procollagens in this network also led to an association of this network with dermatological diseases. The top network identified for the other regenerating condition, 6 week spinal nerve crush, was also associated with cellular movement and cell-to-cell

signalling and showed overlap with the 2DR network with the inclusion of ADAMTS1, COL1A1, F3, FBN1, FN1, TFPI2 and WISP (Figure 5-11). Interestingly, some of these genes have been previously shown to have roles in axon regeneration.

Cell adhesion molecules are thought to play an important role in regeneration (reviewed in Kiryushoko *et al*. 2004). The adhesion molecule thromboplastin (F3) belongs to the Ig superfamily and is expressed on PNS axons. It has been shown to interact with a receptor on Schwann cells and mediates neuron-glial cross talk during development and regeneration (Thomaidou *et al.* 2001). In agreement with a possible role in regeneration this gene has been shown to be upregulated in neurons after peripheral nerve injury (Daniloff *et al.* 1986).

ADAMTS1 is a metalloproteinase and like ECEL1, which was investigated in Chapter 3 (see section 3.3.3.1), has been suggested to have a role in neuronal regeneration. It is upregulated in the hypoglossal nerve after injury (Sasaki *et al.* 2001) and has been shown to have proteolytic activity on the proteoglycan, aggrecan (Kuno *et al.* 2000). This has led to the suggestion that ADAMTS1 secreted at axonal terminals may cleave CSPGs (see also section 1.4.1.2) in the extracellular matrix to make way for axonal outgrowth. Fibronectin (FN1) is also a metalloproteinase and so could be envisioned to have a similar role.

5.6.9 The top IPA network for 6DR reveals a gene that is antagonistically regulated between 2 and 6 weeks after dorsal root crush

Differences in gene expression between 2 and 6 weeks after dorsal root crush has relevance to dorsal root avulsion injury as they may give insight to the intrinsic reasons as to why dorsal root neurons can not regenerate through the DREZ to reinstate functional connections in the spinal cord. The top upregulated network for 6DR (Figure 5-10) is centred around the immediate early gene FOS and is associated with skeletal and muscular system and tissue morphology, cardiovascular system development and function. The network highlights neuregulin (NRG1) as a gene that is upregulated at 6 weeks following dorsal root crush but which is downregulated at 2 weeks after this injury. NRG is an EGF-like growth factor that is thought to be important in the regulation of glial cell function and survival. It has been reported that the expression of this gene in sensory neurons is reduced immediately after peripheral axotomy and returns to normal levels after target reinnervation (Bermingham-McDonogh *et al.* 1997). Another study suggested that a higher level of NRG1 in optic nerves compared to sciatic nerves could contribute to the poor regenerative ability of the former (Martinez *et al.* 2004). Reduction in NRG1 expression is therefore correlated with periods of axon outgrowth whilst overexpression of this gene is associated with reduced regenerative capacity. The upregulation of NRG1 at 6 weeks after dorsal root crush could therefore contribute to the regenerative block of these axons at the DREZ. Conversely, the downregulation of this gene after dorsal column transection could lend further support to the idea that this injury elicits a transcriptional programme conducive to regeneration.

5.7 Question-led analyses and discussion

5.7.1 Is the expression of receptors consistent with a regenerative or non-regenerative phenotype?

Axon outgrowth depends in part, on how well a growth cone can detect and respond to factors in its environment (see also section 1.2.2.1). Neurotrophic factors, growth factors (such as BDNF and GDNF) and laminin have all been shown to be important to the positive regulation of outgrowth. The expression of receptors for these molecules is therefore important in determining growth cone responsiveness. The data was therefore examined for changes in regulation of neurotrophin receptors (Ntrks), growth factor receptors (GFRs) and receptors for laminin (integrins). It might be expected that in the conditions where regeneration is successful (2DR and 6SN) there might be greater upregulation of such receptors than in the non-regenerating conditions however this pattern was only seen for one growth factor receptor, 'platelet-derived growth factor receptor, alpha polypeptide (PDGFRA) which was upregulated 1.48 fold in both 6SN and 2DR (at 3.16 % and 2.1 % FDR, respectively).

5.7.2 Is the expression of putative regeneration associated genes (RAGs) restricted to the regenerating conditions?

Studies of peripheral nerve regeneration have identified 11 consistently upregulated genes (see section 1.5.2.3), suggestive of these genes being important to the process of axonal regeneration. A number of other genes that have been identified through microarray studies as putative RAGs have been overexpressed in DRG neurons *in vitro,* and have stimulated neurite outgrowth. The expression of these genes in our injury conditions was compared (Table 5-24). The upregulation of these genes does not appear to correlate with neuronal regeneration. In fact, these genes are most consistently upregulated in the dorsal column transection condition, a condition in which regeneration is blocked. Regulation of these genes is almost completely absent at 6 weeks after spinal nerve injury in which there is ongoing regeneration, suggesting that they are not necessary for maintenance of axon outgrowth.

Table 5-24: Comparison of changes in expression of putative RAGs after all conditions.
Cells are coloured according to expression.

Gene symbol	'Regenerating'		'Non-regenerating'	
	6SN	2DR	6DR	2DC
NPY				
GAL				
GAP43				
SPRR1A				
CACNA2D				
SOX11				
GADD45a				
ANXA1				
HSP27 (HSPB1)				
CYP1B1				
MMP9				
ARG1				
ATF3				
FN14 (TNFRSF12A)				
ANKRD1				
FLRT3				

not regulated within 50% FDR

upregulated but not within 5% FDR

<2-fold upregulated

>2-fold upregulated

5.7.3 Is regeneration a recapitulation of development?

It is known that during its development, the CNS undergoes a critical period during which plasticity-related genes are expressed. This is thought to account for the regenerative capacity of the mammalian CNS in embryogenesis that is lost developmentally with the expression of plasticity-restricting molecules such as the myelin-associated inhibitors of regeneration. There is contradictory evidence for developmental genes being re-expressed during regeneration (reviewed in (Emery *et al.* 2003)). There was however evidence from the pilot microarray of increased expression of developmental genes after sciatic nerve transection (see section 3.5.2.1).

IPA functional analysis was used to interrogate the data sets for genes that are involved in nervous system development to search for evidence of re-expression of developmental genes in the regenerating conditions. Genes involved in nervous system development and function were significantly represented in all the data sets apart from 6SN (Figure 5-17).

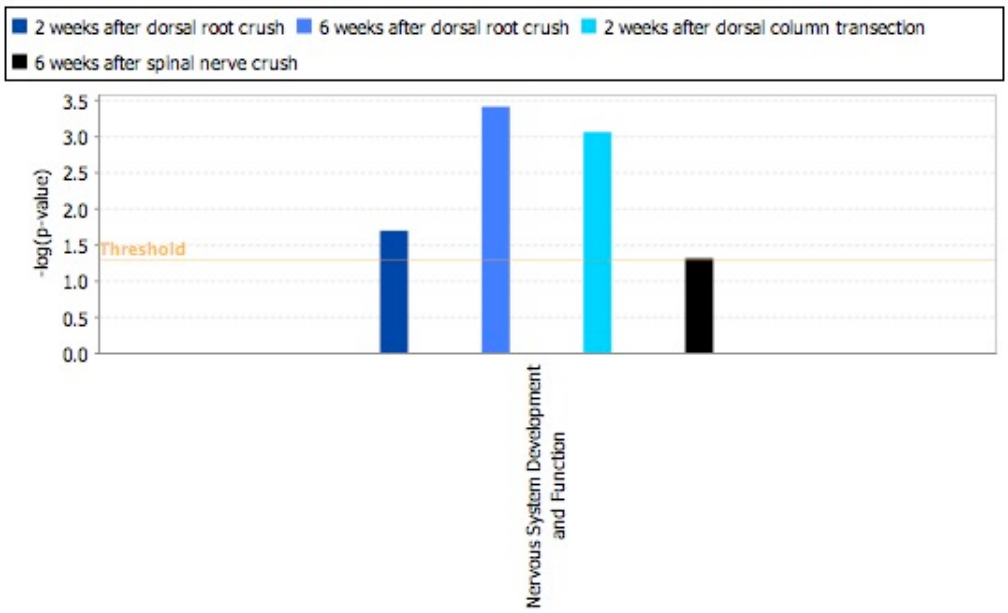

Figure 5-17: IPA analysis of the level of representation of genes involved in 'nervous system development and function' in each data set.

5.7.3.1 The 2DR data set

In the 2DR dataset 'nervous system development and function' was significantly represented (p value)=$2.06E^{-2}$-$4.83E^{-2}$) by 24 genes. The list featured genes involved in the activation of neuroglia and neurons (upregulation of BDNF, CYBB, FN1, IGF1, FOS and NTS and the downregulation of CHGA), ensheathment of neurons (upregulation of CLN11 and POU3F1), migration of neuroglia (upregulation of BDNF, CCL13, CLDN11, FN1, ITGAL and downregulation of NRG1), circadian rhythm (upregulation of DBP, FOS, PER2 and PER3 and downregulation of RAB3A), quantity of CNS cells (upregulations of ADCYAP1, CCND2, EGFR, IGF1, IGFBP6), excitation of neurons (upregulation of BDNF, FOS and NPY) and survival of granule cells (upregulation of ADCYAP1, BDNF and IGF1).

5.7.3.2 The 6DR data set

12 genes contributed to the significant representation of 'nervous system development and function' in the 6DR data set ((p value)=$3.95E^{-4}$- $2.3E^{-2}$). These were genes involved in; chemotaxis of granule cells and granule cell precursors, survival of cells (both associated with upregulation of BDNF and CXCL12), activation of neurons and neuroglia (upregulation of BDNF, FOS, CYBB and GFA, and downregulation of APLN), long term potentiation (upregulation of BDNF, GFAP and NRG1), excitation of neurons and granule cells (upregulation of BDNF and FOS), maturation of neurons (upregulation of BDNF and CDKN1C), binding of axon terminals, branching of peripheral nerves, cell cycle progression, defasiculation, extension of schwann cells, morphology of axon terminals, remyelination and retraction of axon terminals and conduction of axons (all associated with the upregulation of NRG1), generation of action potential, chemokinesis, discharge of granule cells, formation of cells, innervation, rearrangement of axons, generation of

the excitatory post synaptic potential of dorsal root (all associated with upregulation of BDNF), development of motor endplates (downregulation of CHRNE), growth of peripheral nerve and neurons (upregulation of BDNF and NRG1), withdrawal of sensory nerves, quantity of neuroglia and axon branches (upregulation of BDNF, EGFR and NRG1), migration (upregulation of BDNF and NRG1), myelination (upregulation of BDNF, CLDN1 and NRG1), cell to cell contact, (upregulation of CXCL12) and reactivation of astrocytes (upregulation of GFAP).

5.7.3.3 The 2DC data set

80 genes contributed to the significant representation of 'nervous system development and function' in the DC data set ((p value)=8.89E-^{4}- 4.51E^{-2}). Specifically, 16 genes involved in neurogenesis were downregulated (ACSL6, AMIGO3, CNR1, DPYSL4, DRGX, FABP7, GFRA2, GRIK1, LGI1, LSAMP, MT3, NOG, NRG1, RET, SCRG1 and TRPV1) while 17 genes were upregulated (BDNF, CDKN1C, CRIM1, DLX5, DRD2, FRF2, GAL, GFAP, GFRA1, HHIP, MAOA, MET, SOX11, SYN3, TGFBR1, THBS4 and SEM). Other genes contributing to the functional classification were involved in; innervation of neurons and cells (upregulation of BDNF, GAP43 and VCAM1 and downregulation of GFRA2, GRIA2 and NOG), maturation of neurons (upregulation of BDNF, CDKN1C and FGF2), quantity of neurons (upregulation of ADCYAP1, BDNF, CASP3, CCND2, CYBB, DRD2, FGF2, GAL, GFRA1, IRX3 and SERPING1 and downregulation of GFRA2, NOG and RET), quantity of ganglion cells (downregulation of GFRA2 and NOG), quantity of neurites (upregulation of BDNF, GAL and MAOA and downregulation of GFRA2, HTR7 and MAPK10), activation of nerves (upregulation of ADCYAP1 and downregulation of CALCA and TAC1), activation of neurons (upregulation of BDNF and FOS and downregulation of CNR1, PTGER3, RET and TAC1), depolarisation of dorsal horn cells (upregulation of VIP and downregulation of TAC1), depolarisation of neurons (upregulation of ADYCYAP1 and VIP and downregulation of P2RX3 and TAC1), paired-pulse facilitation (upregulation of BDNF and downregulation of UNC13C), patterning of axons (CASP3 and MAOA), recruitment of medium spiny neurons (upregulation of BDNF and FGF2), regeneration of neurons (upregulation of ARG1 and FGF2), synaptic fatigue of synapse (upregulation of BDNF and SYN3), growth of axons (upregulation of BDNF, FGF2, GFRA1, MAOA, MET and SYN3 and downregulation of NRG1 and RET), synaptic transmission (upregulation of BDNF, DRD2, FGF2, FREQ, GABRA5, GAL, KCNMB4, NPY, SLC1A1 and XDH and downregulation of CHRNB4, CHRNE, DLGAP1, GABRG2, GLRB, GRIA2, GRIK1, GRI1, GRM4, HTR7, HTR1D, HTR3A, PCDH8, RIT2 and UNC13C), neuritogenesis (upregulation of ADCYAP1 and FGF2 and downregulation of CACNA1H and GFRA2), survival of motor neurons (upregulation of BDNF, GFRA1 and REG3A and downregulation of GFRA2) and pain behaviour (upregulation of ARRB1 and SCN3A and downregulation of KCNIP3, SCN11A, TAC1 and TRPV1).

5.7.3.4 The 6SN data set

Within the 6SN data set only 2 genes contributed ((p value)=4.94E^{-2}). Both the genes (DBP and PER2) were upregulated and are known to be involved in circadian rhythm.

5.7.3.5 Discussion

The analysis did not provide evidence for a re-expression of developmental genes in the regenerating conditions and regulated genes in the 2DR and 6SN condition appeared to belong to subcategories pertaining to nervous system function rather than nervous system development. Indeed dorsal column transection was the only condition in which genes belonging to developmental subcategories were changed. For example in the neurogenesis category, 17 genes were upregulated including; SOX11, a developmentally expressed transcription factor that is required for neuron survival and outgrowth (Jankowski *et al.* 2006); synapsin III (SYN3), which is highly expressed in growth cones in early development and is required for axonal differentiation (Ferreira *et al.* 2000); cysteine rich motor neuron 1 (CRIM1), a transmembrane protein with a role in CNS development via growth factor binding (Kolle *et al.* 2000) and DLX5, a transcription factor which is required for normal neuronal differentiation during development (Perera *et al.* 2004).

5.7.4 What do the regenerating conditions have in common?

In order to reveal genes that are common to the regenerating conditions, and thus potentially important to the regenerative process, genes were filtered in two ways. Differentially expressed genes identified by ANOVA ($p<0.05$) were filtered using Venn diagrams in Genespring. In addition, genes that were identified by RPA as differentially expressed (<5% FDR) were filtered by Excel based data sorting.

5.7.4.1 Gene filtering using Venn Diagrams

Intuitively, genes that are regulated in the regenerating conditions and not in the non-regenerating conditions are interesting as putative regeneration-associated genes. Venn diagrams were generated using Genespring GX and were used to identify genes that were differentially expressed specifically to the regenerating conditions (2DR and SN). At the 5% significance level 1011 genes are changed after 2DR, genes changed after 6DR and 466 genes changed after 2DC transection were plotted (Figure 5-18a). This allowed the identification of 190 genes that were specific to the regenerating condition (2DR). This process was repeated with the other regenerating condition (6SN) (Figure 5-18b). This identified 101 genes regulated specifically in 6SN. These 101 genes and the 190 genes specific to 2DR were plotted on a third Venn diagram (Figure 5-18c). This allowed the identification of 44 genes that were specifically regulated at the 5% significance level in the regenerating conditions but not in the non-regenerating conditions (Figure 5-19). GO analysis of this list of genes categorised them as belonging to a number of gene categories including development and response to stimulus (Figure 5-18d). No ‘GO’ categories were significantly overrepresented.

Figure 5-18: Identifying regeneration-associated genes using Venn diagrams. Number of regulated genes ($p<0.05$) (in bold) specific to a) 2DR and b) 6SN are identified. c) 44 genes common to 2DR and SN are identified and d) analysed by GO. The number in brackets represents the number of regulated genes that changed >1.5-fold.

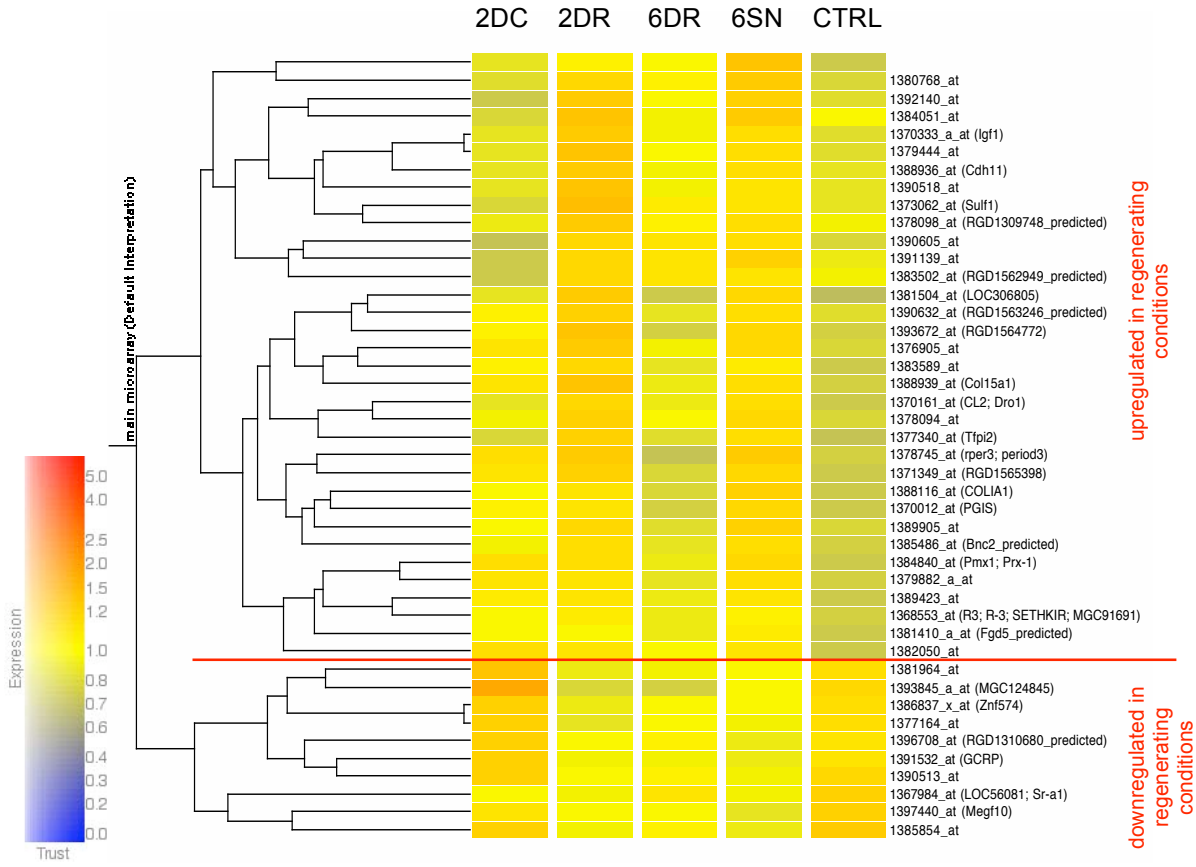

Figure 5-19: Heatmap with hierarchical clustering (centroid or average linkage method) showing the 44 genes identified by Genespring showing differential regulation (at the 5% significance level) in only the regenerating conditions. Cells are coloured by mean normalised signal intensity for each condition. Degree of trust is indicated by the brightness of the cells.

5.7.4.2 Identification of regeneration-associated genes using excel data sorting

Rank products-analysed data files containing fold change values and FDRs for all genes that appeared within a 50% FDR cut-off were merged into a single excel spreadsheet that allowed the data to be sorted and filtered according to a number of different criteria.

When data was filtered to leave only those genes regulated in the regenerating conditions at the 50% FDR level and not in the non- regenerating conditions this yielded a list of 272 genes. A 50% FDR cut-off is however extremely liberal and when these genes were filtered to leave only those that were regulated at the 5% FDR level in at least one of the two conditions, 35 genes remained (Table 5-25) and 11 of which showed an overlap with the list generated by Genespring (Figure 5-16). Of these 35 genes only 3 were regulated within 5% FDR in both the conditions (highlighted in red). These represent candidate regeneration-associated genes.

Table 5-25: Genes regulated within 50% FDR in regenerating conditions but absent at 50% FDR in non-regenerating conditions.

		2DR		SN	
Affy ID	Gene symbol	FC	FDR	FC	FDR
1369484_at	Wisp2	1.43	4.01	1.58	1.23
1370333_a_at	Igf1	1.31	10.8	1.53	1.65
1373062_at	Sulf1	1.22	30.4	1.63	0.67
1373314_at	---	1.44	4.01	1.36	7.84
1373914_at	Shank1	1.21	31.21	1.54	1.8
1376734_at	---	1.4	8.4	2.01	0.09
1377168_at	Cpne9	-1.16	47.33	-1.38	2.34
1377340_at	Tfpi2	1.49	1.83	1.66	0.53
1378094_at	RGD1308084	1.37	6.35	1.44	3.97
1379362_at	---	1.23	28.48	1.4	4.98
1379444_at	---	1.3	11.4	1.54	1.37
1380726_at	LOC306805	1.29	17.06	1.8	0.25
1381556_at	RGD1560014_predicted	1.58	2.25	1.22	36.12
1381819_at	---	1.24	29.88	1.51	1.89
1382599_at	---	1.41	5.53	1.52	1.68
1383875_at	Upk1b	1.21	32.72	1.42	4.7
1384211_at	Col11a1	1.29	14.78	1.6	1.07
1385053_at	---	1.4	7.17	1.73	0.37
1385082_at	---	1.29	15.83	1.44	4.73
1385973_at	---	1.52	1.96	1.37	8.41
1386946_at	Cpt1a	1.18	40.01	1.47	3.66
1387313_at	Myoc	1.36	5.52	1.5	2.16
1388469_at	---	1.38	6.11	1.45	4.07
1388569_at	Serpinf1	1.3	11.71	1.44	3.88
1388936_at	Cdh11	1.27	16.79	1.44	3.36
1389905_at	---	1.47	2.2	1.39	5.99
1390119_at	Sfrp2	1.38	7.09	2.41	0
1390518_at	LOC685462	1.21	33.06	1.56	1.07
1390632_at	RGD1563246_predicted	1.28	15.22	1.44	3.39
1390989_at	RGD1563952_predicted	1.21	32.77	1.45	4.01
1392140_at	Cdh11	1.42	3.18	1.48	2.26
1393346_at	RGD1561673_predicted	1.26	19.63	1.43	3.9
1393809_at	Traf6_predicted	-1.21	36.85	1.48	3.8
1396152_s_at	Igfbp5	1.21	31.36	1.44	3.38
1399069_at	RGD1310351_predicted	1.21	40.1	1.52	1.68

5.7.4.3 Investigating the functions of WISP2 and TFPI2

Two of these putative regeneration associated genes, WISP2 and TFPI2 feature in the top networks identified for the regenerating conditions along with genes that have previously been implicated in regeneration (Figure 5-8 and Figure 5-11). WISP2 and TFPI2 have not been described previously as having functions in axonal injury and regeneration. In an effort to investigate the function of these genes Genespring was used to select genes with a highly similar pattern of expression across all conditions (Pearson correlation coefficient r^2>0.95) which thus show co-regulation, and may function in concert, with the genes of interest. 165 genes passed this criteria for WISP2 and this list was uploaded for analysis by IPA. Of these 165 genes, 114 genes could be mapped to IDs and 86 were network eligible while 82 were function/network eligible. Two significant canonical pathways could be identified as relevant to the list of genes identified as being similar in regulation to WISP2 by Genespring (Figure 5-20a). These were 'Phospholipid degradation' (p =0.0021) and 'Glycerophospholipid metabolism' (p=0.0077). Three genes contributed to both these pathways (PLA1A, PPAP2A, RNF111) 167 genes clustered with TFPI2 in terms of cross-condition expression and were analysed by IPA. Of these 167 genes, 117 genes could be mapped to IDs and 87 were network eligible while 78 were function/network eligible. Four significant canonical pathways (Figure 5-20b) could be identified as relevant to the list of genes identified as being similar in regulation to TFPI2 by Genespring. These were 'Phospholipid degradation' (p=0.0019) (contributed by IGF1, PPP2CB, RNF111, WISP2), 'Glycerophospholipid metabolism' (p=0.0069) (contributed by PLA1A, PPAP2A, RNF111, WISP2), 'Synaptic long term depression' (p=0.0143) (contributed by IGF1, PPP2CB, RNF111, WISP2) and 'Wnt/β-catenin signalling' (p=0.0229) (contributed by FRZB, NLK, PPP2CB, SFRP4).

Genes that cluster with TFPI2 and WISP2 are known to be involved in phospholipid degradation and gylcerophospholipid metabolism. This is perhaps interesting as decreased glycerophospholipid synthesis can lead to suppression of axonal outgrowth (Ikemoto *et al.* 1997). TFPI2 also clusters with genes associated with Wnt/β catenin signalling. This is interesting as activation of this signalling pathway has been shown to promote regeneration in the adult retina after injury (Osakada *et al.* 2007) and is thought to have diverse roles in nervous system development, microtubule dynamics, modulation of synaptic plasticity and regulation of gene expression (Speese and Budnik 2007). Among the genes that are regulated within this pathway is: soluble frizzle-related protein 4 (SFRP4), one of the secreted regulators of wnt that can act to antagonise or enhance its signalling (Nakanishi *et al.* 2006; Bovolenta *et al.* 2008); Neuroleukin (NLK), a neurotrophic factor that promotes the survival of spinal and sensory neurons in culture (Gurney *et al.* 1986); protein phosphatase 2CB (PPP2CB), which can act as an inhibitor of cellular stress signalling (Lammers and Lavi 2007) and, frizzled-related protein (FRZB), a receptor for Wnt. WISP2 and TFPI2 may therefore support neuronal regeneration by participation in Wnt/β catenin signalling.

a)

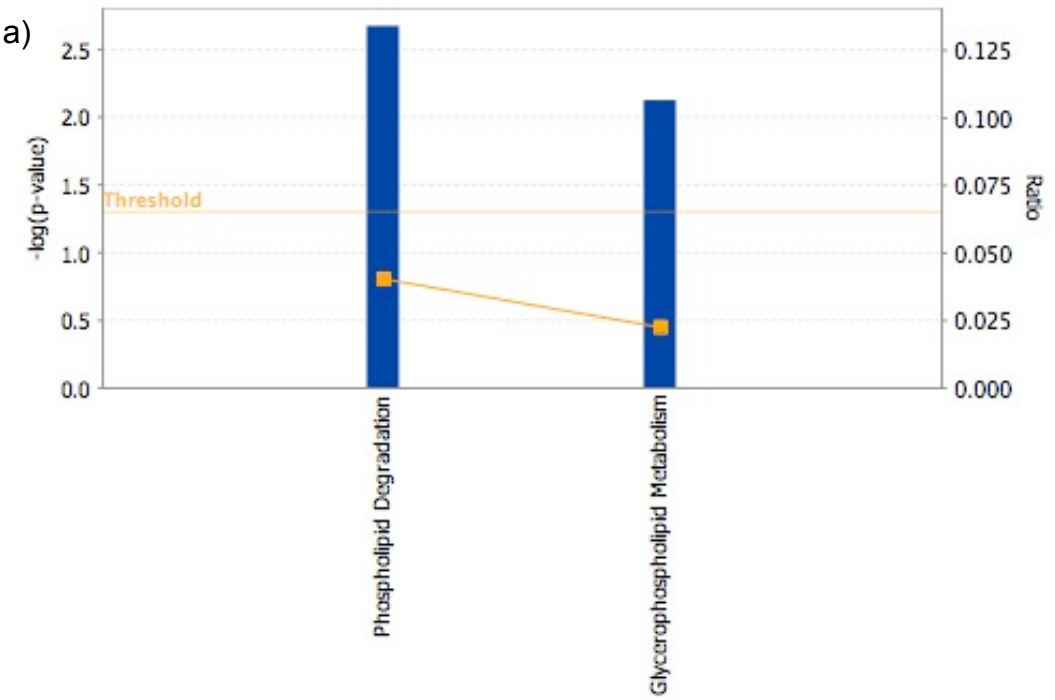

.

b)

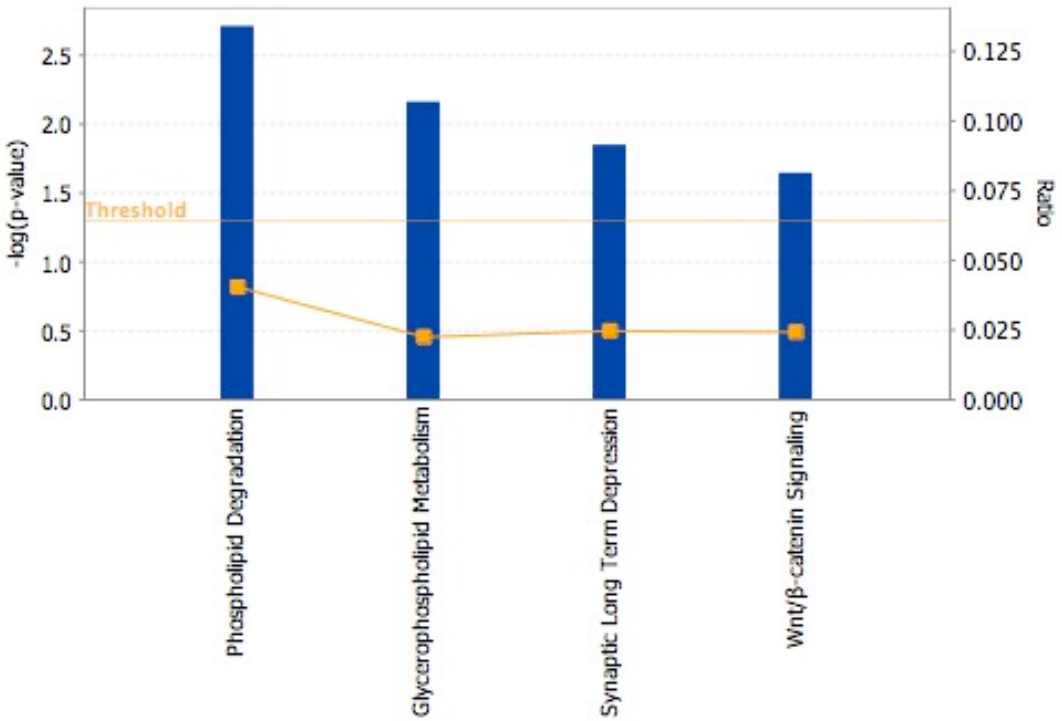

Figure 5-20: IPA analysis of canonical pathways significantly represented by genes with similar regulatory pattern to a) WISP2 and b) TFPI2. Fisher's exact test was used to calculate a p value (shown as blue bars) determining the probability that each biological function assigned to the network is due to chance alone. The ratio (shown as yellow squares) represents the number of differentially expressed genes in a given pathway relative to the number of genes that make up that canonical pathway.

5.7.5 Summary

We wished to determine the transcriptional profiles associated with axonal outgrowth in vivo. We were particularly interested in finding genes whose expression is generally associated with the process of regeneration rather than time point or specific injuries. Thus in order to avoid focussing on transcripts unique to one injury or one time point and another, we used a comparative strategy to look for changes that were common to two different regenerating conditions and were therefore more likely to be involved in the general process of regeneration. We examined global gene expression changes in DRG at 6 weeks after spinal nerve crush and 2 weeks after dorsal root crush (regenerating conditions) and compared this to a 2 week dorsal column transection and a 6 week dorsal root crush (non-regenerating conditions).

The gene expression changes in the DRG after the injuries were associated with both regeneration and neuropathic pain. A number of observations were made that were common to all the injuries such as the activation of complement. Other changes were specific to injury type. Dorsal column transection elicited a transcriptional programme that was quite different from the other injuries but also upregulated known RAGs suggesting that these neurons are primed for growth and that appropriate manipulation of the lesion zone could be beneficial. This injury also elicited a downregulation of neurotransmitter receptors that leads to neuronal hyperexcitability and neuropathic pain after peripheral nerve injury.

The most striking commonality for the regenerating conditions was the upregulation of procollagens, presumably by the non-neuronal cells in the DRG that was not time point dependent. This suggests that factors secreted by non-neuronal cells in the vicinity of a neuron may play an important role in modulating its outgrowth.

Filtering of genes regulated in each condition identified a number of genes associated with regeneration. Two of these genes, WISP2 and TFPI2 are co-regulated with genes involved in gycerophospholipid metabolism while TFPI2 also clusters with genes involved in Wnt/β catenin signalling. These genes were chosen for validation with qRT-PCR (Chapter 6) as putative regeneration associated genes.

6 qRT-PCR validation of microarray data

6.1 Introduction and Aims

Validation is a crucial component of any microarray study. Although commercial microarrays are now generally regarded as reliable and consistent (Barnes *et al.* 2005; Dallas *et al.* 2005; Larkin *et al.* 2005; Petersen *et al.* 2005; Zhu *et al.* 2005; de Reynies *et al.* 2006; Wang *et al.* 2006), they can still generate a large number of false positive and negative results by virtue of the large number of gene expression results they yield. It is therefore still considered good practice that microarray findings are confirmed by an independent gene expression method.

The large quantity of RNA required for Northern blots normally precludes their use in validation and as such qRT-PCR (section 2.10) has become the 'gold standard' for the validation of microarrays. A selection of genes that were differentially expressed within the microarray experiment were therefore validated using qRT-PCR assays using SYBR green chemistry (Section 2.10). qRT-PCR also presented the opportunity to include sham controls for each of the injuries. This allowed us to confirm that gene changes seen in the microarray were due to the injury itself and not some non-specfic effect of anaesthesia and/or tissue damage. In addition, qRT-PCR was performed on RNA extracted from the DRG of individual animals allowing the degree of biological variation in the expression of a given gene to be assessed. This was made possible by pooling samples *after* RNA extraction for the microarray and reserving RNA from separate animal for qRT-PCR. A 6 week time point after dorsal column transection (6DC) that was not investigated using microarrays was also assessed by qRT-PCR to allow temporal changes in gene expression after dorsal column injury to be examined. For the naïve control and all injury conditions (excluding the 6DC condition), the same RNA that was used for the microarray was also used in the qRT-PCR. Additional animals were required for the generation of sham controls and the 6DC injury condition.

Quantitect primer assays for each gene of interest were purchased from Qiagen (Table 2-3). Good quality, total RNA samples were extracted from rat DRG (n=8 rats per condition) (2.8.4.2 , DNase treated and reverse transcribed to cDNA using quantitect RT kit (section 2.8.9.2). qRT-PCR assays were performed in triplicate on each sample using the Opticon 2 real-time thermocycler (section 2.10). Following qRT-PCR, outliers were removed (section 2.10.4.3), and REST-MCS was used to analyse the mean Ct values. Gene expression changes were normalised to a factor calculated from three housekeeping genes whose stability in these injury models was confirmed.

6.1.1 Genes chosen for validation

It is not feasible to validate all the results of a microarray, therefore a small number of genes were selected for further investigation. A number of criteria can be used to select these genes. Many studies have used a 2-fold difference as the cut-off for significance (Miron *et al.* 2006). However, this choice can lead to a loss of a large number of smaller expression changes and fails to eliminate false-positive results (Costigan *et al.* 2002). A cut-off between 1.2 and 1.5-fold combined with statistical significance ($p<0.05$ or, in our case <5% FDR) has been suggested as an improved criteria for gene selection (Li and Wong 2001). Genes selected for validation were therefore not necessarily changed over 2-fold, but changed within the 5% FDR level in at least one of the conditions.

We were particularly interested in genes that were regulated specifically in the regenerating conditions as these represent putative regeneration-associated genes (section 5.7.4). Two of these genes, WISP2 and TFPI2, were regulated at the 5% FDR level in both the regenerating conditions but not regulated within 50% FDR in the non-regenerating conditions and hence were chosen for validation. IGF1 also showed this pattern of regulation but just missed the 5% FDR in the SN injury. IGF1 did however appear in the top IPA network identified for 2DR along with TFPI2 and WISP2 suggesting that these genes may somehow interact. Furthermore, as will be discussed in more detail later, IGF1 has been suggested to have a role in the promotion of axonal outgrowth and regeneration (Thanos *et al.* 1999; Rabinovsky 2004; Salie and Steeves 2005; Koriyama *et al.* 2007) and was therefore also picked for validation.

In a recent comparative study of the neuronal response to dorsal root and sciatic nerve crush (Stam *et al.* 2007) described Ankrd1, a new putative regeneration associated gene, which, when overexpressed in PC12 cells induced neurite outgrowth. This gene did not show expression in our microarray that was consistent with it being associated with regeneration and was therefore further investigated with qRT-PCR as a test of this hypothesis.

Dorsal column transection elicited changes in genes that had also been seen after sciatic nerve transection. This was interesting as it suggested that injuries within the spinal cord could induce the same intrinsic transcriptional programmes that are elicited by peripheral nerve injury. Among the genes that showed regulation only in dorsal column and sciatic nerve transection were SEMA6A (described in section 3.3.3.5) and protein tyrosine phosphatase 5 (PTPN5 or STEP). PTPN5 overexpression in PC12 cells leads to increased cAMP-induced neurite outgrowth suggesting that this gene may have a role in the conditioning lesion effect (see also section 1.4.2.1) (Okamura *et al.* 1999).

Also chosen for validation were two genes that have been well studied in models of nervous system injury. ATF3 (described in section 3.3.3.2) was only significantly induced (within 5% FDR) in the 2 week injury conditions suggesting that this gene is part of the general early response to injury and not a regeneration-associated gene. This hypothesis was therefore tested by qRT-PCR.

BDNF1 was significantly induced in all the conditions except 6 weeks after spinal nerve crush. It has been shown that peripherally derived BDNF1 (resulting from a conditioning lesion) can promote regeneration of ascending sensory neurons after spinal cord injury (Song *et al.* 2008). It is therefore slightly surprising that BDNF is induced in dorsal column transection where regeneration is abortive and in central axotomy at a time-point when regeneration is not occurring, but not in spinal nerve crush at a time-point when axons are still regenerating. qRT-PCR was used to check this unexpected result.

6.2 Results

6.2.1 Precision of real-time RT-PCT

The technical precision or reproducibility of qRT-PCR measurements was assessed by calculation of inter- and intra-assay variations and operator error according to methods described in Section 2.10.3. Linearised threshold values (Ct) were obtained and used to calculate experimental variations. qRT-PCR produces logarithmic data and as such linearised values give a better indication of the true experimental variation.

Table 6-1 : Intra-assay and inter-assay precision.

SAMPLE REPLICATE	RUN 1		RUN 2		RUN 3	
	Ct	Linearised Ct ($x10^{-8}$)	Ct	Linearised Ct ($x10^{-8}$)	Ct	Linearised Ct ($x10^{-8}$)
1	26.56	1.01	27.27	0.62	26.72	0.90
2	26.13	1.36	26.90	0.80	26.52	1.04
3	26.33	1.19	27.30	0.61	26.06	1.42
4	25.97	1.52	26.67	0.94	26.32	1.19
5	26.17	1.32	26.14	1.35	26.51	1.04
6	26.38	1.15	27.01	0.74	26.74	0.89
7	26.19	1.31	26.58	1.00	26.48	1.07
8	26.55	1.02	27.04	0.73	26.35	1.17
9	25.93	1.56	27.00	0.75	26.90	0.80
10	27.03	0.73	26.73	0.90	26.47	1.08
11	26.66	0.94	27.42	0.56	27.04	0.72
12	26.12	1.37	27.34	0.59	26.49	1.06
13	26.74	0.89	27.15	0.67	26.50	1.05
14	26.55	1.02	27.18	0.58	26.45	1.09
15	25.97	1.52	26.94	0.78	26.90	0.80
Mean Ct SD CVexp	26.352 0.312 1.18%	1.19 0.26 21.33%	26.978 0.328 1.22%	0.79 0.21 26.38%	26.563 0.255 0.92%	1.02 0.18 17.51%

Intra-assay variations were 21.33% (Run 1, SD=0.26) and 26.38% (Run 2, SD=0.21). Inter-assay (Run 1- Run 2) and operator-associated experimental variation (Average of Run1 and Run 2) –

Run 3) were 5.05 % and 6.34 % respectively. 0.03 % (Run 1- Run 2). These data suggest that the machine and reagent- associated variation was less than the variation generated through operator associated pipetting errors and indicates good reproducibility between runs.

6.2.2 Validation of qRT-PCR reference genes

The CVexp of several potential reference genes was calculated from the log_2normalised data from each of the 15 microarray chips in the main microarray experiment (Table 6-2). Of these genes UBC was the most variable in the pilot experiment validation. The next four least variable genes (CANX, ATP5B, GAPDH and B2M) were therefore chosen to be assessed independently by qRT-PCR.

Table 6-2: CV_{exp} for selected housekeeping genes calculated across all chips

GENE ID	AFFY. ID	CV_{EXP}
UBC	1398767_at	0.541
CANX	1371686_at	0.579
ATP5B	1380070_at	0.708
GAPDH	1367557_s_a	0.936
B2M	1371440_at	1.114
YWAZ	1395893_at	2.031
TOP1	1369421_at	2.662

The stability and hence their suitability as reference genes for qRT-PCR normalisation was assessed for GAPDH, ATP5B, CANX and B2M using geNorm and Normfinder (section 2.10.4.1). B2M, CANX and ATP5B were found to be the most stable of the 4 genes analysed (Figure 6-1 and Figure 6-2) and these were therefore used to calculate a composite normalisation factor in later analyses in REST-MCS.

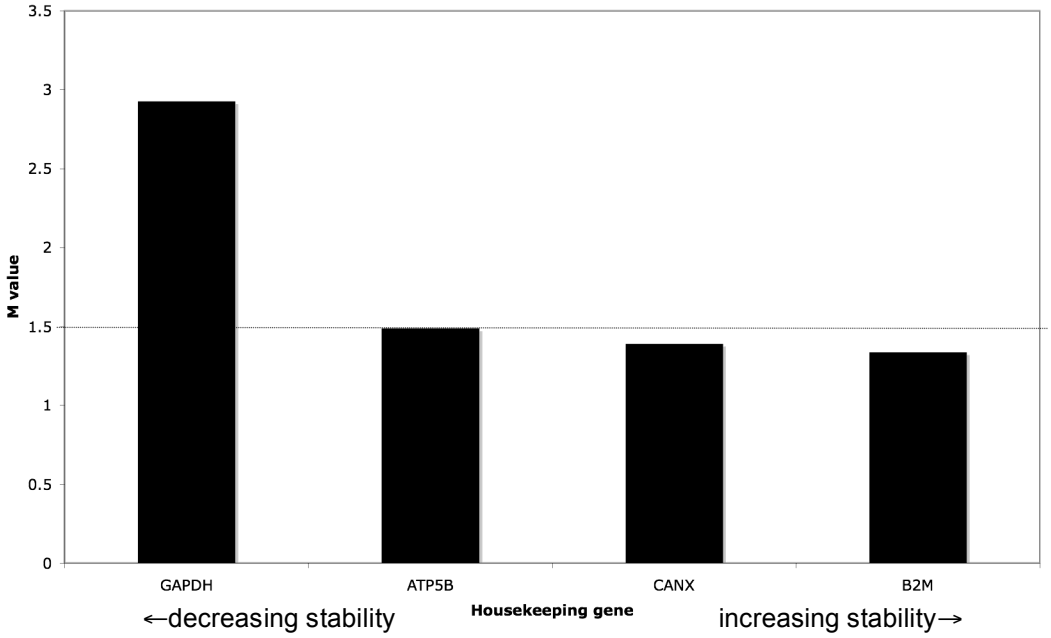

Figure 6-1: HKG evaluation by GeNorm. Of the 4 genes evaluated only 3 were suitable for use as reference genes (M value< 1.5).

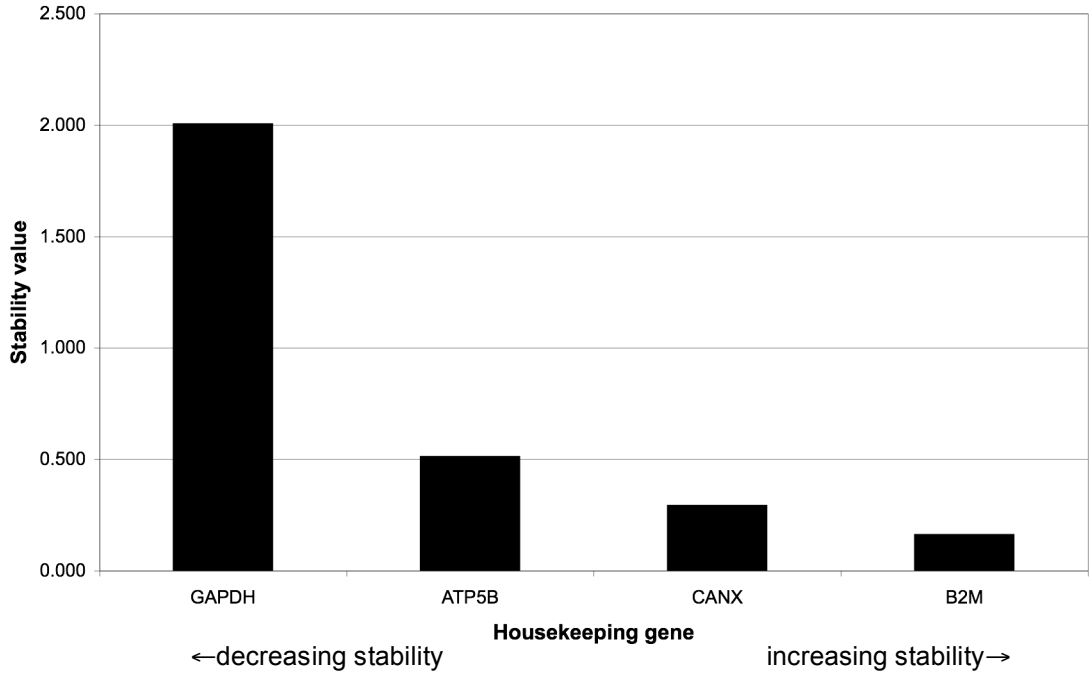

Figure 6-2: HKG evaluation by Normfinder. Genes were ranked in order of stability with B2M as the most stable.

6.2.3 LinReg analysis of well-well reaction efficiencies

LinReg was described in (Sections 2.10.4.4 and 3.3.2). The average reaction efficiency for each gene assay with standard deviation is recorded in Table 6-3 below. These gene specific efficiencies were integrated into the relative expression analysis in REST MCS.

Table 6-3: Gene reaction efficiencies as calculated by LinRegPCR.

GENE SYMBOL	MEAN REACTION EFFICIENCY	STANDARD DEVIATION
B2M	1.782	0.181
CANX	1.762	0.173
GAPDH	1.713	0.135
ATP5B	1.753	0.163
ANKRD1	1.717	0.184
ATF3	1.685	0.203
SLIT3	1.720	0.185
BDNF1	1.735	0.142
IGF1	1.765	0.158
WISP2	1.746	0.206
PTPN5	1.797	0.225
SEMA6A	1.728	0.184
TFPI2	1.766	0.186

6.2.4 qRT-PCR validation of selected genes

qRT-PCR was used to quantify expression changes in selected genes from the microarray experiment. Expression in the DRG after injury was calculated relative to a naïve control and for all groups apart from 6DC, a sham condition appropriate to the injury (section 2.2.7). Each gene validated in this way is dealt with separately in the ensuing sections. Microarray fold-change data was converted to Log_2 expression ratios and for each gene, displayed on a single graph with the Log2 expression ratios generated by REST-MCS for the qRT-PCR data (Figure 6-3 to Figure 6-10). Mean Ct values and CV_{exp} values (as calculated by REST-MCS) are presented for each experimental group and each gene in appendix C.

6.2.4.1 Wnt-1 inducible signalling pathway protein-2 (WISP2) expression

In the microarray WISP2 (1369484_at) was significantly upregulated in both the 6SN (1.6-fold change, 4.01%FDR) and 2DR (1.58-fold change, 1.23% FDR) data sets. This change was validated by qRT-PCR in the 2DR vs. naïve comparison, which showed a significant upregulation in WISP2 expression (p=0.042, pair-wise fixed reallocation test in REST-MCS) (Figure 6-3). Upregulation of the gene was also seen in the 2DR vs. sham comparison although this was insignificant (p=0.127). In the SN vs. naïve and SN vs. sham comparisons qRT-PCR detected a small but insignificant upregulation and downregulation, respectively (p>0.05).

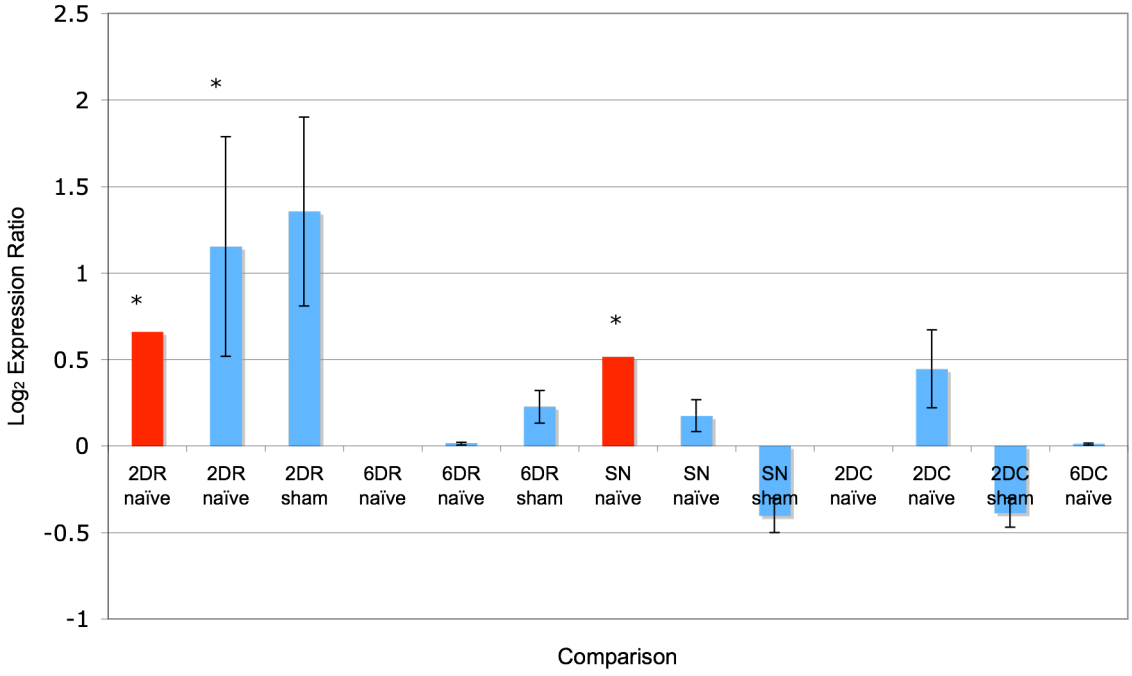

Figure 6-3: qRT-PCR validation of changes in WISP2 expression -comparison of microarray and qRT-PCR data. Red columns show microarray data (*FDR<5%) and blue columns show qRT-PCR data (mean ± S.E.M, n=6-8/group) (*p<0.05 for plotted comparison). Blank columns indicate no change (i.e. ratio=1).

6.2.4.2 Tissue factor pathway inhibitor 2 (TFPI2) expression

The microarray detected changes in TFPI2 (1377340_at) within 50% FDR only for the 6SN (1.49 fold change, 1.83% FDR) and 2DR (1.66 fold change, 0.53% FDR) data sets. This change was validated by qRT-PCR in the 2DR vs. naïve comparison which showed a highly significant upregulation in TFPI2 (p=0.01). This upregulation was also observed in the 2DR vs. sham, 6DR vs. naïve and sham, 6SN vs. naive and sham, and 2DC vs. sham comparisons although insignificant (p>0.05). The upregulation in the 6DR vs. naïve comparison was however significant before normalisation (p=0.028).

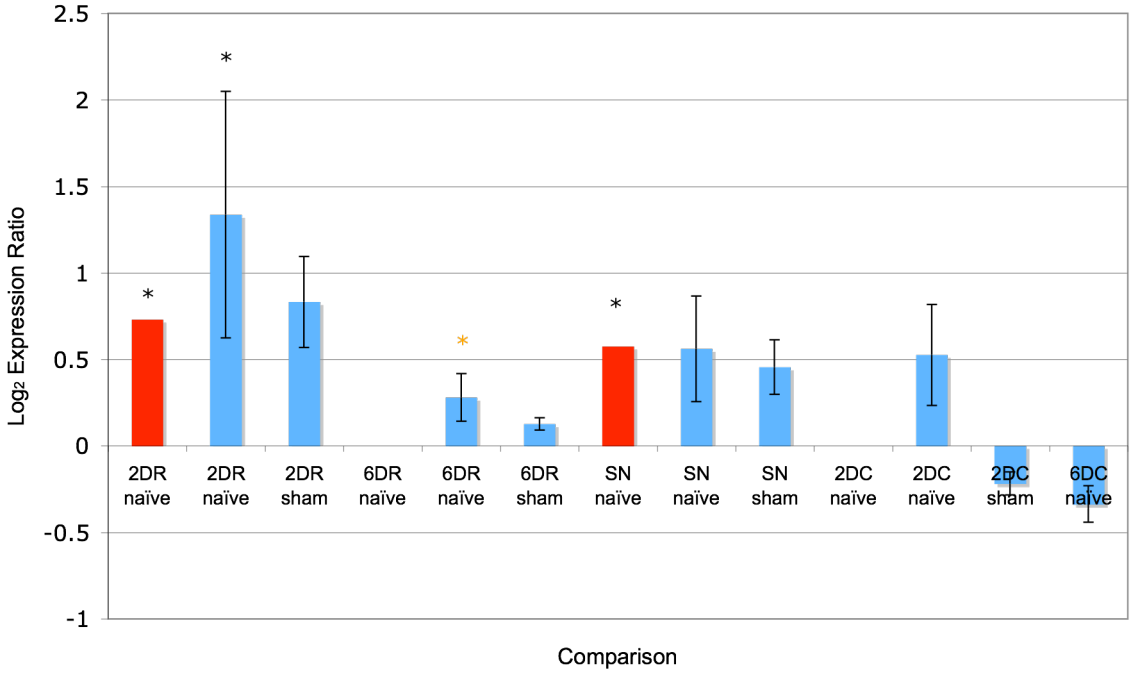

Figure 6-4: qRT-PCR validation of changes in TFPI2 expression -comparison of microarray and qRT-PCR data. Red columns show microarray data (*FDR<5%) and blue columns show qRT-PCR data (mean ± S.E.M, n=6-8/group) (*p<0.05, *p<0.05 before normalisation for plotted comparison).

6.2.4.3 Insulin-like growth factor 1 (IGF1) expression

IGF1 (probe set 1370333_a_at) was upregulated in both the regenerating conditions (1.31-fold, 10.8% FDR in SN and 1.53-fold 1.65% FDR in 2DR). qRT_PCR detected upregulations in 2DR vs. both naïve and sham although these were not significant ($p<0.05$). Small insignificant downregulations of the gene were detected in the SN vs. naïve and sham conditions as well as in 2DC vs. sham. qRT-PCR also detected small and insignificant upregulations of IGF1 in 6DR vs. sham and naïve, 2DC vs. naïve and 6DC vs. naïve conditions. In the 6DR vs. sham condition this change was significant before normalisation to the reference genes ($p=0.007$).

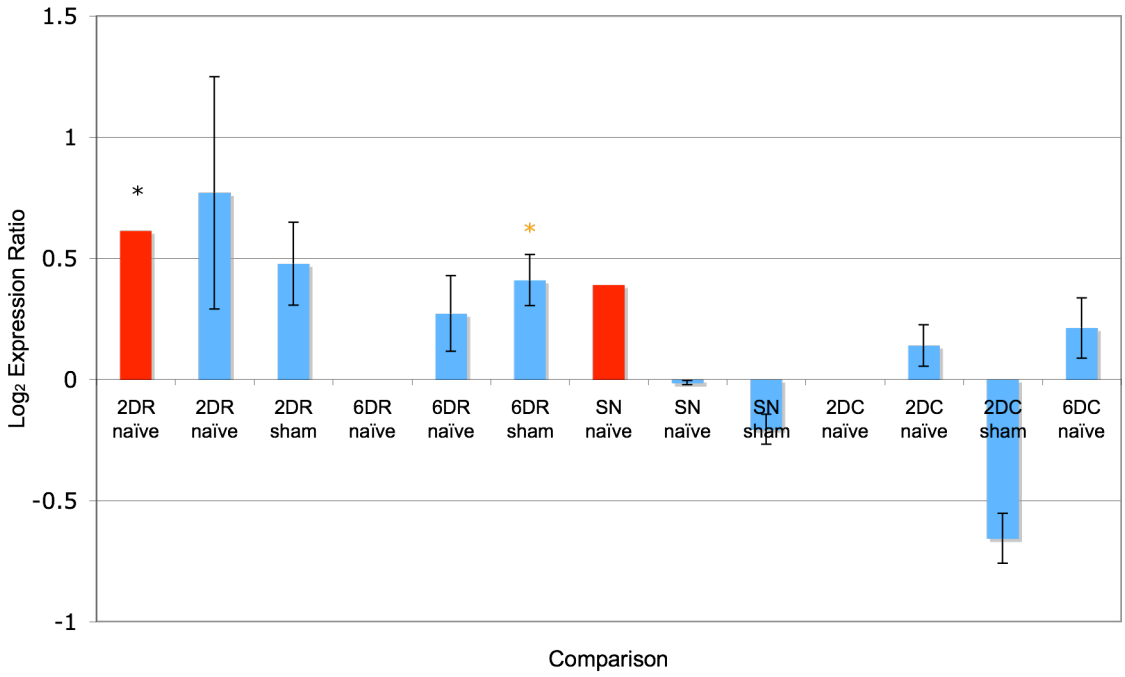

Figure 6-5: qRT-PCR validation of changes in IGF1 expression -comparison of microarray and qRT-PCR data. Red columns show microarray data (*FDR<5%) and blue columns show qRT-PCR data (mean ± S.E.M, n=6-8/group) (*$p<0.05$, *$p<0.05$ before normalisation for plotted comparison).

6.2.4.4 Activating transcription factor 3 (ATF3) expression

In our microarray, ATF3 (probe set 1369268_at) was upregulated in all the conditions but within the 5% FDR cut-off only in the 2DR vs. naïve (2.45-fold change, <0.01% FDR) and 2DC vs. naïve (11.13-fold change, <0.01% FDR) comparisons. qRT-PCR validated the change in the 2DR microarray, detecting a significant upregulation in ATF3 in the 2DR vs. sham comparison (p=0.015). This upregulation was also seen in the 2DR vs. naïve condition although this was not significant (p=0.367). Small, insignificant upregulations were detected in the 6DR vs. naïve and 6DR vs. sham conditions (p=0.984 and p=0.123, respectively) and the 6DR vs. sham comparison was significant before normalisation to reference genes (p=0.001). Changes seen in the SN microarray were also validated, a significant upregulation in the SN vs. naïve comparison was detected by qRT-PCR analysis (p=0.037) although the upregulation seen in SN vs. sham just misses significance (p=0.059). qRT-PCR detected a small upregulation in the 2DC vs. naïve and 2DC vs. sham comparisons although these were not significant (p=0.968 and p=0.241, respectively). A downregulation in ATF3 was detected for 6DC vs. naïve but this was insignificant (p=0.639).

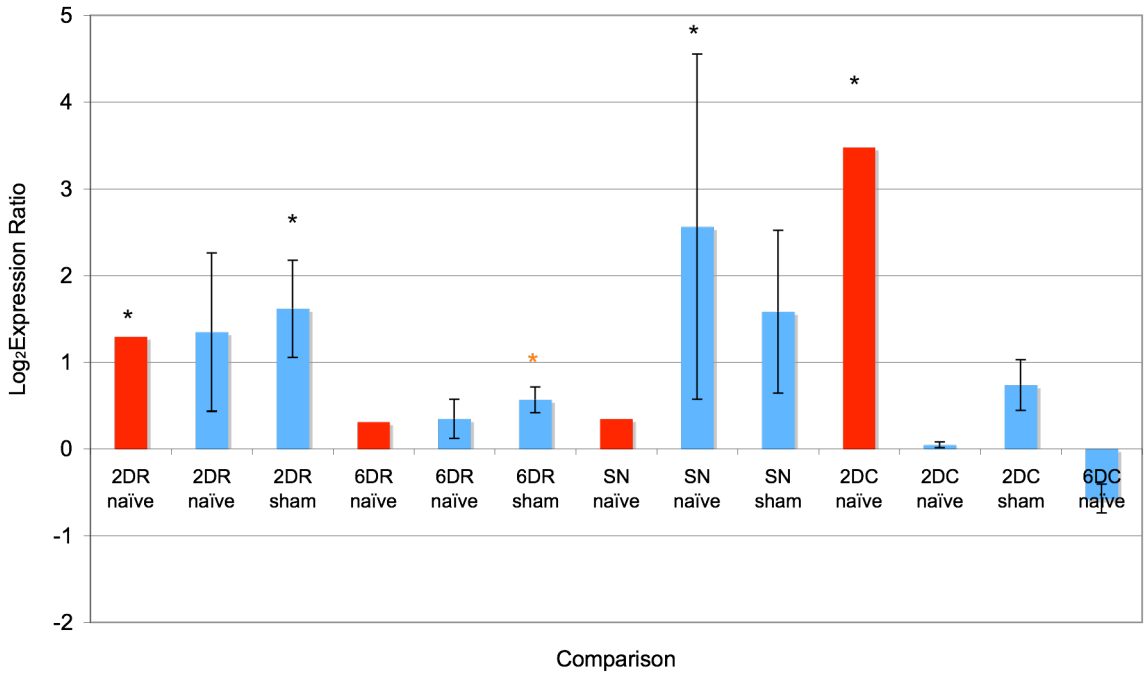

Figure 6-6: qRT-PCR validation of changes in ATF3 expression -comparison of microarray and qRT-PCR data. Red columns show microarray data (*FDR<5%) and blue columns show qRT-PCR data (mean ± S.E.M, n=5-8/group) (*p<0.05, *p<0.05 before normalisation for plotted comparison).

6.2.4.5 Ankyrin repeat domain 1 (ANKRD1) expression

The microarray detected a change in ANKRD1 (probe set 1367664_at) expression in only the 2DC condition (1.77-fold change, 1.77% FDR). This change was also seen in qRT-PCR in the 2DC vs. naïve and 6DC vs. naive comparisons (p=0.004 and p=0.001, respectively) although these were not significant after normalisation to the reference genes (p=0.252 and p=0.368, respectively). In addition, upregulation in ANKRD1 expression was not detected when 2DC was compared to its sham control (p=0.693). qRT-PCR did however detect significant upregulation of ANKRD1 in the 2DR vs. naïve, SN vs. naïve and SN vs. sham comparisons (p=0.001, p=0.002 and p=0.004, respectively). A small upregulation was also seen in the 6DR vs. naïve comparison (p=0.033) but this was insignificant after normalisation (p=0.871).

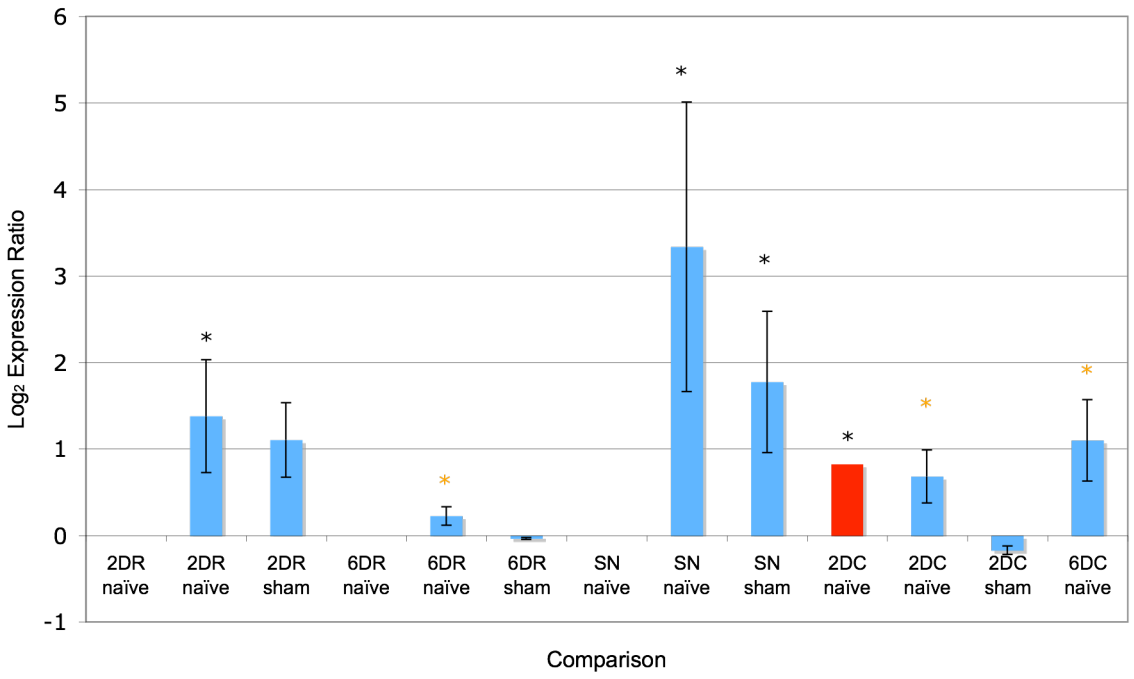

Figure 6-7: qRT-PCR validation of changes in ANKRD1 expression -comparison of microarray and qRT-PCR data. Red columns show microarray data (*FDR<5%) and blue columns show qRT-PCR data (mean ± S.E.M, n=6-8/group) (*p<0.05, *p<0.05 before normalisation for plotted comparison).

6.2.4.6 Semaphorin 6A (SEMA6A) expression

In the microarray SEMA6A (probe set 1376601_at) was significantly upregulated in the 2DC data (3.85-fold change, <0.01% FDR). A small but insignificant upregulation was also detected in the 2DR data set (1.32-fold change, 12.19% FDR) that was reflected in the 2DR vs. naïve and 2DR vs. sham comparisons (p=0.436 and 0.308, respectively). qRT-PCR did not however validate the microarray result for the 2DC data set and instead detected small but insignificant downregulations of the gene in both the 2DC vs. naïve and 2DC vs. sham comparisons (p=0.939 and p=0.076, respectively). A small and insignificant upregulation was however detected for the 6DC vs. naïve comparison (p=0.692). Where the microarray did not detect any difference in the gene for the SN data set, a significant upregulation was detected by qRT-PCR for the SN vs. sham comparison (p=0.038) but the upregulation in the 2DR vs. naïve comparison misses significance (p=0.099). In addition, qRT-PCR detected upregulations in the SN vs. naive and 6DR vs. sham that were significant before normalisation to the reference genes (p<0.05).

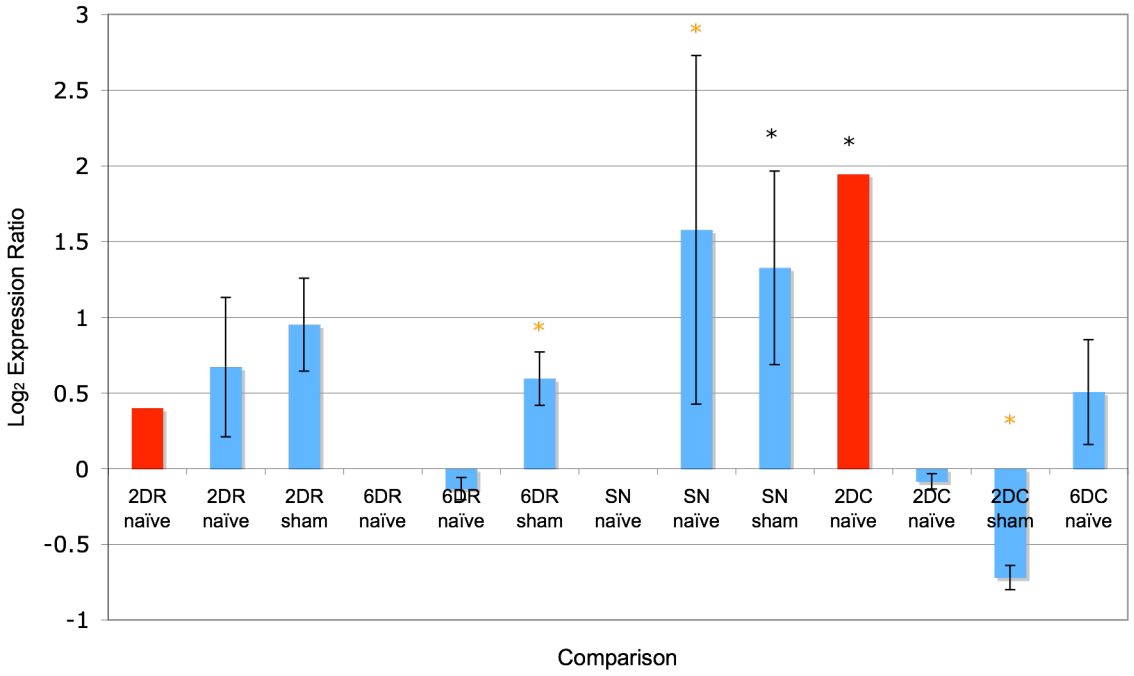

Figure 6-8: qRT-PCR validation of changes in SEMA6A expression -comparison of microarray and qRT-PCR data. Red columns show microarray data (*FDR<5%) and blue columns show qRT-PCR data (log2expression ± S.E.M, n=6-8/group) (*p<0.05, *p<0.05 before normalisation for plotted comparison).

6.2.4.7 Protein tyrosine phosphatase, non-receptor type 5 (PTPN5) expression

In the microarray PTPN5 (probe set 1368421_at) was regulated within the 50% FDR level in only the 2DC data set (2.96-fold change, 0.05% FDR). This change was not validated by qRT-PCR and there was small, insignificant downregulation of this gene in the 2DC vs. sham and 6DC vs. naïve comparisons ($p>0.05$). qRT-PCR did however detect upregulations in this gene in the 2DR and SN comparisons. This change was significant in the SN vs. sham comparison ($p=0.03$) and highly significant before normalisation to reference genes in the SN vs. naïve comparison ($p=0.004$) although just misses significance after nomalisation ($p=0.054$). The upregulation of PTPN5 in the 2DR vs. naïve comparison was significant ($p=0.022$) but the upregulation in the 2DR vs. sham comparison misses significance ($p=0.054$).

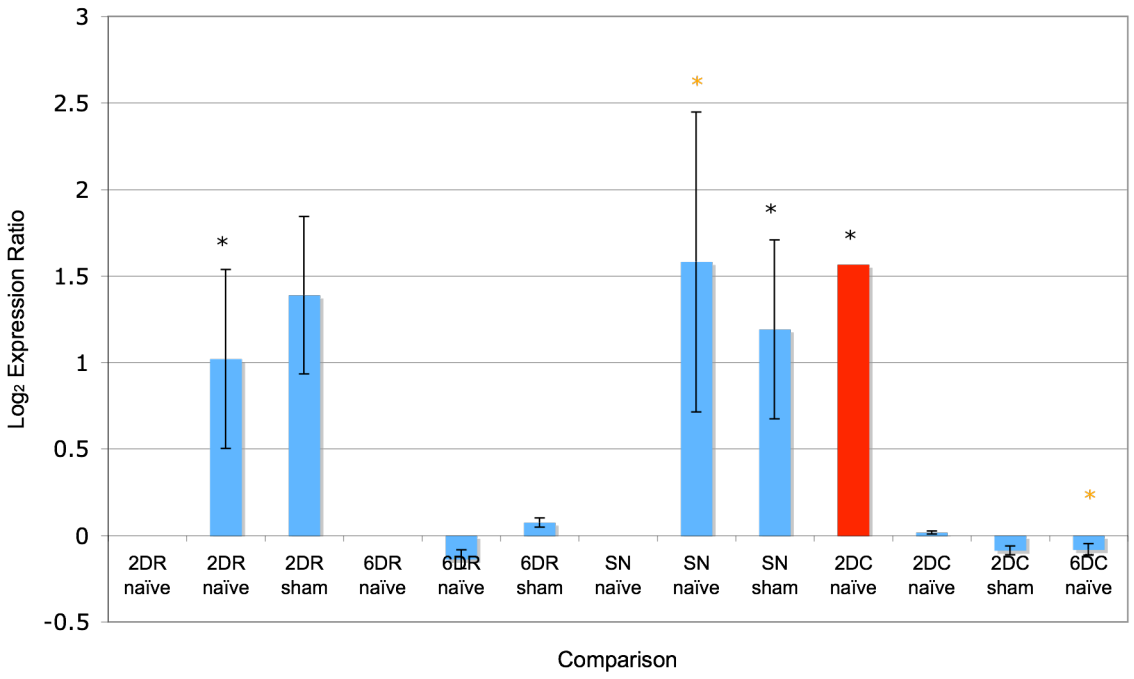

Figure 6-9: qRT-PCR validation of changes in PTPN5 expression -comparison of microarray and qRT-PCR data. Red columns show microarray data (*FDR<5%) and blue columns show qRT-PCR data (log2expression ± S.E.M, n=6-8/group) (*p<0.05, *p<0.05 before normalisation for plotted comparison).

6.2.4.8 Brain-derived neurotrophic factor (BDNF) expression

In the microarray BDNF (probe set 1368677_at) was significantly upregulated in the 2DR (2.86-fold change, <0.01% FDR), 6DR (1.48-fold change, 1.69% FDR) and 2DC (1.57-fold change, 4.7% FDR) data sets. By qRT-PCR, upregulation of this gene was seen in all comparisons except the 2DC vs. naïve and sham and 6DC vs. naïve comparisons that showed small insignificant decreases in BDNF. None of the changes were significant however ($p>0.05$) although the upregulation in the 6DR vs. sham comparison was significant before normalisation ($p=0.013$).

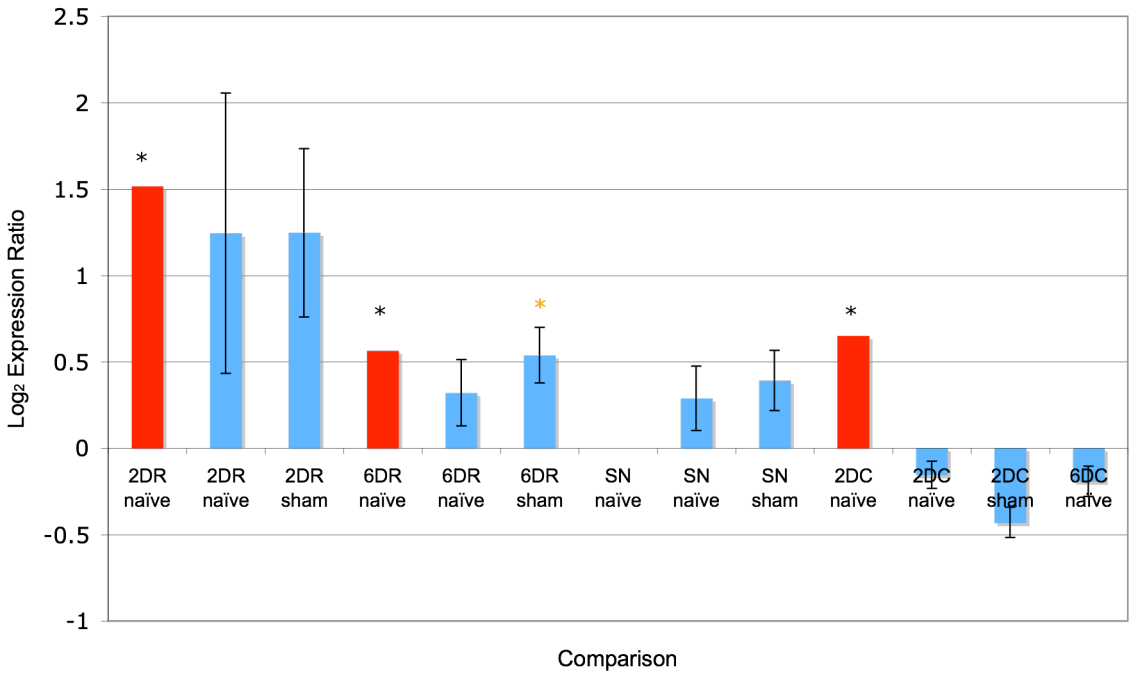

Figure 6-10: qRT-PCR validation of changes in BDNF expression -comparison of microarray and qRT-PCR data. Red columns show microarray data (*FDR<5%) and blue columns show qRT-PCR data (log2expression ± S.E.M, n=6-8/group) (*p<0.05, *p<0.05 before normalisation for plotted comparison).

6.2.5 Section discussion

6.2.5.1 Interpretation of qRT-PCR data

On the whole, the qRT-PCR was consistent with the microarray experiment in that when changes were significant, they were in the same direction and of similar magnitude. Changes in the dorsal column transection microarray were generally not validated however. In addition, qRT-PCR detected regulation in some genes that had not been detected by microarray, consistent with qRT-PCR being a more sensitive technique.

WISP2 and TFPI2 were selected as attractive regeneration associated genes, as they were two of only three genes that were upregulated in the regenerating conditions (<5% FDR) but not regulated (>50% FDR) in the non-regenerating conditions. In addition, IPA provided evidence that they are regulated in two different functional gene networks that are active in the regenerating conditions that also contain IGF1 (**Figure 5-8** and Figure 5-11). qRT-PCR however only validated the changes in these genes in the 2DR condition and hence brings into question whether these genes are truly regeneration associated.

Three genes that did not show a regeneration-associated expression in the microarrays (SEMA6A, PTPN5 and ANKRD1) appeared to show this pattern of expression in the qRT-PCR analysis. Overexpression of ANKRD1 has been shown to stimulate neurite outgrowth in PC12 cells and has been suggested as a candidate transcriptional modulator of regeneration (Stam *et al.* 2007). The results of the qRT-PCR support this. PTPN5 also stimulates neurite growth *in vitro* and hence the results of the qRT-PCR are consistent with this. For SEMA6A, the link to promotion of regeneration appears more tenuous as SEMA6A is known to act as a repulsive signal during development and can cause growth cone collapse (see also section 1.2.2.2). More recent evidence however suggests that this gene may have a role in microtubule dynamics (see also section) (Prislei *et al.* 2008). Additionally, accumulating evidence suggests that class VI semaphorins can act as receptors as well as ligands and thus function in retrograde signalling. The SEMA6A cytoplasmic domain can bind ENA/VASP-like protein (EVL) (Klostermann *et al.* 2000) that can promote actin polymerisation when receptor-bound (Lambrechts *et al.* 2000). ENA/VASP proteins (see also section 1.2.2.1) are concentrated at filopodial tips and are involved in translating extrinsic guidance cues into changes in cytoskeleton and filopodia (Drees and Gertler 2008). The upregulation in SEMA6A in the DRG could therefore result in changes in fillopodial dynamics through retrograde signalling at the growth cone.

The qRT-PCR data also lends support to ATF3 being a regeneration-associated gene. This is in contrast to the microarray results which suggested a timepoint-dependent expression of this gene, consistent with a general immediate-early response to stress as has been reported previously (Hai *et al.* 1999). Also consistent with the idea that ATF3 is a general response to any injury, and not only in injuries where regeneration is successful, is the observation that this gene was upregulated in DRG neurons after spinal cord transection (Huang *et al.* 2006). Other studies have however

suggested that this gene is induced in DRG after peripheral and not after central axonal injury and is downregulated after target innervation (Tsujino *et al.* 2000; Bloechlinger *et al.* 2004). This is consistent with a regeneration-associated expression and also with the qRT-PCR results of this study.

The expression of BDNF was confirmed for the 2 and 6 weeks dorsal root injuries but the relatively large upregulation seen in the microarray for dorsal column transection was not detected. The pattern of regulation for this gene as assessed by qRT-PCR is highly suggestive of it having a time-dependent response to injury out-with the CNS whilst injury within the CNS does not appear to induce its expression.

6.2.5.2 Methodological considerations

In the microarray experiment, samples were pooled to smooth biological variability. In the qRT-PCR cDNA was generated from individual animals to allow biological variability to be assessed. Standard errors were large indicating a high degree of inter-animal variability in gene expression. This may reflect true differences in gene expression levels between animals and could indicate heterogeneity between animals in the severity of the injury although care was taken to be consistent in the length of time that the nerve was crushed and in the distance of the crush from the DRG. In the case of the dorsal column transection injury, care was taken that the placement of the wire knife was consistent. The samples for each group were however usually split between three plates as all samples could not fit on one and an even mix of samples from each condition were placed on each plate to potentially allow direct comparisons between all groups. This may have increased within-group variability and reduced the power of the experiment. An improved design would have all samples for an experimental group, its sham control and the naïve control on a single plate as comparisons between experimental groups were not necessary.

The power of the experiment could have been further improved by increasing the number of samples in each group. In the pilot experiment, gene changes as low as 2.45 fold were validated using a group size of 5-6. Some of the genes that were chosen for validation of the main experiment did however show only a very modest fold change (often less than 2 fold) in the microarray. In hindsight, a power calculation based on the pilot experiment could have been used to predict the sample size required to detect <2-fold changes.

Four HKGs were assessed for general stability over all the injury models, sham control and naïve groups. Although the most stable in the sciatic nerve transection/ naïve and sciatic transection/sham groups, GAPDH was found to be the least stable across all our new injury models. This highlights the importance of validating HKGs for the specific model in question. Indeed, the experiment could have been further improved by performing a separate GeNorm analysis for each of the injury models and its control, providing an injury-specific set of stably expressed housekeeping genes for each model. For a number of the target genes, normalisation against the reference genes resulted in a change in the P-value of the results (orange asterix on figures). This demonstrates the necessity of normalisation of qRT-PCR data to a stably expressed

reference gene or genes in avoiding erroneous conclusions due to differences in starting template amount.

6.3 Preliminary results in human DRGs

We wished to determine if genes that are expressed within the DRG of rats with dorsal root crush are also present at a similar level in human avulsed DRGs to give an indication as to whether the candidate genes revealed by our microarray experiment based on animal injury models are likely to be relevant to dorsal root avulsion (see also sections 1.3.2 and 1.4.1.3) as seen in human patients.

DRGs from three patients who had suffered a dorsal root avulsion injury were obtained at the time of corrective surgery. The details of the patient material are noted in Table 6-4. All patients were young males and this represents the demographic that most commonly presents with dorsal root avulsion injury. Since control human material was unavailable (the acquisition of age-matched post mortem DRGs is difficult and samples of inappropriate age have been used in the past (Rabert *et al.* 2004)), the expression of two genes in dorsal root avulsed human DRGs and dorsal root crush rat DRGs was compared by qRT-PCR. From the injury models available to us, dorsal root crush is the injury that most closely resembles dorsal root avulsion. The 2 genes that were chosen were upregulated at 5% FDR specifically in the 2DR (chondroitin sulphate proteoglycan 2 (CSPG2), 1.99 fold-change, 0.06 % FDR)) and 6DR (high density lipid binding protein (HDLBP), 1.38 fold-change, 4.26 % FDR)) models. qRT-PCR data was normalised using the most stable reference gene from before (B2M).

Table 6-4: Details of human DRG material.

PATIENT ID	AGE	SEX	CAUSE OF INJURY	TIME FROM INJURY TO OPERATION	NOTES
050093	27	Male	Car road traffic accident	6 months	C8 root found in posterior triangle of neck, completely avulsed from spinal cord.
060060	24	Male	Dive from bridge	4 months	C6, C7, C8 and T1 roots found in posterior triangle of the neck, completely avulsed from the spinal cord.
050082	18	Male	Motorbike road traffic accident	3 months	C8 root found in posterior triangle of the neck, completely avulsed from the spinal cord.

6.3.1 Results and discussion

All samples for one target gene and the housekeeping were run in triplicate on a single plate. As before, triplicate Ct values were averaged and REST-MCS was used to quantitate human DRG gene expression relative to the 2DR and 6DR animal tissue. Reaction efficiencies for the human and rat primer assays were calculated using LinReg as before and were used to determine if there was any difference in efficiency between the rat and human primer assays (Table 6-5). The values could not however be used in REST-MCS as only one reaction efficiency per primer assay can be entered. The reaction efficiency for all three genes was therefore set to the default of 2.

Table 6-5: Reaction efficiencies of rat and human primer assays.

GENE	B2M		CSPG2		HDLBP	
Species (n=3/group)	Human	Rat	Human	Rat	Human	Rat
Average efficiency (to 3 s.f.)	1.784	1.710	1.716	1.718	1.732	1.761
Standard deviation (to 3 s.f.)	0.143	0.148	0.128	0.124	0.149	0.163

The expression of CSPG2 and HDLBP was expressed relative to the reference gene B2M for both the rat and human DRGs (Figure 6-11). The difference in the expression of the two genes in human tissue relative to 2DR and 6DR, normalised by B2M, was also quantified (Figure 6-12). The relative expression of both CSPG2 and HDLBP was lower in the human patient material than in the 2DR and 6DR DRGs. This difference was ~4.4-fold and significant for CSPG2 ($p=0.001$ and $p=0.048$ for comparison to 2DR and 6DR, respectively).

The difference in CSPG2 expression in the human and rat material is not attributed to differences in primer efficiencies between the human and rat assays as these were not significantly different ($p>0.05$, 1-way ANOVA). Indeed, it is unsurprising to find that the human DRGs had lower expression of these injury-induced genes given that they were harvested at a much later time point after injury than the rat DRGs (3-6 months vs. 2-6 weeks). These very preliminary data suggest that there is a turning down of injury-induced genes at a late time point after injury and a return to steady state gene expression, possibly due to failed regenerative attempts. Alternatively, these differences could merely represent variation in the constitutive expression of these genes between lumbar and cervical ganglia. Inclusion of a rat control would have allowed confirmation that these two genes are truly injury induced.

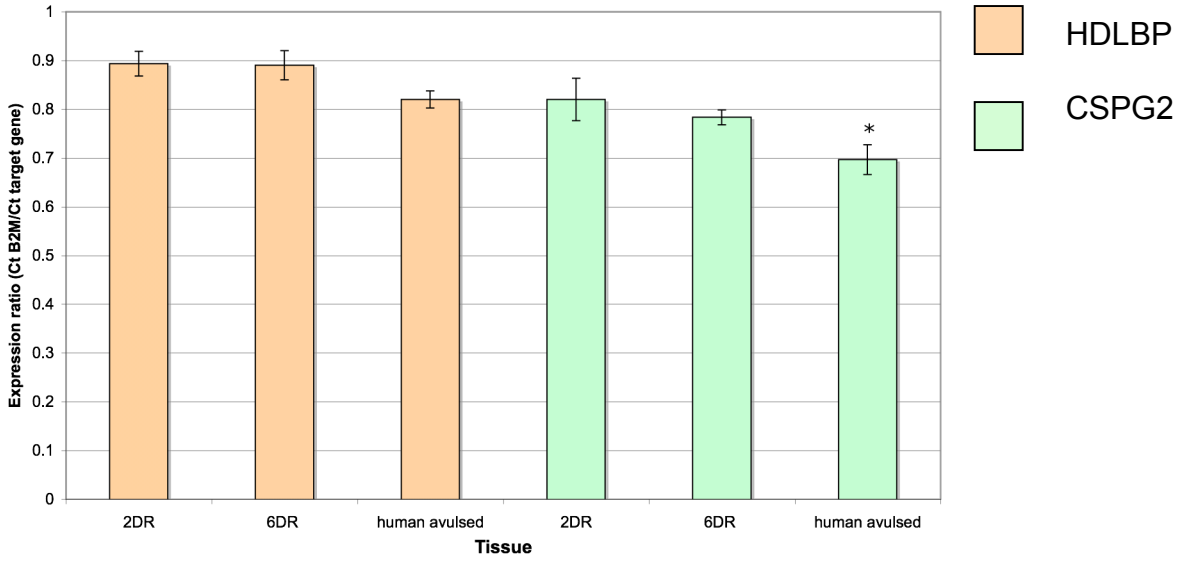

Figure 6-11: Expression of HDLBP and CSPG2 in human avulsed DRG compared to rat DRG with dorsal root crush expressed relative to B2M expression such that a lower expression ratio equates to a lower expression. * significantly different from 2DR and from 6DR ($p<0.05$). Mean ± S.E.M, n=3/group.

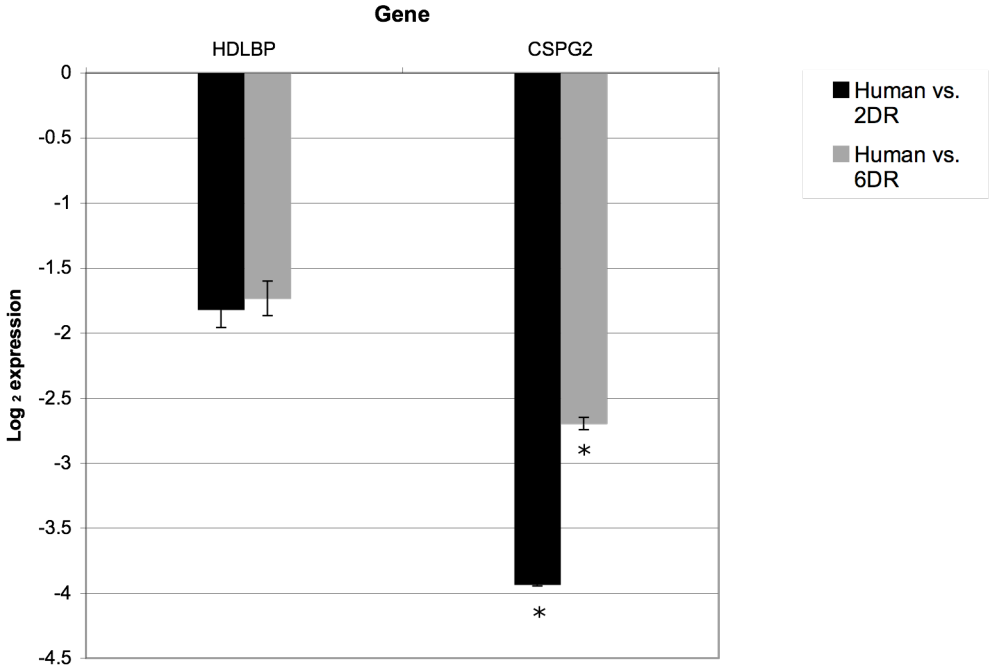

Figure 6-12: Log2 Expression of HDLBP and CSPG2 in human avulsed DRGs relative to rat DRGs (mean ± S.E.M, *$p<0.05$, n=3/group). Data are normalised to the housekeeping gene B2M.

6.4 Chapter summary

The attempted qRT-PCR validation of the microarray data met with mixed success. Improvements could have been made to the design of the experiment to minimise intergroup variability and hence increase the power for detection of small fold changes. The qRT-PCR results for the dorsal column transection animals showed little similarity to the microarray resullts bringing into question the validity of the changes in gene expression detected by these chips. The mixed success of the qRT-PCR validation highlights the importance of validation on a gene-to-gene basis and the dangers of applying a validated status to a whole microarray data set on the basis of a only a few validated genes.

The very preliminary data from the human tissue suggests that two genes that are expressed in rat DRG after injury are also expressed in human avulsed DRGs, albeit at a slightly lower level. As there were was no human control tissue available, the level of gene expression was compared to a rat injury model with relevance to dorsal root avulsion and normalised for differences in starting template to a housekeeping gene. This approach may be useful for future investigations where human control material is unavailable.

7 Final Discussion and future directions

A number of extrinsic and intrinsic factors are thought to contribute to the failure of the CNS to regenerate after injury (section1.4). This project aimed to reveal transcriptional programmes intrinsic to successful neuronal regeneration by examining neuronal gene expression associated with regenerating and regeneration-blocked/arrested DRG neurons. This project also, to the best of our knowledge, represents the first global survey of gene expression changes in the DRG following dorsal column injury, or indeed after any other spinal cord injury.

One of the biggest challenges presented by this, and indeed any other, microarray study is data analysis. Microarrays generate massive volumes of data and as such the application of appropriate analyses methods is of paramount importance. Discrepancies between results of different microarrays may be partially attributed to the diverse range of software available to store and analyse microarray data (Holloway *et al.* 2002; Slonim 2002). Tistone (2003) highlighted the dangers of drawing faulty conclusions from microarray data due to inadequate or inappropriate statistical analysis methods. This project utilised the data analysis facilities at the Sir Henry Wellcome Functional Genomics Facility (SHWGF) and Bioinformatics Research Centre (BRC) at the University of Glasgow. This facility has developed a robust microarray analysis pipeline that consists of three major steps: data normalisation, identification of differentially expressed genes and automated functional interpretation. Data normalisation is an important step that accounts for factors such as differing intensities of dye incorporation; minor irregularities in probe distribution during hybridisation; topographical slide variation or scanner introduced bias (Yang *et al*. 2002). At the SHWFGF, data normalisation is performed using the Robust Multichip Average (RMA) method (Irizarry *et al.* 2003). RMA performs a probe-specific background correction that compensates for non-specific binding, a probe-level multi-chip quantile normalisation to unify perfect match distributions across all chips, and a probe-set summary of the log-normalised probe-level data by median polishing.

Following data normalisation, the SHWFGF utilises the Rank Products (RP) method (Breitling *et al.* 2004), to identify differentially expressed genes. This method has been shown to perform more reliably and consistently than Tusher *et al*.'s (2001) Significance Analysis of Microarrays (SAM) and is particularly useful for small and noisy data sets (Breitling *et al*. 2004b). The method has now been widely adopted and a number of studies published recently have utilised this analysis to reveal differentially regulated genes (Cironi *et al.* 2008; Figueiredo *et al.* 2008; Kozul *et al.* 2008). RP ranks genes according to their expression changes and also provides statistical confidence levels. The final stage of analysis at the SHWFGF, automated functional interpretation, uses Iterative Group Analysis (iGA) (Breitling *et al*. 2004a) to produce a robust biological summary of the physiological processes affected in a given experiment. This method was particularly useful as an aid in the interpretation of the microarray data.

In addition to this pipeline analysis, the microarray data was also analysed using 'Genespring' software, a 'gold standard' proprietary software for microarray analysis, and 'Ingenuity pathways

analysis', a relatively new approach for functional analysis of microarray data. These programmes offered visualisation aids that were not provided with the RPA and IGA analysis and in addition, cross-validation of the analysis methods was achieved by use of multiple analysis tools. Indeed, the two functional analyses (IPA and IGA) showed overlaps in their functional classification of the data.

Ontology based analyses do inevitably have their limitations however. IGA is reliant on existing 'GO ontology' functional annotations where, for virtually every organism only a subset of known genes are annotated (King *et al.* 2003). Both IGA and IPA are reliant on the manual curation of information from published papers and are as such subject to human error in the interpretation of facts. It was also evident that IGA was heavily influenced by genes that appeared in more than one GO category and there was a good deal of redundancy as parent terms and all subordinate daughter terms were represented.

7.1 Main observations

All the injury models elicited changes in hundreds of genes both at 5% FDR and the 5% significance level. The number of genes that were specific to the regenerating conditions was fairly low however. This may reflect the fact that the two regenerating conditions were at two very different time points after injury and it is conceivable that genes which are responsible for initiation of regeneration are not required for maintenance of regeneration and vice versa. This analysis also assumes that regeneration of the central branch of the DRG neuron after dorsal root injury involves activation of the same genes and mechanisms as regeneration after a sciatic or spinal nerve injury. Evidence from a recent study of the response of peripherally and centrally axotomised DRG neurons did however suggest that injuries in these two branches are very different, even at an early time point when regeneration would be taking place in the dorsal root (Stam *et al.* 2007). Taking this into account it is perhaps unsurprising that the degree of overlap in the two regenerating condition is so small.

There was however one striking commonality in the regenerating conditions. This was the upregulation of procollagens. Collagens are usually produced by fibroblasts and are indicative of fibrosis. In the normal sciatic nerve collagen fibrils form part of the perineurium and epineurium, the outer connective tissue sheaths that lend structural support and elasticity to the nerve (Stolinski 1995). After injury, epineurial fibroblasts are known to upregulate collagen mRNAs (Siironen *et al.* 1996). The results from the microarray suggest that procollagens are also upregulated within the DRG during times of axon regeneration. It is unclear however if procollagens upregulated within the DRG could contribute to distal ensheathment of axons during regeneration but the fact that procollagens were not generally upregulated in all injuries suggests that this is not simply a feature of an inflammatory response to injury.

Dorsal column transection elicited a robust transcriptional response in the DRG. This included a large number of genes that were not regulated (>50% FDR) in the other injury models (2827 genes

<50% FDR, 244 <5% FDR). The complete separation of this injury from the others in principal components and correlational analysis further highlighted the uniqueness of the transcriptional response to this type of injury. This may be explained by the fact that dorsal column transection severs mainly ascending large-diameter Aβ fibres whilst leaving the smaller diameter C fibres that make central contacts in the dorsal horn intact. The DRG therefore retains a supply of target-derived factors and remains functional. The difference in the transcriptional response may also be due to the fact that it involved transection rather than crushing of the axons and differences in the response of DRGs to crushing and axotomy has already been demonstrated (Cho *et al.* 1998) and differences in cell death are discussed later.

An interesting finding regarding the neuronal response to dorsal column transection was that a number of known RAGs were expressed. While some of these genes have been demonstrated to promote neurite outgrowth *in vitro*, others have only been associated with regeneration because they are upregulated after a peripheral nerve injury- i.e. they have not been shown to be unregulated in non-regenerating conditions. So does the upregulation of these RAGs mean that dorsal column injury elicits a regenerative transcriptional response or does this mean these genes have nothing to do with regeneration after all? If the former is true, these data may have important implications for treatment of spinal cord injury as it suggests that the neurons may be already intrinsically primed for regeneration given the appropriate extrinsic factors.

7.1.1 Observations with relevance to dorsal root avulsion

Dorsal root avulsion is an intractable injury due to the failure of dorsal root fibres to regenerate though the barrier of the DREZ to enter the spinal cord (see also section 1.4.1.3). It was therefore interesting to compare the neuronal response to dorsal root regeneration to that associated with dorsal root block at the DREZ. Many of the genes that were activated at 2 weeks following dorsal root crush had returned to pre-injury levels at 6 weeks post-injury. IPA network analysis did however reveal one gene that was downregulated at 2 weeks but later upregulated at 6 weeks. This gene was neuregulin 1 (NRG1) (see section 5.6.9). This gene was one of a very few genes that showed an antagonistic pattern of expression at 2 and 6 weeks post-injury (only two others were identified using Excel data sorting) and reduced expression of this gene has been previously shown to correlate with periods of regeneration (Bermingham-McDonogh *et al.* 1997) while elevated levels of this gene has been suggested to contribute to the poor regenerative capacity of optic nerves (Martinez *et al.* 2004). Upregulation of this gene in neurons that are blocked at the DREZ may therefore represent one of the intrinsic factors that contribute to the failure of dorsal root axons to overcome the barrier of the DREZ and may represent an attractive candidate for genetic manipulation.

7.1.2 Putative regeneration associated genes

Wnt-1-inducible signalling pathway protein 2 (WISP2) and tissue factor pathway inhibitor 2 (TFPI2) were identified from the microarray as being novel regeneration-associated genes as they were

common and specific to the regenerating conditions. Further investigation of their function using cluster analysis revealed that they are co-regulated in the injury conditions with genes involved in glycerophospholipid metabolism. In addition, TFPI2 clustered with genes involved in Wnt/β catenin signalling, a pathway that has been implicated in a number of functions including axonal outgrowth (Endo and Rubin 2007). Although the expression of these genes was not fully validated by the qRT-PCR experiments, further investigation of their function and their possible involvement in this pathway would be interesting.

7.1.3 Observations with relevance to neuropathic pain

Although the main focus of the project was the identification of genes that may have a putative role in neuronal regeneration, the study also had relevance to neuropathic pain injury. Chronic spinal pain is a significant problem after spinal cord injury and neuropathic pain is associated with peripheral nerve injuries. An interesting finding was that dorsal column injury elicited many of the changes in ion channels and neurotransmitter receptors that are associated with neuropathic injury models. In addition, a feature of all the injuries was gene expression changes indicative of immune cell infiltration and there was activation of complement in the DRG after all the injuries. The complement pathway has been recently suggested as a novel target for treatment of neuropathic pain (Levin *et al.* 2008).

7.2 Interpretational considerations

Interpretation of the microarray data from this experiment was made extremely complex by the multitude of factors at play in the *in vivo* milieu. Injury to an axon initiates retrograde signalling (section 1.5.2.1) that causes changes in the transcription of many genes within the DRG. The transcriptional programmes that are active at any one time in a neuron will be determined by a number of factors such as nature of the injury (eg. crush or transection), distance and position of injury in relation to the cell body, time from injury and extrinsic signals at the lesion zone. In addition, the DRG is a heterogeneous tissue that contains non-neuronal cells such as macrophage and fibroblasts that are also influenced by injury to neurons in their vicinity. Gene expression changes can therefore also be associated with these non-neuronal cells. Attempts have been made to reveal the factors that are intrinsic to regeneration by dissociating neurons from the extrinsic factors acting on them in vivo and studying them in culture (Szpara *et al.* 2007). Whilst this allows the environmental conditions to be carefully controlled, there are questions as to how valid *in vitro* observations are to the *in vivo* situation. Ultimately, extrinsic and intrinsic factors are coupled in the animal, both influencing the other- remove one and you change the other and as such *in vitro* approaches may not accurately reflect the *in vivo* situation.

Given also that the nature of the injury has such an influence on the transcriptional response of the DRG, we have to ask how clinically relevant animal injury models are. Animal models need to be

reproducible and hence there is a trade off with how clinically relevant they are (it can be argued that it is easier to do a reproducible dorsal column transection than a contusion, easier to do a reproducible dorsal root crush than an avulsion). Indeed it has been shown that there is a difference in cell death after dorsal root avulsion and dorsal root axotomy (Chew *et al.* 2008).

This also highlights another interpretational problem for this project in the fact that different injury models may induce varying levels of cell death. An apparent downregulation in a gene could therefore be attributed to loss of a certain cell subtype relative to control and this loss may be different in each injury. There have been reports of preferential loss of large cells (Bondok and Sansone 1984) whilst others report preferential loss of small cells (Rich *et al.* 1989). Cell death is also thought to vary according to distance of axotomy from the ganglion with injuries that are closer to the cell body producing more rapid and pronounced cell death (Watson 1968). The delay in cell death after very distal injuries could be attributed to the delay for retrograde injury signals (section 1.5.2.1) to reach the cell body. An investigation of the time course and level of cell death after each of our injury models using techniques such as optical dissection would allow us to ascertain to what extent gene expression changes were due to cell death. Information from this would also have relevance to regenerative strategies. If substantial cell death occurs following injury one must first improve neuronal survival (e.g. by providing adequate neurotrophic support) before regeneration can be encouraged via other strategies.

7.3 Methodological considerations

Microarray experiments are expensive and therefore experimental design is constrained by costs. Had resources been available, it would have been possible to hybridise chips with samples from sham-operated controls for each condition. This would have removed genes that were regulated by systemic changes due to tissue damage during surgery. The inclusion of sham-operated samples in the qRT-PCR validation experiments did however provide a compromise that was more financially feasible and allowed us to test surgery effects on a gene-to-gene basis.

Chip costs also dictated the number of replicates that could be performed. For each condition the minimum requirement of three replicates was performed and pooling of samples was applied in order to smooth variation, as recommended for experiments with a small number of chips (Kendziorski *et al.* 2005).

Finally, whilst the dorsal column transection is an injury model which has been well optimised and which produces a reproducible lesion without damage to overlying blood vessels, it is not easily comparable to a crush lesion. There are several spinal cord contusion injury models (Kuhn and Wrathall, 1998; Metz et al. 2000; Young, 2002) which may have been used as an alternative to transection but, as discussed, may not be so reproducible although arguably, more clinically relevant.

7.4 Future directions

A number of aspects of the microarray data provided by this project were interesting and could have been investigated further had there been sufficient time and resources. The qRT-PCR validation could have been expanded to include a larger set of genes and the group size could have been increased to enhance the power of assay to detect smaller gene expression changes. Given the heterogeneity of the DRG, it would have been interesting to determine the locus of the gene expression changes by *in situ* hybridisation on DRG sections. Validated gene expression changes detected in the DRG after injury may not necessarily translate to protein changes in the axon however so further validation using protein techniques such as Western blotting and immunohistochemical analysis of nerve sections is needed. Proteins that localise to growth cones in axon terminals would be of particular interest as regeneration associated genes.

Following confirmation that a gene is translated and expressed at an appropriate location in the neuron, candidate regeneration associated genes may be tested for their ability to stimulate regeneration in *in vitro* assays of DRG neuron growth or *in vivo* using gene silencing technology and transgenic animals. Short interfering RNAs (siRNA) have been successful in silencing a number of target genes *in vitro* thus demonstrating their role in regeneration and neuropathic pain (Jankowski *et al.* 2006; Williams *et al.* 2006; Murray and Shewan 2008; Toth *et al.* 2008). *In vivo* gene silencing is more difficult because of possible off-target effects. Intrathecal and paratracheal administration of siRNA *in vivo* has been shown to relieve chronic neuropathic pain by reducing expression of cation channels in the DRG and their subsequent translocation to the dorsal horn of the spinal cord (Dorn *et al.* 2004; Kasama *et al.* 2007). HSV vectors have been used recently to target short-hairpin RNA to silence genes in the DRG of mice and this may represent a more efficient and targeted method of gene silencing *in vivo* (Anesti *et al.* 2008).

Another interesting line of investigation would be to investigate how manipulations of the lesion zone that promote regeneration in the spinal cord (such as cell grafts), affect gene expression in the DRG after dorsal column transection. This may reveal how the extrinsic factors influence neuronal transcriptional programmes to promote regeneration. In addition, this study provided only a snapshot of gene expression at 2 weeks after dorsal column transection. It would be interesting therefore to examine temporal DRG gene expression after injury. In particular a comparison of very early gene expression (during the period of abortive sprouting) with gene expression at a later time point would be of interest to the identification of regeneration associated genes.

To summarise, this project revealed a number of interesting aspects of the neuronal response to central and peripheral branch injuries and a small number of putative regeneration-associated genes. Further work is however needed to validate these, to elucidate the locus of the observed changes within the DRG and to establish a causal link between their expression and axonal regeneration. The study also provided the first genome-wide study of gene expression after dorsal column transection, which suggested that even after injury within the CNS, DRGs are primed for

regeneration. This has implications for the treatment of SCI and suggests that early interventions to manipulate extrinsic factors at the lesion zone could potentially lead to regeneration and functional recovery.

Appendices

a) Differentially expressed genes (Rank Products Analysis)

i) Pilot microarray

Table 7-1: Genes upregulated (<1% FDR) in the DRG 8 days after sciatic nerve transection.

AFFY. ID.	FDR	MEAN FC	ACC. NO.	GENE SYMBOL	GENE TITLE
1387154_at	0	45.88	NM_012614	Npy	neuropeptide Y
1377146_at	0	28.51	AI412212	RGD:621647	vasoactive intestinal polypeptide
1369268_at	0	14.32	NM_012912	Atf3	activating transcription factor 3
1387088_at	0	12	NM_033237	Gal	galanin
1398243_at	0	8.71	NM_057144	---	---
1368238_at	0	8.82	NM_053289	Pap	pancreatitis-associated protein
1371248_at	0	7.15	BI286387	RGD:1310042	small proline-rich protein 1A (predicted)
1376601_at	0	6.35	BF397526	---	Similar to semaphorin 6A1; semaphorin 6A-1
1368224_at	0	6.62	NM_031531	Spin2c	Serine protease inhibitor
1387396_at	0	5.8	NM_053469	Hamp	hepcidin antimicrobial peptide
1369202_at	0	5.35	NM_017028	Mx2	myxovirus (influenza virus) resistance 2
1377334_at	0	4.8	BG378249	RT1-Ba	RT1 class II, locus Ba
1388451_at	0	3.76	AA817802	---	Transcribed locus
1370883_at	0.07	4.03	Y00480	---	---
1368947_at	0.07	4.12	NM_024127	Gadd45a	growth arrest and DNA-damage-inducible 45 alpha
1368266_at	0.06	3.69	NM_017134	Arg1	arginase 1
1370315_a_at	0.06	3.56	AF026530	Stmn4	stathmin-like 4
1371450_at	0.11	3.02	BE117330	Sox11	SRY-box containing gene 11
1367973_at	0.11	3.2	NM_031530	Ccl2	chemokine (C-C motif) ligand 2
1372734_at	0.1	3.44	AI408095	RGD:727777	small cell adhesion glycoprotein
1386967_at	0.1	3.04	NM_053522	Rhoq	ras homolog gene family, member Q
1388385_at	0.09	3.28	BG371710	Cryba2	crystallin, beta A2
1368421_at	0.09	3.01	NM_019253	Ptpn5	protein tyrosine phosphatase, non-receptor type 5
1367930_at	0.08	2.77	NM_017195	Gap43	growth associated protein 43
1371015_at	0.2	2.73	X52711	Mx1	myxovirus (influenza virus) resistance 1
1388944_at	0.19	2.59	BE109016	Sox11	SRY-box containing gene 11
1367679_at	0.19	3.15	NM_013069	Cd74	CD74 antigen (invariant polpypeptide of major histocompatibility class II antigen-associated)
1368892_at	0.25	2.88	NM_016989	Adcyap1	adenylate cyclase activating polypeptide 1
1370177_at	0.28	2.81	AI548856	PVR	poliovirus receptor
1376836_at	0.27	2.67	BF419655	---	---
1369788_s_at	0.26	2.68	NM_021835	Jun	v-jun sarcoma virus 17 oncogene homolog (avian)
1370383_s_at	0.34	2.97	BI279526	---	---
1370051_at	0.36	2.83	NM_031659	Tgm1	transglutaminase 1
1367664_at	0.38	2.82	L81174	Ankrd1	ankyrin repeat domain 1 (cardiac muscle)
1389006_at	0.4	2.53	AI170394	Mpeg1	Macrophage expressed gene 1
1375951_at	0.47	2.65	AA818521	Thbd	thrombomodulin
1388433_at	0.46	2.63	BI279605	Krt1-19	keratin complex 1, acidic, gene 19
1372042_at	0.53	2.51	BI294844	---	Similar to RIKEN cDNA 9430096L06
1389373_at	0.56	2.42	AI029555	Smad1	SMAD, mothers against DPP homolog 1 (Drosophila)
1367874_at	0.65	2.7	NM_053522	Rhoq	ras homolog gene family, member Q
1371245_a_at	0.93	4.11	BI287300	---	---
1368210_at	0.9	2.31	NM_133311	Il24	interleukin 24
1374280_at	0.95	2.67	AA817812	---	---
1388711_at	0.93	2.42	BF282650	---	Transcribed locus, strongly similar to NP_598751.3 interleukin 13 receptor, alpha 1 [Mus musculus]
1370215_at	1	2.39	AW434057	C1qb	complement component 1, q subcomponent, beta polypeptide

Table 7-2: Genes downregulated (<1% FDR) in the DRG 8 days after sciatic nerve transection.

AFFY. ID.	% FDR	MEAN FC	ACC. NO.	GENE SYMBOL	GENE TITLE
1368751_at	0	-3.6	NM_031778	Kcns3	potassium voltage-gated channel, delayed-rectifier, subfamily S, member 3
1393933_at	0	-3.25	AW144823	RGD:1310938	sortilin-related receptor, L(DLR class) A repeats-containing (predicted)
1371108_a_at	0	-3.82	M74494	Atp1a1	ATPase, Na+/K+ transporting, alpha 1 polypeptide
1374046_at	0	-3.03	BG376092	---	---
1368506_at	0	-3.37	U27767	Rgs4	regulator of G-protein signaling 4
1368821_at	0	-3.23	BI290885	Fstl1	follistatin-like 1
1370556_at	0	-3.06	M24104	---	---
1370517_at	0	-2.88	U18772	RGD:628894	neuronal pentraxin 1
1377457_a_at	0	-2.8	AA850618	RGD:1310938	sortilin-related receptor, L(DLR class) A repeats-containing (predicted)
1377095_at	0	-2.91	BG380409	LOC287847	similar to ataxin 2-binding protein 1 isoform 1; hexaribonucleotide binding protein 1
1369390_a_at	0	-2.82	NM_022850	Dpp6	dipeptidylpeptidase 6
1371077_at	0	-2.63	AI575989	Htr3b	5-hydroxytryptamine (serotonin) receptor 3b
1369428_a_at	0	-2.65	U28430	Htr3a	5-hydroxytryptamine (serotonin) receptor 3a
1371211_a_at	0	-2.78	U02315	Nrg1	neuregulin 1
1369001_at	0	-2.57	NM_052805	Chrna3	cholinergic receptor, nicotinic, alpha polypeptide 3
1388000_at	0	-2.65	AF021923	Slc24a2	solute carrier family 24 (sodium/potassium/calcium exchanger), member 2
1369116_a_at	0	-2.5	NM_017338	Calca	calcitonin/calcitonin-related polypeptide, alpha
1370572_at	0	-2.43	AY030276	Gpr149	G protein-coupled receptor 149
1375242_at	0.05	-2.39	BI296440	---	---
1384132_at	0.05	-2.63	H31111	RGD:1310999	immunoglobulin superfamily, member 4A (predicted)
1369144_a_at	0.05	-2.49	U75448	Kcnd3	potassium voltage gated channel, Shal-related family, member 3
1387065_at	0.32	-2.37	NM_080688	Plcd4	phospholipase C, delta 4
1387309_a_at	0.3	-2.34	AI111480	Grik1	glutamate receptor, ionotropic, kainate 1
1368044_at	0.38	-2.42	NM_022669	Scg2	secretogranin 2
1371003_at	0.36	-2.66	BG378086	Map1b	microtubule-associated protein 1b
1376736_at	0.38	-2.49	BG375419	---	Transcribed locus
1369816_at	0.37	-2.47	NM_013018	Rab3a	RAB3A, member RAS oncogene family
1368182_at	0.36	-2.33	NM_130739	Acsl6	acyl-CoA synthetase long-chain family member 6
1383499_at	0.34	-2.29	BG371995	---	Transcribed locus
1387602_a_at	0.37	-2.26	NM_022189	Htr3b	5-hydroxytryptamine (serotonin) receptor 3b
1370146_at	0.42	-2.54	NM_053296	Glrb	glycine receptor, beta subunit
1393480_at	0.56	-2.38	AW919998	Ppp1r2	protein phosphatase 1, regulatory (inhibitor) subunit 2
1369210_at	0.58	-2.26	NM_030875	Scn1a	sodium channel, voltage-gated, type 1, alpha polypeptide
1374743_at	0.74	-2.27	BE115056	---	---
1376311_at	0.71	-2.22	BM391312	---	Transcribed locus
1390097_at	0.69	-2.36	BI281738	RGD:1306653	TSPY-like 4 (predicted)
1390672_at	0.68	-2.29	BG381258	---	Transcribed locus
1372345_at	0.66	-2.18	AA894210	---	Transcribed locus
1373658_at	0.64	-2.13	AI409259	---	Similar to Rac GTPase-activating protein
1375026_at	0.62	-2.16	AI105369	RGD:1309714	ceroid-lipofuscinosis, neuronal 6 (predicted)
1368853_at	0.61	-2.37	AI227991	Vsnl1	visinin-like 1
1392607_at	0.64	-2.46	BF391141	---	Transcribed locus
1372300_at	0.74	-2.22	BI288838	---	Similar to Polymerase (RNA) II (DNA directed) polypeptide C
1390146_at	0.75	-2.2	BF414998	---	Similar to RIKEN cDNA 2610318G18
1368505_at	0.73	-2.28	U27767	Rgs4	regulator of G-protein signaling 4
1370406_a_at	0.72	-2.31	AB032395	Daf1	decay accelarating factor 1
1369627_at	0.7	-2.31	BG672437	Sv2b	synaptic vesicle glycoprotein 2b
1376842_at	0.71	-2.19	BF395964	---	Transcribed locus
1376987_at	0.73	-2.21	AW523375	RGD1309466_predicted	similar to hypothetical protein FLJ20156 (predicted)
1368822_at	0.72	-2.22	BI290885	Fstl1	follistatin-like 1
1367959_a_at	0.71	-2.41	AF182949	Scn1b	sodium channel, voltage-gated, type I, beta polypeptide

Table 7-2 continued.

1367835_at	0.69	-2.39	NM_019279	Pcsk1n	proprotein convertase subtilisin/kexin type 1 inhibitor
1369000_at	0.91	-2.23	NM_021589	Ntrk1	neurotrophic tyrosine kinase, receptor, type 1
1387235_at	0.89	-2.08	NM_021655	Chga	chromogranin A
1368696_at	0.95	-2.21	NM_022008	Fxyd7	FXYD domain-containing ion transport regulator 7
1376657_at	0.98	-2.27	BE117767	---	Similar to RA175
1368768_at	0.96	-2.08	NM_019265	Scn11a	sodium channel, voltage-gated, type11, alpha polypeptide

ii) Main microarray

Table 7-3: Genes upregulated (<1% FDR) in the DRG 2 weeks after dorsal root crush.

AFFY. ID	% FDR	MEAN FC	ACC. NO.	GENE SYMBOL	GENE TITLE
1368238_at	0	13.64	NM_053289	Pap	pancreatitis-associated protein
1387930_at	0	4.55	L10229	Reg3a	regenerating islet-derived 3 alpha
1368187_at	0	3.71	NM_133298	Gpnmb	glycoprotein (transmembrane) nmb
1387154_at	0	3.18	NM_012614	Npy	neuropeptide Y
1368677_at	0	2.86	NM_012513	Bdnf	brain derived neurotrophic factor
1368359_a_at	0	2.83	NM_030997	Vgf	VGF nerve growth factor inducible
1375010_at	0	2.53	AI177761	Cd68	CD68 antigen
1384063_at	0	2.49	AA958001	Cthrc1	collagen triple helix repeat containing 1
1395126_at	0	2.45	AI011393	Msr2_predicted	macrophage scavenger receptor 2 (predicted)
1369268_at	0	2.45	NM_012912	Atf3	activating transcription factor 3
1373386_at	0	2.49	AI179953	Gjb2	gap junction membrane channel protein beta 2
1390119_at	0	2.41	BF396602	Sfrp2	secreted frizzled-related protein 2
1376750_at	0	2.32	AA963477	---	Transcribed locus
1385751_at	0	2.38	BF408413	Thbs2	thrombospondin 2
1377092_at	0	2.33	BF389682	---	Transcribed locus
1368224_at	0	2.34	NM_031531	Serpina3n	serine (or cysteine) peptidase inhibitor, clade A, member 3N
1392965_a_at	0	2.25	AI028877	Smoc2_predicted	SPARC related modular calcium binding 2 (predicted)
1385248_a_at	0	2.25	AA997590	Ogn_predicted	osteoglycin (predicted)
1370892_at	0	2.27	BI285347	C4a /// C4-2	complement component 4a /// complement component 4, gene 2 ///
1367973_at	0	2.33	NM_031530	Ccl2	chemokine (C-C motif) ligand 2
1384707_at	0	2.25	AI600020	---	Transcribed locus
1392515_at	0	2.24	AI177403	Ly49i9	Ly49 inhibitory receptor 9
1375917_at	0	2.24	BF282961	Gp49b /// LOC499078	glycoprotein 49b /// similar to GP49B1
1367794_at	0	2.19	NM_012488	A2m	alpha-2-macroglobulin
1371057_at	0	2.12	AW520967	Gabra5	gamma-aminobutyric acid (GABA-A) receptor, subunit alpha 5
1390525_a_at	0	2.11	BI284420	Stra6	stimulated by retinoic acid gene 6 homolog (mouse)
1387868_at	0	2.21	BF289368	Lbp	lipopolysaccharide binding protein
1393708_at	0.07	2.07	BE115766	Bhlhb5_predicted	basic helix-loop-helix domain containing, class B5 (predicted)
1382692_at	0.07	2.1	AI045955	RGD1565140_predicted	similar to Clecsf12 protein (predicted)
1388485_at	0.07	2.14	BG380414	Cxcl14	chemokine (C-X-C motif) ligand 14
1370234_at	0.06	2.05	AA893484	Fn1	fibronectin 1
1391435_at	0.06	2.12	BI278687	Pltp_predicted	phospholipid transfer protein (predicted)
1371447_at	0.06	2.01	BG378630	Plac8_predicted	placenta-specific 8 (predicted)
1397889_at	0.06	2	BF402043	---	Transcribed locus
1369947_at	0.06	2.01	NM_031560	Ctsk	cathepsin K
1388142_at	0.06	1.99	AA850991	Cspg2	chondroitin sulfate proteoglycan 2
1373911_at	0.05	2.05	BM389026	Postn_predicted	periostin, osteoblast specific factor (predicted)
1391812_at	0.05	1.99	AI145876	RGD1309172_predicted	Similar to RIKEN cDNA E330026B02 (predicted)
1391106_at	0.05	1.97	BM385061	---	Transcribed locus
1393508_at	0.05	1.98	AI043805	---	Transcribed locus
1382205_at	0.1	1.93	AW527509	---	Transcribed locus
1390866_at	0.1	1.97	AI168981	---	Transcribed locus
1385475_a_at	0.09	1.94	AI030451	Stra6	stimulated by retinoic acid gene 6 homolog (mouse)
1376734_at	0.09	2.01	BI279030	---	Transcribed locus
1387893_at	0.09	1.91	D88250	C1s /// RGD1561715_predicted	complement component 1, s subcomponent
1368459_at	0.09	1.95	NM_024375	Gdf10	growth differentiation factor 10
1394109_at	0.09	2.02	BF558056	Thbs1	Thrombospondin 1
1381504_at	0.12	1.91	AI639412	LOC306805	similar to asporin precursor
1374273_at	0.12	1.88	BG665433	Cxadr	Coxsackie virus and adenovirus receptor
1373628_at	0.12	1.88	AA818342	---	Transcribed locus
1379344_at	0.12	1.88	AI176057	Cybb	Cytochrome b-245, beta polypeptide
1374529_at	0.12	1.89	AI406660	Thbs1	Thrombospondin 1
1368303_at	0.11	1.86	NM_031678	Per2	period homolog 2 (Drosophila)
1368202_a_at	0.17	1.86	NM_024159	Dab2	disabled homolog 2 (Drosophila)

Table 7-3 continued.

1383786_at	0.16	1.84	AW915417	---	Transcribed locus
1389006_at	0.16	1.85	AI170394	---	Transcribed locus, moderately similar to NP_035543.1 sex-limited protein [Mus musculus]
1383210_at	0.21	1.84	BF554576	---	Transcribed locus
1372013_at	0.21	1.86	BG380285	Ifitm1_predicted	interferon induced transmembrane protein 1 (predicted)
1388557_at	0.2	1.83	BF284922	C7 /// Tubb2c	complement component 7 /// tubulin, beta 2c
1398387_at	0.2	1.8	AI009530	MGC72614	Unknown (protein for MGC:72614)
1387348_at	0.21	1.88	BE113270	Igfbp5	insulin-like growth factor binding protein 5
1372254_at	0.23	1.8	AW915763	Serping1	serine (or cysteine) peptidase inhibitor, clade G, member 1
1382108_at	0.22	1.8	AA900536	---	Transcribed locus
1390798_at	0.22	1.81	BF288130	Ptprc	protein tyrosine phosphatase, receptor type, C
1380318_at	0.22	1.81	BF401102	---	Transcribed locus, strongly similar to XP_579933.1 PREDICTED: hypothetical protein XP_579933 [Rattus norvegicus]
1368422_at	0.24	1.82	NM_017149	Meox2	mesenchyme homeobox 2
1370282_at	0.24	1.82	U44948	Csrp2	cysteine and glycine-rich protein 2
1388939_at	0.25	1.79	AA800298	Col15a1	procollagen, type XV
1380726_at	0.25	1.8	BI290633	LOC306805	Similar to asporin precursor
1371245_a_at	0.24	1.91	BI287300	LOC689064	similar to Hemoglobin beta-2 subunit (Hemoglobin beta-2 chain) (Beta-2-globin)
1371102_x_at	0.28	1.9	X05080	MGC72973	beta-glo
1382398_at	0.28	1.77	BF291169	RGD1565710_predicted	similar to MGC68837 protein (predicted)
1381798_at	0.29	1.77	BE114958	LMO7	LIM domain only protein 7
1368223_at	0.31	1.75	NM_024400	Adamts1	a disintegrin-like and metallopeptidse (reprolysin type) with thrombospondin type 1 motif, 1
1369182_at	0.31	1.76	NM_013057	F3	coagulation factor III
1371079_at	0.32	1.79	X73371	Fcgr2b	Fc receptor, IgG, low affinity IIb
1379331_at	0.31	1.78	AA965084	Tnn_predicted	tenascin N (predicted)
1388138_at	0.31	1.8	X89963	Thbs4	thrombospondin 4
1382305_at	0.32	1.76	AI236814	Zfp364_predicted	Zinc finger protein 364 (predicted)
1393351_at	0.31	1.74	BE109501	---	Transcribed locus
1373923_at	0.35	1.73	BF283756	---	Transcribed locus
1387874_at	0.34	1.84	AI230048	Dbp	D site albumin promoter binding protein
1385031_at	0.35	1.73	AI144913	---	Transcribed locus
1391412_at	0.35	1.84	AA996841	Xrn2_predicted	5'-3' exoribonuclease 2 (predicted)
1379766_at	0.34	1.74	AI500952	Sla	Src-like adaptor
1375661_at	0.34	1.74	BE104180	---	Transcribed locus
1368883_at	0.33	1.83	NM_030868	Nov	nephroblastoma overexpressed gene
1393672_at	0.33	1.72	BE117954	Hmcn1_predicted	hemicentin 1 (predicted)
1374726_at	0.35	1.74	AI411941	Fndc1	fibronectin type III domain containing 1
1368419_at	0.36	1.73	AF202115	Cp	ceruloplasmin
1378140_at	0.35	1.74	BI296317	Arl11	ADP-ribosylation factor-like 11
1382431_at	0.36	1.72	AI103530	---	Transcribed locus, strongly similar to XP_520163.1 PREDICTED: similar to ATP-binding cassette transporter 1 [Pan troglodytes]
1372818_at	0.37	1.72	BI284441	Colec12	collectin sub-family member 12
1383946_at	0.37	1.75	AI137640	Cldn1	claudin 1
1390715_at	0.38	1.71	BF396448	Igfbpl1_predicted	insulin-like growth factor binding protein-like 1 (predicted)
1373175_at	0.38	1.72	BI285951	RGD1308734	similar to RIKEN cDNA 1100001H23
1385053_at	0.37	1.73	BE108648	---	Transcribed locus
1370830_at	0.37	1.79	M37394	Egfr	epidermal growth factor receptor
1378057_at	0.38	1.69	BE103354	Flrt3_predicted	fibronectin leucine rich transmembrane protein 3 (predicted)
1367942_at	0.38	1.71	NM_019144	Acp5	acid phosphatase 5, tartrate resistant
1370072_at	0.44	1.69	NM_012608	Mme	membrane metallo endopeptidase
1389754_at	0.45	1.73	AI555295	---	Transcribed locus, moderately similar to XP_529632.1 PREDICTED: hypothetical protein XP_529632 [Pan troglodytes]
1390835_at	0.46	1.76	AI013568	RGD1311123	similar to 1300013J15Rik protein
1375951_at	0.48	1.7	AA818521	Thbd	thrombomodulin
1388459_at	0.48	1.68	AI101782	Col18a1	procollagen, type XVIII, alpha 1
1393891_at	0.49	1.7	BE128699	Col8a1_predicted	procollagen, type VIII, alpha 1 (predicted)
1382153_at	0.5	1.69	AI171821	Clecsf6	C-type (calcium dependent, carbohydrate recognition domain) lectin, superfamily member 6
1368172_a_at	0.5	1.69	BI304009	Lox	lysyl oxidase
1368420_at	0.5	1.69	NM_012532	Cp	ceruloplasmin

Table 7-3 continued.

1398258_at	0.49	1.69	NM_012777	Apod	apolipoprotein D
1392863_at	0.49	1.66	AA817953	Flrt3_predicted	fibronectin leucine rich transmembrane protein 3 (predicted)
1374730_at	0.5	1.7	AI102519	Txnrd3_predicted	Thioredoxin reductase 3 (predicted)
1383391_a_at	0.5	1.71	AI716125	C2	complement component 2
1376799_a_at	0.51	1.68	AA925924	Crlf1_predicted	cytokine receptor-like factor 1 (predicted)
1368395_at	0.53	1.66	NM_012774	Gpc3	glypican 3
1370895_at	0.53	1.67	AI179399	Col5a2	procollagen, type V, alpha 2
1377340_at	0.53	1.66	AI179507	Tfpi2	tissue factor pathway inhibitor 2
1387029_at	0.55	1.67	NM_130409	Cfh	complement component factor H
1375378_at	0.55	1.66	BE108882	LOC499022 /// LOC684079	similar to quaking homolog, KH domain RNA binding isoform HQK-6 /// similar to quaking homolog, KH domain RNA binding isoform HQK-5
1394908_at	0.58	1.65	AW529671	Adcyap1	Adenylate cyclase activating polypeptide 1
1379404_at	0.58	1.66	AI598327	---	Transcribed locus
1395372_at	0.57	1.67	BG668993	Itgb8_predicted	Integrin beta 8 (predicted)
1392557_at	0.57	1.66	BF389151	Bicc1_predicted	Bicaudal C homolog 1 (Drosophila) (predicted)
1393064_at	0.58	1.68	AI709766	RGD1564108_predicted	Similar to hedgehog-interacting protein (predicted)
1387005_at	0.59	1.64	NM_017320	Ctss	cathepsin S
1385397_at	0.6	1.65	AA859085	LOC499991	Ab1-219
1370432_at	0.6	1.64	M72711	Pou3f1	POU domain, class 3, transcription factor 1
1379995_at	0.63	1.64	BE113173	Tubb2b	Tubulin, beta 2b
1367553_x_at	0.65	1.77	NM_033234	Hbb	hemoglobin beta chain complex
1368418_a_at	0.65	1.63	AF202115	Cp	ceruloplasmin
1381145_at	0.66	1.64	BE112469	---	Transcribed locus
1388742_at	0.66	1.63	AA945877	---	---
1373062_at	0.67	1.63	BM388650	---	Transcribed locus
1383291_at	0.66	1.64	BF282631	C7 /// Tubb2c	complement component 7 /// tubulin, beta 2c
1370959_at	0.66	1.64	BI275716	Col3a1	procollagen, type III, alpha 1
1368990_at	0.68	1.62	NM_012940	Cyp1b1	cytochrome P450, family 1, subfamily b, polypeptide 1
1372299_at	0.67	1.63	AI013919	Cdkn1c	cyclin-dependent kinase inhibitor 1C (P57)
1368171_at	0.67	1.64	NM_017061	Lox	lysyl oxidase
1389020_at	0.7	1.62	BM389149	LOC686539	similar to immunoglobulin superfamily containing leucine-rich repeat
1371527_at	0.71	1.61	BI275741	Emp1	epithelial membrane protein 1
1370301_at	0.72	1.62	U65656	Mmp2	matrix metallopeptidase 2
1385229_at	0.72	1.64	AW524146	Pcdh20_predicted	protocadherin 20 (predicted)
1375043_at	0.71	1.63	BF415939	Fos	FBJ murine osteosarcoma viral oncogene homolog
1380692_at	0.72	1.61	BM387127	LOC683869	similar to Retinoblastoma-like protein 1 (107 kDa retinoblastoma-associated protein) (PRB1) (P107)
1376368_at	0.75	1.65	BE095878	Cuedc2_predicted	CUE domain containing 2 (predicted)
1372273_at	0.75	1.61	AA944212	Gypc	glycophorin C (Gerbich blood group)
1371450_at	0.78	1.6	BE117330	---	Transcribed locus
1387767_a_at	0.77	1.65	AF305418	Col2a1	procollagen, type II, alpha 1
1394039_at	0.77	1.62	BM382886	Klf5	Kruppel-like factor 5
1369422_at	0.76	1.61	NM_138850	Fap	fibroblast activation protein
1396872_at	0.77	1.6	AI555260	---	---
1368270_at	0.77	1.62	NM_012907	Apobec1	apolipoprotein B editing complex 1
1394490_at	0.78	1.63	AI502114	Abca1	ATP-binding cassette, sub-family A (ABC1), member 1
1381262_at	0.77	1.66	BG374101	Pbxip1	Pre-B-cell leukemia transcription factor interacting protein 1
1384035_at	0.77	1.62	AW536030	LOC685277 /// LOC686794	similar to liver-specific bHLH-Zip transcription factor
1370240_x_at	0.81	1.69	AI179404	Hba-a1 /// LOC360504	hemoglobin alpha, adult chain 1
1370810_at	0.85	1.6	L09752	Ccnd2	cyclin D2
1367749_at	0.84	1.6	NM_031050	Lum	lumican
1378745_at	0.87	1.6	BG374483	Tmem14a_predicted	Transmembrane protein 14A (predicted)
1387566_at	0.87	1.59	NM_133551	Pla2g4a	phospholipase A2, group IVA (cytosolic, calcium-dependent)
1371349_at	0.92	1.59	AI598402	Col6a1_predicted	procollagen, type VI, alpha 1 (predicted)
1368394_at	0.92	1.63	AF140346	Sfrp4	secreted frizzled-related protein 4
1367902_at	0.98	1.59	NM_022396	Gng11	guanine nucleotide binding protein (G protein), gamma 11
1389966_at	0.97	1.58	AI176126	Col6a3_predicted	procollagen, type VI, alpha 3 (predicted)
1381070_at	0.96	1.59	AI233106	Synpr	Synaptoporin /// Transcribed locus, strongly similar to NP_082328.2 synaptoporin

Table 7-3 continued.

1371913_at	0.98	1.57	BG379319	Tgfbi	transforming growth factor, beta induced
1379696_at	0.98	1.59	BI291833	---	Transcribed locus, moderately similar to XP_576460.1 PREDICTED: similar to hypothetical protein PB402898.00.0 [Rattus norvegicus]
1376905_at	0.97	1.58	BI304147	---	Transcribed locus
1392946_at	0.97	1.57	AI029194	---	Transcribed locus
1389553_at	0.96	1.58	BF393825	Dcir3	dendritic cell inhibitory receptor 3
1378389_at	0.98	1.58	BM385157	---	Transcribed locus, strongly similar to XP_225713.3 PREDICTED: similar to nuclear factor of activated T-cells, cytoplasmic, calcineurin-dependent 1 [Rattus norvegicus]
1374531_at	0.99	1.58	AA926305	---	Transcribed locus

Table 7-4: Genes downregulated (<1% FDR) in the DRG at 2 weeks after dorsal root crush.

AFFY. ID.	% FDR	MEAN FC	ACC. NO.	GENE SYMBOL	GENE TITLE
1387133_at	0	-2.44	NM_053988	Calb2	calbindin 2
1394297_at	0	-2.31	BG670107	Hoxd1_predicted	homeo box D1 (predicted)
1390881_at	0	-2.25	AI172339	Abra	actin-binding Rho activating protein
1370900_at	0.25	-9.32	BM391169	Myh4	myosin, heavy polypeptide 4, skeletal muscle
1367962_at	0.4	-7.31	NM_133424	Actn3	actinin alpha 3
1384269_at	0.5	-1.77	BF386887	---	Transcribed locus
1377163_at	0.57	-1.74	BM385741	Inhbb	inhibin beta-B
1372195_at	0.5	-6.72	BG663128	Tnnc2	troponin C type 2 (fast)
1370033_at	0.44	-5.55	NM_020104	Mlc3	fast myosin alkali light chain
1391575_at	0.4	-1.67	BG380566	---	---
1380306_at	0.36	-1.96	AW435415	---	Transcribed locus
1367626_at	0.42	-5.3	NM_012530	Ckm	creatine kinase, muscle
1391305_at	0.46	-1.62	AI576233	---	---
1387787_at	0.43	-5.11	NM_012605	Myl2	myosin, light polypeptide 2
1368585_at	0.53	-1.66	NM_017110	Cart	cocaine and amphetamine regulated transcript
1395714_at	0.5	-1.53	AT005664	---	---
1388349_at	0.71	-1.75	AA799557	---	---
1367762_at	0.67	-1.58	NM_012659	Sst	somatostatin
1371247_at	0.68	-4.33	BF521859	Ap2a1_predicted /// Ptov1 /// Med25_predicted	Adaptor protein complex AP-2, alpha 1 subunit (predicted) /// Prostate tumor over expressed gene 1 /// Mediator of RNA polymerase II transcription, subunit 25 homolog (yeast) (predicted)
1370198_at	0.65	-2.86	AJ243304	Trdn	triadin
1386907_at	0.67	-2.96	NM_012949	Cpd	Carboxypeptidase D
1368108_at	0.64	-4.05	NM_058213	Atp2a1	ATPase, Ca++ transporting, cardiac muscle, fast twitch 1
1387235_at	0.61	-1.51	NM_021655	Chga	chromogranin A
1378252_at	0.71	-1.62	AI029745	Chodl_predicted	chondrolectin (predicted)
1390355_at	0.68	-2.14	AI575442	Ryr1	ryanodine receptor 1, skeletal muscle
1391153_at	0.73	-1.52	BE101678	---	Transcribed locus
1368554_at	0.7	-1.56	NM_013161	Pnlip	pancreatic lipase
1374677_at	0.97	-2.91	AI577508	LOC684425	similar to Adenylosuccinate synthetase isozyme 1
1376227_at	0.94	-2.08	AI716887	RGD1561064_predicted	similar to myozenin 1 (predicted)
1374934_at	0.91	-1.54	BF405151	Gpr39	G protein-coupled receptor 39
1372296_at	0.88	-1.59	AA800892	RGD1563599_predicted	similar to putative SH3BGR protein (predicted)
1395327_at	0.91	-1.91	AW522341	---	Transcribed locus, weakly similar to XP_580018.1 PREDICTED: hypothetical protein XP_580018 [Rattus norvegicus]
1367896_at	0.89	-3.45	AB030829	Ca3	carbonic anhydrase 3
1370550_at	0.89	-1.48	U31554	Lsamp	limbic system-associated membrane protein

Table 7-5: Genes upregulated (<1% FDR) in the DRG at 6 weeks after dorsal root crush.

AFFY. ID	% FDR	MEAN FC	ACC. NO.	GENE SYMBOL	GENE TITLE
1387902_a_at	0	2.67	L22655	LOC500180 /// LOC500183	similar to IG KAPPA CHAIN V-V REGION K2 PRECURSOR /// similar to IG KAPPA CHAIN V-V REGION K2 PRECURSOR /// similar to NGF-binding Ig light chain /// similar to NGF-binding Ig light chain
1371447_at	0	1.98	BG378630	Plac8_predicted	placenta-specific 8 (predicted)
1368187_at	0	2.11	NM_133298	Gpnmb	glycoprotein (transmembrane) nmb
1371245_a_at	0	1.94	BI287300	LOC689064	similar to Hemoglobin beta-2 subunit (Hemoglobin beta-2 chain) (Beta-2-globin) (Hemoglobin beta chain, minor-form)
1390798_at	0	1.87	BF288130	Ptprc	protein tyrosine phosphatase, receptor type, C
1373386_at	0	2.05	AI179953	Gjb2	gap junction membrane channel protein beta 2
1367553_x_at	0	1.81	NM_033234	Hbb	hemoglobin beta chain complex
1371102_x_at	0	1.8	X05080	MGC72973	beta-glo
1387125_at	0	2.29	NM_053587	S100a9	S100 calcium binding protein A9 (calgranulin B)
1388602_at	0	1.87	AI237358	Cfd	complement factor D (adipsin)
1369705_at	0	2.03	AI169634	Xtrp3	X transporter protein 3
1370967_at	0.08	1.71	BG374683	Cldn10_predicted	Claudin 10 (predicted)
1382083_at	0.15	1.82	BF287593	Coch_predicted	coagulation factor C homolog (Limulus polyphemus) (predicted)
1391446_at	0.29	1.68	AA817742	Ms4a1_predicted	membrane-spanning 4-domains, subfamily A, member 1 (predicted)
1374334_at	0.27	1.87	AI412189	Igha_mapped	immunoglobulin heavy chain (alpha polypeptide) (mapped)
1382305_at	0.25	1.65	AI236814	Zfp364_predicted	Zinc finger protein 364 (predicted)
1368422_at	0.24	1.7	NM_017149	Meox2	mesenchyme homeobox 2
1395126_at	0.28	1.71	AI011393	Msr2_predicted	macrophage scavenger receptor 2 (predicted)
1367985_at	0.26	1.65	NM_013197	Alas2	aminolevulinic acid synthase 2
1397999_at	0.5	1.61	BF386502	Irs2	Insulin receptor substrate 2
1395209_at	0.52	1.6	BM387740	Pank2_predicted	Pantothenate kinase 2 (Hallervorden-Spatz syndrome) (predicted)
1385974_at	0.5	1.92	BM384723	Pard6g_predicted	par-6 partitioning defective 6 homolog gamma (C. elegans) (predicted)
1369182_at	0.52	1.69	NM_013057	F3	coagulation factor III
1368494_at	0.58	2.06	NM_053822	S100a8	S100 calcium binding protein A8 (calgranulin A)
1376750_at	0.72	1.6	AA963477	---	Transcribed locus
1370240_x_at	0.73	1.63	AI179404	Hba-a1 /// LOC360504	hemoglobin alpha, adult chain 1
1375519_at	0.7	1.58	AI237401	LOC287167	globin, alpha
1381997_at	0.71	1.64	BM386227	Adipoq	adiponectin, C1Q and collagen domain containing
1394283_at	0.72	1.57	AW144132	Luc7l2_predicted	LUC7-like 2 (S. cerevisiae) (predicted)
1372264_at	0.7	1.69	BI277460	Pck1	phosphoenolpyruvate carboxykinase 1
1370892_at	0.68	1.62	BI285347	C4a /// C4-2	complement component 4a /// complement component 4, gene 2
1375917_at	0.66	1.61	BF282961	Gp49b /// LOC499078	glycoprotein 49b /// similar to GP49B1
1374122_at	0.73	1.57	BM386808	Myo5c_predicted	myosin VC (predicted)
1379766_at	0.71	1.64	AI500952	Sla	Src-like adaptor
1381798_at	0.77	1.56	BE114958	LMO7	LIM domain only protein 7
1395716_at	0.75	1.58	AW919386	---	---
1370239_at	0.76	1.59	AI179404	Hba-a1 /// LOC360504	hemoglobin alpha, adult chain 1 /// hemoglobin alpha 2 chain
1390777_at	0.74	1.58	AI710051	Sc5d	sterol-C5-desaturase (fungal ERG3, delta-5-desaturase) homolog (S. cerevisae)
1385248_a_at	0.82	1.68	AA997590	Ogn_predicted	osteoglycin (predicted)
1380050_at	0.8	1.58	AA819428	---	Transcribed locus
1388608_x_at	0.83	1.54	AI577319	Hba-a1 /// LOC360504	hemoglobin alpha, adult chain 1
1370607_a_at	0.81	1.54	U02323	Nrg1	neuregulin 1
1370428_x_at	0.84	1.5	AJ249701	RT1-Aw2 /// RT1-A2 /// RT1-A3	RT1 class Ib, locus Aw2 /// RT1 class Ia, locus A2 /// RT1 class I, A3
1367847_at	0.95	1.62	NM_053611	Nupr1	nuclear protein 1

Table 7-6: Genes downregulated (1% FDR) in the DRG at 6 weeks after a dorsal root crush.

AFFY. ID.	% FDR	MEAN FC	ACC. NO.	GENE SYMBOL	GENE TITLE
1387133_at	0	-1.86	NM_053988	Calb2	calbindin 2
1367962_at	0	-9.27	NM_133424	Actn3	actinin alpha 3
1387787_at	0	-8.39	NM_012605	Myl2	myosin, light polypeptide 2
1370033_at	0	-9.08	NM_020104	Mlc3	fast myosin alkali light chain
1384269_at	0	-1.72	BF386887	---	Transcribed locus
1370900_at	0	-14.12	BM391169	Myh4	myosin, heavy polypeptide 4, skeletal muscle
1377106_at	0	-5.94	AW533050	---	Transcribed locus
1372195_at	0	-8.73	BG663128	Tnnc2	troponin C type 2 (fast)
1378252_at	0	-1.66	AI029745	Chodl_predicted	chondrolectin (predicted)
1370971_at	0	-6.99	BI277545	Myh1 /// LOC691644	myosin, heavy polypeptide 1, skeletal muscle, adult
1388604_at	0	-3.1	BI276959	LOC679341 /// LOC686019	similar to Calsequestrin-1 precursor (Calsequestrin, skeletal muscle isoform)
1369928_at	0.08	-4.79	NM_019212	Acta1	actin, alpha 1, skeletal muscle
1367626_at	0.08	-6.48	NM_012530	Ckm	creatine kinase, muscle
1387414_at	0.07	-1.58	NM_024141	Duox2	dual oxidase 2
1390881_at	0.4	-1.66	AI172339	Abra	actin-binding Rho activating protein
1370198_at	0.38	-3.15	AJ243304	Trdn	triadin
1390355_at	0.41	-2.21	AI575442	Ryr1	ryanodine receptor 1, skeletal muscle
1368554_at	0.39	-1.58	NM_013161	Pnlip	pancreatic lipase
1395327_at	0.37	-3.09	AW522341	---	Transcribed locus, weakly similar to XP_580018.1 PREDICTED: hypothetical protein XP_580018 [Rattus norvegicus]
1371247_at	0.45	-5.61	BF521859	Ap2a1_predicted /// Ptov1 /// Med25_predicted	Adaptor protein complex AP-2, alpha 1 subunit (predicted) /// Prostate tumor over expressed gene 1 /// Mediator of RNA polymerase II transcription, subunit 25 homolog (yeast) (predicted)
1386907_at	0.52	-3.23	NM_012949	Cpd	Carboxypeptidase D
1374677_at	0.59	-3.22	AI577508	LOC684425	similar to Adenylosuccinate synthetase isozyme 1 (Adenylosuccinate synthetase, muscle isozyme) (IMP--aspartate ligase 1) (AdSS 1) (AMPSase 1)
1395406_at	0.7	-1.54	BF552212	Sbno1	Sno, strawberry notch homolog 1 (Drosophila)
1372296_at	0.67	-1.58	AA800892	RGD1563599_predicted	similar to putative SH3BGR protein (predicted)
1394297_at	0.88	-1.46	BG670107	Hoxd1_predicted	homeo box D1 (predicted)
1368788_at	0.85	-1.6	NM_019164	Chad	chondroadherin
1367964_at	0.85	-3.21	NM_017185	Tnni2	troponin I type 2 (skeletal, fast)
1384737_at	0.86	-2.11	BF555973	Trdn	Triadin
1368108_at	0.9	-4.15	NM_058213	Atp2a1	ATPase, Ca++ transporting, cardiac muscle, fast twitch 1
1371241_x_at	0.87	-3.57	AF370889	Tpm1	Tropomyosin 1, alpha

Table 7-7: Genes upregulated (<1% FDR) in the DRG at 6 weeks after spinal nerve crush.

AFFY. ID	% FDR	MEAN FC	ACC. NO.	GENE SYMBOL	GENE TITLE
1387125_at	0	3.26	NM_053587	S100a9	S100 calcium binding protein A9 (calgranulin B)
1371245_a_at	0	2.88	BI287300	LOC689064	similar to Hemoglobin beta-2 subunit
1367553_x_at	0	2.58	NM_033234	Hbb	hemoglobin beta chain complex
1370913_at	0	2.57	AI409634	Best5	Best5 protein
1368494_at	0	2.85	NM_053822	S100a8	S100 calcium binding protein A8 (calgranulin A)
1371102_x_at	0	2.51	X05080	MGC72973	beta-glo
1382031_at	0.14	2.38	AA859079	---	Transcribed locus
1370240_x_at	0.12	2.32	AI179404	Hba-a1 /// LOC360504	hemoglobin alpha, adult chain 1 /// hemoglobin alpha 2 chain
1367985_at	0.11	2.34	NM_013197	Alas2	aminolevulinic acid synthase 2
1368021_at	0.1	2.23	NM_130780	Adh1	alcohol dehydrogenase 1 (class I)
1370239_at	0.09	2.28	AI179404	Hba-a1 /// LOC360504	hemoglobin alpha, adult chain 1 /// hemoglobin alpha 2 chain
1375519_at	0.08	2.26	AI237401	LOC287167	globin, alpha
1371447_at	0.08	2.1	BG378630	Plac8_predicted	placenta-specific 8 (predicted)
1388142_at	0.14	2.05	AA850991	Cspg2	chondroitin sulfate proteoglycan 2
1385248_a_at	0.13	2.38	AA997590	Ogn_predicted	osteoglycin (predicted)
1370791_at	0.12	2.46	U16683	Hgfac	Hepatocyte growth factor activator
1385229_at	0.18	2.42	AW524146	Pcdh20_predicted	protocadherin 20 (predicted)
1388608_x_at	0.17	2.07	AI577319	Hba-a1 /// LOC360504	hemoglobin alpha, adult chain 1 /// hemoglobin alpha 2 chain
1387943_at	0.16	2.19	U16686	Defa	defensin, alpha 5, Paneth cell-specific
1374334_at	0.2	2.21	AI412189	Igha_mapped	immunoglobulin heavy chain (alpha polypeptide) (mapped)
1387902_a_at	0.24	2.08	L22655	LOC500180 /// LOC500183	similar to IG KAPPA CHAIN V-V REGION K2 PRECURSOR /// similar to NGF-binding Ig light chain
1369182_at	0.23	1.85	NM_013057	F3	coagulation factor III
1373628_at	0.3	1.85	AA818342	---	Transcribed locus
1370234_at	0.29	1.79	AA893484	Fn1	fibronectin 1 /// fibronectin 1
1370428_x_at	0.28	2.03	AJ249701	RT1-Aw2 /// RT1-A2 /// RT1-A3	RT1 class Ib, locus Aw2 /// RT1 class Ia, locus A2 /// RT1 class I, A3
1387134_at	0.31	1.86	NM_053687	Slfn3	schlafen 3
1375917_at	0.33	1.73	BF282961	Gp49b /// LOC499078	glycoprotein 49b /// similar to GP49B1
1393210_at	0.36	1.7	AI070116	---	---
1389486_at	0.34	1.8	BE108354	---	Transcribed locus
1388557_at	0.4	1.69	BF284922	C7 /// Tubb2c	complement component 7 /// tubulin, beta 2c
1369202_at	0.39	1.78	NM_017028	Mx2	myxovirus (influenza virus) resistance 2
1393508_at	0.38	1.69	AI043805	---	Transcribed locus
1386641_at	0.36	1.7	BF546770	---	Transcribed locus
1392557_at	0.35	1.69	BF389151	Bicc1_predicted	Bicaudal C homolog 1 (Drosophila) (predicted)
1381145_at	0.34	1.68	BE112469	---	Transcribed locus
1387874_at	0.33	1.78	AI230048	Dbp	D site albumin promoter binding protein
1368459_at	0.32	1.81	NM_024375	Gdf10	growth differentiation factor 10
1388602_at	0.34	1.71	AI237358	Cfd	complement factor D (adipsin)
1381859_at	0.33	1.67	BE097018	LOC684063 /// LOC689997	similar to F33H2.2
1382153_at	0.4	1.68	AI171821	Clecsf6	C-type (calcium dependent, carbohydrate recognition domain) lectin, superfamily member 6
1384707_at	0.39	1.68	AI600020	---	Transcribed locus
1392842_at	0.38	1.64	AI072951	---	Transcribed locus, strongly similar to XP_220775.2 PREDICTED: similar to schlafen 5 [Rattus norvegicus]
1368422_at	0.4	1.64	NM_017149	Meox2	mesenchyme homeobox 2
1388138_at	0.39	1.63	X89963	Thbs4	thrombospondin 4
1368304_at	0.4	1.67	NM_053433	Fmo3	flavin containing monooxygenase 3
1387985_a_at	0.39	1.64	AB039825	Obp3	alpha-2u globulin PGCL4
1391428_at	0.38	1.68	AI639162	---	Transcribed locus
1381504_at	0.38	1.65	AI639412	LOC306805	similar to asporin precursor
1390450_a_at	0.39	1.63	AA945955	Ogn_predicted	osteoglycin (predicted)
1387893_at	0.42	1.63	D88250	C1s /// RGD1561715_predicted	complement component 1, s subcomponent
1393064_at	0.43	1.69	AI709766	RGD1564108_predicted	Similar to hedgehog-interacting protein (predicted)
1382587_at	0.46	1.62	AA901257	RGD1307084	Similar to RIKEN cDNA 1110001A07 gene

Table 7-7 continued.

1368474_at	0.53	1.6	NM_012889	Vcam1	vascular cell adhesion molecule 1
1382108_at	0.52	1.59	AA900536	---	Transcribed locus
1390798_at	0.51	1.6	BF288130	Ptprc	protein tyrosine phosphatase, receptor type, C
1388973_at	0.52	1.81	BM388861	Col9a1	procollagen, type IX, alpha 1
1393603_at	0.6	1.76	AA998531	Camp	cathelicidin antimicrobial peptide
1368303_at	0.64	1.81	NM_031678	Per2	period homolog 2 (Drosophila)
1378745_at	0.64	1.64	BG374483	Tmem14a_predicted	Transmembrane protein 14A (predicted)
1388116_at	0.63	1.61	BI285575	Col1a1	procollagen, type 1, alpha 1
1395209_at	0.64	1.59	BM387740	Pank2_predicted	Pantothenate kinase 2 (Hallervorden-Spatz syndrome) (predicted)
1393252_at	0.65	1.68	AA996804	---	Transcribed locus
1370810_at	0.65	1.56	L09752	Ccnd2	cyclin D2
1387319_at	0.67	1.56	NM_019205	Ccl11	chemokine (C-C motif) ligand 11
1381262_at	0.69	1.59	BG374101	Pbxip1	Pre-B-cell leukemia transcription factor interacting protein 1
1388880_at	0.7	1.62	BI278962	---	Transcribed locus
1394940_at	0.72	1.56	BI294811	RGD1311381_predicted	similar to hypothetical protein FLJ20037 (predicted)
1367847_at	0.74	1.6	NM_053611	Nupr1	nuclear protein 1
1368187_at	0.72	1.78	NM_133298	Gpnmb	glycoprotein (transmembrane) nmb
1387756_s_at	0.76	1.65	NM_133294	Hemgn	hemogen
1383708_at	0.82	1.56	BI303923	LOC498564	similar to integrin, beta-like 1
1384063_at	0.85	1.65	AA958001	Cthrc1	collagen triple helix repeat containing 1

Table 7-8: Genes downregulated (<1% FDR) in the DRG at 6 weeks after spinal nerve crush.

AFFY. ID	% FDR	MEAN FC	ACC. NO.	GENE SYMBOL	GENE TITLE
1377106_at	1	-5.79	AW533050	---	Transcribed locus
1370900_at	0.67	-6.6	BM391169	Myh4	myosin, heavy polypeptide 4, skeletal muscle
1372195_at	0.5	-6.89	BG663128	Tnnc2	troponin C type 2 (fast)
1370033_at	0.4	-5.94	NM_020104	Mlc3	fast myosin alkali light chain
1383827_at	0.5	-1.61	AI059119	Tlk1_predicted	tousled-like kinase 1 (predicted)
1387787_at	0.43	-6.72	NM_012605	Myl2	myosin, light polypeptide 2
1370971_at	0.62	-5.37	BI277545	Myh1 /// LOC691644	myosin, heavy polypeptide 1, skeletal muscle, adult /// similar to Myosin heavy chain, skeletal muscle, adult 2 (Myosin heavy chain IIa) (MyHC-IIa)
1370198_at	0.56	-3.27	AJ243304	Trdn	triadin
1384717_at	0.7	-1.55	AA894199	---	---
1367626_at	0.64	-5.08	NM_012530	Ckm	creatine kinase, muscle
1370550_at	0.75	-1.5	U31554	Lsamp	limbic system-associated membrane protein
1388604_at	0.69	-2.82	BI276959	LOC679341 /// LOC686019	similar to Calsequestrin-1 precursor (Calsequestrin, skeletal muscle isoform)
1385491_at	0.64	-1.71	BF403514	RGD1560435_predicted	similar to KIAA1183 protein (predicted)
1371247_at	0.6	-5.01	BF521859	Ap2a1_predicted /// Ptov1 /// Med25_predicted	Adaptor protein complex AP-2, alpha 1 subunit (predicted) /// Prostate tumor over expressed gene 1 /// Mediator of RNA polymerase II transcription, subunit 25 homolog (yeast) (predicted)
1369928_at	0.62	-4.4	NM_019212	Acta1	actin, alpha 1, skeletal muscle
1399073_at	0.65	-1.55	BI274378	Otub1_predicted	OTU domain, ubiquitin aldehyde binding 1 (predicted)
1387133_at	0.61	-1.48	NM_053988	Calb2	calbindin 2
1374677_at	0.68	-3.21	AI577508	LOC684425	similar to Adenylosuccinate synthetase isozyme 1 (AdSS 1) (AMPSase 1)
1368108_at	0.75	-4.04	NM_058213	Atp2a1	ATPase, Ca++ transporting, cardiac muscle, fast twitch 1
1386907_at	0.86	-2.99	NM_012949	Cpd	Carboxypeptidase D
1380695_at	0.82	-1.49	BM386352	---	Transcribed locus, strongly similar to XP_580081.1 PREDICTED: hypothetical protein XP_580081 [Rattus norvegicus]
1393555_at	0.78	-1.68	BG153357	Hspcb	similar to heat shock protein 1, beta
1393615_at	0.75	-1.48	AI059603	RGD1561030_predicted	similar to DEP domain containing 6 (predicted)
1390630_at	0.76	-1.48	BE112446	---	Transcribed locus
1382441_at	0.85	-1.53	AI556402	Arid1b	AT rich interactive domain 1B (Swi1 like)
1390881_at	0.93	-1.6	AI172339	Abra	actin-binding Rho activating protein

Table 7-9: Genes upregulated (<1% FDR) in the DRG at 2 weeks after dorsal column transection.

AFFY. ID	% FDR	MEAN FC	ACC. NO.	GENE SYMBOL	GENE TITLE
1377146_at	0	87.59	AI412212	Vip	vasoactive intestinal polypeptide
1387154_at	0	29.13	NM_012614	Npy	neuropeptide Y
1368238_at	0	13.01	NM_053289	Pap	pancreatitis-associated protein
1369268_at	0	11.13	NM_012912	Atf3	activating transcription factor 3
1398243_at	0	9.65	NM_057144	Vsnl1	Visinin-like 1
1384035_at	0	7.67	AW536030	LOC685277 /// LOC686794	similar to liver-specific bHLH-Zip transcription factor
1387088_at	0	6.14	NM_033237	Gal	galanin
1368266_at	0	5.87	NM_017134	Arg1	arginase 1
1392863_at	0	5.69	AA817953	Flrt3_predicted	fibronectin leucine rich transmembrane protein 3 (predicted)
1393573_at	0	5.23	AI575628	Pde6b_predicted	phosphodiesterase 6B, cGMP, rod receptor, beta polypeptide (predicted)
1381070_at	0	4.99	AI233106	Synpr	Synaptoporin
1371450_at	0	5.03	BE117330	---	Transcribed locus
1383210_at	0	4.95	BF554576	---	Transcribed locus
1375661_at	0	4.76	BE104180	---	Transcribed locus
1371248_at	0	4.8	BI286387	LOC499660	similar to Cornifin A (Small proline-rich protein 1A) (SPR1A) (SPRR1)
1382868_at	0	4.33	BM387083	Sema6a_predicted	sema domain, transmembrane domain (TM), and cytoplasmic domain, (semaphorin) 6A (predicted)
1378057_at	0	4.24	BE103354	Flrt3_predicted	fibronectin leucine rich transmembrane protein 3 (predicted)
1392862_at	0	4.25	AA859389	Sema6a_predicted	Sema domain, transmembrane domain (TM), and cytoplasmic domain, (semaphorin) 6A (predicted)
1378700_at	0	3.85	BF403674	---	Transcribed locus
1376601_at	0	3.85	BF397526	Sema6a_predicted	sema domain, transmembrane domain (TM), and cytoplasmic domain, (semaphorin) 6A (predicted)
1374276_at	0	3.79	BE104102	LOC685277	Similar to liver-specific bHLH-Zip transcription factor
1373513_at	0	3.61	AI012419	---	Transcribed locus
1371057_at	0	3.56	AW520967	Gabra5	gamma-aminobutyric acid (GABA-A) receptor, subunit alpha 5
1368947_at	0	3.52	NM_024127	Gadd45a	growth arrest and DNA-damage-inducible 45 alpha
1388433_at	0	3.34	BI279605	Krt1-19	keratin complex 1, acidic, gene 19
1393477_at	0	3.35	AI548924	---	---
1370883_at	0	3.35	Y00480	RT1-Da	RT1 class II, locus Da
1369649_at	0	3.32	AF400662	Cacna2d1	calcium channel, voltage-dependent, alpha2/delta subunit 1
1368359_a_at	0	3.35	NM_030997	Vgf	VGF nerve growth factor inducible
1384803_at	0	3.42	BI283351	RGD1565626_predicted /// RGD1561089_predicted /// LOC686064 /// LOC686125	RGD1565626 (predicted) /// hypothetical protein LOC686125
1386552_at	0	3.24	BF284027	---	Transcribed locus
1388451_at	0	3.16	AA817802	---	Transcribed locus
1368000_at	0	3.14	NM_016994	C3	complement component 3
1382692_at	0	3.04	AI045955	RGD1565140_predicted	similar to Clecsf12 protein (predicted)
1377334_at	0	3.07	BG378249	RT1-Ba	RT1 class II, locus Ba
1370383_s_at	0	3.04	BI279526	RT1-Db1	RT1 class II, locus Db1
1388944_at	0	2.9	BE109016	---	Transcribed locus
1368421_at	0.05	2.96	NM_019253	Ptpn5	protein tyrosine phosphatase, non-receptor type 5
1382017_at	0.05	2.83	AI012949	Rbp2	retinol binding protein 2, cellular
1368657_at	0.05	2.96	NM_133523	Mmp3	matrix metallopeptidase 3
1368188_at	0.05	2.76	NM_017233	Hpd	4-hydroxyphenylpyruvic acid dioxygenase
1376390_at	0.05	2.76	BF395317	Ms4a11_predicted	membrane-spanning 4-domains, subfamily A, member 11 (predicted
1367679_at	0.05	2.73	NM_013069	Cd74	CD74 antigen (invariant polypeptide of major histocompatibility complex, class II antigen-associated)

Table 7-9 continued.

1397823_at	0.05	2.72	BE117531	Cacna2d1	Calcium channel, voltage-dependent, alpha2/delta subunit 1
1371079_at	0.04	2.75	X73371	Fcgr2b	Fc receptor, IgG, low affinity IIb
1377168_at	0.04	2.74	AI412673	Cpne9	copine family member IX
1370315_a_at	0.04	2.66	AF026530	Stmn4	stathmin-like 4
1389528_s_at	0.04	2.71	BI288619	Jun	Jun oncogene
1370892_at	0.04	2.66	BI285347	C4a /// C4-2	complement component 4a /// complement component 4, gene 2 ///
1383536_at	0.08	2.63	AI712541	Dhfr	Dihydrofolate reductase
1384036_s_at	0.08	2.6	AW536030	---	---
1398390_at	0.08	2.53	AA892854	LOC498335	similar to Small inducible cytokine B13 precursor (CXCL13) (B lymphocyte chemoattractant) (CXC chemokine BLC)
1387908_at	0.13	2.6	AF239157	Rasd1	RAS, dexamethasone-induced 1
1369788_s_at	0.13	2.41	NM_021835	Jun	Jun oncogene
1381190_at	0.13	2.45	AI598833	Prpf8	Pre-mRNA processing factor 8
1370177_at	0.12	2.43	AI548856	PVR	poliovirus receptor
1389696_at	0.12	2.44	BF409820	---	Transcribed locus
1381798_at	0.12	2.4	BE114958	LMO7	LIM domain only protein 7
1387283_at	0.12	2.68	NM_134350	Mx2	myxovirus (influenza virus) resistance 2
1370249_at	0.12	2.34	AI008680	Bzrp	benzodiazepine receptor, peripheral
1387930_at	0.11	2.62	L10229	Reg3a	regenerating islet-derived 3 alpha
1382638_at	0.11	2.3	AI058645	Flrt3_predicted	Fibronectin leucine rich transmembrane protein 3 (predicted)
1388711_at	0.13	2.31	BF282650	Il13ra1	interleukin 13 receptor, alpha 1
1376100_at	0.12	2.35	BI274903	Tubb6	tubulin, beta 6
1382960_at	0.14	2.3	BE108047	---	Transcribed locus
1371913_at	0.14	2.29	BG379319	Tgfbi	transforming growth factor, beta induced
1376750_at	0.13	2.29	AA963477	---	Transcribed locus
1388557_at	0.13	2.25	BF284922	C7 /// Tubb2c	complement component 7 /// tubulin, beta 2c
1379957_at	0.13	2.23	BE107457	Slfn8	schlafen 8 /// schlafen 8
1383805_at	0.14	2.33	BG666454	RGD1561817_predicted	similar to Traf2 and NCK interacting kinase, splice variant 4 (predicted)
1368353_at	0.14	2.23	NM_017009	Gfap	glial fibrillary acidic protein
1377092_at	0.14	2.26	BF389682	---	Transcribed locus
1374404_at	0.14	2.3	BI288619	Jun	Jun oncogene
1397400_at	0.14	2.25	BM391846	---	Transcribed locus, moderately similar to XP_580018.1 PREDICTED: hypothetical protein XP_580018 [Rattus norvegicus]
1373368_at	0.15	2.22	BI279680	LOC684050	similar to procollagen C-endopeptidase enhancer 2
1370822_at	0.16	2.39	AF307302	RT1-Ba	RT1 class II, locus Ba
1387221_at	0.16	2.27	NM_024356	Gch	GTP cyclohydrolase 1
1376799_a_at	0.15	2.19	AA925924	Crlf1_predicted	cytokine receptor-like factor 1 (predicted)
1390687_at	0.15	2.2	AI556803	Plek	pleckstrin
1383946_at	0.16	2.24	AI137640	Cldn1	claudin 1
1380100_at	0.17	2.16	AW526268	RGD1561817_predicted	similar to Traf2 and NCK interacting kinase, splice variant 4 (predicted)
1372734_at	0.17	2.16	AI408095	Smagp	small cell adhesion glycoprotein
1368419_at	0.17	2.15	AF202115	Cp	ceruloplasmin
1368923_at	0.17	2.14	AB023896	Ecel1	endothelin converting enzyme-like 1
1390282_at	0.16	2.22	BI274639	LOC687052	similar to cytochrome P450, family 2, subfamily s, polypeptide 1
1371033_at	0.17	2.44	AI715202	RT1-Bb	RT1 class II, locus Bb
1382619_at	0.17	2.13	AI072460	---	Transcribed locus
1370428_x_at	0.17	2.83	AJ249701	RT1-Aw2 /// RT1-A2 /// RT1-A3	RT1 class Ib, locus Aw2 /// RT1 class Ia, locus A2 /// RT1 class I, A3
1384013_at	0.17	2.12	BF524215	Chl1	cell adhesion molecule with homology to L1CAM
1388496_at	0.16	2.18	AI103600	Flnc_predicted	filamin C, gamma (actin binding protein 280) (predicted)
1392946_at	0.2	2.1	AI029194	---	Transcribed locus
1370391_at	0.19	2.15	U23407	Crabp2	cellular retinoic acid binding protein 2
1378531_at	0.19	2.09	AI555775	---	Transcribed locus
1376911_at	0.19	2.12	BM386385	---	Transcribed locus
1368224_at	0.19	2.18	NM_031531	Serpina3n	serine (or cysteine) peptidase inhibitor, clade A, member 3N

Table 7-9 continued.

1369904_at	0.2	2.06	NM_012956	Gabrb1	gamma-aminobutyric acid (GABA-A) receptor, subunit beta 1
1387893_at	0.2	2.06	D88250	C1s /// RGD1561715_predicted	complement component 1, s subcomponent
1367930_at	0.22	2.05	NM_017195	Gap43	growth associated protein 43
1376562_at	0.24	2.11	BI291396	RGD1561817_predicted	similar to Traf2 and NCK interacting kinase, splice variant 4 (predicted)
1372359_at	0.24	2.07	BI291423	RGD1310090	similar to 2310043K02Rik protein
1393679_at	0.26	2.04	BE102362	---	Transcribed locus
1387005_at	0.26	2.03	NM_017320	Ctss	cathepsin S
1379766_at	0.27	2.02	AI500952	Sla	Src-like adaptor
1381145_at	0.27	2.02	BE112469	---	Transcribed locus
1390713_at	0.26	2.01	BF410051	---	Transcribed locus
1390798_at	0.28	1.99	BF288130	Ptprc	protein tyrosine phosphatase, receptor type, C
1374280_at	0.28	2.01	AA817812	Cbln2	cerebellin 2 precursor protein
1388547_at	0.34	2.01	BE328951	Cldn4	claudin 4
1372516_at	0.35	1.98	AI317842	Kif22	kinesin family member 22
1388045_a_at	0.35	1.96	D83348	Cdh22	cadherin 22
1371447_at	0.35	1.96	BG378630	Plac8_predicted	placenta-specific 8 (predicted)
1370830_at	0.35	2.1	M37394	Egfr	epidermal growth factor receptor
1389579_at	0.34	1.97	BI284372	---	Transcribed locus
1368412_a_at	0.34	2	D45412	Ptpro	protein tyrosine phosphatase, receptor type, O
1381341_at	0.34	2.01	BE111796	Gabbr1	Gamma-aminobutyric acid (GABA) B receptor 1
1369029_at	0.34	1.96	NM_057194	Plscr1	phospholipid scramblase 1
1383234_at	0.35	1.98	BF405850	---	Transcribed locus
1390525_a_at	0.34	1.94	BI284420	Stra6	stimulated by retinoic acid gene 6 homolog (mouse)
1393508_at	0.4	1.96	AI043805	---	Transcribed locus
1391605_at	0.4	2	BG666431	---	Transcribed locus, strongly similar to XP_342569.2 PREDICTED: similar to protein tyrosine phosphatase, receptor type, T isoform 1 precursor [Rattus norvegicus]
1370913_at	0.39	2	AI409634	Best5	Best5 protein
1388742_at	0.39	1.95	AA945877	---	---
1381331_at	0.39	2.01	AI638953	Cklfsf1	chemokine-like factor super family 1
1383391_a_at	0.4	1.93	AI716125	C2	complement component 2
1390450_a_at	0.4	1.95	AA945955	Ogn_predicted	osteoglycin (predicted)
1372254_at	0.4	1.91	AW915763	Serping1	serine (or cysteine) peptidase inhibitor, clade G, member 1 G,
1368590_at	0.4	1.96	NM_080776	Mmp16	matrix metalloproteinase 16
1382031_at	0.4	2	AA859079	---	Transcribed locus
1388419_at	0.4	1.95	AW915005	Acly	ATP citrate lyase
1389373_at	0.4	1.93	AI029555	Smad1	MAD homolog 1 (Drosophila)
1396451_at	0.41	1.96	BF393275	---	Transcribed locus
1373357_at	0.41	1.91	BI291467	---	Transcribed locus
1392110_at	0.4	2.08	AA818585	---	Transcribed locus
1367847_at	0.45	1.92	NM_053611	Nupr1	nuclear protein 1
1383936_at	0.45	1.9	BM386842	Emilin2_predicted	Elastin microfibril interfacer 2 (predicted)
1394908_at	0.45	1.94	AW529671	Adcyap1	Adenylate cyclase activating polypeptide 1
1394940_at	0.44	1.9	BI294811	RGD1311381_predicted	similar to hypothetical protein FLJ20037 (predicted)
1395126_at	0.44	1.99	AI011393	Msr2_predicted	macrophage scavenger receptor 2 (predicted)
1368892_at	0.44	1.94	NM_016989	Adcyap1	adenylate cyclase activating polypeptide 1
1379995_at	0.45	1.94	BE113173	Tubb2b	Tubulin, beta 2b
1379573_at	0.45	1.88	AA818730	Ctps_predicted	Cytidine 5'-triphosphate synthase (predicted)
1369182_at	0.45	1.91	NM_013057	F3	coagulation factor III
1370382_at	0.45	2.01	BI279526	RT1-Bb	RT1 class II, locus Bb
1369705_at	0.46	1.94	AI169634	Xtrp3	X transporter protein 3
1374273_at	0.47	1.88	BG665433	Cxadr	Coxsackie virus and adenovirus receptor
1375043_at	0.46	1.88	BF415939	Fos	FBJ murine osteosarcoma viral oncogene homolog
1368418_a_at	0.46	1.88	AF202115	Cp	ceruloplasmin
1396208_at	0.46	1.9	BM389807	Ggtla1	gamma-glutamyltransferase-like activity 1

Table 7-9 continued.

1368422_at	0.47	1.9	NM_017149	Meox2	mesenchyme homeobox 2
1381089_at	0.49	1.93	BE114458	---	Transcribed locus
1391630_at	0.5	1.86	BF420033	---	Transcribed locus, strongly similar to XP_236458.3 PREDICTED: similar to T-box transcription factor TBX18 [Rattus norvegicus]
1396263_at	0.51	1.86	BI301147	---	Transcribed locus, strongly similar to XP_234584.3 PREDICTED: similar to RIKEN cDNA 4831426I19 [Rattus norvegicus]
1389006_at	0.5	1.88	AI170394	---	Transcribed locus, moderately similar to NP_035543.1 sex-limited protein [Mus musculus]
1375056_at	0.51	1.87	AA943310	---	---
1371527_at	0.57	1.84	BI275741	Emp1	epithelial membrane protein 1
1393469_at	0.56	1.84	BE102340	---	---
1382153_at	0.6	1.84	AI171821	Clecsf6	C-type (calcium dependent, carbohydrate recognition domain) lectin, superfamily member 6
1367974_at	0.6	1.84	NM_012823	Anxa3	annexin A3
1387134_at	0.63	2.06	NM_053687	Slfn3	schlafen 3
1385475_a_at	0.64	1.83	AI030451	Stra6	stimulated by retinoic acid gene 6 homolog (mouse)
1371245_a_at	0.65	1.87	BI287300	LOC689064	similar to Hemoglobin beta-2 subunit (Hemoglobin beta-2 chain) (Beta-2-globin) (Hemoglobin beta chain, minor-form)
1371988_at	0.65	1.82	AA892549	Man1a_predicted	mannosidase 1, alpha (predicted)
1376652_at	0.71	1.85	BF418957	C1qa	complement component 1, q subcomponent, alpha polypeptide
1379404_at	0.71	1.82	AI598327	---	Transcribed locus
1367849_at	0.72	1.84	NM_013026	Sdc1	syndecan 1
1393638_at	0.71	1.82	AI549199	Ptger4	Prostaglandin E receptor 4 (subtype EP4)
1393210_at	0.72	1.81	AI070116	---	---
1397361_x_at	0.74	1.84	AI407549	---	---
1387113_at	0.74	1.81	NM_053335	Ctbp2	C-terminal binding protein 2
1370075_at	0.74	1.86	NM_130400	Dhfr	dihydrofolate reductase
1381682_at	0.78	1.83	BE106750	---	---
1387007_at	0.8	1.82	NM_012959	Gfra1	glial cell line derived neurotrophic factor family receptor alpha 1
1396835_at	0.81	1.79	BE095505	---	Transcribed locus, strongly similar to XP_579880.1 PREDICTED: hypothetical protein XP_579880 [Rattus norvegicus]
1375270_at	0.81	1.8	BM384026	---	Transcribed locus
1391383_at	0.81	1.84	BF413778	Crtac1	cartilage acidic protein 1
1372042_at	0.81	1.82	BI294844	Cmtm3_predicted	CKLF-like MARVEL transmembrane domain containing 3 (predicted)
1389496_at	0.82	1.8	BI300893	Akap7	A kinase (PRKA) anchor protein 7
1382305_at	0.82	1.8	AI236814	Zfp364_predicted	Zinc finger protein 364 (predicted)
1385248_a_at	0.81	1.79	AA997590	Ogn_predicted	osteoglycin (predicted)
1388674_at	0.84	1.78	AI010427	Cdkn1a	cyclin-dependent kinase inhibitor 1A
1368834_at	0.84	1.78	AA894330	Camk2d	calcium/calmodulin-dependent protein kinase II, delta
1386529_at	0.85	1.85	BF564309	---	Transcribed locus
1388792_at	0.9	1.81	AI599423	Gadd45g	growth arrest and DNA-damage-inducible 45 gamma
1375825_at	0.89	1.86	BM382867	---	---
1368021_at	0.9	1.82	NM_130780	Adh1	alcohol dehydrogenase 1 (class I)
1374171_at	0.9	1.78	AI170507	---	Transcribed locus
1370234_at	0.92	1.77	AA893484	Fn1	fibronectin 1
1375145_at	0.94	1.79	AI548036	RGD1565886_predicted	RGD1565886 (predicted)
1373575_at	0.94	1.76	BE111722	LOC498279	similar to NADH dehydrogenase (ubiquinone) Fe-S protein 2
1374557_at	0.94	1.76	BF394235	LOC362065	CG6210-like
1381755_x_at	0.94	1.76	BI288309	RGD1304563_predicted	similar to RIKEN cDNA 4831426I19 (predicted)
1377161_at	0.94	1.78	BG378317	---	Transcribed locus
1368332_at	0.94	1.77	NM_133624	Gbp2	guanylate nucleotide binding protein 2
1385751_at	0.93	1.77	BF408413	Thbs2	thrombospondin 2
1391660_at	0.93	1.78	AI412900	---	Transcribed locus, moderately similar to XP_576460.1 PREDICTED: similar to hypothetical protein PB402898.00.0

Table 7-9 continued.

1370628_at	0.93	1.88	M34097	Gzmb	granzyme B
1376204_at	0.93	1.76	AW531412	---	Transcribed locus
1373975_at	0.94	1.8	AI232716	LOC368066	similar to indolethylamine N-methyltransferase
1375917_at	0.94	1.75	BF282961	Gp49b /// LOC499078	glycoprotein 49b /// similar to GP49B1
1390937_at	0.94	1.75	AW523875	RGD1309051	similar to chromosome 14 open reading frame 50
1383291_at	0.96	1.77	BF282631	C7 /// Tubb2c	complement component 7 /// tubulin, beta 2c
1368708_a_at	0.97	1.76	NM_012547	Drd2	dopamine receptor 2
1389368_at	0.97	1.77	AW253242	Cnksr3	Cnksr family member 3
1369713_at	0.98	1.77	M99418	Cckbr	cholecystokinin B receptor
1374065_at	0.99	1.74	BG378920	Met	Met proto-oncogene
1373911_at	1	1.91	BM389026	Postn_predicted	periostin, osteoblast specific factor (predicted)

Table 7-10: Genes downregulated (<1% FDR) in the DRG at 2 weeks after dorsal column transection.

AFFY. ID.	% FDR	MEAN FC	ACC. NO.	GENE SYMBOL	GENE TITLE
1387133_at	0	-4.94	NM_053988	Calb2	calbindin 2
1388349_at	0	-5.16	AA799557	---	---
1374787_at	0	-4.04	BI282169	---	Transcribed locus
1377163_at	0	-3.81	BM385741	Inhbb	inhibin beta-B
1376980_at	0	-3.72	BF285539	---	Transcribed locus
1391575_at	0	-3.49	BG380566	---	---
1382914_at	0	-3.36	AA924097	---	Transcribed locus
1370900_at	0	-9.97	BM391169	Myh4	myosin, heavy polypeptide 4, skeletal muscle
1368407_at	0	-3.09	NM_022605	Hpse	heparanase
1374035_at	0	-3.08	BI296482	---	Transcribed locus
1385731_at	0	-3.07	BE113552	---	Transcribed locus
1390530_at	0	-3.14	AI169239	---	Transcribed locus
1387065_at	0	-2.95	NM_080688	Plcd4	phospholipase C, delta 4
1371077_at	0	-2.92	AI575989	Htr3b	5-hydroxytryptamine (serotonin) receptor 3b
1394297_at	0	-3.03	BG670107	Hoxd1_predicted	homeo box D1 (predicted)
1396366_at	0	-3.07	BF409020	---	Transcribed locus
1370214_at	0	-2.83	AI175539	Pvalb	parvalbumin
1391563_at	0	-2.95	AA963184	RGD1565148_predicted	similar to melanoma associated antigen (mutated) 1-like 1 (predicted)
1384269_at	0	-2.93	BF386887	---	Transcribed locus
1377106_at	0	-6.9	AW533050	---	Transcribed locus
1393952_at	0	-2.74	BI278833	RGD1561424_predicted	similar to CTCL tumor antigen se57-1 (predicted)
1396676_at	0	-2.87	BF394718	---	Transcribed locus
1380828_at	0	-2.69	AI145413	Gabra1	gamma-aminobutyric acid A receptor, alpha 1
1371211_a_at	0	-2.61	U02315	Nrg1	neuregulin 1
1382439_at	0	-2.72	AI070686	Itgb6	integrin, beta 6
1387309_a_at	0	-2.64	AI111480	Grik1	glutamate receptor, ionotropic, kainate 1
1393299_at	0	-2.68	BF567794	Dpp10	dipeptidylpeptidase 10
1369001_at	0	-2.6	NM_052805	Chrna3	cholinergic receptor, nicotinic, alpha polypeptide 3
1369144_a_at	0	-2.6	NM_031739	Kcnd3	potassium voltage gated channel, Shal-related family, member 3
1370033_at	0	-8.31	NM_020104	Mlc3	fast myosin alkali light chain
1367962_at	0	-7.24	NM_133424	Actn3	actinin alpha 3
1369428_a_at	0	-2.58	U28430	Htr3a	5-hydroxytryptamine (serotonin) receptor 3a
1381499_at	0	-2.57	BM390226	---	Transcribed locus
1391764_at	0	-2.58	BE119571	---	Transcribed locus
1372195_at	0	-8.75	BG663128	Tnnc2	troponin C type 2 (fast)
1370404_at	0	-2.49	AF440736	LOC266776	cystatin TE-1
1386695_at	0.03	-2.45	BF565756	---	---
1394252_at	0.03	-2.48	BG668764	Spock3_predicted	sparc/osteonectin, cwcv and kazal-like domains proteoglycan 3 (predicted)

Table 7-10 continued.

1398623_at	0.03	-2.46	AI454607	Chrnb4	cholinergic receptor, nicotinic, beta polypeptide 4
1390958_at	0.12	-2.43	AW528339	---	Transcribed locus
1378288_at	0.12	-2.36	BI292167	RGD1311100_predicted	similar to RIKEN cDNA D630035O19 (predicted)
1371049_at	0.12	-2.37	BF413467	Dpysl4	dihydropyrimidinase-like 4
1369137_at	0.12	-2.36	NM_017194	Chrne	cholinergic receptor, nicotinic, epsilon polypeptide
1396276_at	0.11	-2.34	BG662898	---	Transcribed locus
1394097_at	0.11	-2.38	AA849706	---	Transcribed locus
1382123_at	0.11	-2.33	AI574734	---	---
1387787_at	0.11	-7.08	NM_012605	Myl2	myosin, light polypeptide 2
1385491_at	0.1	-2.46	BF403514	RGD1560435_predicted	similar to KIAA1183 protein (predicted)
1368749_at	0.1	-2.35	NM_053954	Kcns1	K+ voltage-gated channel, subfamily S, 1
1386310_at	0.1	-2.38	AI412779	---	Transcribed locus
1381233_at	0.1	-2.29	AW528010	---	Transcribed locus
1371212_at	0.1	-2.41	U02315	Nrg1	neuregulin 1
1388604_at	0.11	-3.41	BI276959	LOC679341 /// LOC686019	similar to Calsequestrin-1 precursor (Calsequestrin, skeletal muscle isoform)
1382924_at	0.11	-2.31	AA850195	Pank1_predicted	pantothenate kinase 1 (predicted)
1370971_at	0.11	-5.96	BI277545	Myh1 /// LOC691644	myosin, heavy polypeptide 1, skeletal muscle, adult /// similar to Myosin heavy chain, skeletal muscle, adult 2
1378470_at	0.11	-2.26	BM384409	Paqr5	progestin and adipoQ receptor family member V
1393933_at	0.11	-2.25	AW144823	Sorl1_predicted	sortilin-related receptor, L(DLR class) A repeats-containing (predicted)
1384393_at	0.1	-2.27	BE120370	---	Transcribed locus
1390362_at	0.1	-2.24	BF394081	---	Transcribed locus
1370439_a_at	0.1	-2.29	M34052	Kcnc2	potassium voltage gated channel, Shaw-related subfamily, member 2
1371247_at	0.11	-5.89	BF521859	Ap2a1_predicted /// Ptov1 /// Med25_predicted	Adaptor protein complex AP-2, alpha 1 subunit (predicted) /// Prostate tumor over expressed gene 1 /// Mediator of RNA polymerase II transcription, subunit 25 homolog (yeast) (predicted)
1378310_at	0.11	-2.24	BG669018	RGD1562710_predicted	similar to neuromedin B precursor - rat (predicted)
1388968_at	0.13	-2.2	BF402642	---	Transcribed locus
1386907_at	0.12	-3.69	NM_012949	Cpd	Carboxypeptidase D
1395333_at	0.12	-2.21	AW533483	LOC679370 /// LOC688790	similar to Myelin P2 protein
1367626_at	0.12	-5.55	NM_012530	Ckm	creatine kinase, muscle
1396040_at	0.13	-2.23	BE108568	Shank1	SH3 and multiple ankyrin repeat domains 1
1386119_at	0.13	-2.3	BE110033	LOC689147	Hypothetical protein LOC689147
1368958_at	0.13	-2.16	NM_017294	Pacsin1	protein kinase C and casein kinase substrate in neurons 1
1395487_at	0.13	-2.19	BF400826	---	Transcribed locus
1368740_at	0.13	-2.2	NM_012721	P2rxl1	purinergic receptor P2X-like 1, orphan receptor
1387058_at	0.12	-2.17	NM_017225	Pctp	phosphatidylcholine transfer protein
1385043_at	0.12	-2.19	AA924649	RGD1565362_predicted	similar to channel-interacting PDZ domain protein isoform 1 (predicted)
1387602_a_at	0.12	-2.17	NM_022189	Htr3b	5-hydroxytryptamine (serotonin) receptor 3b
1392221_at	0.12	-2.18	BE114215	RGD1562371_predicted	Similar to GREB1 protein isoform a (predicted)
1379458_at	0.12	-2.18	AW533900	RGD1566178_predicted	similar to Kelch-like protein 14 (predicted)
1394837_at	0.13	-2.2	BF405797	---	---
1369928_at	0.14	-4.76	NM_019212	Acta1	actin, alpha 1, skeletal muscle
1378876_at	0.14	-2.13	BE114024	---	Transcribed locus
1378111_at	0.14	-2.14	AI576002	---	Transcribed locus
1367762_at	0.14	-2.15	NM_012659	Sst	somatostatin
1368524_at	0.13	-2.16	NM_012856	Kcnc1	potassium voltage gated channel, Shaw-related subfamily, member 1
1371089_at	0.13	-2.13	AA945082	---	Transcribed locus
1374743_at	0.13	-2.16	BE115056	RGD1565362_predicted	similar to channel-interacting PDZ domain protein isoform 1 (predicted)

Table 7-10 continued.

1370198_at	0.14	-3.34	AJ243304	Trdn	triadin
1368751_at	0.15	-2.14	NM_031778	Kcns3	potassium voltage-gated channel, delayed-rectifier, subfamily S, member 3
1396542_at	0.15	-2.14	BF393011	---	Transcribed locus
1369677_at	0.15	-2.21	X55812	---	---
1368853_at	0.16	-2.16	NM_012686	Vsnl1	visinin-like 1
1375518_at	0.16	-4.07	AI104533	Ttn	titin
1376225_at	0.16	-2.11	BF411924	Csen	Calsenilin, presenilin binding protein, EF hand transcription factor
1393626_at	0.16	-2.11	BF562507	Sorl1_predicted	sortilin-related receptor, L(DLR class) A repeats-containing (predicted)
1368561_at	0.17	-2.11	NM_033352	Abcd2	ATP-binding cassette, sub-family D (ALD), member 2
1383582_at	0.18	-2.1	BG377582	Tmem54	transmembrane protein 54
1379894_at	0.18	-2.09	AI501165	RGD1310110_predicted	similar to 3632451O06Rik protein (predicted)
1368108_at	0.21	-4.61	NM_058213	Atp2a1	ATPase, Ca++ transporting, cardiac muscle, fast twitch 1
1374677_at	0.21	-3.33	AI577508	LOC684425	similar to Adenylosuccinate synthetase isozyme 1
1393253_at	0.2	-2.13	BF408799	Zfp365	zinc finger protein 365
1367733_at	0.2	-2.14	NM_019291	Ca2	carbonic anhydrase 2
1375026_at	0.2	-2.07	AI105369	LOC688757	Hypothetical protein LOC688757
1372423_at	0.22	-2.07	BI286396	Perp_predicted	PERP, TP53 apoptosis effector (predicted)
1378136_at	0.23	-2.06	BF403749	---	---
1376944_at	0.22	-2.08	AI407163	Prlr	Prolactin receptor
1375066_at	0.25	-2.05	H33003	RGD1563319_predicted	similar to RIKEN cDNA 6330512M04 gene (predicted)
1380455_at	0.25	-2.04	BM389422	---	Transcribed locus, moderately similar to XP_853274.1 PREDICTED: hypothetical protein XP_848181 [Canis familiaris]
1384866_at	0.25	-2.04	AI070096	Entpd3	ectonucleoside triphosphate diphosphohydrolase 3
1377857_at	0.25	-2.08	BF291163	---	Transcribed locus
1369953_a_at	0.25	-2.05	BI285141	Cd24	CD24 antigen
1392880_at	0.26	-2.04	BG665051	---	---
1370517_at	0.26	-2.03	U18772	Nptx1	neuronal pentraxin 1
1391153_at	0.27	-2.04	BE101678	---	Transcribed locus
1394412_at	0.27	-2.06	AI144648	Tmem16c_predicted	transmembrane protein 16C (predicted)
1381575_at	0.28	-3.1	AI638986	---	Transcribed locus
1368506_at	0.28	-2.01	U27767	Rgs4	regulator of G-protein signaling 4
1384080_at	0.28	-2.06	AA924955	---	Transcribed locus
1385633_at	0.28	-2.03	AA817878	---	Transcribed locus
1368554_at	0.29	-2.03	NM_013161	Pnlip	pancreatic lipase
1394821_at	0.29	-2.04	BF399731	---	Transcribed locus
1394578_at	0.29	-2.04	BI299761	Gria2	Glutamate receptor, ionotropic, AMPA2
1383566_at	0.29	-2	AW527690	---	Transcribed locus
1395546_at	0.29	-2.02	AW529685	---	Transcribed locus
1391656_at	0.29	-2.03	AI101416	---	---
1390652_at	0.28	-2.02	BF390059	---	Transcribed locus
1371162_at	0.28	-2.01	AJ311952	Mrga10	nuclear receptor MrgA10 RF-amide G protein-coupled receptor
1394577_at	0.29	-2.02	BI279384	---	Transcribed locus
1388060_at	0.29	-1.98	U71294	Syt12	synaptotagmin XII
1377773_at	0.29	-2	AW522872	---	Transcribed locus, weakly similar to NP_766020.1 RIKEN cDNA C030002O17 [Mus musculus]
1384737_at	0.29	-2.32	BF555973	Trdn	Triadin
1370625_at	0.3	-1.99	AF044201	Faim2	Fas apoptotic inhibitory molecule 2
1392189_at	0.3	-2.01	BE105136	RGD1562092_predicted	similar to regulatory factor X 4 variant (predicted)
1398649_at	0.3	-1.98	AA819827	Slitrk3_predicted	SLIT and NTRK-like family, member 3 (predicted)
1385321_at	0.29	-2.04	AW532713	LOC683275 /// LOC688502	similar to heterogeneous nuclear ribonucleoprotein methyltransferase-like 4 /// similar to Protein arginine N-methyltransferase 4
1386120_at	0.31	-1.99	BF393607	LOC679389 /// LOC689147	hypothetical protein LOC679389 /// hypothetical protein LOC689147

Table 7-10 continued.

1384236_at	0.3	-1.97	BI281089	---	CDNA clone IMAGE:7315883
1377457_a_at	0.31	-1.97	AA850618	Sorl1_predicted	sortilin-related receptor, L(DLR class) A repeats-containing (predicted)
1380865_at	0.31	-1.96	BM385284	---	Transcribed locus
1390707_at	0.32	-1.95	BI281632	Rgs10	regulator of G-protein signalling 10
1395327_at	0.32	-2.31	AW522341	---	Transcribed locus, weakly similar to XP_580018.1 PREDICTED: hypothetical protein XP_580018 [Rattus norvegicus]
1369035_a_at	0.32	-1.96	AB073753	Kcnj6	potassium inwardly-rectifying channel, subfamily J, member 6
1370124_at	0.32	-1.94	NM_053968	Mt3	metallothionein 3
1375242_at	0.32	-1.96	BI296440	LOC687797	similar to tumor suppressor candidate 5
1378026_at	0.31	-1.95	BE109912	---	Transcribed locus
1373637_at	0.32	-1.97	BG372823	---	---
1378105_at	0.34	-1.93	BF289201	---	Transcribed locus
1397497_at	0.34	-1.96	BF391164	---	Transcribed locus
1367745_at	0.33	-1.92	NM_031143	Dgkz	diacylglycerol kinase zeta
1371241_x_at	0.33	-3.05	AF370889	Tpm1	Tropomyosin 1, alpha
1394295_at	0.36	-1.97	BG672252	---	Transcribed locus
1370556_at	0.35	-1.95	M24104	Vamp1	vesicle-associated membrane protein 1
1383014_at	0.35	-1.94	AI639078	---	Transcribed locus
1384696_at	0.35	-1.93	BE113106	MGC116197	similar to RIKEN cDNA 1700001E04
1396023_at	0.35	-1.94	AW522736	---	Transcribed locus
1378252_at	0.36	-2.02	AI029745	Chodl_predicted	chondrolectin (predicted)
1369043_at	0.35	-1.92	NM_012971	Kcna4	potassium voltage-gated channel, shaker-related subfamily, member 4
1390881_at	0.35	-1.95	AI172339	Abra	actin-binding Rho activating protein
1391246_at	0.36	-1.92	BF390318	RGD1561985_predicted	similar to dystrobrevin alpha isoform 1 (predicted)
1390710_x_at	0.35	-1.91	AA850618	Sorl1_predicted	sortilin-related receptor, L(DLR class) A repeats-containing (predicted)
1384923_at	0.35	-1.92	AI137998	---	Transcribed locus, strongly similar to XP_236620.3 PREDICTED: similar to RIKEN cDNA 6430571L13 gene [Rattus norvegicus]
1397840_at	0.36	-1.93	BF563826	---	Transcribed locus
1369755_at	0.35	-1.9	AF106624	B3gat2	beta-1,3-glucuronyltransferase 2 (glucuronosyltransferase S)
1394070_at	0.36	-1.9	AA893087	---	---
1368182_at	0.39	-1.89	NM_130739	Acsl6	acyl-CoA synthetase long-chain family member 6
1382147_at	0.39	-1.88	AI229479	LOC363915	similar to CG14446-PA
1370546_at	0.39	-1.91	U75361	Unc13c	unc-13 homolog C (C. elegans)
1367964_at	0.41	-2.79	NM_017185	Tnni2	troponin I type 2 (skeletal, fast)
1368789_at	0.42	-1.88	NM_020072	Acpp	acid phosphatase, prostate
1395536_at	0.42	-1.88	BG673248	---	Transcribed locus
1379814_at	0.43	-1.9	AW532796	---	CDNA clone IMAGE:7302159
1384655_at	0.44	-1.85	AW142820	Kirrel3_predicted	kin of IRRE like 3 (Drosophila) (predicted)
1388506_at	0.46	-1.86	AW144509	Dsp	desmoplakin
1369116_a_at	0.46	-1.86	NM_017338	Calca	calcitonin/calcitonin-related polypeptide, alpha
1374046_at	0.46	-1.87	BG376092	Hs3st2	heparan sulfate (glucosamine) 3-O-sulfotransferase 2
1382965_at	0.45	-1.88	AA996630	Amigo3	Amphoterin induced gene and ORF 3
1368768_at	0.46	-1.85	NM_019265	Scn11a	sodium channel, voltage-gated, type XI, alpha
1380228_at	0.45	-1.91	BG672066	RGD1306880_predicted	similar to hypothetical protein MGC47816 (predicted)
1386922_at	0.46	-1.88	AI408948	Ca2	carbonic anhydrase 2
1379054_at	0.47	-1.88	BF391881	Kcnc1	Potassium voltage gated channel, Shaw-related subfamily, member 1
1383642_at	0.46	-1.87	BG374114	---	---
1390355_at	0.47	-2.12	AI575442	Ryr1	ryanodine receptor 1, skeletal muscle
1390146_at	0.49	-1.86	BF414998	---	---
1378857_at	0.49	-1.86	AI716196	LOC678833	similar to transcription elongation factor A (SII)-like 5
1387375_at	0.52	-1.83	NM_031855	Khk	ketohexokinase
1388000_at	0.52	-1.83	AF021923	Slc24a2	solute carrier family 24 (sodium/potassium/calcium exchanger), member 2

Table 7-10 continued.

1371570_at	0.52	-1.85	AI406266	Scrt1_predicted	scratch homolog 1, zinc finger protein (Drosophila) (predicted)
1376928_at	0.53	-1.89	BE106737	RGD1565950_predicted	Similar to A disintegrin-like and metalloprotease (reprolysin type) with thrombospondin type 1 motif, 2 (predicted)
1370078_at	0.53	-1.85	NM_021758	---	Transcribed locus
1368124_at	0.53	-1.82	NM_133578	Dusp5	dual specificity phosphatase 5
1369158_at	0.53	-1.82	NM_016996	Casr	calcium-sensing receptor
1377374_at	0.53	-1.84	AI146055	---	Transcribed locus
1391653_at	0.55	-1.83	BE120391	Gabrg2	gamma-aminobutyric acid A receptor, gamma 2
1377924_at	0.57	-1.84	BE113414	---	Transcribed locus
1373697_at	0.57	-2.36	BG378588	Mybpc2_predicted	myosin binding protein C, fast-type (predicted)
1372755_at	0.57	-1.83	AI102073	Mal2	mal, T-cell differentiation protein 2
1394786_at	0.58	-1.85	AW526631	Sorl1_predicted	sortilin-related receptor, L(DLR class) A repeats-containing (predicted)
1378163_at	0.58	-1.83	AA817956	---	Transcribed locus
1380011_at	0.57	-1.81	BM383573	---	Transcribed locus, moderately similar to XP_576460.1 PREDICTED: similar to hypothetical protein PB402898.00.0
1393040_at	0.58	-1.83	BE097656	---	Transcribed locus
1398099_at	0.58	-1.82	AW527241	---	---
1393262_at	0.61	-1.84	BG379771	---	Transcribed locus, strongly similar to XP_574942.1 PREDICTED: similar to regulatory factor X-associated protein [Rattus norvegicus]
1376424_at	0.61	-1.82	BF412664	---	Transcribed locus
1379510_at	0.62	-1.83	BF546306	---	Transcribed locus
1393197_at	0.63	-1.8	BG376055	Abhd8_predicted	abhydrolase domain containing 8 (predicted)
1393547_at	0.63	-1.8	BE101549	RGD1560399_predicted	similar to hypothetical protein C630023L15 (predicted)
1375690_at	0.63	-1.84	AI138004	---	---
1376463_at	0.64	-1.81	AA955579	---	Transcribed locus
1384202_at	0.64	-1.8	BI287326	RGD1566317_predicted	similar to Tescalcin (predicted)
1384780_at	0.64	-1.8	BF402747	Cpne4_predicted	copine IV (predicted)
1372745_at	0.64	-2.14	BE112453	---	---
1370111_at	0.66	-1.81	NM_019314	Kcnn2	potassium intermediate/small conductance calcium-activated channel, subfamily N, member 2
1371052_at	0.68	-1.82	AA859752	Nog	noggin
1374528_at	0.67	-1.79	BF418764	Rgs3	Regulator of G-protein signalling 3
1378107_at	0.67	-1.81	AI146051	---	Transcribed locus
1391013_at	0.67	-1.86	AW523567	Pcdh8	Protocadherin 8
1383220_at	0.68	-1.8	BE114231	Kcnip4	Kv channel interacting protein 4
1390815_at	0.68	-1.82	BF282870	Cnnm1_predicted	cyclin M1 (predicted)
1370550_at	0.68	-1.77	U31554	Lsamp	limbic system-associated membrane protein
1394522_at	0.68	-1.78	AW527950	---	Transcribed locus, weakly similar to XP_508524.1 PREDICTED: similar to phospholipase C, beta 3 (phosphatidylinositol-specific) [Pan troglodytes]
1377828_at	0.68	-1.8	BG672090	Tmem16c_predicted	transmembrane protein 16C (predicted)
1388891_at	0.68	-1.79	BG374285	---	Transcribed locus
1374785_at	0.68	-1.78	BG380471	RGD1565373_predicted	similar to CD69 antigen (p60, early T-cell activation antigen) (predicted)
1387821_at	0.7	-1.8	NM_017313	Rab3ip	RAB3A interacting protein
1384158_at	0.69	-1.82	AW522416	---	Transcribed locus
1368351_at	0.69	-1.77	NM_017247	Scn10a	sodium channel, voltage-gated, type 10, alpha polypeptide
1398306_at	0.69	-2.31	J02811	Ampd1	adenosine monophosphate deaminase 1 (isoform M)
1396459_at	0.69	-1.78	BE096723	Isl2	Insulin related protein 2 (islet 2)
1382011_at	0.69	-1.78	AI100797	---	Transcribed locus, strongly similar to NP_796210.2 plasma membrane calcium ATPase 3 [Mus musculus]
1389550_at	0.7	-1.77	BM385941	Sh3gl2	SH3-domain GRB2-like 2
1385826_at	0.72	-1.78	AA860047	---	Transcribed locus
1381001_at	0.73	-1.78	BE105897	Kbtbd3_predicted	Kelch repeat and BTB (POZ) domain containing 3 (predicted)

Table 7-10 continued.

1384756_at	0.75	-1.79	BF394311	Slc43a2_predicted	Solute carrier family 43, member 2 (predicted)
1380107_a_at	0.75	-1.76	BM384521	RGD1305719_predicted	similar to putative N-acetyltransferase Camello 2 (predicted)
1385311_at	0.75	-1.8	BI274649	Slco5a1_predicted	solute carrier organic anion transporter family, member 5A1 (predicted)
1383542_at	0.78	-1.76	BI282819	---	Transcribed locus
1381445_at	0.77	-1.79	AA996810	Esrrg	Estrogen-related receptor gamma
1391521_at	0.78	-1.75	AA858748	Casp12	Caspase 12
1368255_at	0.78	-1.78	NM_017354	Hnt	neurotrimin
1368339_at	0.78	-1.78	NM_012521	S100g	S100 calcium binding protein G
1388802_at	0.78	-1.76	AI579422	Bex1	brain expressed X-linked 1
1374363_at	0.78	-1.75	AI232693	RGD1306028	similar to hypothetical protein FLJ30473
1376311_at	0.78	-1.78	BM391312	RGD1563465_predicted	similar to netrin G1 (predicted)
1388543_at	0.81	-1.77	BI291257	RGD1306289_predicted	similar to HTPAP protein (predicted)
1396127_at	0.8	-1.76	BF288545	---	---
1368801_at	0.81	-1.76	NM_053342	Cxxc4	CXXC finger 4
1397983_at	0.82	-1.76	BF403330	---	Transcribed locus
1391326_at	0.82	-1.75	BE095733	RGD1562292_predicted	similar to homeotic protein Hox B5 - mouse (predicted)
1398298_at	0.82	-1.75	NM_012852	Htr1d	5-hydroxytryptamine (serotonin) receptor 1D
1393404_at	0.81	-1.74	BF554746	---	Transcribed locus, strongly similar to NP_808376.1 reticulon 4 receptor-like 1 [Mus musculus]
1391200_at	0.81	-1.76	AW530290	---	Transcribed locus
1370606_at	0.81	-1.76	U22830	P2ry1	purinergic receptor P2Y, G-protein coupled 1
1383499_at	0.81	-1.75	BG371995	---	---
1370125_at	0.82	-1.77	NM_019189	Ngef_predicted	Neuronal guanine nucleotide exchange factor (predicted)
1371554_at	0.82	-2.2	AA799471	LOC688173	similar to Telethonin (Titin cap protein)
1394290_at	0.82	-1.77	BG669921	---	Transcribed locus
1370944_at	0.82	-1.75	AI230238	Col10a1	procollagen, type X, alpha 1
1391547_at	0.83	-1.8	AI045669	---	CDNA clone IMAGE:7320555
1375032_at	0.83	-1.76	AI412533	RGD1565261_predicted	similar to kinase non-catalytic C-lobe domain (KIND) containing 1 isoform b (predicted)
1388741_at	0.85	-2.06	AW533234	LOC683555 /// LOC688915	similar to cardiomyopathy associated 5
1388139_at	0.85	-3.66	BI277586	LOC691644	similar to Myosin heavy chain, skeletal muscle, adult 2a
1390123_at	0.85	-1.76	BI279036	Tmem45b	transmembrane protein 45b
1379374_at	0.85	-1.76	AW526088	Prg1	plasticity related gene 1
1398182_at	0.86	-1.75	BF411782	---	Transcribed locus
1388037_at	0.87	-1.74	J05087	Atp2b3	ATPase, Ca++ transporting, plasma membrane 3
1392865_at	0.87	-1.75	BG371594	---	---
1385445_at	0.89	-1.81	BE119167	---	Transcribed locus, strongly similar to XP_233112.3 PREDICTED: similar to extracellular matrix protein QBRICK [Rattus norvegicus]
1391879_at	0.89	-1.74	AA964161	---	Transcribed locus
1376893_at	0.9	-1.74	AI406821	Vmp_predicted	vesicular membrane protein p24 (predicted)
1367896_at	0.9	-1.49	AB030829	Ca3	carbonic anhydrase 3
1387799_at	0.9	-1.74	AF129400	Fxyd2	FXYD domain-containing ion transport regulator 2
1383554_at	0.89	-1.76	AW142796	RGD1566282_predicted	similar to RIKEN cDNA D330045A20 (predicted)
1392950_at	0.9	-2.31	BF552973	Myot_predicted	myotilin (predicted)
1395714_at	0.9	-1.73	AT005664	---	---
1374934_at	0.9	-1.79	BF405151	Gpr39	G protein-coupled receptor 39
1369165_at	0.9	-1.73	NM_021771	Trpc3	transient receptor potential cation channel, subfamily C, member 3
1394545_at	0.9	-1.73	AA998459	Spire2_predicted	spire homolog 2 (Drosophila) (predicted)
1377942_at	0.92	-1.73	AI101595	---	Transcribed locus

b) Ingenuity pathways analysis

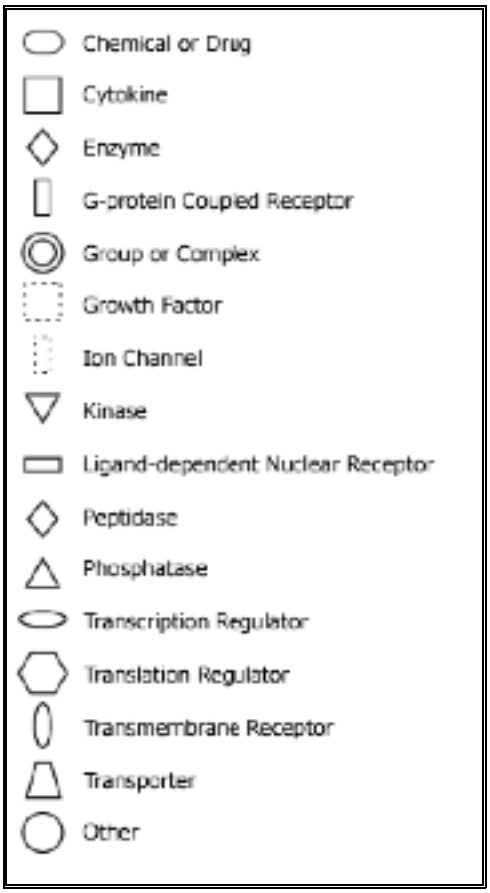

Figure 7-1: Key to IPA node types used in networks.

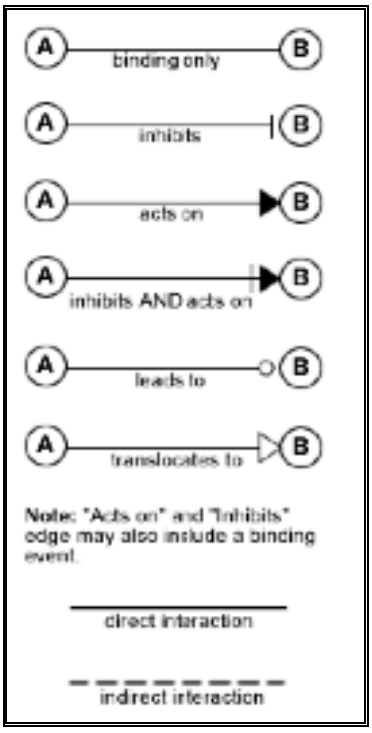

Figure 7-2: Key to IPA edge types used in networks.

c) qRT-PCR descriptive statistics

i) Pilot microarray

Table 7-11: Descriptive statistics for genes investigated in validation of pilot microarray

GENE	GROUP	FINAL N	MEAN CT (±S.E)	CV%
ECEL1	naïve	5	33.228 (0.259)	0.779
	sham	5	33.580 (0.405)	1.206
	sciatic trans.	6	29.582 (0.349)	1.180
ATF3	naive	5	30.432 (0.283)	0.930
	sham	6	31.033 (0.452)	1.457
	sciatic trans.	6	26.960 (0.250)	0.927
MX2	naive	5	29.690 (0.282)	0.950
	sham	6	30.587 (0.382)	1.249
	sciatic trans.	6	29.065 (0.270)	0.929
NPTX1	naive	6	26.227 (0.363)	1.384
	sham	6	27.720 (0.356)	1.284
	sciatic trans.	6	29.542 (0.651)	2.204
SEMA6A	naive	6	28.737 (0.359)	1.249
	sham	6	30.683 (0.511)	1.665
	sciatic trans	6	28.108 (0.461)	1.640

ii) Main microarray

Table 7-12: ATF3 descriptive statistics

GROUP	FINAL N	MEAN CT (±S.E)	CV%
Naïve ctrl	8	29.521 (0.952)	3.225
2DR	8	27.845 (0.348)	1.250
2DR sham	7	28.917 (0.296)	1.024
6DR	7	28.087 (0.344)	1.225
6DR sham	8	29.528 (0.165)	0.559
SN	7	25.709 (0.810)	3.151
SN sham	7	27.603 (0.627)	2.271
2DC	7	28.926 (0.602)	2.081
2DC sham	5	29.702 (0.235)	0.791
6DC	5	29.134 (0.263)	0.903

Table 7-13: ANKRD1 descriptive statistics

GROUP	FINAL N	MEAN CT (±S.E)	CV%
Naïve ctrl	6	36.175 (0.268)	0.741
2DR	6	34.513 (0.270)	0.782
2DR sham	8	34.893 (0.481)	1.378
6DR	7	34.946 (0.394)	1.127
6DR sham	8	35.566 (0.380)	1.068
SN	7	31.503 (0.421)	1.336
SN sham	8	33.579 (0.567)	1.689
2DC	7	34.786 (0.244)	0.701
2DC sham	7	34.371 (0.481)	1.399
6DC	5	33.656 (0.205)	0.615

Table 7-14: SEMA6A descriptive statistics

GROUP	FINAL N	MEAN CT (±S.E)	CV%
Naïve ctrl	7	31.129 (0.956)	3.071
2DR	8	30.386 (0.230)	0.757
2DR sham	8	30.566 (0.287)	0.939
6DR	8	39.369 (0.269)	0.886
6DR sham	8	31.778 (0.353)	1.111
SN	8	28.741 (0.521)	1.813
SN sham	8	30.224 (0.534)	1.767
2DC	8	30.728 (0.279)	0.908
2DC sham	8	29.624 (0.288)	0.927
6DC	7	29.393 (0.380)	1.293

Table 7-15: PTPN5 descriptive statistics

GROUP	FINAL N	MEAN CT (±S.E)	CV%
Naïve ctrl	5	30.988 (0.371)	1.197
2DR	8	29.881 (0.290)	0.971
2DR sham	6	30.567 (0.209)	0.684
6DR	6	30.283 (0.298)	0.984
6DR sham	7	30.983 (0.456)	1.472
SN	8	28.754 (0.467)	1.624
SN sham	8	29.979 (0.369)	1.231
2DC	7	30.493 (0.369)	1.210
2DC sham	8	30.213 (0.263)	0.870
6DC	7	30.061 (0.227)	0.755

Table 7-16: BDNF descriptive statistics

GROUP	FINAL N	MEAN CT (±S.E)	CV%
Naïve ctrl	8	27.450 (0.770)	2.807
2DR	7	25.990 (0.455)	1.751
2DR sham	6	26.542 (0.295)	1.111
6DR	8	26.124 (0.310)	1.187
6DR sham	7	27.453 (0.316)	1.151
SN	8	26.669 (0.435)	1.629
SN sham	7	26.997 (0.487)	1.804
2DC	8	27.138 (0.418)	1.540
2DC sham	8	26.408 (0.366	1.386
6DC	7	26.603 (0.318)	1.195

Table 7-17: IGF1 descriptive statistics

GROUP	FINAL N	MEAN CT (±S.E)	CV%
Naïve ctrl	8	26.290 (0.704)	2.678
2DR	8	25.453 (0.382)	1.501
2DR sham	8	25.049 (0.240)	0.958
6DR	7	25.064 (0.249)	0.993
6DR sham	8	26.195 (0.236)	0.901
SN	8	25.930 (0.385)	1.485
SN sham	8	25.490 (0.379)	1.487
2DC	8	25.630 (0.421)	1.643
2DC sham	8	24.644 (0.394)	1.599
6DC	7	24.977 (0.326)	1.305

Table 7-18: WISP2 descriptive statistics

GROUP	FINAL N	MEAN CT (±S.E)	CV%
Naïve ctrl	8	31.074 (0.405)	1.303
2DR	8	29.745 (0.476)	1.600
2DR sham	8	30.425 (0.302)	0.993
6DR	8	30.145 (0.551)	1.828
6DR sham	7	31.071 (0.397)	1.278
SN	8	30.473 (0.408)	1.339
SN sham	8	29.780 (0.467)	1.568
2DC	8	30.021 (0.372)	1.239
2DC sham	8	29.354 (0.416)	1.417
6DC	6	29.985 (0.365)	1.217

Table 7-19: TFPI2 descriptive statistics

GROUP	FINAL N	MEAN CT (±S.E)	CV%
Naïve ctrl	7	33.014 (0.508)	1.539
2DR	7	31.487 (0.244)	0.775
2DR sham	8	31.516 (0.230)	0.730
6DR	7	31.779 (0.152)	0.478
6DR sham	8	32.565 (0.346)	1.062
SN	7	31.953 (0.316)	0.989
SN sham	8	32.320 (0.253)	0.783
2DC	7	31.884 (0.435)	1.364
2DC sham	7	31.436 (0.453)	1.441
6DC	5	32.370 (0.213)	0.658

References

Abankwa, D., P. Kury and H. W. Muller (2002). "Dynamic changes in gene expression profiles following axotomy of projection fibres in the Mammalian CNS." Mol Cell Neurosci **21**(3): 421-35.

Adam, F., T. Sourisseau, R. Metivier, Y. Le Page, C. Desbois, D. Michel and G. Salbert (2000). "COUP-TFI (chicken ovalbumin upstream promoter-transcription factor I) regulates cell migration and axogenesis in differentiating P19 embryonal carcinoma cells." Mol Endocrinol **14**(12): 1918-33.

Aimone, J. B., J. L. Leasure, V. M. Perreau and M. Thallmair (2004). "Spatial and temporal gene expression profiling of the contused rat spinal cord." Experimental Neurology **189**: 204-221.

Alberi, S., M. Raggenbass, F. de Bilbao and M. Dubois-Dauphin (1996). "Axotomized neonatal motoneurons overexpressing the bcl2 proto-oncogene retain functional electrophysiological properties." Proc Natl Acad Sci U S A **93**(9): 3978-83.

Alvares, D. and M. Fitzgerald (1999). "Building blocks of pain: the regulation of key molecules in spinal sensory neurones during development and following peripheral axotomy." Pain **Suppl 6**: S71-85.

Ambron, R. T. and E. T. Walters (1996). "Priming events and retrograde injury signals. A new perspective on the cellular and molecular biology of nerve regeneration." Mol Neurobiol **13**(1): 61-79.

Andersen, C. L., J. L. Jensen and T. F. Orntoft (2004). "Normalization of real-time quantitative reverse transcription-PCR data: a model-based variance estimation approach to identify genes suited for normalization, applied to bladder and colon cancer data sets." Cancer Res **64**(15): 5245-50.

Andersen, L. B. and D. J. Schreyer (1999). "Constitutive expression of GAP-43 correlates with rapid, but not slow regrowth of injured dorsal root axons in the adult rat." Exp Neurol **155**(2): 157-64.

Anesti, A. M., P. J. Peeters, I. Royaux and R. S. Coffin (2008). "Efficient delivery of RNA Interference to peripheral neurons in vivo using herpes simplex virus." Nucleic Acids Res **36**(14): e86.

Antunes Bras, J. M., A. M. Laporte, J. J. Benoliel, S. Bourgoin, A. Mauborgne, M. Hamon, F. Cesselin and M. Pohl (1999). "Effects of peripheral axotomy on cholecystokinin neurotransmission in the rat spinal cord." J Neurochem **72**(2): 858-67.

Araki, T. and J. Milbrandt (1996). "Ninjurin, a novel adhesion molecule, is induced by nerve injury and promotes axonal growth." Neuron **17**(2): 353-61.

Araki, T., R. Nagarajan and J. Milbrandt (2001). "Identification of genes induced in peripheral nerve injury." The Journal of Biological Chemistry **276**(36): 34131-34141.

Asano, A., H. K. Jin and T. Watanabe (2003). "Mouse Mx2 gene: organization, mRNA expression and the role of the interferon-response promoter in its regulation." Gene **306**: 105-13.

Averill, S., D. R. Davis, P. J. Shortland, J. V. Priestley and S. P. Hunt (2002). "Dynamic pattern of reg-2 expression in rat sensory neurons after peripheral nerve injury." J Neurosci **22**(17): 7493-501.

Averill, S., J. J. Inglis, V. R. King, S. W. Thompson, W. B. Cafferty, P. J. Shortland, S. P. Hunt, B. L. Kidd and J. V. Priestley (2008). "Reg-2 expression in dorsal root ganglion neurons after adjuvant-induced monoarthritis." Neuroscience **155**(4): 1227-36.

Bahr, M. and C. Przyrembel (1995). "Myelin from peripheral and central nervous system is a nonpermissive substrate for retinal ganglion cell axons." Exp Neurol **134**(1): 87-93.

Bandtlow, C. E. (2003). "Regeneration in the central nervous system." Experimental Gerontology **38**: 79-86.

Bardin, L., J. Lavarenne and A. Eschalier (2000). "Serotonin receptor subtypes involved in the spinal

antinociceptive effect of 5-HT in rats." Pain **86**(1-2): 11-8.

Bareyre, F. M. and M. E. Schwab (2003). "Inflammation, degeneration and regeneration in the injured spinal cord: insights from DNA microarrays." Trends Neurosci **26**(10): 555-63.

Barnes, M., J. Freudenberg, S. Thompson, B. Aronow and P. Pavlidis (2005). "Experimental comparison and cross-validation of the Affymetrix and Illumina gene expression analysis platforms." Nucleic Acids Res **33**(18): 5914-23.

Barnett, S. C. and J. S. Riddell (2004). "Olfactory ensheathing cells (OECs) and the treatment of CNS injury: advantages and possible caveats." J Anat **204**(1): 57-67.

Barnett, S. C. and J. S. Riddell (2007). "Olfactory ensheathing cell transplantation as a strategy for spinal cord repair--what can it achieve?" Nat Clin Pract Neurol **3**(3): 152-61.

Batchelor, P. E. and D. W. Howells (2003). "CNS regeneration: clinical possibility or basic science fantasy?" Journal of Clinical Neuroscience **10**(5): 523-534.

Befort, K., L. Karchewski, C. Lanoue and C. J. Woolf (2003). "Selective up-regulation of the growth arrest DNA damage-inducible gene Gadd45 alpha in sensory and motor neurons after peripheral nerve injury." Eur J Neurosci **18**(4): 911-22.

Bennett, D. L., T. J. Boucher, M. P. Armanini, K. T. Poulsen, G. J. Michael, J. V. Priestley, H. S. Phillips, S. B. McMahon and D. L. Shelton (2000). "The glial cell line-derived neurotrophic factor family receptor components are differentially regulated within sensory neurons after nerve injury." J Neurosci **20**(1): 427-37

Berdan, R. C., J. C. Easaw and R. Wang (1993). "Alterations in membrane potential after axotomy at different distances from the soma of an identified neuron and the effect of depolarization on neurite outgrowth and calcium channel expression." J Neurophysiol **69**(1): 151-64.

Bergman, E., B. T. Fundin and B. Ulfhake (1999). "Effects of aging and axotomy on the expression of neurotrophin receptors in primary sensory neurons." J Comp Neurol **410**(3): 368-86.

Bermingham-McDonogh, O., Y. T. Xu, M. A. Marchionni and S. S. Scherer (1997). "Neuregulin expression in PNS neurons: isoforms and regulation by target interactions." Mol Cell Neurosci **10**(3-4): 184-95.

Bethea, J. R. and W. D. Dietrich (2002). "Targeting the host inflammatory response in traumatic spinal cord injury." Curr Opin Neurol **15**(3): 355-60.

Bi, J., N. P. Tsai, Y. P. Lin, H. H. Loh and L. N. Wei (2006). "Axonal mRNA transport and localized translational regulation of kappa-opioid receptor in primary neurons of dorsal root ganglia." Proc Natl Acad Sci U S A **103**(52): 19919-24.

Bi, J., N. P. Tsai, H. Y. Lu, H. H. Loh and L. N. Wei (2007). "Copb1-facilitated axonal transport and translation of kappa opioid-receptor mRNA." Proc Natl Acad Sci U S A **104**(34): 13810-5.

Birder, L. A. and E. R. Perl (1999). "Expression of alpha2-adrenergic receptors in rat primary afferent neurones after peripheral nerve injury or inflammation." J Physiol **515 (Pt 2)**: 533-42.

Bisby, M. A. (1985). "Enhancement of the conditioning lesion effect in rat sciatic motor axons after superimposition of conditioning and test lesions." Exp Neurol **90**(2): 385-94.

Blackmore, M. and P. C. Letourneau (2006). "L1, beta1 integrin, and cadherins mediate axonal regeneration in the embryonic spinal cord." J Neurobiol **66**(14): 1564-83.

Bloechlinger, S., L. A. Karchewski and C. J. Woolf (2004). "Dynamic changes in glypican-1 expression in dorsal root ganglion neurons after peripheral and central axonal injury." Eur J Neurosci **19**(5): 1119-32.

Boeshans, K. M., T. C. Mueser and B. Ahvazi (2007). "A three-dimensional model of the human transglutaminase 1: insights into the understanding of lamellar ichthyosis." J Mol Model **13**(1): 233-46.

Bondok, A. A. and F. M. Sansone (1984). "Retrograde and transganglionic degeneration of sensory neurons after a peripheral nerve lesion at birth." Exp Neurol **86**(2): 322-30.

Bonilla, I. E., K. Tanabe and S. M. Strittmatter (2002). "Small proline-rich repeat protein 1A is expressed by axotomized neurons and promotes axonal outgrowth." J Neurosci **22**(4): 1303-15.

Bos, J. L. (2003). "Epac: a new cAMP target and new avenues in cAMP research." Nat Rev Mol Cell Biol **4**(9): 733-8.

Bovolenta, P., P. Esteve, J. M. Ruiz, E. Cisneros and J. Lopez-Rios (2008). "Beyond Wnt inhibition: new functions of secreted Frizzled-related proteins in development and disease." J Cell Sci **121**(Pt 6): 737-46.

Bradbury, E. J., G. Burnstock and S. B. McMahon (1998). "The expression of P2X3 purinoreceptors in sensory neurons: effects of axotomy and glial-derived neurotrophic factor." Mol Cell Neurosci **12**(4-5): 256-68.

Brazma, A., P. Hingamp, J. Quackenbush, G. Sherlock, P. Spellman, C. Stoeckert, J. Aach, W. Ansorge, C. A. Ball, H. C. Causton, T. Gaasterland, P. Glenisson, F. C. Holstege, I. F. Kim, V. Markowitz, J. C. Matese, H. Parkinson, A. Robinson, U. Sarkans, S. Schulze-Kremer, J. Stewart, R. Taylor, J. Vilo and M. Vingron (2001). "Minimum information about a microarray experiment (MIAME)-toward standards for microarray data." Nat Genet **29**(4): 365-71.

Bregman, B. S., E. Kunkel-Bagden, L. Schnell, H. Dai, D. Gao and M. E. Schwab (1995). "Recovery from spinal cord injury mediated by antibodies to neurite growth inhibitors." Nature **378**: 498-501.

Breitling, R., A. Amtmann and P. Herzyk (2004). "Iterative group Analysis (iGA): A simple tool to enhance sensitivity and facilitate interpretation of microarray experiments." BMC Bioinformatics **5**(34).

Breitling, R., P. Armengaud, A. Amtmann and P. Herzyk (2004). "Rank products: A simple, yet powerful, new method to detect differentially regulated genes in replicated microarray experiments." FEBS Letters **573**: 83-92.

Bretin, S., S. Reibel, E. Charrier, M. Maus-Moatti, N. Auvergnon, A. Thevenoux, J. Glowinski, V. Rogemond, J. Premont, J. Honnorat and C. Gauchy (2005). "Differential expression of CRMP1, CRMP2A, CRMP2B, and CRMP5 in axons or dendrites of distinct neurons in the mouse brain." J Comp Neurol **486**(1) 1-17.

Bron, R., M. Vermeren, N. Kokot, W. Andrews, G. E. Little, K. J. Mitchell and J. Cohen (2007). "Boundary cap cells constrain spinal motor neuron somal migration at motor exit points by a semaphorin-plexin mechanism." Neural Develop **2**: 21.

Broude, E., M. McAtee, M. S. Kelley and B. S. Bregman (1997). "c-Jun expression in adult rat dorsal root ganglion neurons: differential response after central or peripheral axotomy." Exp Neurol **148**(1): 367-77.

Brumovsky, P., M. Watanabe and T. Hokfelt (2007). "Expression of the vesicular glutamate transporters-1 and -2 in adult mouse dorsal root ganglia and spinal cord and their regulation by nerve injury." Neuroscience **147**(2): 469-90.

Burnett, M. G. and E. L. Zager (2004). "Pathophysiology of peripheral nerve injury: a brief review." Neurosurgery Focus **16**(5): 1-7.

Burns, M. J., G. J. Nixon, C. A. Foy and N. Harris (2005). "Standardisation of data from real-time quantitative PCR methods - evaluation of outliers and comparison of calibration curves." BMC Biotechnol **5**: 31.

Buss, A., G. A. Brook, B. Kakulas, D. Martin, R. Franzen, J. Schoenen, J. Noth and A. B. Schmitt (2004). "Gradual loss of myelin and formation of an astrocytic scar during Wallerian degeneration in the human spinal cord." Brain **127**: 34-44.

Cafferty, W. B., N. J. Gardiner, P. Das, J. Qiu, S. B. McMahon and S. W. Thompson (2004). "Conditioning injury-induced spinal axon regeneration fails in interleukin-6 knock-out mice." J Neurosci **24**(18): 4432-43.

Cafferty, W. B., N. J. Gardiner, I. Gavazzi, J. Powell, S. B. McMahon, J. K. Heath, J. Munson, J. Cohen and S. W. Thompson (2001). "Leukemia inhibitory factor determines the growth status of injured adult sensory neurons." J Neurosci **21**(18): 7161-70.

Cai, D., K. Deng, W. Mellado, J. Lee, R. R. Ratan and M. T. Filbin (2002). "Arginase I and polyamines act downstream from cyclic AMP in overcoming inhibition of axonal growth MAG and myelin in vitro." Neuron **35**(4): 711-9.

Cajal, S. R. (1928). Degeneration and Regeneration of the Nervous System, Vols. 1 & 2. London, Oxford University Press.

Cameron, A. A., G. Vansant, W. Wu, D. J. Carlo and C. R. Ill (2003). "Identification of reciprocally regulated gene modules in regenerating dorsal root ganglion neurons and activated peripheral or central nervous system glia." J Cell Biochem **88**(5): 970-85.

Carmel, J. B., A. Galante, P. Soteropoulos, P. Tolias, M. Recce, W. Young and R. P. Hart (2001). "Gene expression profiling of acute spinal cord injury reveals spreading inflammatory signals and neuron loss." Physiol Genomics **7**(2): 201-13.

Caroni, P. and M. E. Schwab (1988). "Antibody against myelin-associated inhibitor of neurite growth neutralises nonpermissive substrate properties of CNS white matter." Neuron **1**: 85-96.

Carroll, S. L., M. L. Miller, P. W. Frohnert, S. S. Kim and J. A. Corbett (1997). "Expression of neuregulins and their putative receptors, ErbB2 and ErbB3, is induced during Wallerian degeneration." The Journal of Neuroscience **17**(5): 1642-1659.

Chadan, S., K. L. Moya, M. M. Portier and G. Filliatreau (1994). "Identification of a peripherin dimer: changes during axonal development and regeneration of the rat sciatic nerve." J Neurochem **62**(5): 1894-905.

Chao, M. (2003). "Neurotrophins and their receptors: a convergence point for many signalling pathways." Nature Neuroscience **4**: 299-309.
Chen, D. F., S. Jhaveri and G. E. Schneider (1995). "Intrinsic changes in developing retinal neurons result in regenerative failure of their axons." Proceedings of the National Academy of Sciences USA **92**: 7287-7291.

Chen, D. F., G. E. Schneider, J. C. Martinou and S. Tonegawa (1997). "Bcl-2 promotes regeneration of severed axons in mammalian CNS." Nature **385**(6615): 434-9.

Cheng, C., C. A. Webber, J. Wang, Y. Xu, J. A. Martinez, W. Q. Liu, D. McDonald, G. F. Guo, M. D. Nguyen and D. W. Zochodne (2008). "Activated RHOA and peripheral axon regeneration." Exp Neurol.

Chew, D. J., V. H. Leinster, M. Sakthithasan, L. G. Robson, T. Carlstedt and P. J. Shortland (2008). "Cell death after dorsal root injury." Neurosci Lett **433**(3): 231-4.

Cho, H. J., J. K. Kim, H. C. Park, J. K. Kim, D. S. Kim, S. O. Ha and H. S. Hong (1998). "Changes in brain-derived neurotrophic factor immunoreactivity in rat dorsal root ganglia, spinal cord, and gracile nuclei following cut or crush injuries." Exp Neurol **154**(1): 224-30.

Cho, H. J., J. K. Kim, X. F. Zhou and R. A. Rush (1997). "Increased brain-derived neurotrophic factor immunoreactivity in rat dorsal root ganglia and spinal cord following peripheral inflammation." Brain Res **764**(1-2): 269-72.

Chong, M. S., M. L. Reynolds, N. Irwin, R. E. Coggeshall, P. C. Emson, L. I. Benowitz and C. J. Woolf (1994). "GAP-43 expression in primary sensory neurons following central axotomy." J Neurosci **14**(7): 4375-84.

Chong, M. S., C. J. Woolf, N. S. Haque and P. N. Anderson (1999). "Axonal regeneration from injured dorsal roots into the spinal cord of adult rats." J Comp Neurol **410**(1): 42-54.

Chuaqui, R. F., R. F. Bonner, C. J. M. Best, J. W. Gillespie, M. J. Flaig, S. M. Hewitt, J. L. Phillips, D. B. Krizman, M. A. Tangrea, M. Ahram, W. M. Lineham, V. Knezevic and M. R. Emmert-Buck (2002). "Post-analysis follow-up and validation of microarray experiments." Nature Genetics **32**: 509-514.

Cironi, L., N. Riggi, P. Provero, N. Wolf, M. L. Suva, D. Suva, V. Kindler and I. Stamenkovic (2008). "IGF1 is a common target gene of Ewing's sarcoma fusion proteins in mesenchymal progenitor cells." PLoS ONE **3**(7): e2634.

Collazos-Castro, J. E., V. C. Muneton-Gomez and M. Nieto-Sampedro (2005). "Olfactory glia transplantation into cervical spinal cord contusion injuries." J Neurosurg Spine **3**(4): 308-17.

Cope, L. M., R. A. Irizarry, H. A. Jaffee, Z. Wu and T. P. Speed (2004). "A benchmark for Affymetrix GeneChip expression measures." Bioinformatics **20**(3): 323-31.

Costigan, M., K. Befort, L. Karchewski, R. S. Griffin, D. D'Urso, A. Allchorne, J. Sitarski, J. W. Mannion, R. E. Pratt and C. J. Woolf (2002). "Replicate high-density rat genome oligonucleotide microarrays reveal hundreds of regulated genes in the dorsal root ganglion after peripheral nerve injury." BMC Neurosci **3**: 16.

Costigan, M., K. Befort, L. Karchewski, R. S. Griffin, D. D'Urso, A. Allchorne, J. Sitarski, R. J. Mannion, R. E. Pratt and C. J. Woolf (2002). "Replicate high-density rat genome oligonucleotide microarrays reveal hundreds of regulated genes in the dorsal root ganglion after peripheral nerve injury." BMC Neuroscience **3** 16-33.

Costigan, M., T. A. Samad, A. Allchorne, C. Lanoue, S. Tate and C. J. Woolf (2003). "High basal expression and injury-induced down regulation of two regulator of G-protein signaling transcripts, RGS3 and RGS4 in primary sensory neurons." Mol Cell Neurosci **24**(1): 106-16.

Dallas, P. B., N. G. Gottardo, M. J. Firth, A. H. Beesley, K. Hoffmann, P. A. Terry, J. R. Freitas, J. M. Boag, A. J. Cummings and U. R. Kees (2005). "Gene expression levels assessed by oligonucleotide microarray analysis and quantitative real-time RT-PCR -- how well do they correlate?" BMC Genomics **6**(1): 59.

Danielsen, N., G. Lundborg and M. Frizell (1986). "Nerve repair and axonal transport: outgrowth delay and regeneration rate after transection and repair of rabbit hypoglossal nerve." Brain Res **376**(1): 125-32.

Daniloff, J. K., G. Levi, M. Grumet, F. Rieger and G. M. Edelman (1986). "Altered expression of neuronal cell adhesion molecules induced by nerve injury and repair." J Cell Biol **103**(3): 929-45.

David, S. and A. J. Aguayo (1981). "Axonal elongation into peripheral nervous system bridges after central nervous system injury in adult rats." Science **214**: 931-933.

Davison, S. P., T. V. McCaffrey, M. N. Porter and E. Manders (1999). "Improved nerve regeneration with neutralization of transforming growth factor-beta1." Laryngoscope **109**(4): 631-5.

De Biase, A., S. M. Knoblach, S. Di Giovanni, C. Fan, A. Molon, E. P. Hoffman and A. I. Faden (2005). "Gene expression profiling of experimental traumatic spinal cord injury as a function of distance from impac site and injury severity." Physiol Genomics **22**(3): 368-81.

de Celis, J. F. and S. Bray (1997). "Feed-back mechanisms affecting Notch activation at the dorsoventral boundary in the Drosophila wing." Development **124**(17): 3241-51.

De Leon, M., R. L. Nahin, C. A. Molina, D. D. De Leon and M. A. Ruda (1995). "Comparison of c-jun, junB, and junD mRNA expression and protein in the rat dorsal root ganglia following sciatic nerve transection." J Neurosci Res **42**(3): 391-401.

De Leon, M., A. A. Welcher, R. H. Nahin, Y. Liu, M. A. Ruda, E. M. Shooter and C. A. Molina (1996). "Fatty acid binding protein is induced in neurons of the dorsal root ganglia after peripheral nerve injury." J Neurosci Res **44**(3): 283-92.

de Reynies, A., D. Geromin, J. M. Cayuela, F. Petel, P. Dessen, F. Sigaux and D. S. Rickman (2006). "Comparison of the latest commercial short and long oligonucleotide microarray technologies." BMC Genomics **7**: 51.

de Wit, J. and J. Verhaagen (2003). "Role of semaphorins in the adult nervous system." Prog Neurobiol **71**(2-3): 249-67.

Dent, E. W. and F. B. Gertler (2003). "Cytoskeletal dynamics and transport in growth cone motility and axor guidance." Neuron **40**: 209-227.

Dergham, P., B. Ellezam, C. Essagian, H. Avedissian, W. D. Lubell and L. McKerracher (2002). "Rho signalling pathway targeted to promote spinal cord repair." The Journal of Neuroscience **22**(15): 6570-6577

Dheda, K., J. F. Huggett, S. A. Bustin, M. A. Johnson, G. Rook and A. Zumla (2004). "Validation of housekeeping genes for normalizing RNA expression in real-time PCR." Biotechniques **37**(1): 112-4, 116, 118-9.

Di Giovanni, S., A. I. Faden, A. Yakovlev, J. S. Duke-Cohan, T. Finn, M. Thouin, S. Knoblach, A. De Biase, B. S. Bregman and E. P. Hoffman (2005). "Neuronal plasticity after spinal cord injury: identification of a gene cluster driving neurite outgrowth." Faseb J **19**(1): 153-4.

Di Giovanni, S., S. M. Knoblach, C. Brandoli, S. A. Aden, E. P. Hoffman and A. I. Faden (2003). "Gene profiling in spinal cord injury shows role of cell cycle neuronal death." Annual Neurology **53**: 454-468.

Di Giovanni, S., S. M. Knoblach, C. Brandoli, S. A. Aden, E. P. Hoffman and A. I. Faden (2003). "Gene profiling in spinal cord injury shows role of cell cycle in neuronal death." Ann Neurol **53**(4): 454-68.

Dib-Hajj, S., J. A. Black, P. Felts and S. G. Waxman (1996). "Down-regulation of transcripts for Na channel alpha-SNS in spinal sensory neurons following axotomy." Proc Natl Acad Sci U S A **93**(25): 14950-4.

Dib-Hajj, S. D., L. Tyrrell, J. A. Black and S. G. Waxman (1998). "NaN, a novel voltage-gated Na channel, is expressed preferentially in peripheral sensory neurons and down-regulated after axotomy." Proc Natl Acad Sci U S A **95**(15): 8963-8.

Dodd, J. and A. Schuchardt (1995). "Axon guidance: A compelling case for repelling growth cones." Cell **81** 471-474.

Dorn, G., S. Patel, G. Wotherspoon, M. Hemmings-Mieszczak, J. Barclay, F. J. Natt, P. Martin, S. Bevan, A. Fox, P. Ganju, W. Wishart and J. Hall (2004). "siRNA relieves chronic neuropathic pain." Nucleic Acids Res **32**(5): e49.

Drees, F. and F. B. Gertler (2008). "Ena/VASP: proteins at the tip of the nervous system." Curr Opin Neurobiol **18**(1): 53-9.

Dube, G. R., K. L. Kohlhaas, L. E. Rueter, C. S. Surowy, M. D. Meyer and C. A. Briggs (2005). "Loss of functional neuronal nicotinic receptors in dorsal root ganglion neurons in a rat model of neuropathic pain." Neurosci Lett **376**(1): 29-34.

Dusart, I., A. Ghoumari, R. Wehrle, M. P. Morel, L. Bouslama-Oueghlani, E. Camand and C. Sotelo (2005). "Cell death and axon regeneration of Purkinje cells after axotomy: challenges of classical hypotheses of axon regeneration." Brain Res Brain Res Rev **49**(2): 300-16.

Eddleston, M. and L. Mucke (1993). "Molecular profile of reactive astrocytes-Implications for their role in neurologic disease." Neuroscience **54**: 15-36.

Ehlers, M. D. (2004). "Deconstructing the axon: Wallerian degeneration and the ubiquitin-proteasome system." Trends in Neurosciences **27**(1): 3-6.

Ekstrom, P. A., U. Mayer, A. Panjwani, D. Pountney, J. Pizzey and D. A. Tonge (2003). "Involvement of alpha7beta1 integrin in the conditioning-lesion effect on sensory axon regeneration." Mol Cell Neurosci **22**(3): 383-95.

Emery, D. L., N. C. Royo, I. Fischer, K. E. Saatman and T. K. McIntosh (2003). "Plasticity following injury to the adult central nervous system: is recapitulation of a developmental state worth promoting?" J

Neurotrauma **20**(12): 1271-92.

Endo, Y. and J. S. Rubin (2007). "Wnt signaling and neurite outgrowth: insights and questions." Cancer Sci **98**(9): 1311-7.

Fawcett, J. W. (1992). "Intrinsic neuronal determinants of regeneration." Trends Neurosci **15**(1): 5-8.

Fawcett, J. W. and R. A. Asher (1999). "The glial scar and central nervous system repair." Brain Research Bulletin **49**(6): 377-391.

Fawcett, J. W., E. Housden, L. Smith-Thomas and R. L. Meyer (1989). "The growth of axons in three dimensional astrocyte cultures." Developmental Biology **135**: 449-458.

Fernandes, K. and W. Tetzlaff (2001). Gene expression in axotomised neurons: Identifying the intrinsic determinants of axonal growth. Axoal regeneration in the central nervous system. N. Ingoglia and M. Murray. New York, Marcel Dekker**:** 219-266.

Ferreira, A., H. T. Kao, J. Feng, M. Rapoport and P. Greengard (2000). "Synapsin III: developmental expression, subcellular localization, and role in axon formation." J Neurosci **20**(10): 3736-44.

Figueiredo, A., A. M. Fortes, S. Ferreira, M. Sebastiana, Y. H. Choi, L. Sousa, B. Acioli-Santos, F. Pessoa, R. Verpoorte and M. S. Pais (2008). "Transcriptional and metabolic profiling of grape (Vitis vinifera L.) leaves unravel possible innate resistance against pathogenic fungi." J Exp Bot **59**(12): 3371-81.

Fodor, S., J. Read, M. Pirrung, L. Stryer, A. Lu and D. Solas (1991). "Light-directed spatially addressable parallel chemical synthesis." Science **251**(4995): 767-773.

Forman, D. S. and R. A. Berenberg (1978). "Regeneration of motor axons in the rat sciatic nerve studied by labeling with axonally transported radioactive proteins." Brain Res **156**(2): 213-25.

Forman, D. S., D. K. Wood and S. DeSilva (1979). "Rate of regeneration of sensory axons in transected rat sciatic nerve repaired with epineurial sutures." J Neurol Sci **44**(1): 55-9.

Francis, J. S., M. Dragunow and M. J. During (2004). "Over expression of ATF-3 protects rat hippocampal neurons from in vivo injection of kainic acid." Brain Res Mol Brain Res **124**(2): 199-203.

Franklin, J. L., B. E. Berechid, F. B. Cutting, A. Presente, C. B. Chambers, D. R. Foltz, A. Ferreira and J. S. Nye (1999). "Autonomous and non-autonomous regulation of mammalian neurite development by Notch1 and Delta1." Curr Biol **9**(24): 1448-57.

Fukuoka, T., A. Tokunaga, E. Kondo, K. Miki, T. Tachibana and K. Noguchi (1998). "Change in mRNAs for neuropeptides and the GABA(A) receptor in dorsal root ganglion neurons in a rat experimental neuropathic pain model." Pain **78**(1): 13-26.

Gallinat, S., M. Yu, A. Dorst, T. Unger and T. Herdegen (1998). "Sciatic nerve transection evokes lasting up-regulation of angiotensin AT2 and AT1 receptor mRNA in adult rat dorsal root ganglia and sciatic nerves." Brain Res Mol Brain Res **57**(1): 111-22.

Gao, Y., K. Deng, J. Hou, J. B. Bryson, A. Barco, E. Nikulina, T. Spencer, W. Mellado, E. R. Kandel and M. T. Filbin (2004). "Activated CREB is sufficient to overcome inhibitors in myelin and promote spinal axon regeneration in vivo." Neuron **44**(4): 609-21.

Garnier, M., P. F. Zaratin, G. Ficalora, M. Valente, L. Fontanella, M. H. Rhee, K. J. Blumer and M. A. Scheideler (2003). "Up-regulation of regulator of G protein signaling 4 expression in a model of neuropathic pain and insensitivity to morphine." J Pharmacol Exp Ther **304**(3): 1299-306.

Gaudet, A. D., S. J. Williams, L. P.-R. Hwi and M. S. Ramer (2004). "Regulation of TRPV2 by axotomy in sympathetic, but not sensory neurons." Brain Research **1017**: 155-162.

Gavazzi, I., J. Stonehouse, A. Sandvig, J. N. Reza, L. S. Appiah-Kubi, R. Keynes and J. Cohen (2000). "Peripheral, but not central, axotomy induces neuropilin-1 mRNA expression in adult large diameter primary

sensory neurons." J Comp Neurol **423**(3): 492-9.

George, E. B., J. D. Glass and J. W. Griffin (1995). "Axotomy-induced axonal degeneration is mediated by calcium influx through ion-specific channels." The Journal of Neuroscience **15**(10): 6445-6452.
Ghooray, G. T. and G. F. Martin (1993). "The development of myelin in the spinal cord of the North American opossum and its possible role in loss of rubrospinal plasticity. A study using myelin basic protein and galactocerebroside immuno-histochemistry." Brain Res Dev Brain Res **72**(1): 67-74.

Giger, R. J., R. J. Pasterkamp, S. Heijnen, A. J. Holtmaat and J. Verhaagen (1998). "Anatomical distribution of the chemorepellent semaphorin III/collapsin-1 in the adult rat and human brain: predominant expression in structures of the olfactory-hippocampal pathway and the motor system." J Neurosci Res **52**(1): 27-42.

Gillardon, F., L. Klimaschewski, H. Wickert, S. Krajewski, J. C. Reed and M. Zimmermann (1996). "Expression pattern of candidate cell death effector proteins Bax, Bcl-2, Bcl-X, and c-Jun in sensory and motor neurons following sciatic nerve transection in the rat." Brain Res **739**(1-2): 244-50.

Gillardon, F., H. Wickert and M. Zimmermann (1994). "Differential expression of bcl-2 and bax mRNA in axotomized dorsal root ganglia of young and adult rats." Eur J Neurosci **6**(10): 1641-4.

Glass, J. D., D. G. Culver, A. I. Levey and N. R. Nash (2002). "Very early activation of m-calpain in peripheral nerve during Wallerian degeneration." Journal of the Neurological Sciences **196**: 9-20.

Godfrey, T. E. and L. A. Kelly (2005). "Development of quantitative reverse transcriptase PCR assays for measuring gene expression." Methods Mol Biol **291**: 423-45.

Goldberg, D. J. and D. W. Burmeister (1986). "Stages in axon formation: Observations of growth of Aplysia axons in culture using video-enhanced contrast-differential interference contrast microscopy." Journal of Cell Biology **103**: 1921-1931.

Golz, G., L. Uhlmann, D. Ludecke, N. Markgraf, R. Nitsch and S. Hendrix (2006). "The cytokine/neurotrophin axis in peripheral axon outgrowth." Eur J Neurosci **24**(10): 2721-30.

Gonzalez-Hernandez, T. and A. Rustioni (1999). "Expression of three forms of nitric oxide synthase in peripheral nerve regeneration." J Neurosci Res **55**(2): 198-207.

GrandPre, T., S. Li and S. M. Strittmatter (2002). "Nogo-66 receptor antagonist peptide promotes axonal regeneration." Nature **417**: 547-551.

Griffin, R. S., M. Costigan, G. J. Brenner, C. H. Ma, J. Scholz, A. Moss, A. J. Allchorne, G. L. Stahl and C. J. Woolf (2007). "Complement induction in spinal cord microglia results in anaphylatoxin C5a-mediated pair hypersensitivity." J Neurosci **27**(32): 8699-708.

Gurgo, R. D., K. S. Bedi and V. Nurcombe (2002). "Current concepts in central nervous system regeneration." Journal of Clinical Neuroscience **9**(6): 613-617.

Gurney, M. E., S. P. Heinrich, M. R. Lee and H. S. Yin (1986). "Molecular cloning and expression of neuroleukin, a neurotrophic factor for spinal and sensory neurons." Science **234**(4776): 566-74.

Hai, T., C. D. Wolfgang, D. K. Marsee, A. E. Allen and U. Sivaprasad (1999). "ATF3 and stress responses." Gene Expr **7**(4-6): 321-35.

Hall, A. (1998). "Rho GTPases and the actin cytoskeleton." Science **279**: 509-514.

Hamdi, M., H. E. Popeijus, F. Carlotti, J. M. Janssen, C. van der Burgt, P. Cornelissen-Steijger, B. van de Water, R. C. Hoeben, K. Matsuo and H. van Dam (2008). "ATF3 and Fra1 have opposite functions in JNK- and ERK-dependent DNA damage responses." DNA Repair (Amst) **7**(3): 487-96.

Han, J., L. Han, P. Tiwari, Z. Wen and J. Q. Zheng (2007). "Spatial targeting of type II protein kinase A to filopodia mediates the regulation of growth cone guidance by cAMP." J Cell Biol **176**(1): 101-11.

Hashimoto, M., M. Koda, H. Ino, K. Yoshinaga, A. Murata, M. Yamazaki, K. Kojima, K. Chiba, C. Mori and H. Moriya (2005). "Gene expression profiling of cathepsin D, metallothioneins-1 and -2, osteopontin, and tenascin-C in a mouse spinal cord injury model by cDNA microarray analysis." Acta Neuropathol **109**(2): 165-80.

Haviv, L., D. Gillo, F. Backouche and A. Bernheim-Groswasser (2008). "A cytoskeletal demolition worker: myosin II acts as an actin depolymerization agent." J Mol Biol **375**(2): 325-30.

Herdegen, T., C. E. Fiallos-Estrada, W. Schmid, R. Bravo and M. Zimmermann (1992). "The transcription factors c-JUN, JUN D and CREB, but not FOS and KROX-24, are differentially regulated in axotomized neurons following transection of rat sciatic nerve." Brain Res Mol Brain Res **14**(3): 155-65.

Hochman, S. (2007). "Spinal Cord." Curr Biol **17**(22): R950-R955.

Hokfelt, T., X. Zhang and Z. Wiesenfeld-Hallin (1994). "Messenger plasticity in primary sensory neurons following axotomy and its functional implications." Trends Neurosci **17**(1): 22-30.

Holloway, A. J., R. K. van Laar, R. W. Tothill and D. D. L. Bowtell (2002). "Options available-from start to finish- for obtaining data from DNA microarrays II." Nature Genetics **32**: 481-489.

Holmes, F. E., S. Mahoney, V. R. King, A. Bacon, N. C. Kerr, V. Pachnis, R. Curtis, J. V. Priestley and D. Wynick (2000). "Targeted disruption of the galanin gene reduces the number of sensory neurons and their regenerative capacity." Proc Natl Acad Sci U S A **97**(21): 11563-8.

Horvath, C. M. (2004). "The Jak-STAT pathway stimulated by interleukin 6." Sci STKE **2004**(260): tr9.

Hotta, A., R. Inatome, J. Yuasa-Kawada, Q. Qin, H. Yamamura and S. Yanagi (2005). "Critical role of collapsin response mediator protein-associated molecule CRAM for filopodia and growth cone development in neurons." Mol Biol Cell **16**(1): 32-9.

Hu, F. and S. M. Strittmatter (2008). "The N-terminal domain of Nogo-A inhibits cell adhesion and axonal outgrowth by an integrin-specific mechanism." J Neurosci **28**(5): 1262-9.

Hu, P., A. L. Bembrick, K. A. Keay and E. M. McLachlan (2007). "Immune cell involvement in dorsal root ganglia and spinal cord after chronic constriction or transection of the rat sciatic nerve." Brain Behav Immun **21**(5): 599-616.

Hu, P. and E. M. McLachlan (2002). "Macrophage and lymphocyte invasion of dorsal root ganglia after peripheral nerve lesions in the rat." Neuroscience **112**(1): 23-38.

Huang, D. W., L. McKerracher, P. E. Braun and S. David (1999). "A therapeutic vaccine approach to stimulate axon regeneration in the adult mammalian spinal cord." Neuron **24**: 639-647.

Huang, W. L., D. Robson, M. C. Liu, V. R. King, S. Averill, P. J. Shortland and J. V. Priestley (2006). "Spinal cord compression and dorsal root injury cause up-regulation of activating transcription factor-3 in large-diameter dorsal root ganglion neurons." Eur J Neurosci **23**(1): 273-8.

Hulsebosch, C. E., G. Y. Xu, J. R. Perez-Polo, K. N. Westlund, C. P. Taylor and D. J. McAdoo (2000). "Rodent model of chronic central pain after spinal cord contusion injury and effects of gabapentin." J Neurotrauma **17**(12): 1205-17.

Ikemoto, A., T. Kobayashi, S. Watanabe and H. Okuyama (1997). "Membrane fatty acid modifications of PC12 cells by arachidonate or docosahexaenoate affect neurite outgrowth but not norepinephrine release." Neurochem Res **22**(6): 671-8.

Irizarry, R. A., B. Hobbs, F. Collin, Y. D. Beazer-Barclay, K. J. Antonellis, U. Scherf and T. P. Speed (2003). "Exploration, normalization, and summaries of high density oligonucleotide array probe level data." Biostatistics **4**(2): 249-64.

Irizarry, R. A., B. Hobbs, F. Collin, Y. D. Beazer-Barclay, K. J. Antonellis, U. Scherf and T. P. Speed (2003). "Exploration, normalisation and summaries of high density oligonucleotide array probe level data."

Biostatistics **4**: 249-264.

Ishikawa, K., M. Tanaka, J. A. Black and S. G. Waxman (1999). "Changes in expression of voltage-gated potassium channels in dorsal root ganglion neurons following axotomy." Muscle Nerve **22**(4): 502-7.

Iwata, T., K. Namikawa, M. Honma, N. Mori, S. Yachiku and H. Kiyama (2002). "Increased expression of mRNAs for microtubule disassembly molecules during nerve regeneration." Brain Res Mol Brain Res **102**(1-2): 105-9.

Jacob, J. M. and I. G. McQuarrie (1991). "Axotomy accelerates slow component b of axonal transport." J Neurobiol **22**(6): 570-82.

Jacob, J. M. and I. G. McQuarrie (1993). "Acceleration of axonal outgrowth in rat sciatic nerve at one week after axotomy." J Neurobiol **24**(3): 356-67.

Jankowski, M. P., P. K. Cornuet, S. McIlwrath, H. R. Koerber and K. M. Albers (2006). "SRY-box containing gene 11 (Sox11) transcription factor is required for neuron survival and neurite growth." Neuroscience **143**(2): 501-14.

Ji, R. R., Q. Zhang, X. Zhang, F. Piehl, T. Reilly, R. F. Pettersson and T. Hokfelt (1995). "Prominent expression of bFGF in dorsal root ganglia after axotomy." Eur J Neurosci **7**(12): 2458-68.

Jiang, Y. Q., J. Pickett and M. M. Oblinger (1994). "Comparison of changes in beta-tubulin and NF gene expression in rat DRG neurons under regeneration-permissive and regeneration-prohibitive conditions." Brain Res **637**(1-2): 233-41.

Jiao, J., X. Huang, R. A. Feit-Leithman, R. L. Neve, W. Snider, D. A. Dartt and D. F. Chen (2005). "Bcl-2 enhances Ca(2+) signaling to support the intrinsic regenerative capacity of CNS axons." Embo J **24**(5): 1068-78.

Jin, H. K., A. Takada, Y. Kon, O. Haller and T. Watanabe (1999). "Identification of the murine Mx2 gene: interferon-induced expression of the Mx2 protein from the feral mouse gene confers resistance to vesicular stomatitis virus." J Virol **73**(6): 4925-30.

Jin, K., J. Chen, K. Kawaguchi, R. L. Zhu, R. A. Stetler, R. P. Simon and S. H. Graham (1996). "Focal ischemia induces expression of the DNA damage-inducible gene GADD45 in the rat brain." Neuroreport **7**(11): 1797-802.

Jin, Z. and S. M. Strittmatter (1997). "Rac1 mediates collapsin-1-induced growth cone collapse." Journal of Neuroscience **17**: 6256-6263.

Jongsma, H., N. Danielsen, F. Sundler and M. Kanje (2000). "Alteration of PACAP distribution and PACAP receptor binding in the rat sensory nervous system following sciatic nerve transection." Brain Res **853**(2): 186-96.

Jourdain, I., S. Lachkar, E. Charbaut, B. Gigant, M. Knossow, A. Sobel and P. A. Curmi (2004). "A synergistic relationship between three regions of stathmin family proteins is required for the formation of a stable complex with tubulin." Biochem J **378**(Pt 3): 877-88.

Kamijo, Y., J. Koyama, S. Oikawa, Y. Koizumi, K. Yokouchi, N. Fukushima and T. Moriizumi (2003). "Regenerative process of the facial nerve: rate of regeneration of fibers and their bifurcations." Neurosci Res **46**(2): 135-43.

Karchewski, L. A., S. Bloechlinger and C. J. Woolf (2004). "Axonal injury-dependent induction of the peripheral benzodiazepine receptor in small-diameter adult rat primary sensory neurons." Eur J Neurosci **20**(3): 671-83.

Kasama, S., M. Kawakubo, T. Suzuki, T. Nishizawa, A. Ishida and J. Nakayama (2007). "RNA interference-mediated knock-down of transient receptor potential vanilloid 1 prevents forepaw inflammatory hyperalgesia in rat." Eur J Neurosci **25**(10): 2956-63.

Kashiba, H., B. Hyon and E. Senba (1998). "Glial cell line-derived neurotrophic factor and nerve growth factor receptor mRNAs are expressed in distinct subgroups of dorsal root ganglion neurons and are differentially regulated by peripheral axotomy in the rat." Neurosci Lett **252**(2): 107-10.

Kashiba, H., K. Noguchi, Y. Ueda and E. Senba (1994). "Neuropeptide Y and galanin are coexpressed in rat large type A sensory neurons after peripheral transection." Peptides **15**(3): 411-6.

Kashiba, H. and E. Senba (1999). "Up- and down-regulation of BDNF mRNA in distinct subgroups of rat sensory neurons after axotomy." Neuroreport **10**(17): 3561-5.

Kataoka, K., M. Kanje and L. B. Dahlin (2007). "Induction of activating transcription factor 3 after different sciatic nerve injuries in adult rats." Scand J Plast Reconstr Surg Hand Surg **41**(4): 158-66.

Kato, R., S. Kiryu-Seo and H. Kiyama (2002). "Damage-induced neuronal endopeptidase (DINE/ECEL) expression is regulated by leukemia inhibitory factor and deprivation of nerve growth factor in rat sensory ganglia after nerve injury." J Neurosci **22**(21): 9410-8.

Kendziorski, C., R. A. Irizarry, K. S. Chen, J. D. Haag and M. N. Gould (2005). "On the utility of pooling biological samples in microarray experiments." Proc Natl Acad Sci U S A **102**(12): 4252-7.

Kenney, A. M. and J. D. Kocsis (1997). "Temporal variability of jun family transcription factor levels in peripherally or centrally transected adult rat dorsal root ganglia." Brain Res Mol Brain Res **52**(1): 53-61.

Kerschensteiner, M., M. E. Schwab, J. W. Lichtman and T. Misgeld (2005). "In vivo imaging of axonal degeneration and regeneration in the injured spinal cord." Nat Med **11**(5): 572-7.

Kim, D. K., S. B. Han, S. T. Hong, Y. J. Choi, W. Sun, D. Geum and H. Kim (2008). "Expression of Sox11 and Brn transcription factors during development and following transient forebrain ischemia in the rat." Neurosci Lett **433**(3): 259-64.

Kim, D. S., J. O. Choi, H. D. Rim and H. J. Cho (2002). "Downregulation of voltage-gated potassium channel alpha gene expression in dorsal root ganglia following chronic constriction injury of the rat sciatic nerve." Brain Res Mol Brain Res **105**(1-2): 146-52.

King, O. D., R. E. Foulger, S. S. Dwight, J. V. White and F. P. Roth (2003). "Predicting gene function from patterns of annotation." Genome Res **13**(5): 896-904.

Kiryu-Seo, S. (2006). "Identification and functional analysis of damage-induced neuronal endopeptidase (DINE), a nerve injury associated molecule." Anat Sci Int **81**(1): 1-6.

Kiryu-Seo, S., R. Kato, T. Ogawa, S. Nakagomi, K. Nagata and H. Kiyama (2008). "Neuronal injury-inducible gene is synergistically regulated by ATF3, c-Jun, and STAT3 through the interaction with Sp1 in damaged neurons." J Biol Chem **283**(11): 6988-96.

Kiryushko, D., V. Berezin and E. Bock (2004). "Regulators of neurite outgrowth: role of cell adhesion molecules." Ann N Y Acad Sci **1014**: 140-54.

Klostermann, A., B. Lutz, F. Gertler and C. Behl (2000). "The orthologous human and murine semaphorin 6A-1 proteins (SEMA6A-1/Sema6A-1) bind to the enabled/vasodilator-stimulated phosphoprotein-like protein (EVL) via a novel carboxyl-terminal zyxin-like domain." J Biol Chem **275**(50): 39647-53.

Kolle, G., K. Georgas, G. P. Holmes, M. H. Little and T. Yamada (2000). "CRIM1, a novel gene encoding a cysteine-rich repeat protein, is developmentally regulated and implicated in vertebrate CNS development and organogenesis." Mech Dev **90**(2): 181-93.

Koriyama, Y., K. Homma, K. Sugitani, Y. Higuchi, T. Matsukawa, D. Murayama and S. Kato (2007). "Upregulation of IGF-I in the goldfish retinal ganglion cells during the early stage of optic nerve regeneration." Neurochem Int **50**(5): 749-56.

Kottis, V., P. Thibault, D. Mikol, Z. C. Xiao, R. Zhang, P. Dergham and P. E. Braun (2002). "Oligodendrocyte-myelin glycoprotein (OMgp) is an inhibitor of neurite outgrowth." Journal of

Neurochemistry **82**: 1566-1569.

Kozul, C. D., A. P. Nomikos, T. H. Hampton, L. A. Warnke, J. A. Gosse, J. C. Davey, J. E. Thorpe, B. P.

Kuhn, P. L. and J. R. Wrathall (1998). "A mouse model of graded contusive spinal cord injury." J Neurotrauma **15**(2): 125-40.

Jackson, M. A. Ihnat and J. W. Hamilton (2008). "Laboratory diet profoundly alters gene expression and confounds genomic analysis in mouse liver and lung." Chem Biol Interact **173**(2): 129-40.

Krekoski, C. A., I. M. Parhad and A. W. Clark (1996). "Attenuation and recovery of nerve growth factor receptor mRNA in dorsal root ganglion neurons following axotomy." J Neurosci Res **43**(1): 1-11.

Kubo, T., T. Yamashita, A. Yamaguchi, K. Hosokawa and M. Tohyama (2002). "Analysis of genes induced in peripheral nerve after axotomy using cDNA microarrays." J Neurochem **82**(5): 1129-36.

Kuno, K., Y. Okada, H. Kawashima, H. Nakamura, M. Miyasaka, H. Ohno and K. Matsushima (2000). "ADAMTS-1 cleaves a cartilage proteoglycan, aggrecan." FEBS Lett **478**(3): 241-5.

Kury, P., D. Abankwa, F. Kruse, R. Greiner-Petter and H. Werner Muller (2004). "Gene expression profiling reveals multiple novel intrinsic and extrinsic factors associated with axonal regeneration failure." European Journal of Neuroscience **19**: 32-42.

Lambrechts, A., A. V. Kwiatkowski, L. M. Lanier, J. E. Bear, J. Vandekerckhove, C. Ampe and F. B. Gertler (2000). "cAMP-dependent protein kinase phosphorylation of EVL, a Mena/VASP relative, regulates its interaction with actin and SH3 domains." J Biol Chem **275**(46): 36143-51.

Lammers, T. and S. Lavi (2007). "Role of type 2C protein phosphatases in growth regulation and in cellular stress signaling." Crit Rev Biochem Mol Biol **42**(6): 437-61.

Landry, M., K. Holmberg, X. Zhang and T. Hokfelt (2000). "Effect of axotomy on expression of NPY, galanin, and NPY Y1 and Y2 receptors in dorsal root ganglia and the superior cervical ganglion studied with double-labeling in situ hybridization and immunohistochemistry." Exp Neurol **162**(2): 361-84.

Larkin, J. E., B. C. Frank, H. Gavras, R. Sultana and J. Quackenbush (2005). "Independence and reproducibility across microarray platforms." Nat Methods **2**(5): 337-44.

LeBlanc, A. C. and J. F. Poduslo (1990). "Axonal modulation of myelin gene expression in the peripheral nerve." Journal of Neuroscience Research **26**: 317-326.

LeDoux, M. S., L. Xu, J. Xiao, B. Ferrell, D. L. Menkes and R. Homayouni (2006). "Murine central and peripheral nervous system transcriptomes: comparative gene expression." Brain Res **1107**(1): 24-41.

Lee, M.-L. T., F. C. Kuo, G. A. Whitmore and J. Skiar (2000). "Importance of replication in microarray gene expression studies: Statistical methods and evidence from repetitive cDNA hybridizations." Proceedings of the National Academy of Sciences USA **97**(18): 9834-9839.

Lehmann, M., A. Fournier, I. Selles-Navarro, P. Dergham and A. Sebok (1999). "Inactivation of Rho signalling pathway promotes CNS axon regeneration." Journal of Neuroscience **19**: 7537-7547.

Levin, M. E., J. G. Jin, R. R. Ji, J. Tong, J. D. Pomonis, D. J. Lavery, S. W. Miller and L. W. Chiang (2008). "Complement activation in the peripheral nervous system following the spinal nerve ligation model of neuropathic pain." Pain **137**(1): 182-201.

Levy, D. and D. W. Zochodne (2000). "Increased mRNA expression of the B1 and B2 bradykinin receptors and antinociceptive effects of their antagonists in an animal model of neuropathic pain." Pain **86**(3): 265-71.

Li, C. and W. H. Wong (2001). "Model-based analysis of oligonucleotide arrays: expression index computation and outlier detection." Proc Natl Acad Sci U S A **98**(1): 31-6.

Li, J., M. Pankratz and J. A. Johnson (2002). "Differential gene expression patterns revealed by oligoncleotide versus long cDNA arrays." Toxicological Science **69**: 383-390.

Lieberman, A. R. (1971). "The axon reaction: A review of the principle features of perikaryon responses to axon injury." International Reviews in Neurobiology **14**: 49-124.

Liedtke, W., E. E. Leman, R. E. Fyffe, C. S. Raine and U. K. Schubart (2002). "Stathmin-deficient mice develop an age-dependent axonopathy of the central and peripheral nervous systems." Am J Pathol **160**(2): 469-80.

Liu, C. L., A. M. Jin and B. H. Tong (2003). "Detection of gene expression pattern in the early stage after spinal cord injury by gene chip." Chin J Traumatol **6**(1): 18-22.

Livesey, F. J. (2003). "Strategies for microarray analysis of limiting amounts of RNA." Briefings in Functional Genomics and Proteomics. **2**(1): 31-36.

Livesey, F. J., J. A. O'Brien, M. Li, A. G. Smith, L. J. Murphy and S. P. Hunt (1997). "A Schwann cell mitogen accompanying regeneration of motor neurons." Nature **390**(6660): 614-8.

Lozeron, P., C. Krarup and H. Schmalbruch (2004). "Regeneration of unmyelinated and myelinated sensory nerve fibres studied by a retrograde tracer method." J Neurosci Methods **138**(1-2): 225-32.

Lu, X. and P. M. Richardson (1991). "Inflammation near the nerve cell body enhances axonal regeneration." J Neurosci **11**(4): 972-8.

Lund, L. M. and I. G. McQuarrie (1996). "Axonal regrowth upregulates beta-actin and Jun D mRNA expression." J Neurobiol **31**(4): 476-86.

Luo, L., R. C. Salunga, H. Guo, A. Bittner, K. C. Joy, J. E. Galindo, H. Xiao, K. E. Rogers, J. S. Wan, M. R. Jackson and M. G. Erlander (1999). "Gene expression profiles of laser-captured adjacent neuronal subtypes." Nat Med **5**(1): 117-22.

Luo, Y., D. Raible and J. A. Raper (1993). "Collapsin: a protein in brain that induces the collapse and paralysis of neuronal growth cones." Cell **75**(2): 217-27.

Luo, Z. D., S. R. Chaplan, E. S. Higuera, L. S. Sorkin, K. A. Stauderman, M. E. Williams and T. L. Yaksh (2001). "Upregulation of dorsal root ganglion (alpha)2(delta) calcium channel subunit and its correlation with allodynia in spinal nerve-injured rats." J Neurosci **21**(6): 1868-75.

Ma, W. and M. A. Bisby (1998). "Partial and complete sciatic nerve injuries induce similar increases of neuropeptide Y and vasoactive intestinal peptide immunoreactivities in primary sensory neurons and their central projections." Neuroscience **86**(4): 1217-34.

Ma, W. and M. A. Bisby (1999). "Increase of galanin mRNA in lumbar dorsal root ganglion neurons of adult rats after partial sciatic nerve ligation." Neurosci Lett **262**(3): 195-8.

Mandys, V., R. van der Neut, P. R. Bar and W. H. Gispen (1991). "Cultivation of rat fetal spinal cord slices in a semi-solid medium: a new approach to studying axonal outgrowth and regeneration." J Neurosci Methods **38**(1): 63-9.

Martinez, J. C., C. Malave, I. Bosch, C. Castillo, J. Nunez, G. M. Villegas and R. Villegas (2004). "A real-time quantitative PCR comparative study between rat optic and sciatic nerves: determination of neuregulin-1 mRNA levels." Brain Res Mol Brain Res **130**(1-2): 49-60.

Mauti, O., E. Domanitskaya, I. Andermatt, R. Sadhu and E. T. Stoeckli (2007). "Semaphorin6A acts as a gate keeper between the central and the peripheral nervous system." Neural Develop **2**: 28.

McKerracher, L., S. David, D. L. Jackson, V. Kottis, R. J. Dunn and P. E. Braun (1994). "Identification of myelin-associated glycoprotein as a major myelin-derived inhibitor of neurite growth." Neuron **13**: 805-811.

McKerracher, L. and M. J. Winton (2002). "Nogo on the go." Neuron **36**: 345-348.

McPhail, L. T., J. F. Borisoff, B. Tsang, L. P. Hwi, J. M. Kwiecien and M. S. Ramer (2007). "Protracted myelin clearance hinders central primary afferent regeneration following dorsal rhizotomy and delayed neurotrophin-3 treatment." Neurosci Lett **411**(3): 206-11.

McQuarrie, I. G. (1975). "Nerve regeneration and thyroid hormone treatment." J Neurol Sci **26**(4): 499-502.

McQuarrie, I. G. and J. M. Jacob (1991). "Conditioning nerve crush accelerates cytoskeletal protein transport in sprouts that form after a subsequent crush." J Comp Neurol **305**(1): 139-47.

Medeiros, N. A., D. T. Burnette and P. Forscher (2006). "Myosin II functions in actin-bundle turnover in neuronal growth cones." Nat Cell Biol **8**(3): 215-26.

Menetski, J., S. Mistry, M. Lu, J. S. Mudgett, R. M. Ransohoff, J. A. Demartino, D. E. Macintyre and C. Abbadie (2007). "Mice overexpressing chemokine ligand 2 (CCL2) in astrocytes display enhanced nociceptive responses." Neuroscience **149**(3): 706-14.

Metz, G. A., A. Curt, H. van de Meent, I. Klusman, M. E. Schwab and V. Dietz (2000). "Validation of the weight-drop contusion model in rats: a comparative study of human spinal cord injury." J Neurotrauma **17**(1): 1-17.

Merry, D. E., D. J. Veis, W. F. Hickey and S. J. Korsmeyer (1994). "bcl-2 protein expression is widespread in the developing nervous system and retained in the adult PNS." Development **120**(2): 301-11.

Michael, G. J. and J. V. Priestley (1999). "Differential expression of the mRNA for the vanilloid receptor subtype 1 in cells of the adult rat dorsal root and nodose ganglia and its downregulation by axotomy." J Neurosci **19**(5): 1844-54.

Mika, J. (2008). "Modulation of microglia can attenuate neuropathic pain symptoms and enhance morphine effectiveness." Pharmacol Rep **60**(3): 297-307.

Miron, M., O. Z. Woody, A. Marcil, C. Murie, R. Sladek and R. Nadon (2006). "A methodology for global validation of microarray experiments." BMC Bioinformatics **7**: 333.

Morales, M., N. McCollum and E. F. Kirkness (2001). "5-HT(3)-receptor subunits A and B are co-expressed in neurons of the dorsal root ganglion." J Comp Neurol **438**(2): 163-72.

Morest, D. K. and D. A. Cotanche (2004). "Regeneration of the inner ear as a model of neural plasticity." Journal of Neuroscience Research **78**: 455-460.

Morgan, B. P. and P. Gasque (1996). "Expression of complement in the brain: role in health and disease." Immunol Today **17**(10): 461-6.

Morris, R. J. and M.-C. Tiveron (1994). "How the growth cone recognizes and responds to its environment." Developmental Biology **5**: 391-402.

Moskowitz, P. F., R. Smith, J. Pickett, A. Frankfurter and M. M. Oblinger (1993). "Expression of the class III beta-tubulin gene during axonal regeneration of rat dorsal root ganglion neurons." J Neurosci Res **34**(1): 129-34.

Mudge, A. W. (1981). "Effect of non-neuronal cells on peptide content of cultured sensory neurones." J Exp Biol **95**: 195-203.

Mulder, H., Y. Zhang, N. Danielsen and F. Sundler (1997). "Islet amyloid polypeptide and calcitonin gene-related peptide expression are down-regulated in dorsal root ganglia upon sciatic nerve transection." Brain Res Mol Brain Res **47**(1-2): 322-30.

Murphy, P. G., J. Grondin, M. Altares and P. M. Richardson (1995). "Induction of interleukin-6 in axotomized sensory neurons." J Neurosci **15**(7 Pt 2): 5130-8.

Murray, A. J. and D. A. Shewan (2008). "Epac mediates cyclic AMP-dependent axon growth, guidance and

regeneration." Mol Cell Neurosci **38**(4): 578-88.

Naik, A. K., S. Pathirathna and V. Jevtovic-Todorovic (2008). "GABA(A) receptor modulation in dorsal root ganglia in vivo affects chronic pain after nerve injury." Neuroscience **154**(4): 1539-53.

Nakamura, F., R. G. Kalb and S. M. Strittmatter (2000). "Molecular basis of semaphorin-mediated axon guidance." J Neurobiol **44**(2): 219-29.

Nakanishi, R., M. Shimizu, M. Mori, H. Akiyama, S. Okudaira, B. Otsuki, M. Hashimoto, K. Higuchi, M. Hosokawa, T. Tsuboyama and T. Nakamura (2006). "Secreted frizzled-related protein 4 is a negative regulator of peak BMD in SAMP6 mice." J Bone Miner Res **21**(11): 1713-21.

Nakazawa, T., H. Morii, M. Tamai and N. Mori (2005). "Selective upregulation of RB3/stathmin4 by ciliary neurotrophic factor following optic nerve axotomy." Brain Res **1061**(2): 97-106.

Nath, R. K., B. Kwon, S. E. Mackinnon, J. N. Jensen, S. Reznik and S. Boutros (1998). "Antibody to transforming growth factor beta reduces collagen production in injured peripheral nerve." Plast Reconstr Surg **102**(4): 1100-6; discussion 1107-8.

Nath, R. K., S. E. Mackinnon, J. N. Jensen and W. C. Parks (1997). "Spatial pattern of type I collagen expression in injured peripheral nerve." J Neurosurg **86**(5): 866-70.

Nesic, O., N. M. Svrakic, G. Y. Xu, D. McAdoo, K. N. Westlund, C. E. Hulsebosch, Z. Ye, A. Galante, P. Soteropoulos, P. Tolias, W. Young, R. P. Hart and J. R. Perez-Polo (2002). "DNA microarray analysis of the contused spinal cord: effect of NMDA receptor inhibition." J Neurosci Res **68**(4): 406-23.

Neuman, K., A. Soosaar, H. O. Nornes and T. Neuman (1995). "Orphan receptor COUP-TF I antagonizes retinoic acid-induced neuronal differentiation." J Neurosci Res **41**(1): 39-48.

Neumann, S., F. Bradke, M. Tessier-Lavigne and A. I. Basbaum (2002). "Regeneration of sensory axons within the injured spinal cord induced by intraganglionic cAMP elevation." Neuron **34**(6): 885-93.

Neumann, S. and C. J. Woolf (1999). "Regeneration of dorsal column fibers into and beyond the lesion site following adult spinal cord injury." Neuron **23**: 83-91.

Newton, R. A., S. Bingham, P. D. Davey, A. D. Medhurst, V. Piercy, P. Raval, A. A. Parsons, G. J. Sanger, C. P. Case and S. N. Lawson (2000). "Identification of differentially expressed genes in dorsal root ganglia following partial sciatic nerve injury." Neuroscience **95**(4): 1111-20.

Ng, W. P. and A. M. Lozano (1999). "Neuronal age influences the response to neurite outgrowth inhibitory activity in the central and peripheral nervous systems." Brain Res **836**(1-2): 49-61.

Nicholson, R., J. Small, A. K. Dixon, D. Spanswick and K. Lee (2003). "Serotonin receptor mRNA expression in rat dorsal root ganglion neurons." Neurosci Lett **337**(3): 119-22.

Noguchi, K., E. Senba, Y. Morita, M. Sato and M. Tohyama (1990). "Alpha-CGRP and beta-CGRP mRNAs are differentially regulated in the rat spinal cord and dorsal root ganglion." Brain Res Mol Brain Res **7**(4): 299-304.

O'Brien, J. J. and N. M. Nathanson (2007). "Retrograde activation of STAT3 by leukemia inhibitory factor in sympathetic neurons." J Neurochem **103**(1): 288-302.

Obata, K., H. Yamanaka, T. Fukuoka, D. Yi, A. Tokunaga, N. Hashimoto, H. Yoshikawa and K. Noguchi (2003). "Contribution of injured and uninjured dorsal root ganglion neurons to pain behavior and the changes in gene expression following chronic constriction injury of the sciatic nerve in rats." Pain **101**(1-2): 65-77.

Oblinger, M. M., J. Wong and L. M. Parysek (1989). "Axotomy-induced changes in the expression of a type III neuronal intermediate filament gene." J Neurosci **9**(11): 3766-75.

Okamura, A., S. Goto, T. Nishi, T. Hamasaki and Y. Ushio (1999). "Overexpression of striatal enriched

phosphatase (STEP) promotes the neurite outgrowth induced by a cAMP analogue in PC12 cells." Brain Res Mol Brain Res **67**(1): 1-9.

Okuse, K., S. R. Chaplan, S. B. McMahon, Z. D. Luo, N. A. Calcutt, B. P. Scott, A. N. Akopian and J. N. Wood (1997). "Regulation of expression of the sensory neuron-specific sodium channel SNS in inflammatory and neuropathic pain." Mol Cell Neurosci **10**(3-4): 196-207.

Omeis, I. A., Y. C. Hsu and M. S. Perin (1996). "Mouse and human neuronal pentraxin 1 (NPTX1): conservation, genomic structure, and chromosomal localization." Genomics **36**(3): 543-5.

Osakada, F., S. Ooto, T. Akagi, M. Mandai, A. Akaike and M. Takahashi (2007). "Wnt signaling promotes regeneration in the retina of adult mammals." J Neurosci **27**(15): 4210-9.

Park, P. J., Y. A. Cao, S. Y. Lee, J.-W. Kim, M. S. Chang, R. Hart and S. Choi (2004). "Current issues for DNA microarrays: platform comparison double linear amplification, and universal RNA reference." Journal of Biotechnology **112**: 225-245.

Park, S. Y., J. Y. Choi, R. U. Kim, Y. S. Lee, H. J. Cho and D. S. Kim (2003). "Downregulation of voltage-gated potassium channel alpha gene expression by axotomy and neurotrophins in rat dorsal root ganglia." Mol Cells **16**(2): 256-9.

Pasterkamp, R. J., P. N. Anderson and J. Verhaagen (2001). "Peripheral nerve injury fails to induce growth of lesioned ascending dorsal column axons into spinal cord scar tissue expressing the axon repellent Semaphorin3A." European Journal of Neuroscience **13**: 457-471.

Pasterkamp, R. J. and J. Verhaagen (2001). "Emerging roles for semaphorins in neural regeneration." Brain Research Reviews **35**: 36-54.

Pasterkamp, R. J. and J. Verhaagen (2006). "Semaphorins in axon regeneration: developmental guidance molecules gone wrong?" Philos Trans R Soc Lond B Biol Sci **361**(1473): 1499-511.

Pearson, A. G., C. W. Gray, J. F. Pearson, J. M. Greenwood, M. J. During and M. Dragunow (2003). "ATF3 enhances c-Jun-mediated neurite sprouting." Brain Res Mol Brain Res **120**(1): 38-45.

Perera, M., G. R. Merlo, S. Verardo, L. Paleari, G. Corte and G. Levi (2004). "Defective neuronogenesis in the absence of Dlx5." Mol Cell Neurosci **25**(1): 153-61.

Perlson, E., S. Hanz, K. F. Medzihradszky, A. L. Burlingame and M. Fainzilber (2004). "From snails to sciatic nerve: Retrograde injury signaling from axon to soma in lesioned neurons." J Neurobiol **58**(2): 287-94.

Petersen, D., G. V. Chandramouli, J. Geoghegan, J. Hilburn, J. Paarlberg, C. H. Kim, D. Munroe, L. Gangi, J. Han, R. Puri, L. Staudt, J. Weinstein, J. C. Barrett, J. Green and E. S. Kawasaki (2005). "Three microarray platforms: an analysis of their concordance in profiling gene expression." BMC Genomics **6**(1): 63.

Pettersson, L. M., L. B. Dahlin and N. Danielsen (2004). "Changes in expression of PACAP in rat sensory neurons in response to sciatic nerve compression." Eur J Neurosci **20**(7): 1838-48.

Pfaffl, M. W., G. W. Horgan and L. Dempfle (2002). "Relative expression software tool (REST) for group-wise comparison and statistical analysis of relative expression results in real-time PCR." Nucleic Acids Res **30**(9): e36.

Prinjha, R. K., S. E. Moore, M. Vinson, S. Blake, R. Morrow, G. Christie, D. Michalovich, D. L. Simmons and F. S. Walsh (2000). "Inhibitor of neurite outgrowth in humans." Nature **403**: 383-384.

Prislei, S., S. Mozzetti, F. Filippetti, M. De Donato, G. Raspaglio, L. Cicchillitti, G. Scambia and C. Ferlini (2008). "From plasma membrane to cytoskeleton: a novel function for semaphorin 6A." Mol Cancer Ther **7**(1): 233-41.

Profyrus, C., S. S. Cheema, D. W. Zang, M. F. Azari, K. Boyle and S. Petratos (2004). "Degenerative and

regenerative mechanisms governing spinal cord injury." Neurobiology of Disease **15**: 415-436.

Qiu, J., W. B. Cafferty, S. B. McMahon and S. W. Thompson (2005). "Conditioning injury-induced spinal axon regeneration requires signal transducer and activator of transcription 3 activation." J Neurosci **25**(7): 1645-53.

Qiu, J., D. Cai, H. Dai, M. McAtee, P. N. Hoffman, B. S. Bregman and M. T. Filbin (2002). "Spinal axon regeneration induced by elevation of cyclic AMP." Neuron **34**(6): 895-903.

Qiu, Y., A. J. Cooney, S. Kuratani, F. J. DeMayo, S. Y. Tsai and M. J. Tsai (1994). "Spatiotemporal expression patterns of chicken ovalbumin upstream promoter-transcription factors in the developing mouse central nervous system: evidence for a role in segmental patterning of the diencephalon." Proc Natl Acad Sci U S A **91**(10): 4451-5.

Quaglia, X., A. T. Beggah, C. Seidenbecher and A. D. Zurn (2008). "Delayed priming promotes CNS regeneration post-rhizotomy in Neurocan and Brevican-deficient mice." Brain **131**(Pt 1): 240-9.

Rabert, D., Y. Xiao, Y. Yiangou, D. Kreder, L. Sangameswaran, M. R. Segal, C. A. Hunt, R. Birch and P. Anand (2004). "Plasticity of gene expression in injured human dorsal root ganglia revealed by GeneChip oligonucleotide microarrays." J Clin Neurosci **11**(3): 289-99.

Rabinovsky, E. D. (2004). "The multifunctional role of IGF-1 in peripheral nerve regeneration." Neurol Res **26**(2): 204-10.

Radtke, C., M. Sasaki, K. L. Lankford, P. M. Vogt and J. D. Kocsis (2008). "Potential of olfactory ensheathing cells for cell-based therapy in spinal cord injury." J Rehabil Res Dev **45**(1): 141-52.

Rajeevan, M. S., S. D. Veron, N. Taysavang and E. R. Unger (2001). "Validation of array-based gene expression profiles by real-time (kinetic) RT-PCR." Journal of Molecular Diagnostics **3**(1): 26-31.

Ramakers, C., J. M. Ruijter, R. H. Deprez and A. F. Moorman (2003). "Assumption-free analysis of quantitative real-time polymerase chain reaction (PCR) data." Neurosci Lett **339**(1): 62-6.

Ramer, M. S., T. Bishop, P. Dockery, M. S. Mobarak, D. O'Leary, J. P. Fraher, J. V. Priestley and S. B. McMahon (2002). "Neurotrophin-3-mediated regeneration and recovery of proprioception following dorsal rhizotomy." Molecular and Cellular Neuroscience **19**: 239-249.

Ramer, M. S., I. Duraisingam, J. V. Priestley and S. B. McMahon (2001). "Two-tiered inhibition of axon regeneration at the dorsal root entry zone." J Neurosci **21**(8): 2651-60.

Ravelli, R. B., B. Gigant, P. A. Curmi, I. Jourdain, S. Lachkar, A. Sobel and M. Knossow (2004). "Insight into tubulin regulation from a complex with colchicine and a stathmin-like domain." Nature **428**(6979): 198-202.

Rende, M., M. Morales, E. Brizi, R. Bruno, F. Bloom and P. P. Sanna (1999). "Modulation of serotonin 5-HT3 receptor expression in injured adult rat spinal cord motoneurons." Brain Res **823**(1-2): 234-40.

Resnick, D. K., C. Schmitt, G. S. Miranpuri, V. K. Dhodda, J. Isaacson and R. Vemuganti (2004). "Molecular evidence of repair and plasticity following spinal cord injury." Neuroreport **15**(5): 837-9.

Rezajooi, K., M. Pavlides, J. Winterbottom, W. B. Stallcup, P. J. Hamlyn, A. R. Lieberman and P. N. Anderson (2004). "NG2 proteoglycan expression in the peripheral nervous system: upregulation following injury and comparison with CNS lesions." Mol Cell Neurosci **25**(4): 572-84.

Rich, K. M., S. P. Disch and M. E. Eichler (1989). "The influence of regeneration and nerve growth factor or the neuronal cell body reaction to injury." J Neurocytol **18**(5): 569-76.

Riddell, J. S., M. Enriquez-Denton, A. Toft, R. Fairless and S. C. Barnett (2004). "Olfactory ensheathing cell grafts have minimal influence on regeneration at the dorsal root entry zone following rhizotomy." Glia **47**(2): 150-67.

Robinson, M., M. C. Parsons Perez, L. Tebar, J. Palmer, A. Patel, D. Marks, A. Sheasby, C. De Felipe, R. Coffin, F. J. Livesey and S. P. Hunt (2004). "FLRT3 is expressed in sensory neurons after peripheral nerve injury and regulates neurite outgrowth." Mol Cell Neurosci **27**(2): 202-14.

Rodriguez, F. J., A. Valero-Cabre and X. Navarro (2004). "Regeneration and functional recovery following peripheral nerve injury." Drug Discovery Today: Disease Models **1**(2): 177-185.

Rohm, B., A. Ottemeyer, M. Lohrum and A. W. Puschel (2000). "Plexin/neuropilin complexes mediate repulsion by the axonal guidance signal semaphorin 3A." Mech Dev **93**(1-2): 95-104.

Romero, M. I., N. Rangappa, M. G. Garry and G. M. Smith (2001). "Functional regeneration of chronically injured sensory afferents into adult spinal cord after neurotrophin gene therapy." The Journal of Neuroscience **21**(21): 8408-8416.

Rossi, F., S. Gianola and L. Corvetti (2007). "Regulation of intrinsic neuronal properties for axon growth and regeneration." Prog Neurobiol **81**(1): 1-28.

Rosslenbroich, V., L. Dai, S. L. Baader, A. A. Noegel, V. Gieselmann and J. Kappler (2005). "Collapsin response mediator protein-4 regulates F-actin bundling." Exp Cell Res **310**(2): 434-44.

Rudge, J. S. and J. Silver (1990). "Inhibition of neurite outgrowth on astroglial scars in vitro." Journal of Neuroscience **10**: 3594-3603.

Rudomin, P. and R. F. Schmidt (1999). "Presynaptic inhibition in the vertebrate spinal cord revisited." Exp Brain Res **129**(1): 1-37.

Sahay, A., C. H. Kim, J. P. Sepkuty, E. Cho, R. L. Huganir, D. D. Ginty and A. L. Kolodkin (2005). "Secreted semaphorins modulate synaptic transmission in the adult hippocampus." J Neurosci **25**(14): 3613-20.

Salie, R. and J. D. Steeves (2005). "IGF-1 and BDNF promote chick bulbospinal neurite outgrowth in vitro." Int J Dev Neurosci **23**(7): 587-98.

Sasaki, M., K. Ishizaki, H. Obata and F. Goto (2001). "Effects of 5-HT2 and 5-HT3 receptors on the modulation of nociceptive transmission in rat spinal cord according to the formalin test." Eur J Pharmacol **424**(1): 45-52.

Sasaki, M., S. Seo-Kiryu, R. Kato, S. Kita and H. Kiyama (2001). "A disintegrin and metalloprotease with thrombospondin type1 motifs (ADAMTS-1) and IL-1 receptor type 1 mRNAs are simultaneously induced in nerve injured motor neurons." Brain Res Mol Brain Res **89**(1-2): 158-63.

Schafers, M., C. Schmidt, C. Vogel, K. V. Toyka and C. Sommer (2002). "Tumor necrosis factor-alpha (TNF) regulates the expression of ICAM-1 predominantly through TNF receptor 1 after chronic constriction injury of mouse sciatic nerve." Acta Neuropathol **104**(2): 197-205.

Schmidt, E. F. and S. M. Strittmatter (2007). "The CRMP family of proteins and their role in Sema3A signaling." Adv Exp Med Biol **600**: 1-11.

Schmitt, A. B., S. Breuer, J. Liman, A. Buss, C. Schlangen, K. Pech, E. M. Hol, G. A. Brook, J. Noth and F.-W. Schwaiger (2003). "Identification of regeneration-associated genes after central and peripheral nerve injury." BMC Neuroscience **4**: 8-20.

Schmitt, C., G. S. Miranpuri, V. K. Dhodda, J. Isaacson, R. Vemuganti and D. K. Resnick (2006). "Changes in spinal cord injury-induced gene expression in rat are strain-dependent." Spine J **6**(2): 113-9.

Schmittgen, T. D. and B. A. Zakrajsek (2000). "Effect of experimental treatment on housekeeping gene expression: validation by real-time, quantitative RT-PCR." J Biochem Biophys Methods **46**(1-2): 69-81.

Schnell, L., S. Fearn, H. Klassen, M. E. Schwab and V. H. Perry (1999). "Acute inflammatory responses to mechanical lesions in the CNS: differences between brain and spinal cord." Eur J Neurosci **11**(10): 3648-58.

Schnoor, M., P. Cullen, J. Lorkowski, K. Stolle, H. Robenek, D. Troyer, J. Rauterberg and S. Lorkowski (2008). "Production of type VI collagen by human macrophages: a new dimension in macrophage functional heterogeneity." J Immunol **180**(8): 5707-19.

Schroeder, A., O. Mueller, S. Stocker, R. Salowsky, M. Leiber, M. Gassmann, S. Lightfoot, W. Menzel, M. Granzow and T. Ragg (2006). "The RIN: an RNA integrity number for assigning integrity values to RNA measurements." BMC Mol Biol **7**: 3.

Schwab, M. E. (1993). "Experimental aspects of spinal cord regeneration." Curr Opin Neurol Neurosurg **6**(4): 549-53.

Schwegler, G., M. E. Schwab and J. P. Kapfhammer (1995). "Increased collateral sprouting of primary afferents in the myelin-free spinal cord." J Neurosci **15**(4): 2756-67.

Seijffers, R., A. J. Allchorne and C. J. Woolf (2006). "The transcription factor ATF-3 promotes neurite outgrowth." Mol Cell Neurosci **32**(1-2): 143-54.

Seijffers, R., C. D. Mills and C. J. Woolf (2007). "ATF3 increases the intrinsic growth state of DRG neurons to enhance peripheral nerve regeneration." J Neurosci **27**(30): 7911-20.

Selvey, S., E. W. Thompson, K. Matthaei, R. A. Lea, M. G. Irving and L. R. Griffiths (2001). "Beta-actin--an unsuitable internal control for RT-PCR." Mol Cell Probes **15**(5): 307-11.

Sestan, N., S. Artavanis-Tsakonas and P. Rakic (1999). "Contact-dependent inhibition of cortical neurite growth mediated by notch signaling." Science **286**(5440): 741-6.

Shehab, S. A., R. C. Spike and A. J. Todd (2003). "Evidence against cholera toxin B subunit as a reliable tracer for sprouting of primary afferents following peripheral nerve injury." Brain Res **964**(2): 218-27.

Shi, T. J., K. Holmberg, Z. Q. Xu, H. Steinbusch, J. de Vente and T. Hokfelt (1998). "Effect of peripheral nerve injury on cGMP and nitric oxide synthase levels in rat dorsal root ganglia: time course and coexistence." Pain **78**(3): 171-80.

Shi, T. S., U. Winzer-Serhan, F. Leslie and T. Hokfelt (2000). "Distribution and regulation of alpha(2)-adrenoceptors in rat dorsal root ganglia." Pain **84**(2-3): 319-30.

Siironen, J., M. Sandberg, V. Vuorinen and M. Roytta (1992). "Laminin B1 and collagen type IV gene expression in transected peripheral nerve: reinnervation compared to denervation." J Neurochem **59**(6): 2184-92.

Siironen, J., E. Vuorio, M. Sandberg and M. Roytta (1996). "Expression of type I and III collagen and laminin beta1 after rat sciatic nerve crush injury." J Peripher Nerv Syst **1**(3): 209-21.

Sleeper, A. A., T. R. Cummins, S. D. Dib-Hajj, W. Hormuzdiar, L. Tyrrell, S. G. Waxman and J. A. Black (2000). "Changes in expression of two tetrodotoxin-resistant sodium channels and their currents in dorsal root ganglion neurons after sciatic nerve injury but not rhizotomy." J Neurosci **20**(19): 7279-89.

Slonim, D. K. (2002). "From patterns to pathways: gene-expression data analysis comes of age." Nature Genetics **32**: 502-508.

Smith, D. S. and J. H. Skene (1997). "A transcription-dependent switch controls competence of adult neurons for distinct modes of axon growth." J Neurosci **17**(2): 646-58.

Son, S. J., K. M. Lee, S. M. Jeon, E. S. Park, K. M. Park and H. J. Cho (2007). "Activation of transcription factor c-jun in dorsal root ganglia induces VIP and NPY upregulation and contributes to the pathogenesis of neuropathic pain." Exp Neurol **204**(1): 467-72.

Song, G., C. Cechvala, D. K. Resnick, R. J. Dempsey and V. L. Rao (2001). "GeneChip analysis after acute spinal cord injury in rat." J Neurochem **79**(4): 804-15.

Song, H., G. Ming, Z. He, M. Lehmann, L. McKerracher, M. Tessier-Lavigne and M. Poo (1998).

"Conversion of neuronal growth cone responses from repulsion to attraction by cyclic nucleotides." Science **281**(5382): 1515-8.

Song, X. Y., F. Li, F. H. Zhang, J. H. Zhong and X. F. Zhou (2008). "Peripherally-derived BDNF promotes regeneration of ascending sensory neurons after spinal cord injury." PLoS ONE **3**(3): e1707.

Speese, S. D. and V. Budnik (2007). "Wnts: up-and-coming at the synapse." Trends Neurosci **30**(6): 268-75.

Spencer, T., M. Domeniconi, Z. Cao and M. T. Fibin (2003). "New roles for old proteins in adult CNS axonal regeneration." Current Opinion in Neurobiology **13**: 133-139.

Spencer, T., M. Domeniconi, Z. Cao and M. T. Filbin (2003). "New roles for old proteins in adult CNS axonal regeneration." Curr Opin Neurobiol **13**(1): 133-9.

Spencer, T. and M. T. Filbin (2004). "A role for cAMP in regeneration of the adult mammalian CNS." J Anat **204**(1): 49-55.

Speth, C., M. P. Dierich and P. Gasque (2002). "Neuroinvasion by pathogens: a key role of the complement system." Mol Immunol **38**(9): 669-79.

Stam, F. J., H. D. MacGillavry, N. J. Armstrong, M. C. de Gunst, Y. Zhang, R. E. van Kesteren, A. B. Smit and J. Verhaagen (2007). "Identification of candidate transcriptional modulators involved in successful regeneration after nerve injury." Eur J Neurosci **25**(12): 3629-37.

Stark, G. R., I. M. Kerr, B. R. Williams, R. H. Silverman and R. D. Schreiber (1998). "How cells respond to interferons." Annu Rev Biochem **67**: 227-64.

Sten Shi, T. J., X. Zhang, K. Holmberg, Z. Q. Xu and T. Hokfelt (1997). "Expression and regulation of galanin-R2 receptors in rat primary sensory neurons: effect of axotomy and inflammation." Neurosci Lett **237**(2-3): 57-60.

Stobart, M. J., D. Parchaliuk, S. L. Simon, J. Lemaistre, J. Lazar, R. Rubenstein and J. D. Knox (2007). "Differential expression of interferon responsive genes in rodent models of transmissible spongiform encephalopathy disease." Mol Neurodegener **2**: 5.

Stolinski, C. (1995). "Structure and composition of the outer connective tissue sheaths of peripheral nerve." J Anat **186 (Pt 1)**: 123-30.

Stoll, G., S. Jander and R. R. Myers (2002). "Degeneration and regeneration of the peripheral nervous system: From Augustus Waller's observations to neuroinflammation." Journal of the Peripheral Nervous System. **7**: 13-27.

Stoll, G. and H. W. Muller (1999). "Nerve injury, axonal degeneration and neural regeneration: basic insights." Brain Pathology **9**: 313-325.

Sugitani, K., T. Matsukawa, Y. Koriyama, T. Shintani, T. Nakamura, M. Noda and S. Kato (2006). "Upregulation of retinal transglutaminase during the axonal elongation stage of goldfish optic nerve regeneration." Neuroscience **142**(4): 1081-92.

Sun, Y. and R. E. Zigmond (1996). "Leukaemia inhibitory factor induced in the sciatic nerve after axotomy is involved in the induction of galanin in sensory neurons." Eur J Neurosci **8**(10): 2213-20.

Sun, Y. and R. E. Zigmond (1996). "Involvement of leukemia inhibitory factor in the increases in galanin and vasoactive intestinal peptide mRNA and the decreases in neuropeptide Y and tyrosine hydroxylase mRNA in sympathetic neurons after axotomy." J Neurochem **67**(4): 1751-60.

Sweigreiter, R., A. R. Walmsley, B. Niederost, D. R. Zimmermann, T. Oertle, E. Casademunt, S. Frentzel, G. Dechant, A. Mir and C. E. Bandtlow (2004). "Versican V2 and the central inhibitory domain of Nogo-A inhibit neurite growth via p75NTR/NgR-independent pathways that converge at RhoA." Molecular and Celllular Neuroscience **27**: 163-174.

Szpara, M. L., K. Vranizan, Y. C. Tai, C. S. Goodman, T. P. Speed and J. Ngai (2007). "Analysis of gene expression during neurite outgrowth and regeneration." BMC Neurosci **8**: 100.

Tachibana, T., K. Noguchi and M. A. Ruda (2002). "Analysis of gene expression following spinal cord injury in rat using complementary DNA microarray." Neuroscicence Letters **327**: 133-137.

Tanabe, K., I. Bonilla, J. A. Winkles and S. M. Strittmatter (2003). "Fibroblast growth factor-inducible-14 is induced in axotomized neurons and promotes neurite outgrowth." J Neurosci **23**(29): 9675-86.

Tanaka, T., M. Minami, T. Nakagawa and M. Satoh (2004). "Enhanced production of monocyte chemoattractant protein-1 in the dorsal root ganglia in a rat model of neuropathic pain: possible involvement in the development of neuropathic pain." Neurosci Res **48**(4): 463-9.

Tandrup, T., C. J. Woolf and R. E. Coggeshall (2000). "Delayed loss of small dorsal root ganglion cells after transection of the rat sciatic nerve." J Comp Neurol **422**(2): 172-80.

Taniuchi, M., H. B. Clark, J. B. Schweitzer and E. M. Johnson, Jr. (1988). "Expression of nerve growth factor receptors by Schwann cells of axotomized peripheral nerves: ultrastructural location, suppression by axonal contact, and binding properties." J Neurosci **8**(2): 664-81.

Teng, F. Y. and B. L. Tang (2006). "Axonal regeneration in adult CNS neurons--signaling molecules and pathways." J Neurochem **96**(6): 1501-8.

Thanos, P. K., S. Okajima, D. A. Tiangco and J. K. Terzis (1999). "Insulin-like growth factor-I promotes nerve regeneration through a nerve graft in an experimental model of facial paralysis." Restor Neurol Neurosci **15**(1): 57-71.

Thellin, O., W. Zorzi, B. Lakaye, B. De Borman, B. Coumans, G. Hennen, T. Grisar, A. Igout and E. Heinen (1999). "Housekeeping genes as internal standards: use and limits." J Biotechnol **75**(2-3): 291-5.

Thomaidou, D., D. Coquillat, S. Meintanis, M. Noda, G. Rougon and R. Matsas (2001). "Soluble forms of NCAM and F3 neuronal cell adhesion molecules promote Schwann cell migration: identification of protein tyrosine phosphatases zeta/beta as the putative F3 receptors on Schwann cells." J Neurochem **78**(4): 767-78.

Thompson, S. W., J. V. Priestley and A. Southall (1998). "gp130 cytokines, leukemia inhibitory factor and interleukin-6, induce neuropeptide expression in intact adult rat sensory neurons in vivo: time-course, specificity and comparison with sciatic nerve axotomy." Neuroscience **84**(4): 1247-55.

Tilstone, C. (2003). "Vital Statistics." Nature **424**: 610-612.

Toft, A., D. T. Scott, S. C. Barnett and J. S. Riddell (2007). "Electrophysiological evidence that olfactory cell transplants improve function after spinal cord injury." Brain **130**(Pt 4): 970-84.

Toth, C., S. Y. Shim, J. Wang, Y. Jiang, G. Neumayer, C. Belzil, W. Q. Liu, J. Martinez, D. Zochodne and M. D. Nguyen (2008). "Ndel1 promotes axon regeneration via intermediate filaments." PLoS ONE **3**(4): e2014.

Tsuji, L., T. Yamashita, T. Kubo, T. Madura, H. Tanaka, K. Hosokawa and M. Tohyama (2004). "FLRT3, a cell surface molecule containing LRR repeats and a FNIII domain, promotes neurite outgrowth." Biochem Biophys Res Commun **313**(4): 1086-91.

Tsujino, H., E. Kondo, T. Fukuoka, Y. Dai, A. Tokunaga, K. Miki, K. Yonenobu, T. Ochi and K. Noguchi (2000). "Activating transcription factor 3 (ATF3) induction by axotomy in sensory and motoneurons: A novel neuronal marker of nerve injury." Mol Cell Neurosci **15**(2): 170-82.

Tusher, V. G., R. Tibshirani and G. Chu (2001). "Significance analysis of microarrays applied to the ionizing radiation response." Proceedings of the National Academy of Sciences USA **28**(9): 5116-5121.

Uberti, D., E. Meli and M. Memo (2002). "Expression of cell-cycle-related proteins and excitoxicity." Amino

Acids **23**(1-3): 27-30.

Usdin, T. B., E. Mezey, D. C. Button, M. J. Brownstein and T. I. Bonner (1993). "Gastric inhibitory polypeptide receptor, a member of the secretin-vasoactive intestinal peptide receptor family, is widely distributed in peripheral organs and the brain." Endocrinology **133**(6): 2861-70.

Uwanogho, D., M. Rex, E. J. Cartwright, G. Pearl, C. Healy, P. J. Scotting and P. T. Sharpe (1995). "Embryonic expression of the chicken Sox2, Sox3 and Sox11 genes suggests an interactive role in neuronal development." Mech Dev **49**(1-2): 23-36.

Valder, C. R., J. J. Liu, Y. H. Song and Z. D. Luo (2003). "Coupling gene chip analyses and rat genetic variances in identifying potential target genes that may contribute to neuropathic allodynia development." J Neurochem **87**(3): 560-73.

Vandesompele, J., K. De Preter, F. Pattyn, B. Poppe, N. Van Roy, A. De Paepe and F. Speleman (2002). "Accurate normalization of real-time quantitative RT-PCR data by geometric averaging of multiple internal control genes." Genome Biol **3**(7): RESEARCH0034.

Vargas, M. E. and B. A. Barres (2007). "Why is Wallerian degeneration in the CNS so slow?" Annu Rev Neurosci **30**: 153-79.

Velardo, M. J., C. Burger, P. R. Williams, H. V. Baker, M. C. Lopez, T. H. Mareci, T. E. White, N. Muzyczka and P. J. Reier (2004). "Patterns of gene expression reveal a temporally orchestrated wound healing response in the injured spinal cord." The Journal of Neuroscience **24**(39): 8562-8576.

Verdu, E. and X. Navarro (1997). "Comparison of immunohistochemical and functional reinnervation of skin and muscle after peripheral nerve injury." Exp Neurol **146**(1): 187-98.

Verge, V. M., Z. Wiesenfeld-Hallin and T. Hokfelt (1993). "Cholecystokinin in mammalian primary sensory neurons and spinal cord: in situ hybridization studies in rat and monkey." Eur J Neurosci **5**(3): 240-50.

Waller, A. (1850). "Experiments of the section of the Glossopharyngeal and Hypoglossal nerves of the frog, and observations of the alterations produced thereby in the structure of their primitive fibres." Philosophical Transactions of the Royal Society of London **140**: 423-429.

Wallquist, W., J. Zelano, S. Plantman, S. J. Kaufman, S. Cullheim and H. Hammarberg (2004). "Dorsal root ganglion neurons up-regulate the expression of laminin-associated integrins after peripheral but not central axotomy." J Comp Neurol **480**(2): 162-9.

Wang, H., H. Sun, K. Della Penna, R. J. Benz, J. Xu, D. L. Gerhold, D. J. Holder and K. S. Koblan (2002). "Chronic neuropathic pain is accompanied by global changes in gene expression and shares pathobiology with neurodegenerative diseases." Neuroscience **114**(3): 529-46.

Wang, X., S. J. Chun, H. Treloar, T. Vartanian, C. A. Greer and S. M. Strittmatter (2002). "Localization of Nogo-A and Nogo-66 inhibition of axonal regeneration." Journal of Neuroscience **22**: 5505-5515.

Wang, Y., C. Barbacioru, F. Hyland, W. Xiao, K. L. Hunkapiller, J. Blake, F. Chan, C. Gonzalez, L. Zhang and R. R. Samaha (2006). "Large scale real-time PCR validation on gene expression measurements from two commercial long-oligonucleotide microarrays." BMC Genomics **7**: 59.

Watson, W. E. (1968). "Observations on the nucleolar and total cell body nucleic acid of injured nerve cells." J Physiol **196**(3): 655-76.

Waxman, S. G., J. D. Kocsis and J. A. Black (1994). "Type III sodium channel mRNA is expressed in embryonic but not adult spinal sensory neurons, and is reexpressed following axotomy." J Neurophysiol **72**(1): 466-70.

Werner, A., M. Willem, L. L. Jones, G. W. Kreutzberg, U. Mayer and G. Raivich (2000). "Impaired axonal regeneration in alpha7 integrin-deficient mice." The Journal of Neuroscience **20**(5): 1822-1830.

Williams, K. L., M. Rahimtula and K. M. Mearow (2006). "Heat shock protein 27 is involved in neurite

extension and branching of dorsal root ganglion neurons in vitro." J Neurosci Res **84**(4): 716-23.

Willis, D., K. W. Li, J. Q. Zheng, J. H. Chang, A. Smit, T. Kelly, T. T. Merianda, J. Sylvester, J. van Minnen and J. L. Twiss (2005). "Differential transport and local translation of cytoskeletal, injury-response, and neurodegeneration protein mRNAs in axons." J Neurosci **25**(4): 778-91.

Wong, J. and M. M. Oblinger (1990). "A comparison of peripheral and central axotomy effects of neurofilament and tubulin gene expression in rat dorsal root ganglion neurons." The Journal of Neuroscience **10**(7): 2215-2222.

Wong, J. and M. M. Oblinger (1990). "Differential regulation of peripherin and neurofilament gene expression in regenerating rat DRG neurons." J Neurosci Res **27**(3): 332-41.

Woodham, P., P. N. Anderson, W. Nadim and M. Turmaine (1989). "Satellite cells surrounding axotomised rat dorsal root ganglion cells increase expression of a GFAP-like protein." Neurosci Lett **98**(1): 8-12.

Wu, D., W. Huang, P. M. Richardson, J. V. Priestley and M. Liu (2008). "TRPC4 in rat dorsal root ganglion neurons is increased after nerve injury and is necessary for neurite outgrowth." J Biol Chem **283**(1): 416-26.

Xiao, L., Z. L. Ma, X. Li, Q. X. Lin, H. P. Que and S. J. Liu (2005). "cDNA microarray analysis of spinal cord injury and regeneration related genes in rat." Sheng Li Xue Bao **57**(6): 705-13.

Xu, X. J., T. Hokfelt, T. Bartfai and Z. Wiesenfeld-Hallin (2000). "Galanin and spinal nociceptive mechanisms: recent advances and therapeutic implications." Neuropeptides **34**(3-4): 137-47.

Xu, Z. Q., T. J. Shi, M. Landry and T. Hokfelt (1996). "Evidence for galanin receptors in primary sensory neurones and effect of axotomy and inflammation." Neuroreport **8**(1): 237-42.

Yamashita, T., H. Higuchi and M. Tohyama (2002). "The p75 receptor transduces the signal from myelin-associated glycoprotein to Rho." Journal of Cell Biology **157**: 567-570.

Yang, E. K., K. Takimoto, Y. Hayashi, W. C. de Groat and N. Yoshimura (2004). "Altered expression of potassium channel subunit mRNA and alpha-dendrotoxin sensitivity of potassium currents in rat dorsal root ganglion neurons after axotomy." Neuroscience **123**(4): 867-74.

Yang, L., F.-X. Zhang, F. Huang, Y.-J. Lu, G.-D. Li, L. Bao, H.-S. Xiao and X. Zhang (2004). "Peripheral nerve injury induces trans-synaptic modification of channels, receptors and signal pathways in rat dorsal spinal cord." European Journal of Neuroscience **19**: 871-883.

Yang, Y. H., S. Dudoit, P. Luu, D. M. Lin, V. Peng, J. Ngai and T. P. Speed (2002). "Normalization for cDNA microarray data: a robust composite method addressing single and multiple slide sytematic variation." Nucleic Acids Research **20**(4): e15.

Yasuhara, F., G. R. Gomes, E. R. Siu, C. I. Suenaga, E. Marostica, C. S. Porto and M. F. Lazari (2008). "Effects of the Antiestrogen Fulvestrant (ICI 182,780) on Gene Expression of the Rat Efferent Ductules." Biol Reprod.

Yi, X. N., L. F. Zheng, J. W. Zhang, L. Z. Zhang, Y. Z. Xu, G. Luo and X. G. Luo (2006). "Dynamic changes in Robo2 and Slit1 expression in adult rat dorsal root ganglion and sciatic nerve after peripheral and central axonal injury." Neurosci Res **56**(3): 314-21.

Yiangou, Y., P. Facer, R. Birch, L. Sangameswaran, R. Eglen and P. Anand (2000). "P2X3 receptor in injured human sensory neurons." Neuroreport **11**(5): 993-6.

Young, W. (2002). "Spinal cord contusion models." Prog Brain Res **137**: 231-55.

Yuan, T. F. (2008). "Olfactory ensheathing cells transplantation for spinal cord injury treatment: still a long way to go." Med Hypotheses **71**(1): 153-4.

Zhai, Q., J. Wang, A. Kim, Q. Liu, R. Watts, E. Hoopfer, T. Mitchison, L. Luo and Z. He (2003). "Involvement of the Ubiquitin-Proteasome system in the early stages of Wallerian Degeneration." Neuron

39: 217-225.

Zhang, K. H., H. S. Xiao, P. H. Lu, J. Shi, G. D. Li, Y. T. Wang, S. Han, F. X. Zhang, Y. J. Lu, X. Zhang and X. M. Xu (2004). "Differential gene expression after complete spinal cord transection in adult rats: an analysis focused on a subchronic post-injury stage." Neuroscience **128**(2): 375-88.

Zhang, Q., R. R. Ji, R. Lindsay and T. Hokfelt (1995). "Effect of growth factors on substance P mRNA expression in axotomized dorsal root ganglia." Neuroreport **6**(9): 1309-12.

Zhang, X., L. Bao, U. Arvidsson, R. Elde and T. Hokfelt (1998). "Localization and regulation of the delta-opioid receptor in dorsal root ganglia and spinal cord of the rat and monkey: evidence for association with the membrane of large dense-core vesicles." Neuroscience **82**(4): 1225-42.

Zhang, X., L. Bao, T. J. Shi, G. Ju, R. Elde and T. Hokfelt (1998). "Down-regulation of mu-opioid receptors in rat and monkey dorsal root ganglion neurons and spinal cord after peripheral axotomy." Neuroscience **82**(1): 223-40.

Zhang, X., A. Dagerlind, R. P. Elde, M. N. Castel, C. Broberger, Z. Wiesenfeld-Hallin and T. Hokfelt (1993). "Marked increase in cholecystokinin B receptor messenger RNA levels in rat dorsal root ganglia after peripheral axotomy." Neuroscience **57**(2): 227-33.

Zhang, X., Z. Wiesenfeld-Hallin and T. Hokfelt (1994). "Effect of peripheral axotomy on expression of neuropeptide Y receptor mRNA in rat lumbar dorsal root ganglia." Eur J Neurosci **6**(1): 43-57.

Zhang, X., Z. O. Xu, T. J. Shi, M. Landry, K. Holmberg, G. Ju, Y. G. Tong, L. Bao, X. P. Cheng, Z. Wiesenfeld-Hallin, A. Lozano, J. Dostrovsky and T. Hokfelt (1998). "Regulation of expression of galanin and galanin receptors in dorsal root ganglia and spinal cord after axotomy and inflammation." Ann N Y Acad Sci **863**: 402-13.

Zhang, Y., R. Roslan, D. Lang, M. Schachner, A. R. Lieberman and P. N. Anderson (2000). "Expression of CHL1 and L1 by neurons and glia following sciatic nerve and dorsal root injury." Molecular and Cellular Neuroscience **16**: 71-96.

Zhang, Y., K. Tohyama, J. K. Winterbottom, N. S. Haque, M. Schachner, A. R. Lieberman and P. N. Anderson (2001). "Correlation between putative inhibitory molecules at the dorsal root entry zone and failure of dorsal root axonal regeneration." Mol Cell Neurosci **17**(3): 444-59.

Zhao, Y., J. Xiao, M. Ueda, Y. Wang, M. Hines, T. S. Nowak, Jr. and M. S. Ledoux (2008). "Glial elements contribute to stress-induced torsinA expression in the CNS and peripheral nervous system." Neuroscience.

Zhu, B., G. Ping, Y. Shinohara, Y. Zhang and Y. Baba (2005). "Comparison of gene expression measurements from cDNA and 60-mer oligonucleotide microarrays." Genomics **85**(6): 657-65.

Zimmermann, M. (2001). "Pathobiology of neuropathic pain." Eur J Pharmacol **429**(1-3): 23-37.

Znaor, L., S. Lovric, Q. Hogan and D. Sapunar (2007). "Association of neural inflammation with hyperalgesia following spinal nerve ligation." Croat Med J **48**(1): 35-42.

Zvarova, K., E. Murray and M. A. Vizzard (2004). "Changes in galanin immunoreactivity in rat lumbosacral spinal cord and dorsal root ganglia after spinal cord injury." J Comp Neurol **475**(4): 590-603.